ЖУРНАЛ
ПРИКЛАДНОЙ ХИМИИ

JOURNAL OF
APPLIED CHEMISTRY
OF THE USSR

(ZHURNAL PRIKLADNOI KHIMY)

IN ENGLISH TRANSLATION

VOL. 30 NO. 7

CONSULTANTS BUREAU, INC.
227 WEST 17TH STREET, NEW YORK 11, N. Y.
an agency for the interpretation of international knowledge

SOVIET RESEARCH
in
CATALYSIS

Chemistry Collection No. 3. Covers all aspects of catalysis; papers selected from all Soviet chemical journals translated by Consultants Bureau, 1949-1955.

Sections may be purchased separately as follows:

I.	Theoretical and Sundry Associated Effects	262 pages	$50.–	
IIa.	General	250 pages	50.–	$125.–
IIb.	General	250 pages	50.–	
IIc.	General: Reduction-Oxidation and Fischer-Tropsch	214 pages	50.–	
III.	Hydrogenation Dehydrogenation Cracking	294 pages	50.–	
IV.	Isomerization Alkylation Dehydration	274 pages		$50.–
V.	Polymerization Friedel-Crafts Zeigler	128 pages		30.–

The Collection, comprising 1,672 pages, 262 papers may be purchased as a unit for **$200.00**

Individual papers are available separately – Table of Contents on request.

CONSULTANTS BUREAU, INC.

227 WEST 17TH STREET, NEW YORK 11, N. Y.

JOURNAL OF APPLIED CHEMISTRY OF THE USSR

(ZHURNAL PRIKLADNOI KHIMII)

Volume 30, No. 7

July, 1957

(A Publication of the Academy of Sciences of the U. S. S. R.)

IN ENGLISH TRANSLATION

Copyright, 1958

CONSULTANTS BUREAU, INC.

227 West 17th Street

New York 11, N. Y.

Printed in the United States

	Domestic	Foreign
Annual Subscription	$60.00	$65.00
Annual Subscription for libraries of non-profit academic institutions	20.00	25.00
Single Issue	7.50	

Note: The sale of photostatic copies of any portion of this copyright translation is expressly prohibited by the copyright owners.

SIGNIFICANCE OF ABBREVIATIONS MOST FREQUENTLY ENCOUNTERED IN SOVIET PERIODICALS

FIAN	Phys. Inst. Acad. Sci. USSR.
GDI	Water Power Inst.
GITI	State Sci.-Tech. Press
GITTL	State Tech. and Theor. Lit. Press
GONTI	State United Sci.-Tech. Press
Gosenergoizdat	State Power Press
Goskhimizdat	State Chem. Press
GOST	All-Union State Standard
GTTI	State Tech. and Theor. Lit. Press
IL	Foreign Lit. Press
ISN (Izd. Sov. Nauk)	Soviet Science Press
Izd. AN SSSR	Acad. Sci. USSR Press
Izd. MGU	Moscow State Univ. Press
LEIIZhT	Leningrad Power Inst. of Railroad Engineering
LET	Leningrad Elec. Engr. School
LETI	Leningrad Electrotechnical Inst.
LETIIZhT	Leningrad Electrical Engineering Research Inst. of Railroad Engr.
Mashgiz	State Sci.-Tech. Press for Machine Construction Lit.
MEP	Ministry of Electrical Industry
MES	Ministry of Electrical Power Plants
MESEP	Ministry of Electrical Power Plants and the Electrical Industry
MGU	Moscow State Univ.
MKhTI	Moscow Inst. Chem. Tech.
MOPI	Moscow Regional Pedagogical Inst.
MSP	Ministry of Industrial Construction
NII ZVUKSZAPIOI	Scientific Research Inst. of Sound Recording
NIKFI	Sci. Inst. of Modern Motion Picture Photography
ONTI	United Sci.-Tech. Press
OTI	Division of Technical Information
OTN	Div. Tech. Sci.
Stroiizdat	Construction Press
TOE	Association of Power Engineers
TsKTI	Central Research Inst. for Boilers and Turbines
TsNIEL	Central Scientific Research Elec. Engr. Lab.
TsNIEL-MES	Central Scientific Research Elec. Engr. Lab.–Ministry of Electric Power Plants
TsVTI	Central Office of Economic Information
UF	Ural Branch
VIESKh	All-Union Inst. of Rural Elec. Power Stations
VNIIM	All-Union Scientific Research Inst. of Meteorology
VNIIZhDT	All-Union Scientific Research Inst. of Railroad Engineering
VTI	All-Union Thermotech. Inst.
VZEI	All-Union Power Correspondence Inst.

Note: Abbreviations not on this list and not explained in the translation have been transliterated, no further information about their significance being available to us. – Publisher.

SEPARATION OF CALCIUM CHLORIDE FROM SOLVAY SPENT LIQUOR THROUGH CALCIUM HYDROXYCHLORIDE

I. I. Volnov and E. I. Latysheva

One of the important disadvantages of the Solvay process for soda production is the accumulation of enormous amounts of the so-called distillation liquor (spent liquor), formed in the ammonia stills during treatment of the $NaHCO_3$ mother liquor with slaked lime.

Work on profitable methods of using distillation liquors in the soda industry has continued from the earliest days of the ammonia–soda process, and in recent years at one soda works of the USSR calcium chloride has been made on a large scale by evaporation of the distillation liquor after removal of suspended $CaCO_3$, $Ca(OH)_2$ and $CaSO_4 \cdot 2H_2O$ and dissolved $CaSO_4$ and $Ca(OH)_2$ [1].

The purpose of the present investigation was to determine the possibility of partial separation of calcium chloride from the liquor in the form of the basic salt $CaCl_2 \cdot 3Ca(OH)_2 \cdot 12H_2O$, with omission of the evaporation stage, and also the possibility of separation of $CaCl_2$ in the form of $CaCl_2 \cdot 3Ca(OH)_2 \cdot 12H_2O$ at a definite stage of evaporation of the liquor.

This investigation is justified by the fact that, according to available published data, calcium hydroxychloride may have direct applications in the building industry [2-4].

The exact composition, conditions of formation, and stability limits of basic calcium chlorides, formed by interaction of $CaCl_2$ solutions with $Ca(OH)_2$ solution, were determined by one of the present authors under the guidance of S. Z. Makarov [5, 6] in a systematic study of solubility in the three-component system $CaCl_2$–$Ca(OH)_2$–H_2O at + 5, 10, 30, 40, 50, 55, 75°.

On the basis of these results and literature data a polythermal diagram was plotted in temperature – wt. % $CaCl_2$ coordinates, from which it is possible to determine the regions of formation of eight solid phases: $Ca(OH)_2$, $CaCl_2 \cdot 3Ca(OH)_2 \cdot 12H_2O$, $CaCl_2 \cdot Ca(OH)_2 \cdot H_2O$, $CaCl_2 \cdot 2H_2O$, α-, β- and γ-$CaCl_2 \cdot 4H_2O$ and $CaCl_2 \cdot 6H_2O$.

Analysis of these results shows that in the particular case of a liquor containing from 8 to 10% $CaCl_2$, with the presence of 5-6% NaCl ignored in the first approximation, to separate part of the $CaCl_2$ in the form of $CaCl_2 \cdot 3Ca(OH)_2 \cdot 12H_2O$ it is necessary to carry out the process at a temperature not higher than 5°; the amount of calcium chloride which can be bound in the form of the basic salt will not be larger, as at 0° the equilibrium concentration at the point $Ca(OH)_2 + CaCl_2 \cdot 3Ca(OH)_2 \cdot 12H_2O$ is 6.8 wt. %.

As data on the behavior of the system at temperatures < 0° were not available, it was decided to study the system at temperatures below zero in order to obtain precise data on the separation region of $CaCl_2 \cdot 3Ca(OH)_2 \cdot 12H_2O$ and to find the boundary between the $CaCl_2 \cdot 3Ca(OH)_2 \cdot H_2O$ area and the ice area.

With regard to the possibility of isolation of $CaCl_2$ through the basic chloride at a definite stage of evaporation of the liquor, the situation is more favorable.

Comparison of Bodrov's data [1] on the variation of the composition of distillation liquor during evaporation with the polythermal data shows that from solutions of $CaCl_2$ of moderate concentrations (from 18.75 to 30.50 wt. % $CaCl_2$ but no higher), formed at definite stages of evaporation of the liquor, with the presence of 3-8% NaCl neglected in the first approximation, it is possible to separate considerable amounts of $CaCl_2$ in the form of $CaCl_2 \cdot 3Ca(OH)_2 \cdot 12H_2O$.

It is evident that a separate investigation is required to find the optimum conditions of separation of $CaCl_2$ through $CaCl_2 \cdot 3Ca(OH)_2 \cdot 12H_2O$ from solutions without impurities, from the original distillation liquor, and from the liquor at a definite stage of evaporation.

EXPERIMENTAL

Solubility isotherm at −20° for the system $CaCl_2$–$Ca(OH)_2$–H_2O. The starting materials for the study of this system were $CaCl_2 \cdot 6H_2O$ of analytical grade from the Karpov Works, Moscow, and $Ca(OH)_2$ from the Stalin Chemical Reagent Works.

Definite amounts of calcium chloride solution of increasing concentration were added to milk of lime contained in a glass vessel for solubility determinations. The vessel was contained in a Dewar flask filled with ice + NaCl freezing mixture. The temperature was regulated to the nearest ± 0.5°. The composition of the solid phases was determined by the "residue" method. Alkalinity was determined by titration with 0.1 N HCl solution Cl^- by the Volhard method, and Ca^{++} by precipitation as oxalate followed by titration with 0.1 N $KMnO_4$ solution.

The results are given in Table 1 and plotted in a triangular phase diagram (Fig. 1).

TABLE 1

Isotherm at −20° for the System $CaCl_2$–$Ca(OH)_2$–H_2O

Points No.	Time (in hours)	Liquid phase (wt. %)		Residue (wt. %)		Solid phase*
		$Ca(OH)_2$	$CaCl_2$	$Ca(OH)_2$	$CaCl_2$	
7	24	0.09	20.40	0.50	9.73	Ice + 1, 3, 12
8	24	0.06	22.20	35.08	20.21	1, 3, 12
5	24	0.08	28.30	9.30	26.55	1, 3, 12
2	30	0.09	32.77	—	—	
4	34	0.07	33.68	20.26	27.27	1, 3, 12
3	35	0.08	33.90	10.48	36.62	1, 3, 12 + $CaCl_2 \cdot 6H_2O$
1	25	—	34.1	—	—	$CaCl_2 \cdot 6H_2O$

* The numbers given for the solid phase in this and subsequent tables represent the composition of $CaCl_2 \cdot 3Ca(OH)_2 \cdot 12H_2O$.

The isotherm at −20° shows the existence of 3 solid phases – ice, $CaCl_2 \cdot 3Ca(OH)_2 \cdot 12H_2O$ and $CaCl_2 \cdot 6H_2O$. By plotting multiple points for the system (given in the paper [4]) and multiple points for ice + $CaCl_2 \cdot 3Ca(OH)_2 \cdot 12H_2O$ and $CaCl_2 \cdot 3Ca(OH)_2 \cdot 12H_2O$ + $CaCl_2 \cdot 6H_2O$ (given in Table 1) on the temperature – wt. % $CaCl_2$ polythermal diagram (Fig. 2), it is possible to determine by interpolation the triple point for ice + $Ca(OH)_2$ + + $CaCl_2 \cdot 3Ca(OH)_2 \cdot 12H_2O$ at −5° and 6% $CaCl_2$ by weight.

Therefore we may now say with certainty that considerable amounts of calcium chloride cannot be isolated in the form of $CaCl_2 \cdot 3Ca(OH)_2 \cdot 12H_2O$ from distillation liquor even at subzero temperatures.*

* It must be pointed out that the new data obtained for the system $CaCl_2$–$Ca(OH)_2$–H_2O also give an idea of the processes which occur under the conditions which determine the structure of cement stone with additions of calcium chloride at subzero temperatures.

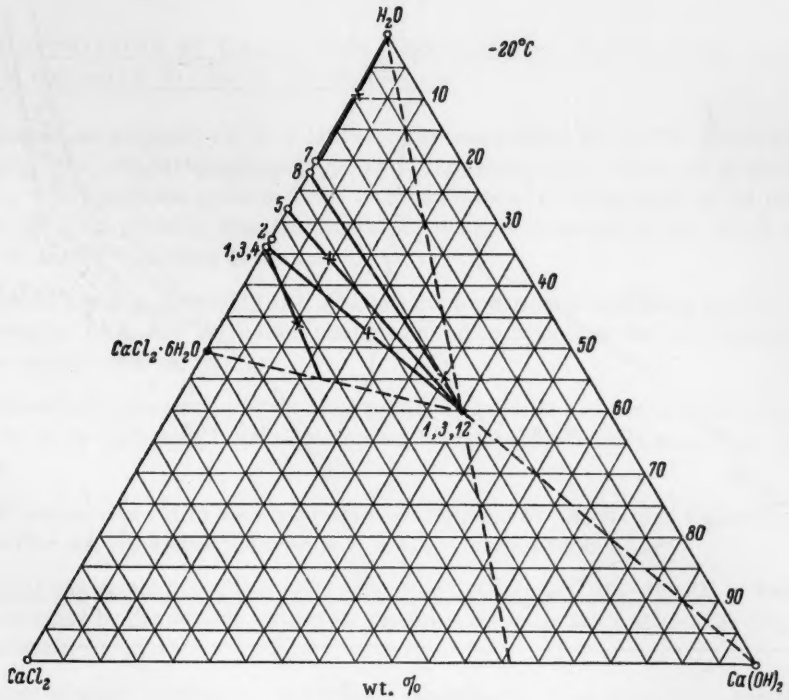

Fig. 1. Solubility isotherm at −20° for the system $CaCl_2$–$Ca(OH)_2$–H_2O.

Conditions for separation of $CaCl_2$ aqueous solutions without impurities, in the form of $CaCl_2 \cdot 3Ca(OH)_2 \cdot 12H_2O$. Solutions containing 10% $CaCl_2$ (corresponding to the approximate composition of distillation liquor) and 22% $CaCl_2$ (corresponding to the composition of this liquor at a definite evaporation stage) were chosen for the study.

It was found that dry $Ca(OH)_2$ cannot always be used for separation of $CaCl_2 \cdot 3Ca(OH)_2 \cdot 12H_2O$; this depends on the concentration of the $CaCl_2$ solution. For example, if slaked lime is added to calcium chloride solution of moderate concentration (22% by weight) at room temperature, lumps are formed. The lime evidently becomes coated with the basic salt and this retards the reaction. This does not occur when dry $Ca(OH)_2$ is added to dilute $CaCl_2$ solutions (up to 10%).

Therefore, for solutions containing over 10% $CaCl_2$ by weight, milk of lime rather than dry $Ca(OH)_2$ should be used, and $CaCl_2$ should be added in the milk of lime in order to reach equilibrium more quickly. Milk of lime should not be used for separation of $CaCl_2$ from solutions containing 10% and less of $CaCl_2$, as the solution is diluted, and the result lies outside the limits of existence of the compound $CaCl_2 \cdot 3Ca(OH)_2 \cdot 12H_2O$ (see Fig. 2).

Moreover, in the first case (22% solution) $CaCl_2$ solution should be added with continuous stirring to milk of lime heated to about 50-60°, the solution should be allowed to cool slowly to room temperature, and it should then be cooled to about + 1° (in order to obtain maximum yield); in the second case (10% solution), dry $Ca(OH)_2$ should be added by portions to $CaCl_2$ solution heated to 50-60°, the subsequent procedure being the same as for 22% solution. Crystalline, easily filterable precipitates of $CaCl_2 \cdot 3Ca(OH)_2 \cdot 12H_2O$ (Fig. 3) are obtained only if these procedures are followed; for 10% solutions equilibrium is reached in about 1.5 days, and for 22% solutions, in 3.5 days.

Conditions for maximum yields of $CaCl_2 \cdot 3Ca(OH)_2 \cdot 12H_2O$ from 10% and 22% solutions of $CaCl_2$ are given in Table 2.

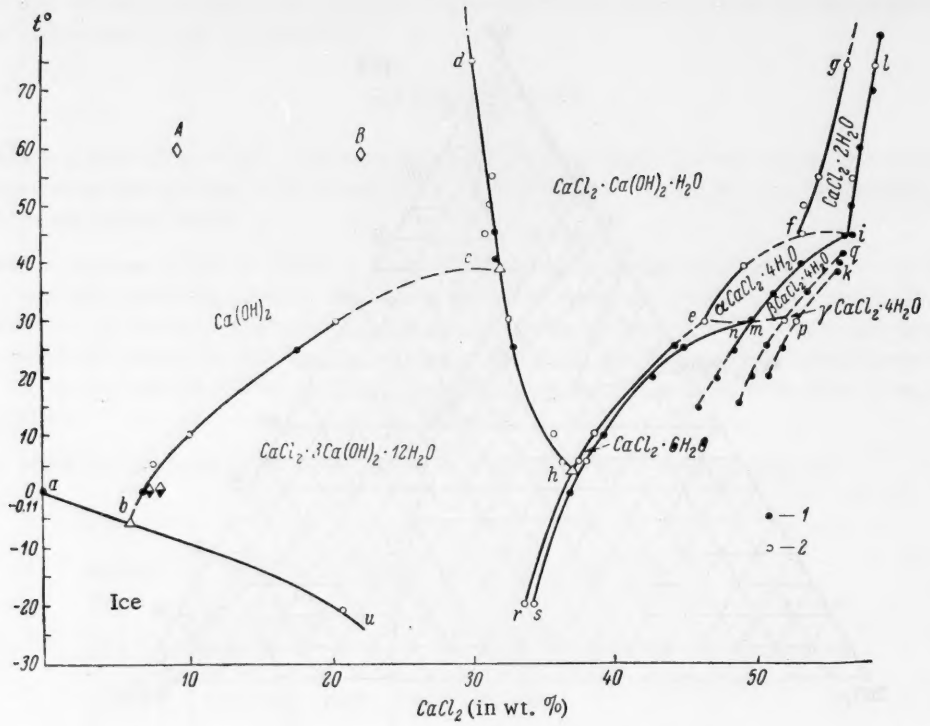

Fig. 2. Solubility polytherm for the system $CaCl_2$–$Ca(OH)_2$–H_2O. Data: 1) From the literature; 2) the author's.

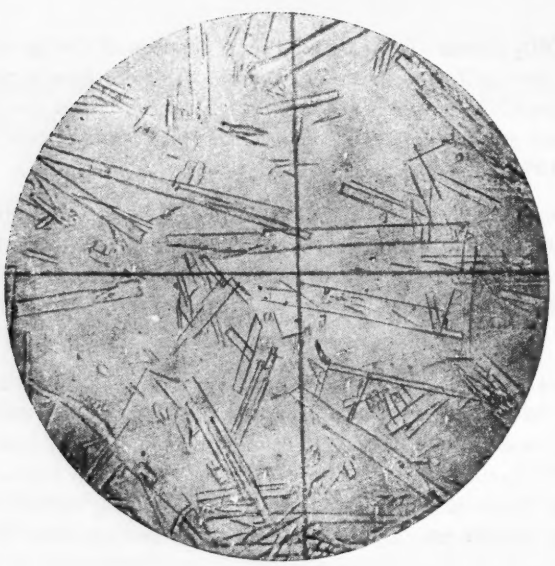

Fig. 3. Micrograph of the salt $CaCl_2 \cdot Ca(OH)_2 \cdot 12H_2O$.

In the polythermal diagram (Fig. 2) points representing the compositions of the original solutions in Experiments A and B are denoted by rhombs, and the points representing the compositions of the corresponding liquid phases at the end of the experiments, by half-black rhombs.

Conditions for Separation of $CaCl_2$ from the Original Distillation Liquor and from the Liquor at a Definite Stage of Evaporation

A synthetic liquor was prepared (s. g. 1.112) with the composition (in wt. %): $CaCl_2$ 10.03, NaCl 4.99, $Ca(OH)_2$ 0.09, $CaSO_4$ 0.16, NH_4OH 0.001, and a series of experiments was carried out in the same conditions as for Experiment A. The results are given in Table 3 (Experiment A^1). Comparison of the results of Experiments A and A^1 shows that the yield of $CaCl_2$ from the distillation liquor is somewhat higher, 26.1% instead of 20.3%, probably owing to the salting-out effect of the impurities.

It must be pointed out that Bodrov [1] also observed the formation of needlelike crystals of calcium hydroxychlorides in the slaking of lime with distillation liquor followed by cooling of the lime suspension to below 15°, but the quantitative aspects were not studied.

For an experiment with distillation liquor after partial evaporation, on the basis of Bodrov's data [1] a solution (s. g. 1.24) of the following composition (in wt. %) was synthesized: $CaCl_2$ 21.5, NaCl 6.5, $CaSO_4$ 0.90, $Ca(OH)_2$ 0.03.

Experiment B^1 was carried out in the conditions of Experiment B; the yield of $CaCl_2$ was 65.7%, which is considerably higher than the yield obtained from pure $CaCl_2$ solution (Table 3).

Physicochemical characteristics of the hydroxychloride $CaCl_2 \cdot 3Ca(OH)_2 \cdot 12H_2O$. Data in the literature, and earlier results obtained by the present author [5], show that the basic salt $CaCl_2 \cdot 3Ca(OH)_2 \cdot 12H_2O$ has the following characteristics.

The salt consists of white, transparent, needlelike crystals (Fig. 3) of the rhombic system, with refractive indices $N_g = 1.513$, $N_m = 1.532$, $N_h = 1.535$ [7]; the optic axial angle $2V = 44.6°$ [8]; s. g. 1.67 [5]. The salt decomposes in water and alcohols to give a solution of $CaCl_2$ and $Ca(OH)_2$; it dissolves without decomposition in an aqueous solution containing 85 g/liter of $CaCl_2$ and in solutions of ethyl, butyl, and amyl alcohols containing 130, 54 and 48 g/liter of $CaCl_2$ respectively [9], in glycerol [5], and in sugar solution [10].

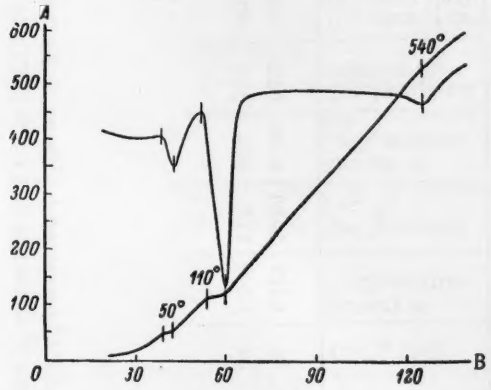

Fig. 4. Heating curve of $CaCl_2 \cdot 3Ca(OH)_2 \cdot 12H_2O$. A) Temperature (in °C), B) time (minutes).

The salt is hygroscopic; after dehydration to the composition $CaCl_2 \cdot 3Ca(OH)_2$ it absorbs more than 12 moles of water per mole in three days when exposed to water vapor [11]. It is carbonated in an atmosphere of CO_2 [9].

The heating curve of $CaCl_2 \cdot 3Ca(OH)_2 \cdot 12H_2O$ (Fig. 4) has 3 consecutive endothermic effects, which show that the salt is stable up to + 50°, and decomposes above this temperature into $Ca(OH)_2$ and a solution of $CaCl_2$. The effect at 111° represents evaporation of water, and the effect at 540° represents decomposition of $Ca(OH)_2$ into CaO and H_2O [5].

Conversion of $CaCl_2 \cdot 3Ca(OH)_2 \cdot 12H_2O$ into $CaCl_2$ solution with recovery of $Ca(OH)_2$. We also studied the conversion of $CaCl_2 \cdot 3Ca(OH)_2 \cdot 12H_2O$ into $CaCl_2$ solution, with recovery of $Ca(OH)_2$, as described in a patent [12], as quantitative data are not given in this patent. It follows from the polythermal diagram (Fig. 2) that treatment of $CaCl_2 \cdot 3Ca(OH)_2 \cdot 12H_2O$ with water at 50-60° can yield solutions containing up to 32% $CaCl_2$ and pure $Ca(OH)_2$. To calculate the minimum amount of water required for the decomposition, we plotted the boundary of the fields for $Ca(OH)_2$ and $CaCl_2 \cdot 3Ca(OH)_2 \cdot 12H_2O$ at 55° and the point representing the composition of $CaCl_2 \cdot 3Ca(OH)_2 \cdot 12H_2O$ on a

TABLE 2

Conditions for Separation of $CaCl_2$ from its Aqueous Solutions through $CaCl \cdot 3Ca(OH)_2 \cdot 12H_2O$

Experiment	Amount (g)		$Ca(OH)_2$ content of milk of lime (wt. %)	Amount of $CaCl_2$ (ml)	Density of $CaCl_2$ solution	$CaCl_2$ content (wt. %)	Amount of $CaCl_2$ solution (g)	Total weight of mixture (g)	Duration of experiment (hrs)	Temperature (°C)		Wt. (g)		Amount (wt. %)				Solid phase	Amount of mother liquor (%)	Yield (%)
														liquid phase		residue				
	$Ca(OH)_2$	water								initial	final	liquid phase	residue	$Ca(OH)_2$	$CaCl_2$	$Ca(OH)_2$	$CaCl_2$			
A	6.6	—	—	50	1.083	10.0	54.15	60.75	37	60	1	40.0	20.75	0.10	6.41	29.09	13.95	1,3,12	36.2	20.3
B	18	31	36.7	50	1.198	22.0	59.95	108.95	81	60	1	51.45	57.50	0.15	7.75	29.56	14.59	1,3,12	35.5	51.6

TABLE 3

Conditions for Separation of $CaCl_2$ from Distillation Liquor through $CaCl_2 \cdot 3Ca(OH)_2 \cdot 12H_2O$

Experiment	Amount (g)		$Ca(OH)_2$ content of milk of lime (wt. %)	Amount of $CaCl_2$ (ml)	Density of $CaCl_2$ solution	$CaCl_2$ content (wt. %)	Amount of $CaCl_2$ solution (g)	Total weight of mixture (g)	Duration of experiment (hrs)	Temperature (°C)		Wt. (g)		Amount (wt. %)				Solid phase	Amount of mother liquor (%)	Yield (%)
														liquid phase		residue				
	$Ca(OH)_2$	water								initial	final	liquid phase	residue	$Ca(OH)_2$	$CaCl_2$	$Ca(OH)_2$	$CaCl_2$			
A^1	6.6	—	—	50	1.112	10.03	55.60	62.20	39	60	+1	40.0 *	22.2	0.12	5.18	30.96	15.42	1,3,12	25.0	26.1
B^1	18	31	36.7	50	1.240	21.5	62.0	11.1	81	60	+1	51.6 **	59.4	0.15	6.81	31.29	16.53	1,3,12	26.0	65.7

*Liquid phase of Experiment A^1 contained 4.12% wt. % NaCl and 0.16 wt. % $CaSO_4$. The "residue" contained 1.81 wt. % NaCl, traces of $CaSO_4$.
**Liquid phase of Experiment B^1 contained 3.71 wt. % NaCl and 0.09 wt. % $CaSO_4$. The "residue" contained 2.07 wt. % NaCl, traces of $CaSO_4$.

triangular phase diagram (Fig. 5). This point was joined to the water corner and it was thus found that to obtain 30% $CaCl_2$ solution, $CaCl_2 \cdot 3Ca(OH)_2 \cdot 12H_2O$ must be treated with 5-6% water on the weight of the basic chloride taken. However, experiments carried out with this amount of water gave a mass of poor filterability.

Better filterability was obtained when 50 g of $CaCl_2 \cdot 3Ca(OH)_2 \cdot 12H_2O$ was stirred with 8 g of water (i. e., ~14 %) in a thermostat at 50° for 20 hours. The weight ratio of the liquid and solid phases formed was 1 : 1. The liquid phase contained 24.6% $CaCl_2$ (point D in Fig. 5). Thus, this method can be used for binding $CaCl_2$ in the form of $CaCl_2 \cdot 3Ca(OH)_2 \cdot 12H_2O$ from weak solutions of $CaCl_2$ (not less than 10%); decomposition of the basic salt at 50° in presence of 14% of water gives a solution containing 24% $CaCl_2$. By prolonged washing of the "residue" with water in an atmosphere free from CO_2 it is possible to obtain $Ca(OH)_2$ containing about 1.2% of $CaCO_3$ and traces of $Fe^{\cdots}$.

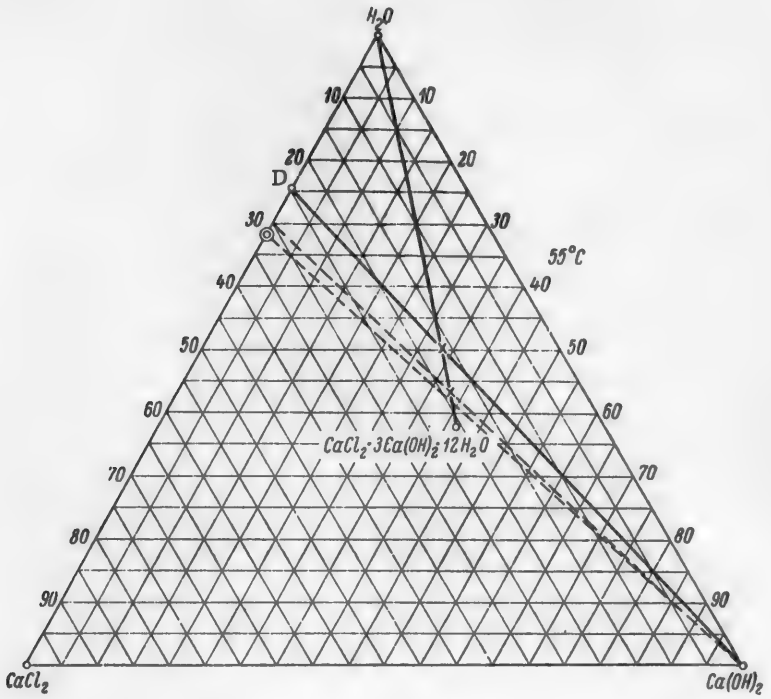

Fig. 5. Conditions for conversion of calcium hydroxychloride into $CaCl_2$ and $Ca(OH)_2$.

SUMMARY

1. By addition of dry $Ca(OH)_2$ to aqueous solutions of $CaCl_2$ of about 10% concentration it is possible to separate, at 1°, $CaCl_2$ in the form of the hydroxychloride $CaCl_2 \cdot 3Ca(OH)_2 \cdot 12H_2O$, in a crystalline, easily filterable form in ~ 20% yield.

2. $CaCl_2$ can be obtained in ~ 26 % yield from distillation liquors in the Solvay process under these conditions.

3. If aqueous solutions of $CaCl_2$ of about 22% concentration, without impurities, are added to milk of lime containing 36.7% of $Ca(OH)_2$ by weight, $CaCl_2$ can be separated at + 1° in ~ 50% yield under the above conditions.

4. $CaCl_2$ can be separated in ~65% yield from distillation liquors evaporated down to 21.5% $CaCl_2$.

5. According to the literature, calcium hydroxychloride

$$CaCl_2 \cdot 3Ca(OH)_2 \cdot 12H_2O$$

can be utilized in the building industry.

6. Decomposition of the hydroxychloride at 50° with 14% of water on the weight of the basic chloride gives 24% solutions of $CaCl_2$.

LITERATURE CITED

[1] D. S. Bodrov, Author's Summary of Candidate's Dissertation, All-Union Institute of the Building Industry, Ministry of the Chemical Industry USSR, Kharkov (1953).

[2] W. Pitt, Chem. Eng. and Mining Rev., 21, 242, 65 (1928).

[3] V. M. Moskvin, Hardening Accelerators for Concrete (ONTI, 1937)* p. 110.

[4] V. F. Zhuravlev, Chemistry of Cements (Goskhimizdat, 1951)* pp. 179-181.

[5] I. I. Volnov, Author's Summary of Candidate's Dissertation, Institute of General and Inorganic Chemistry, Acad. Sci. USSR (Moscow, 1952).

[6] S. Z. Makarov and I. I. Volnov, Ann. Sector Phys.-Chem. Analysis 24, 320 (1954).

[7] C. Bunn, L. Clark and J. Clifford, Proc. Royal Soc., A, 151, 141 (1935).

[8] G. Perhrman and G. R. W. Mylius, Acta. AcadAboensis Mat. Phys., VIII, 9, 9 (1935).

[9] A. Ditte, C. R., 91, 576 (1880).

[10] F. A. H. Schreinemakers, Chem. Wekblad, 8, 683 (1911).

[11] F. W. Kliugstedt, Acta Acad. Aboensis Mat. Phys., IX, 1, 1-29 (1935).

[12] D. R. P., 15, 493, Pechiney Co. (1886).

Received November 21, 1955

*In Russian

ISOTHERMS FOR THE RECIPROCAL AQUEOUS SYSTEM AMMONIUM MONOPHOSPHATE – SODIUM NITRATE – WATER AT + 30, + 20 AND 0°

S. Ya. Shpunt

Scientific Research Institute of Fertilizers and Insectofungicides

In one of the alternative processes developed in the Scientific Research Institute of Fertilizers and Insectofungicides [1] for the nitric acid conversion of phosphates, calcium ions are precipitated as calcium sulfate by addition of sodium sulfate to the extract obtained in this process.

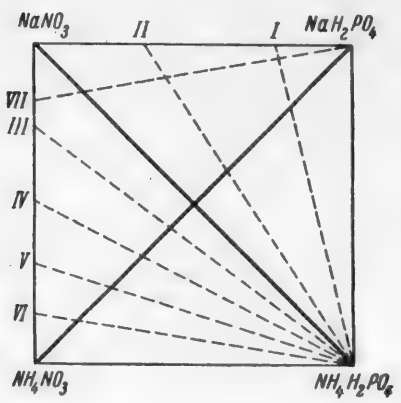

Fig. 1. Position of the internal sections on a horizontal projection for the system $NaNO_3-NH_4H_2PO_4-H_2O$.

The solution, after neutralization with ammonia, contains a mixture of ammonium monophosphate and sodium nitrate. An investigation of the reciprocal aqueous system ammonium monophohphate – sodium nitrate – water was undertaken with the object of finding methods for separation of these salts.

In order to plot the polytherm for the reciprocal system $NaNO_3-NH_4H_2PO_4-H_2O$ and to obtain isotherms for any temperatures by interpolation, we had previously investigated 7 internal sections [2]:

32.0% $NaNO_3$ + 68.0% $NaH_2PO_4 \rightarrow NH_4H_2PO_4$	(I)
74.7% $NaNO_3$ + 25.3% $NaH_2PO_4 \rightarrow NH_4H_2PO_4$	(II)
74.0% $NaNO_3$ + 26.0% $NH_4NO_3 \rightarrow NH_4H_2PO_4$	(III)
48.5% $NaNO_3$ + 51.5% $NH_4NO_3 \rightarrow NH_4H_2PO_4$	(IV)
31.2% $NaNO_3$ + 68.8% $NH_4NO_3 \rightarrow NH_4H_2PO_4$	(V)
78.5% NH_4NO_3 + 21.5% $NaNO_3 \rightarrow NH_4H_2PO_4$	(VI)
86.7% $NaNO_3$ + 13.3% $NH_4NO_3 \rightarrow NaH_2PO_4$	(VII)

The positions of the sections are shown (Fig. 1) in a horizontal projection for the system $NaNO_3-NH_4H_2PO_4-H_2O$. Each of these sections may be regarded as a polytherm for a ternary system consisting of a salt, water, and a complex component containing 2 salts in definite proportions. The individual results of investigations of the internal sections are given in the tables and diagrams for the quaternary system.

Diagrams for the ternary systems, and diagonal and internal sections for the quaternary systems [3-6] investigated by the visual polythermal method, can be used to plot isotherms for the quaternary systems for any temperatures within the range studied. We have plotted isotherms for + 30, + 20 and 0° and verified them by the isothermal method.

The polythermal and isothermal data are compared in Table 1 and in Figures 2, 3 and 4.

The isotherms for + 30, + 20 and 0°, on which the isohydric lines are shown (Figures 2, 3 and 4) contain four crystallization areas; $NaNO_3$, NH_4NO_3, $NH_4H_2PO_4$ and $NaH_2PO_4 \cdot 2H_2O$. The multiple points on the isotherms

TABLE 1

Curves: JM, FM, MN, BN, and DN of the Isotherms at 30, 20 and 0°

Points	Composition of solution (in moles per 100 moles of dry salts)					Method
	$NaNO_3$	NH_4NO_3	$NH_4H_2PO_4$	NaH_2PO_4	H_2O	
	Isotherm for +30°					
	Curve $NaH_2PO_4 \cdot 2H_2O + NaNO_3$					
J	58.8	—	—	41.2	479	Isothermal
	59.4	—	—	40.6	485	Polythermal
	$NaH_2PO_4 \cdot 2H_2O + NH_4H_2PO_4 + NaNO_3$					
M	43.3	—	17.8	38.9	378	Isothermal
	Curve *FM* $NH_4H_2PO_4 + NaH_2PO_4 \cdot 2H_2O$					
F	—	—	24.9	75.1	536	Isothermal
	—	—	24.9	75.1	536	Polythermal
	13.1	—	22.0	64.9	445	Isothermal
	25.0	—	22.1	52.9	456	Polythermal
	39.7	—	17.9	42.4	382	Isothermal
	$NH_4H_2PO_4 + NaNO_3 + NaH_2PO_4 \cdot 2H_2O$					
M	43.3	—	17.8	38.9	378	Isothermal
	Curve *MN* $NH_4H_2PO_4 + NaNO_3 + NaH_2PO_4 \cdot 2H_2O$					
M	43.3	—	17.8	38.9	378	Isothermal
	$NaNO_3 + NH_4H_2PO_4$					
	59.6	—	19.4	21.0	400	Isothermal
	77.7	—	22.3	—	408	Polythermal
	67.5	24.0	8.5	—	377	Polythermal
	64.1	30.3	5.6	—	336	Isothermal
	49.4	48.2	2.4	—	275	Isothermal
	47.5	50.6	1.9	—	255	Polythermal
	36.2	62.7	1.1	—	191	Isothermal
	$NH_4H_2PO_4 + NaNO_3 + NH_4NO_3$					
N	27.5	71.7	0.8	—	147	Isothermal
	Curve *BN* $NaNO_3 + NH_4NO_3$					
B	27.1	72.9	—	—	147	Polythermal
	$NH_4H_2PO_4 + NaNO_3 + NH_4NO_3$					
N	27.5	71.7	0.8	—	147	Isothermal
	Curve *DN* $NH_4H_2PO_4 + NH_4NO_3$					
D	—	98.8	1.2	—	192	Isothermal
	20.0	79.1	0.9	—	159	Isothermal
	21.1	77.3	1.6	—	161	Polythermal
	$NH_4H_2PO_4 + NH_4NO_3 + NaNO_3$					
N	27.5	71.7	0.8	—	147	Isothermal

TABLE 1 (continued)

Points	Composition of solution (in moles per 100 moles of dry salts)					Method
	$NaNO_3$	NH_4NO_3	$NH_4H_2PO_4$	NaH_2PO_4	H_2O	
			Isotherm for +20°			
			Curve *JM*			
			$NaNO_3 + NaH_2PO_4 \cdot 2H_2O$			
J	71.7	—	—	28.3	540	Isothermal
	71.0	—	—	29.0	542	Polythermal
	69.2	—	9.0	21.8	495	Isothermal
			$NaNO_3 + NaH_2PO_4 \cdot 2H_2O + NH_4H_2PO_4$			
M	63.4	—	18.5	18.1	446	Isothermal
			Curve FM			
			$NaH_2PO_4 \cdot 2H_2O + NH_4H_2PO_4$			
F	—	—	24.9	75.1	621	Polythermal
	8.0	—	22.9	69.1	566	Isothermal
	15.1	—	21.6	63.3	538	Isothermal
	25.0	—	22.0	53.0	553	Polythermal
	35.4	—	20.3	44.3	486	Isothermal
	61.2	—	18.5	20.3	447	Isothermal
			$NaNO_3 + NaH_2PO_4 \cdot 2H_2O + NH_4H_2PO_4$			
M	63.4	—	18.5	18.1	446	Isothermal
			Curve *MN*			
			$NaH_2PO_4 \cdot 2H_2O + NH_4H_2PO_4 + NaNO_3$			
M	63.4	—	18.5	18.1	446	Isothermal
			$NaNO_3 + NH_4H_2PO_4$			
	78.5	—	21.5	—	445	Polythermal
	67.9	24.1	8.0	—	408	Polythermal
	64.3	30.9	4.8	—	350	Isothermal
	49.0	48.9	2.1	—	267	Isothermal
	47.6	50.6	1.8	—	276	Polythermal
	39.6	59.2	1.2	—	212	Isothermal
	32.7	66.2	1.1	—	188	Isothermal
			$NaNO_3 + NH_4H_2PO_4 + NH_4NO_3$			
N	30.3	68.9	0.8	—	171	Isothermal

TABLE 1 (continued)

Points	Composition of solution (in moles per 100 moles of dry salts)					Method
	$NaNO_3$	NH_4NO_3	$NH_4H_2PO_4$	NaH_2PO_4	H_2O	
			Curve *BN*			
			$NaNO_3 + NH_4NO_3$			
B	30.4	69.6	—	—	178	Polythermal
			$NaNO_3 + NH_4H_2PO_4 + NH_4NO_3$			
N	30.3	68.9	0.8	—	171	Isothermal
			Curve *DN*			
			$NH_4NO_3 + NH_4H_2PO_4$			
D	—	98.7	1.3	—	236	Isothermal
	—	98.8	1.2	—	239	Polythermal
	4.8	94.0	1.2	—	226	Isothermal
	9.4	89.5	1.1	—	216	Isothermal
	17.4	81.6	1.0	—	199	Isothermal
	20.5	78.6	0.9	—	193	Isothermal
	21.2	77.1	1.7	—	207	Polythermal
	27.4	71.7	0.9	—	175	Isothermal
	29.8	69.4	0.8	—	172	Polythermal
			$NaNO_3 + NH_4H_2PO_4 + NH_4NO_3$			
N	30.3	68.9	0.8	—	171	Isothermal
	30.9	68.2	0.9	—	162	Polythermal
			Isotherm for 0° Curve *JM*			
			$NaNO_3 + NaH_2PO_4 \cdot 2H_2O$			
J	81.3	—	—	18.7	657	Isothermal
	81.4	—	—	18.6	667	Polythermal
	79.3	—	6.6	14.1	597	Isothermal
	70.4	10.6	—	19.0	590	Polythermal
			$NaNO_3 + NH_4H_2PO_4 + NaH_2PO_4 \cdot 2H_2O$			
M	79.5	—	20.1	0.4	558	Isothermal

TABLE 1 (continued)

Points	Composition of solution (in moles per 100 moles of dry salts)					Method
	$NaNO_3$	NH_4NO_3	$NH_4H_2PO_4$	NaH_2PO_4	H_2O	
			Curve *FM*			
			$NaH_2PO_4 \cdot 2H_2O + NH_4H_2PO_4$			
F	—	—	24.1	75.9	937	Isothermal
	—	—	24.3	75.7	931	Polythermal
	21.3	—	23.0	55.7	852	Isothermal
	25.2	—	21.5	53.3	825	Polythermal
	44.3	—	21.4	34.3	733	Isothermal
	59.2	—	20.6	20.2	692	Isothermal
			$NaNO_3 + NH_4H_2PO_4 + NaH_2PO_4 \cdot 2H_2O$			
M	79.5	—	20.1	0.4	558	Isothermal
			Curve *MN*			
			$NaNO_3 + NH_4H_2PO_4 + NaH_2PO_4 \cdot 2H_2O$			
M	79.5	—	20.1	0.4	558	Isothermal
			$NaNO_3 + NH_4H_2PO_4$			
	80.4	—	19.6	—	539	Polythermal
	71.3	21.1	7.6	—	483	Isothermal
	68.8	24.4	6.8	—	477	Polythermal
	59.6	37.0	3.4	—	420	Isothermal
	51.1	46.9	2.0	—	341	Isothermal
	47.8	50.8	1.4	—	321	Polythermal
	43.1	55.7	1.2	—	287	Isothermal
			$NaNO_3 + NH_4H_2PO_4 + NH_4NO_3$			
N	37.9	61.2	0.9	—	255	Isothermal
			Curve *BN*			
			$NaNO_3 + NH_4NO_3$			
B	37.4	62.6	—	—	265	Polythermal
			$NaNO_3 + NH_4H_2PO_4 + NH_4NO_3$			
N	37.9	61.2	0.9	—	255	Isothermal
			Curve *DN*			
			$NH_4H_2PO_4 + NH_4NO_3$			
D	—	98.1	1.9	—	395	Isothermal
	—	98.0	2.0	—	402	Polythermal
	12.3	86.1	1.6	—	338	Isothermal
	21.2	77.3	1.5	—	326	Polythermal
	27.4	71.4	1.2	—	292	Isothermal
	30.8	68.0	1.2	—	289	Polythermal
	34.4	64.5	1.1	—	264	Isothermal
			$NaNO_3 + NH_4H_2PO_4 + NH_4NO_3$			
N	37.9	61.2	0.9	—	255	Isothermal

TABLE 2

Multiple Points for the Reciprocal System $NaNO_3-NH_4H_2PO_4-H_2O$

Points	Composition of solution (in moles per 100 moles of dry salts)					Solid phases	Method
	$NaNO_3$	NH_4NO_3	$NH_4H_2PO_4$	NaH_2PO_4	H_2O		
	Isotherm for +30°						
A	100.0	—	—	—	490	$NaNO_3$	Polythermal
B	27.1	72.9	—	—	147	$NaNO_3 + NH_4NO_3$	
C	—	100.0	—	—	186	NH_4NO_3	
D	—	98.8	1.2	—	192	$NH_4NO_3 + NH_4H_2PO_4$	Isothermal
E	—	—	100.0	—	1477	$NH_4H_2PO_4$	
F	—	—	24.9	75.1	536	$NH_4H_2PO_4 + NaH_2PO_4 \cdot 2H_2O$	
F	—	—	24.9	75.1	536	$NH_4H_2PO_4 + NaH_2PO_4 \cdot 2H_2O$	Polythermal
H	—	—	—	100.0	628	$NaH_2PO_4 \cdot 2H_2O$	
J	58.8	—	—	41.2	479	$NaH_2PO_4 \cdot 2H_2O + NaNO_3$	Isothermal
J	59.4	—	—	40.6	485	$NaH_2PO_4 \cdot 2H_2O + NaNO_3$	Polythermal
M	43.3	—	17.8	38.9	378	$NH_4H_2PO_4 + NaNO_3 + NaH_2PO_4 \cdot 2H_2O$	Isothermal
N	27.5	71.7	0.8	—	147	$NH_4H_2PO_4 + NaNO_3 + NH_4NO_3$	Isothermal
	Isotherm for +20°						
A	100.0	—	—	—	555	$NaNO_3$	Polythermal
B	30.4	69.6	—	—	178	$NaNO_3 + NH_4NO_3$	
C	—	100.0	—	—	277	NH_4NO_3	
D	—	98.7	1.3	—	236	$NH_4NO_3 + NH_4H_2PO_4$	Isothermal
D *	—	98.8	1.2	—	239	$NH_4NO_3 + NH_4H_2PO_4$	
E	—	—	100.0	—	1824	$NH_4H_2PO_4$	Polythermal
F	—	—	24.9	75.1	621	$NaH_2PO_4 \cdot 2H_2O + NH_4H_2PO_4$	
H	—	—	—	100.0	789	$NaH_2PO_4 \cdot 2H_2O$	
J	71.7	—	—	28.3	540	$NaNO_3 + NaH_2PO_4 \cdot 2H_2O$	Isothermal
J	71.0	—	—	29.0	542	$NaNO_3 + NaH_2PO_4 \cdot 2H_2O$	Polythermal
M	63·4	—	18.5	18.1	446	$NaNO_3 + NaH_2PO_4 \cdot 2H_2O + NH_4H_2PO_4$	Isothermal
N	30.3	68.9	0.8	—	171	$NaNO_3 + NH_4H_2PO_4 + NH_4NO_3$	
	Isotherm for 0°						
A	100.0	—	—	—	654	$NaNO_3$	Polythermal
B	37.4	62.6	—	—	265	$NaNO_3 + NH_4NO_3$	
C	—	100.0	—	—	385	NH_4NO_3	
D	—	98.1	1.9	—	395	$NH_4H_2PO_4 + NH_4NO_3$	Isothermal
D *	—	98.0	2.0	—	402	$NH_4H_2PO_4 + NH_4NO_3$	Polythermal
E	—	—	100.0	—	2833	$NH_4H_2PO_4$	Isothermal
F	—	—	24.1	75.9	937	$NaH_2PO_4 \cdot 2H_2O + NH_4H_2PO_4$	
F	—	—	24.3	75.7	931	$NaH_2PO_4 \cdot 2H_2O + NH_4H_2PO_4$	Polythermal
H	—	—	—	100.0	1150	$NaH_2PO_4 \cdot 2H_2O$	
J	81.3	—	—	18.7	657	$NaNO_3 + NaH_2PO_4 \cdot 2H_2O$	Isothermal
J	81.4	—	—	18.6	667	$NaNO_3 + NaH_2PO_4 \cdot 2H_2O$	Polythermal
M	79.5	—	20.1	0.4	558	$NaNO_3 + NH_4H_2PO_4 + NaH_2PO_4 \cdot 2H_2O$	Isothermal
N	37.9	61.2	0.9	—	255	$NaNO_3 + NH_4H_2PO_4 + NH_4NO_3$	

*Polythermal data of Bergman and Bochkarev [7].

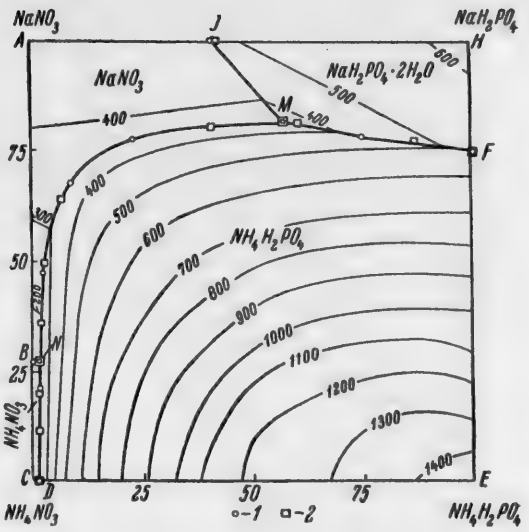

Fig. 2. Isotherm for + 30°. Data: 1) Polythermal, 2) isothermal.

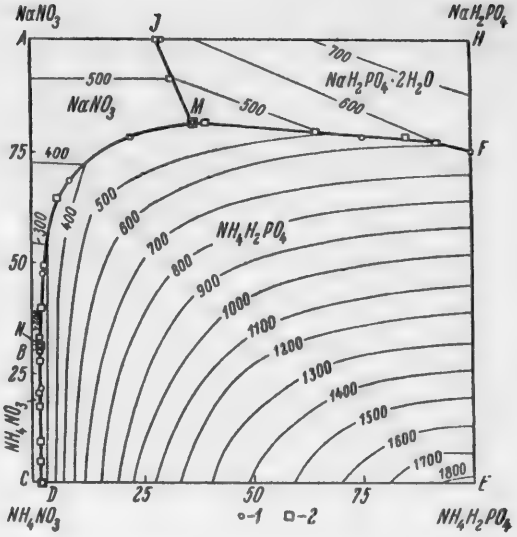

Fig. 3. Isotherm for + 20°. Data: 1) Polythermal, 2) isothermal.

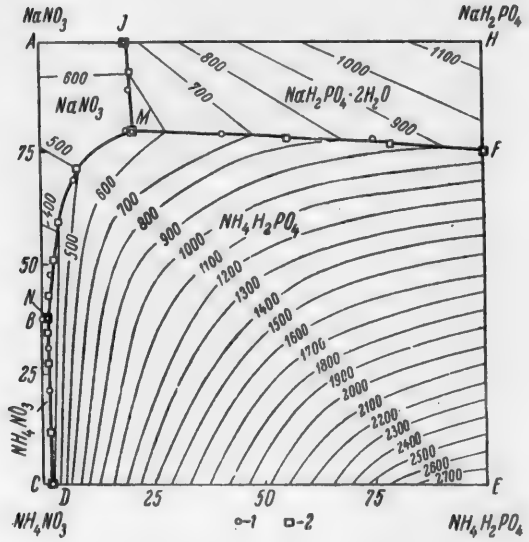

Fig. 4. Isotherm for 0°. Data: 1) Polythermal, 2) isothermal.

correspond to the following combinations of three saturation solid phases:

$$M — NH_4H_2PO_4 + NaNO_3 + NaH_2PO_4 \cdot 2H_2O$$
$$N — NH_4H_2PO_4 + NaNO_3 + NH_4NO_3.$$

A comparison of the isotherms in the temperature range from + 30° to 0° shows that the composition of the solution at the Point M, which is at a considerable distance to the right of the $NaNO_3$—$NH_4H_2PO_4$ diagonal at 30°, approaches this diagonal with decrease of temperature and lies upon it at 0°. Thus, 0° represents a transition of the Point M from a congruent to an incongruent point. Consequently, the crystallization area of monosodium phosphate increases with decrease of temperature, while the sodium nitrate area correspondingly decreases. The composition of the solution corresponding to the Point N changes little with decrease of temperature. The compositions of the solutions at the multiple points of the isotherms for + 30, + 20 and 0° are given in Table 2.

SUMMARY

1. Polythermal data for ternary systems, data for the diagonal and internal sections of the reciprocal aqueous system ammonium monophosphate—sodium nitrate—water, and results obtained in special isothermal investigations, have been used to plot isotherms for + 30, + 20 and 0°.

2. It is shown that no double salts or solid solutions are formed in the system.

3. The isotherms for the system between + 30 and 0° have four crystallization fields: $NaH_2PO_4 \cdot 2H_2O$;

$NaNO_3$; $NH_4H_2PO_4$ and NH_4NO_3, and two multiple points with three salts in the solid phase: M) $NH_4H_2PO_4$ + + $NaH_2PO_4 \cdot 2H_2O$ + $NaNO_3$; N) $NaNO_3$ + NH_4NO_3 + $NH_4H_2PO_4$.

LITERATURE CITED

[1] S. I. Volfkovich, A. P. Belopolsky and A. I. Loginova, Bull. Acad. Sci. USSR, Chem. Ser. 5 (1940).

[2] S. Ya. Shpunt, J. Appl. Chem. 20, 3 (1957).

[3] S. Ya. Shpunt, J. Appl. Chem. 13, 1, 9-18 (1940).

[4] S. Ya. Shpunt, J. Appl. Chem. 13, 1, 19-28 (1940).

[5] S. Ya. Shpunt, J. Appl. Chem. 19, 3, 293 (1946).

[6] S. Ya. Shpunt, J. Appl. Chem. 20, 7, 685 (1947).

[7] A. G. Bergman and P. F. Bochkarev, Bull. Acad. Sci. USSR, Chem. Ser. 1, 248 (1938).

Received October 12, 1955

REMOVAL OF SCALE FROM STEELS AT ELEVATED TEMPERATURES

B. S. Krasikov and B. I. Lavrentyev

Solutions of acids with added inhibitors of acid corrosion [1-3], mostly of organic origin, are now widely used for pickling of steels in order to remove scale. However, a defect common to this type of inhibitors is the sharp decrease of their protective action when the solution temperature is raised to 50° and over, which is a consequence of the adsorptive mode of action of the inhibitors [1, 4] (surface-active substances).

It is to be expected, on the basis of the electrochemical theory of solution of metals in acids [5, 6], that contact deposition of metals with high hydrogen overvoltages on the steel surface should result in a sharp decrease of the rate of hydrogen discharge on the metal and thereby retard dissolution of the metal (iron) [7].

It has been reported in the literature [8, 9] that contact deposition of lead and tin may be used for protection of iron in pickling; moreover, an electrochemical (cathodic) method of scale removal, in which the steel is protected by electrodeposited coatings of tin or lead [1], has been used in practice. However, this method is not used very extensively.

With high outputs, it becomes necessary to accelerate descaling processes, primarily by a further increase of temperature to 65-70°, in order to raise the production rate without the use of additional equipment. This problem can be solved sucessfully if additives capable of reducing the dissolution of iron at these temperatures can be found.

A study has been made of the temperature range in which "ChM" additive is effective in the pickling of various steels, in order to compare the effectiveness of this additive with the inhibiting action of coatings of various metals formed by contact deposition. It was assumed that retardation of hydrogen ion discharge will be primarily determined by the continuity of the metal coating, and much less so by its thickness.

EXPERIMENTAL

The method used was extremely simple; steel specimens of known weight were placed in the pickling liquor, extracted after a certain time, dried, and weighed. Specimens covered with a continuous layer of scale were made by the action of heat in a muffle furnace at 900° for an hour. The clean metal specimens were made from steel rods by mechanical cleaning. Different types of steel (Table 1) were studied; by their contents, they belonged to UI-10A and 10-60 steel grades.

The beakers containing the pickling liquor were kept at constant temperature to within ± 0.5°; the liquor consisted of 15% H_2SO_4 (pure, and with various additives).

RESULTS AND DISCUSSION

The results obtained in determination of the rate of scale removal from steel U6A are given in Figure 1 and Table.2.

The graph shows that the rate of scale removal at a given temperature is practically independent of the presence of additives in the solution; this indicates that the additives, regardless of their nature, are adsorbed or deposited only on the clean metal, free from scale.

TABLE 1

Compositions of Different Steels

Alloying additions (%)						Steel grades
C	Mn	Si	ΣP, S	Ni	Cr	
0.11	0.29	0.29	0.03	0.20	0.21	U1A
0.44	0.31	0.26	0.03	0.18	0.20	U4A
0.53	0.27	0.30	0.026	0.23	0.23	U5A
0.64	0.29	0.24	0.03	0.20	0.24	U6A
0.72	0.29	0.29	0.027	0.18	0.20	U7A
0.80	0.33	0.31	0.03	0.19	0.21	U8A
0.90	0.30	0.26	0.03	0.20	0.22	U9A
1.03	0.28	0.29	0.03	0.23	0.19	U10A
0.12	0.78	0.28	0.062	0.33	0.29	10
0.42	0.76	0.24	0.069	0.34	0.34	40
0.50	0.82	0.24	0.070	0.31	0.33	50
0.63	0.80	0.27	0.064	0.31	0.29	60

TABLE 2

Effect of Solution Temperature on the Rate of Scale Removal from U6A Steel

Solution	Time for removal of scale (min) at solution temperature (°C)						
	15	25	35	45	55	65	70
15%- H_2SO_4	82	49	28	24	15	10	9
15%- H_2SO_4+4 g/l "ChM".	86	50	25	20	16	10	8
15%- H_2SO_4 + 0.5 g/l $SnSO_4$	84	49	27	22	16	10	8

Data on the rates of scale removal at various temperatures, determined from the inflection points of curves similar to those shown in Figure 1, are summarized in Table 2. It follows from these results that increase of temperature from 45 to 70° produced approximately a threefold increase in the rate of scale removal.

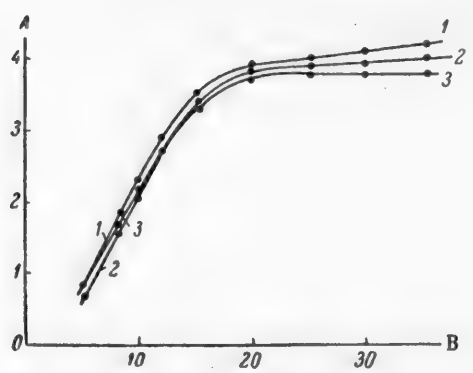

Fig. 1. Rate of removal of scale from U6A steel at 55°. A) $(\Delta m)/m \cdot 100\%$, B) time (min). Pickling in solutions of: 1) 15% H_2SO_4, 2) 15% H_2SO_4 + 4 g "ChM" per liter, 3) 15% H_2SO_4 + 0.5 g $SnSO_4$/liter.

The protective action of an additive is usually represented by the formula [3]:

$$Z = \frac{\rho_0 - \rho}{\rho_0} \cdot 100\%.$$

The results of experiments on the pickling of U6A steel in 15% H_2SO_4 with various additives are summarized in Table 3.

These results show that the protective action of "ChM" decreases sharply with rise of temperature, whereas the protective action of metal coatings formed by contact deposition changes very little with the temperature. It also follows from these results that a coating of tin formed by contact deposition has the best protective action, and the subsequent experiments were therefore carried out with additions of salts of this metal only.

TABLE 3

Protective Action of Various Additives at Different Temperatures (Steel U6A)

Solution	Protective action (in %) at solution temperature (°C)						
	15	25	35	45	55	65	70
14% H_2SO_4 + 4 g "ChM" per liter	87	83	79	72	56	30	12
15% H_2SO_4 + 0.5 g $CuSO_4$ per liter	19	24	21	28	23	26	28
15% H_2SO_4 + 0.5 g $PbSO_4$ per liter	78	72	69	64	50	39	33
15% H_2SO_4 + 0.5 g $SnSO_4$ per liter	93	95	93	92	88	87	88

The protective action of tin in solutions with different contents of $SnSO_4$ was studied. It was found that dense films of tin are deposited on steels when the tin concentration in the solution is 0.01 g/liter (Table 4) and over; it follows that it is possible to use H_2SO_4 solutions with added tin until the tin contents are completely exhausted.

TABLE 4

Effect of $SnSO_4$ Concentration in 15% H_2SO_4 Solution on the Protective Action of Tin

Temperature (in °C)	Protective action (in %) at $SnSO_4$ concentrations (in g/liter):					
	0.5	0.2	0.1	0.05	0.02	0.01
25	95	95	96	94	93	93
45	92	94	94	91	91	92
65	87	86	88	86	86	82

TABLE 5

Protective Action of a Pickling Liquor During Prolonged Use at 65° Original Solution: 15% H_2SO_4 + 0.5 g/liter $SnSO_4$; Volume 250 ml Each Batch of Metal Treated for 12 Minutes

Solution No.	Protective action (in %) for different areas of metal (in dm^2) passed through the solution						
	12	24	48	72	84	96	108
1	87	86	87	84	86	39	21
2	86	87	85	86	84	80	26
3	87	85	88	85	86	79	22

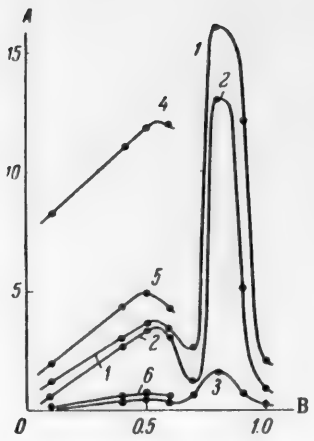

Fig. 2. Losses of metal in the pickling of different steels at 65°. A) $(\Delta m)/m \cdot 100\%$, B) C content of steel (%). Pickling in solutions of: 1 and 4) 15% H_2SO_4, 2 and 5) 15% H_2SO_4 + 4g "ChM" per liter, 3 and 6) 15% H_2SO_4 + 0.5 g $SnSO_4$ per liter. Curves: 1, 2, 3) UI-10A Steel; 4, 5, 6) 10-60 Steel.

Experiments on this were carried out, and the results are given in Table 5. It is seen that the protective action of the tin first remains without change as the amount of metal passed through the solution increases, and then falls sharply. The thickness of the contact deposit of tin can be calculated from the total surface area of the specimens passed through the solution; according to our data, this film is not greater than 0.01 micron thick (the tin consumption is 0.05-0.07 g per 1 m^2 of metal surface).

It was also found that accumulation of $FeSO_4$ in the solution has no influence on the protective action of tin (up to 90 g of iron, calculated as the metal, per liter).

Interesting results were obtained in experiments on the dissolution of various steels in presence of "ChM" additive and $SnSO_4$ in 15% H_2SO_4 solution. For comparison, the results obtained in pure 15% H_2SO_4 are also given (Fig. 2). All the experiments were carried out at 65°, with exposure times of 1 hour. From these results a number of conclusions can be drawn both concerning the nature of the protective action of additives, and concernint the mechanism of dissolution of steels.

The sharp increase in the dissolution rates of U8A and U9A steels as compared with other steels is noteworthy. This may be explained by the differences in the crystalline structure of the steels; it is known [10] that this changes from a ferrite structure (0.8% C) to a pearlite structure (0.82% C) and then to a cementite structure (0.82% C)*; if changes in the steel microstructure as the result of tempering at 900° (when the specimens were coated with the layer of scale) are also taken into account, it appears that adsorptional differences of the different microcrystalline structures [11], together with the appreciably varying rates of pickling of the annealed steels, lead to the effect described above.

Special metallographic investigations were not carried out but nevertheless it may be suggested that because of the lowest density of the films (formed both by contact deposition, and by adsorption) on pearlite steel, in conjunction with the troostite structure of the tempered specimens, very sharp increases of the rate of attack on certain steels (U8A and U9A) are possible.

The greater adsorption of the additives on ferrite and cementite steels, in conjunction with the martensitic (or sorbitic) structure of the tempered specimens, makes some of the specimens studied relatively resistant to sulfuric acid.

The films formed on the steel surface by adsorption or by contact deposition affect only the absolute dissolution rates of the steel specimens, while the form of the dissolution rate – steel composition curves will be largely determined by the microcrystalline structure of the steel.

Increased manganese contents in the steel raise the dissolution rate of the iron considerably. Within the limits of a single crystalline structure of the steels (0.1-0.5% C) the dissolution rate of iron increases approximately linearly with increasing carbon content.

Changes in the microcrystalline structure of the steels should primarily affect the rate of the anodic process (ionization of iron); differences of bonding energy between the atoms in different crystalline structures determine the amounts of energy required to break down the bonds in these structures. The parallel course of the curves for the variation of the dissolution rate with carbon content in presence of "ChM" additive (Fig. 2, Curve 2) and in pure H_2SO_4 (Fig. 2, Curve 1) indicates that the anodic and cathodic processes are retarded to about the same extent by the additive; this is in harmony with other published results [12]. Addition of tin salts produces a different effect; here a leveling of the rates of attack on steels of different structures is clearly seen, i. e., the anodic process is no longer the determining factor. From the high values of hydrogen overvoltage on tin, and

*Possibly 0.89% C – Publisher's note.

from the data in Figure 2 (Curve 3) it may be concluded that formation of tin coatings greatly retards the discharge of hydrogen ions and also partly creates purely mechanical obstacles to the passage of iron ions into solution.

These experiments showed that protection of iron with tin has a number of advantages: 1) the inhibiting effect of a tin film formed by contact deposition is greater at 70° than that of "ChM" additive at 35°; 2) the carbon content of steels has considerably less influence if tin is used; 3) if tin is used, the risk of hydrogen accumulation in steel is diminished at 65-70° (with short pickling times); 4) with the use of tin it is easy to control the pickling time by the almost complete cessation of hydrogen evolution after complete removal of the scale.

The tin films can be removed from steel articles either by treatment with hot (95-100°) 10-20% NaOH solution, or by contact deposition of copper on the tinned steel articles. A solution of 15-20 g/liter of $CuSO_4 \cdot 5H_2O$ in 15% H_2SO_4 is used for this purpose. The tin is then dissolved in the form of $SnSO_4$. This method is particularly suited for wire and cable factories, where contact deposits of copper on tin are used as "lubricant" in drawing the wire. The tin is completely recovered and recycled. The copper content of the solution used for deposition can be taken down to 0.03-0.05 g/liter, when the last traces of copper are removed by addition of the appropriate amount of finely divided metallic tin and the solution of $SnSO_4$ in 15% H_2SO_4 is used for adding to pure 15% H_2SO_4 in the pickling liquor.

LITERATURE CITED

[1] V. I. Lainer and N. T. Kudryavtsev, Fundamentals of Electroplating, 1 (Metallurgy Press, 1953).*

[2] D. V. Stepanov and A. A. Timokhin, Metal Industry Herald 1, 2 (1934).

[3] S. A. Balezin, V. P. Barannik and P. N. Putilova, Use of Inhibitors of Acid Corrosion (Metallurgy Press, 1948).*

[4] M. A. Loshkarev, A. A. Krivtsov and A. A. Kriukova, J. Phys. Chem. 23, 221 (1949).

[5] A. I. Shultin, J. Phys. Chem. 18, 61 (1944).

[6] Ya. V. Durdin, Sci. Mem. Leningrad State Univ., Ser. Chem. Sci. 3, 4 (1939).

[7] A. N. Frumkin, V. S. Bagotskii, Z. A. Iofa and B. N. Kabanov, Kinetics of Electrode Processes (Izd. MGU, 1952).

[8] C. P. Watts, Traus. Electroch. Soc., 67, 259 (1937).

[9] V. O. Krenig and E. M. Zaretsky, Corrosion and Its Prevention 6, 4, 16 (1940).

[10] A. P. Gulyaev, Metallography (Defense Press, 1948).*

[11] S. P. Makaryeva, J. Phys. Chem. 17, 160 (1943); N. T. Kudryavtseva and B. V. Ershler, Proc. Acad. Sci. USSR 72, 363 (1950).

[12] V. A. Kuznetsov and Z. A. Iofa, J. Phys. Chem. 21, 2 (1947).

Received October 27, 1955

*In Russian.

THE CORROSION STABILITY OF GALVANIC FILMS DEPOSITED ON A PASSIVATED SURFACE

L. I. Kadaner and A. Kh. Masik

In a series of papers we have published previously [1-6], and in subsequent papers by Belyaev [7, 8], Khersonskii, Lyashchenko and Stepanova [9], Rosental [10], etc., it has been shown that preliminary passivation favors an appreciable decrease in porosity, and leads to an increase in the stability of the link between the galvanic film and the metal base.

During an investigation of the favorable influence of passivation, we established, by using the crystal count method [11], that preliminary passivation increases the homogeneity of the plated surface. Iron and copper samples which had been preliminary passivated or had been left unpassivated were plated under identical conditions in an acid tinning electrolyte, free from surface active materials and colloids, in order to give a better definition of the individual crystals. The iron was passivized by immersion for 30 seconds in concentrated nitric acid (s. p. 1.36) at 4-8°. Copper was passivated in a solution containing 10% of potassium dichromate and 2% sulfuric acid at 45°. In the case of both the copper and iron samples which had been passivated under the same electrolysis conditions, there was formed a considerably larger number of crystals than in the unpassivated samples (Figures 1 and 2) this testifies to the greater homogeneity of the passivated surface.

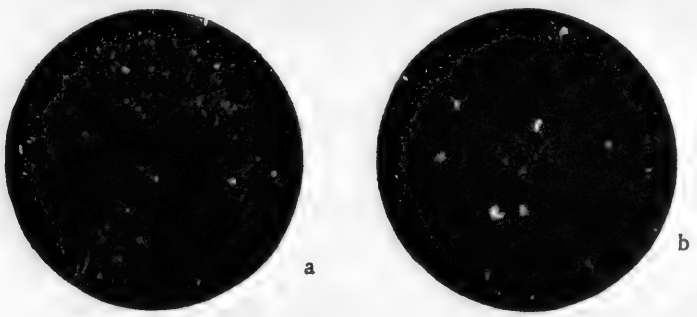

Fig. 1. Electrolytic tin deposits. a) On passivated iron; b) on unpassivated iron.

The greater homogeneity of the passivated surface favors the formation of more highly dispersed, less porous films.

In an earlier paper, we suggested that the passive film is completely reduced at the beginning of the electrolysis [12]. Special tests showed that the passive film is actually reduced, but, it is not completely reduced. Thus, the potential of passivated iron samples, on which zinc has been deposited in an acid electrolyte, and which has been subsequently removed by a two-hour treatment with boiling 10% sodium hydroxide, remained 0.12-0.16 volt more positive than that of unpassivated samples subjected to the same treatment. During electrodeposition of zinc in an alkaline electrolyte, the oxide film was reduced to a lesser extent; the potential of passivated samples on which zinc had been deposited in an alkaline medium, followed by complete removal, remained 0.18-0.22 volts more positive than unpassivated samples treated identically.

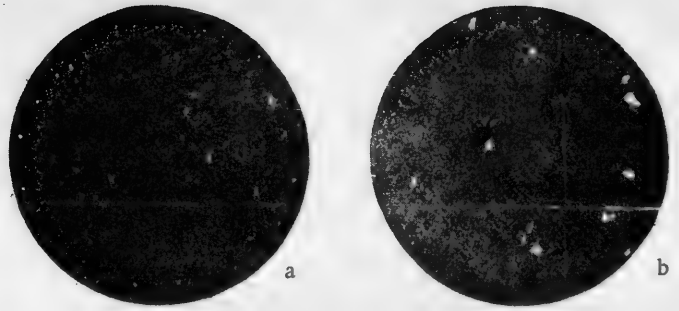

Fig. 2. Electrolytic tin deposits. a) On passivated copper; b) on unpassivated copper.

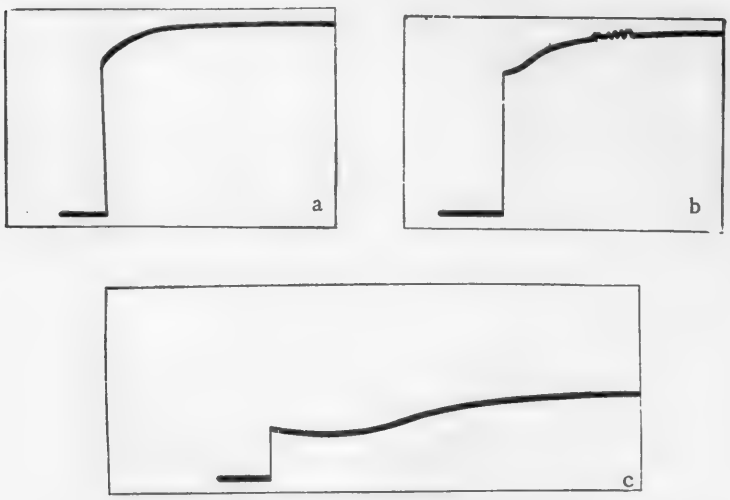

Fig. 3. Oscillograms for potential change with time during electrolytic deposition of tin in an acid electrolyte. a) Unpassivated iron, $D_{cathode}$ = = 1 ampere/dm^2; b) passivated iron, $D_{cathode}$ = 1 ampere/dm^2; c) passivated iron, $D_{cathode}$ = 0.2 ampere/dm^2.

Control tests showed that during treatment of passivated and unpassivated samples in 10% sodium hydroxide solution, a difference in potential of the order of 0.17-0.20 volt was maintained between passivated and unpassivated samples.

That the passive film is only partly reduced, can be seen from a consideration of the oscillograms illustrating the change in potential with time in the initial stages of electrolysis. During deposition of tin on unpassivated iron (Fig. 3a), the cathode potential at the point where the current is switched on becomes immediately more negative, and subsequently shifts to more negative values, as the result of concentration polarization, caused by deposition of tin on the cathode surface, leading accordingly, to a decrease in Sn^{++} concentration in the

neighborhood of the cathode. During deposition of tin on passivated surfaces, there is observed a retardation in potential growth (the practically horizontal part of the curve), which is the result of the fact that on switching on the current, reduction of the oxide film occurs first, and only when this has finished does the tin start to be deposited. Naturally, at higher current densities, reduction of the passive film proceeds at a faster rate. Accordingly, at current densities of 1 ampere/dm^2 (Fig. 3b) the duration of the retardation of potential change is one fifth to one sixth that when the current density is 0.2 ampere/dm^2 (Fig. 3c).

The metal crystals are precipitated apparently, only on those parts where the passive film has been reduced; on the other parts of the surface, in the pores, the passive film is preserved until the end of the electrolysis, and this favors screening of the unplated parts by the growing deposit. The effect of the pores was discovered on measuring the potentials of samples covered with a zinc deposit 0.5 microns thick. The potential of the passivated zinc plated samples, as a result of the passive film still left in the pores, proved to be 0.1-0.2 volt more positive than the potential of unpassivated zinc plated samples.

The conservation of the passive film on the unplated parts is also indicated by the following fact. Tin was deposited in the course of 2-3 seconds in an acid electrolyte on passivated and unpassivated iron samples, using a current density of 2 amperes/dm^2, this corresponds to a mean thickness of the deposit of 0.04 microns. Naturally, with such a "thickness", the tin layer was far from being continuous. These samples were kept for 14 months in a hot chamber, after which the surface of the unpassivized samples was covered with a continuous layer of rust, while the surface of the passivated samples remained completely untarnished.

Experiments which we carried out with the aid of radioactive S^{35} also demonstrated that the film is not completely reduced. Unfortunately, we were unable to use the radioactive isotopes of oxygen, which have a very short half-life period. Accordingly, we used sulfide films as the object of our work. It is known that preliminary treatment of gold in an aqueous-alcohol solution of the alkali metal sulfides ensures stable combination of the electrolytic copper deposits with the gold.

Gold plates were immersed for 20 seconds in an aqueous-alcohol solution of sodium sulfide, prepared from sulfur containing the radioactive isotope S^{35}, the plates were then carefully washed in a stream of water and dried, the radioactivity of the same was then measured on a type "B" counter. An impulse count (after subtraction of the background) indicated 365 impulses/minute. Copper was then deposited in the course of 10 seconds on plates treated in this way, from an acid electrolyte at a current density of 1.5 amperes/dm^2. After the electrolysis, the radioactivity of the samples decreased appreciably, the count rate was down to 145 impulses/minute, indicating partial removal of the film.

Thus, during passivation in solutions of an oxidizing agent, a greater degree of homogeneity is attained than during normal preparation — etching and pickling. When the current is switched on, the film is partly reduced; under such conditions there is obtained a larger number of active parts as compared with normal preparation methods. As a result there is formed a large number of fine crystals, and this leads to a more complete coverage of the surface of the metal base. In fact, the surface of combination of the basic metal with its coat proves to be greater. As a result there is attained a smaller porosity and greater stability of the coupling with the base metal. The lower porosity of the coating, together with the maintenance of the film on the uncoated parts, should ensure enhanced corrosion resistance.

Doubt, however, has arisen as to how essential is the effect of passivation on corrosion resistance. It might be assumed that the porosity of the coatings deposited on steel surfaces prepared as usual, and on passivated steel surfaces, is the same, and that it simply does not show up completely when the coating deposited on the passivated surface is tested, since the passive film left on the uncovered parts (pores) prevents manifestation of the pores during the short time of the action of reagent. During a more prolonged period of the action of corrosion agents, as a result of the reduction of the passive film, the corrosion resistance of the passivated and unpassivated samples.

In order to establish the effect of passivation on corrosion resistance, we tested both cathodic and anodic coatings, on iron.

Corrosion of Cathodic Coatings. Test materials were nickel, tin, and copper coatings on iron.

Electrolytes of the following composition were used for plating (in g/liter): 1) $SnSO_4$ 30, H_2SO_4 90, cresol 8, carpenter's glue 2; current density $D_{cathode}$ = 1 ampere/dm^2; 2) $NiSO_4 \cdot 7H_2O$ 180, $Na_2SO_4 \cdot 10H_2O$ 40,

$MgSO_4 \cdot 7H_2O$ 45, H_3BO_3 20, NaCl 7; current density $D_{cathode}$ = 0.8 amperes/dm^2; 3) $CuSO_4 \cdot 5H_2O$ 200, H_2SO_4 50; current density $D_{cathode}$ = 1 ampere/dm^2.

The iron was passivated in concentrated nitric acid (s. g. 1.36) at 4-8°.

The corrosion resistance of the nickel and tin coatings were evaluated by external appearances, and also, in addition to this, on the basis of corrosion attacks — seats of corrosion. The stability of the copper coatings was evaluated by the loss in weight of the sample.

The tinned iron samples with a coating thickness of 3 microns were tested over a period of 80 days in a desiccator over 3% sodium chloride solution at a temperature of 22-26°. In addition, samples with coating thicknesses of 3, 5 and 10 microns were tested by immersion for 13 hours in an 8% solution of sodium chloride at 18-20°. In all cases, during the whole period of the test, the preliminarily passivated and unpassivated samples were kept under absolutely identical conditions.

TABLE 1

Number of Corrosion Spots on Tinned Iron After Immersion in 8% Sodium Chloride Solution

Thickness of the tin layer (in microns)	Number of corrosion pits per 100 cm^2	
	passivated iron	unpassivated iron
3	5	60
5	4	48
10	0	15

Assessment of corrosion attacks showed considerably higher corrosion stability in the case of the samples passivated beforehand. The number of corrosion spots on the passivated samples after testing in 8% sodium chloride solution was 10-12 times less than the number on the unpassivated samples (Table 1).

As can be seen from the photograph, the outward appearance of the tinned samples which had been preliminarily passivated, and were tested in a desiccator over the solution (Fig. 4), and also of similar samples tested by immersion in NaCl solution, was much better than that of unpassivated samples.

Nickel coated iron samples with a thickness of 3 and 5 μ of nickel, were tested by immersion for 18.5 hours in an 8% solution of sodium chloride. In addition, nickel coated samples with coating thicknesses of 3, 5, and 10μ were tested in the course of 85 days in the open air under a shelter (in order to avoid the direct action of atmospheric deposits), the temperature variations during this time were from 0 to +28°.

TABLE 2

Number of Corrosion Pits on Nickel Coated Iron After Immersion for 18.5 hours in 8% NaCl Solution

Thickness of the nickel layer (in μ)	Number of corrosion pits per 100 cm^2	
	passivated iron	unpassivated iron
3	136	240
5	32	147

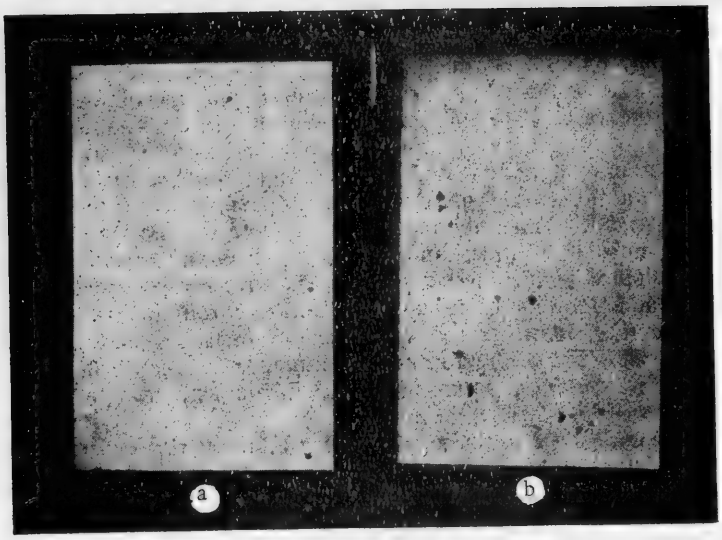

Fig. 4. Tinned samples after 80 days in a desiccator over a 3% NaCl solution. a) Passivated; b) unpassivated.

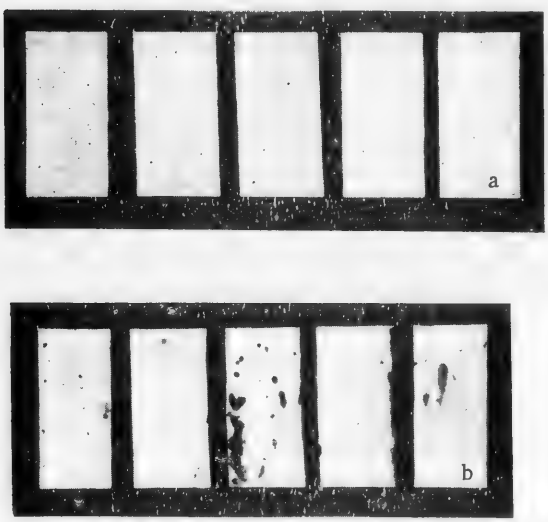

Fig. 5. Tinned samples after 13 hours immersion in an 8% NaCl solution. Thickness of tin layer 3μ. a) Passivated; b) unpassivated.

Assessment of corrosion attacks showed appreciably less differences between passivated and unpassivated samples as compared with the tinned iron. All the same, the number of corrosion pits on the passivated samples was 2-4.5 times less (Table 2).

With respect to external appearances, the nickel plated samples which had been passivated beforehand, after testing by immersion in an 8% sodium chloride solution, also differed from the unpassivated samples to a lesser extent than the tinned samples (Figs. 6 and 7), this corresponds to the comparative results on porosity we obtained earlier. Passivated nickel samples and unpassivated samples tested in the open, were found to differ even less from each other (Fig. 8), although the differences were very appreciable.

Copper coated iron samples, in which the thickness of the copper layer was 3 μ, were tested by immersion for 24 hours in 3% sulfuric acid. Losses in weight of samples passivated beforehand (0.0084 g) were 20% less than than in the case of unpassivated samples (0.0105 g). The losses in weight decreased to an even greater extent (0.0063 g), when, after passivation, the samples were coated in the course of 8 seconds in an acid copper electrolyte, containing 8 g/liter of carpenter's glue, after which, coating with copper was finished in the usual acid electrolyte.

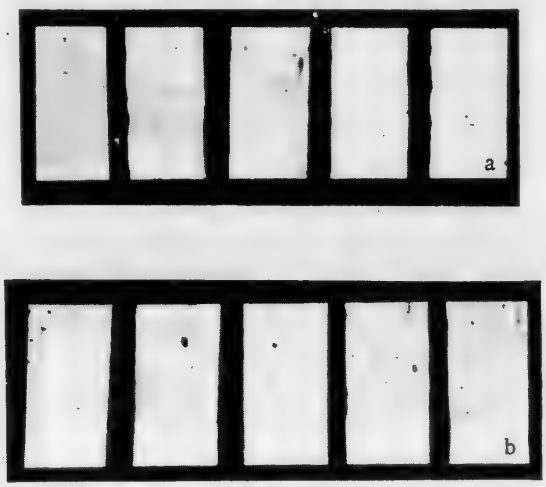

Fig. 6. Nickel plated samples after immersion for 18.5 hours in 8% NaCl solution. Thickness of nickel layer 3 μ. a) Passivated; b) unpassivated.

Corrosion of Anodic Coatings. The test objects in this case were zinc and tin coatings (the tin coatings were anodic with respect to iron in a series of organic acids).

Electrolytes of the following composition were used for zinc plating (in g/liter): $ZnSO_4 \cdot 7H_2O$ 215, $Na_2SO_4 \cdot 10H_2O$ 30, $Al_2(SO_4)_3 \cdot 18H_2O$ 30, NaCl 5; current density $D_{cathode}$ = 1.5 amperes/dm^2.

Corrosion resistance was evaluated on the basis of the loss in weight on testing by emmersion in an electrolyte, and by the increase in weight on testing in the atmosphere.

The zinc coated samples with a zinc deposit 2 μ thick were tested by immersion for 13 hours in a 0.3% sodium chloride solution. In this case passivation of the iron was carried out by anodic treatment at a current density of D_{anode} = 10 amperes/dm^2 * in a solution containing 98% sulfuric acid and 10 g/liter of potassium dichromate. In all the remaining cases, passivation was carried out in concentrated nitric acid. The zinc coated samples with zinc coatings 3 and 5 μ thick were also tested in the open atmosphere over a period of a month (31 days).

The loss in weight of passivated zinc coated samples on immersion in 0.3% sodium chloride solution, was, on an average, 20% less than in the case of the unpassivated samples.

---

*The ammeter needle falls practically to zero as passivation proceeds.

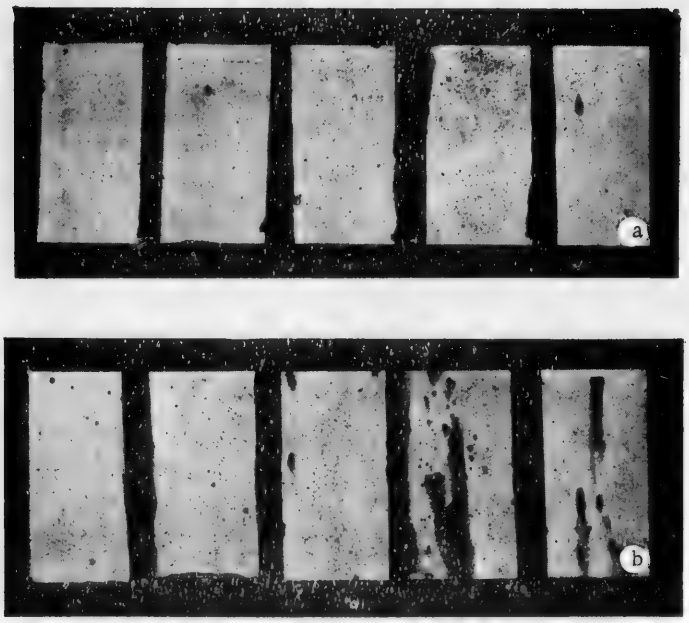

Fig. 7. Nickel coated samples after immersion for 18.5 hours in an 8% sodium chloride solution. Thickness of the nickel layer 5μ. a) Passivated; b) unpassivated.

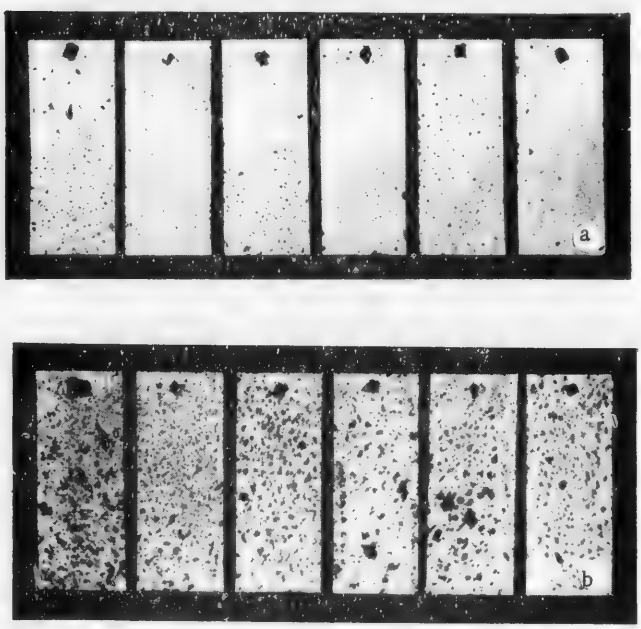

Fig. 8. Nickel coated samples after corrosion testing for 85 days in the open air (under shelter). a) Passivated; b) unpassivated.

TABLE 3

Change in Weight of Zinc Coated Samples After Testing in the Open Atmosphere

Thickness of zinc coating	Duration of test in the open (in days)	Increase in weight (in g)	
		passivated iron	unpassivated iron
3	8	0.0007	0.0010
3	31	0.0012	0.0016
5	8	0.0010	0.0012
5	31	0.0013	0.0014

Changes in weight in passivated samples on testing in the open are also considerably smaller than for unpassivated samples (Table 3).

Tin coated samples were tested by immersion for 5 hours in 1% oxalic acid solution, in which tin is anodic with respect to iron. Losses in weight of passivated samples proved to be less by 25-35%.

In considering the reason for the positive effect of preliminary passivation in enhancing corrosion resistance, it is essential to point out that the presence of the preserved passive film in the pores will not favor slowing down of the corrosion of anodic coatings. On the other hand, during the initial period, the presence of the passive film will even somewhat accelerate corrosion, since the emf of the Zn-ferric-oxide couple will be considerably greater than that of the Zn-Fe couple. Nevertheless, the decisive, long acting factor which determines the decrease in the rate of both anodic and cathodic coatings deposited on a passivated surface, is the decreased porosity.

SUMMARY

1. Preliminary passivation of iron increases the corrosion resistance of both cathodic and anodic galvanized coatings.

2. Passivation increases the degree of homogeneity of the coated surface, which leads to more highly dispersed, less porous coatings.

3. The passive film partly remains on the uncoated parts of the surface of the metal being coated (in the pores), and this, coupled with a lower porosity of the coating, ensures enhanced corrosion resistance.

LITERATURE CITED

[1] L. I. Kadaner, Electrolytic Tin Plating. Dzerzhinsk (1945).

[2] L. I. Kadaner, Sci. Trans. Kharkov Inst. Soviet Trade, 1, 107 (1957).

[3] L. I. Kadaner, Thesis 77528 (1948).

[4] L. I. Kadaner, Ukrainian Chem. J. XVII, 5, 727 (1951).

[5] L. I. Kadaner, J. Appl. Chem. XXV, 8, 850 (1952).

[6] L. I. Kadaner, Ukrainian Chem. J. XVII, 5, 723 (1951).

[7] P. P. Belyaev, Trans. NIIKhIMMASh, 11, 3 (1951).

[8] P. P. Belyaev, Trans. Conference on Electrochemistry, Izd. AN SSSR 4 (1953).

[9] G. Khersonsky, I. P. Lyashchenko, T. N. Olenina and D. V. Stepanov, Bulletin of Investions, 1, 90 (1950).

[10] M. Rosental, Metalurgia (Rumanian) 4, 4-5, 57 (1953).

[11] A. T. Vagramyan, "Electrocoating of Metals," Izd. AN SSSR (1950).

[12] L. I. Kadaner, Trans. Conference on Electrochemistry, Izd. AN SSSR 421 (1953).

Received August 5, 1955

THE EMF OF SOME GALVANIC CIRCUITS IN CRYOLITE – ALUMINA MELTS

V. P. Mashovets and A. A. Revazyan

All-Union Aluminum-Magnesium Institute

In any electrolysis process the electrode processes are determined by the nature of the ions present in the electrolyte, and by the ratio of the discharge potentials of these ions.

The nature of the ions present in cryolite – alumina melts has not, as yet, been clarified. While nothing is known of the nature of the ions present in such melts, it follows that nothing can be said of their potentials. Accordingly, the main criterion for assessing the mechanism of electrolysis of a cryolite – alumina melt is the ratio of the decomposition potentials of the components NaF, AlF_3 and Al_2O_3 which are present in the electrolyte. The material which is subjected to electrochemical decomposition is that which requires the least expenditure of energy, taking into account irreversible processes (overvoltage).

Of the three components – NaF, AlF_3 and Al_2O_3 – the one with the lowest decomposition voltage is alumina. Consequently, the primary electrochemical process which occurs during electrolysis of cryolite–alumina melts, should be decomposition of alumina. This assumption is open to doubt in view of the differences in the values obtained for the decomposition voltage of alumina obtained by various authors, these values ranging from 0.98 to 1.8 volts; the methods used for establishing these values were based on measurements of I – V curves and back emf, using carbon anodes; these experimental values also disagree with the thermodynamic values of 1.10-1.12 volts [1, 2].

The reason for this lack of reproducibility is the insufficient accuracy of the method of measuring the back emf and of constructing I – V curves; determination of the reversible decomposition potential of Al_2O_3 by measuring the emf of galvanic elements is free from this drawback. Under conditions of complete reversibility of the circuit, the energy expended in the electrochemical decomposition of alumina should be equal to the energy liberated during the reverse interaction of the products obtained on the electrodes to form the original material. The emf of the circuit and the decomposition voltage of the alumina should be exactly the same in absolute value. In order to eliminate the influence of the heat of solution of alumina on the value of the emf, measurements must be carried out in a melt saturated with Al_2O_3, in which the free energy of solid and dissolved Al_2O_3 will be equal.

The decomposition voltage of Al_2O_3 and consequently, the emf of the circuit in dilute solutions, should differ from the corresponding values for solid Al_2O_3, since the free energies of formation (or decomposition) differ in dilute and saturated solutions of Al_2O_3.

As a result of experimental (apparatus) difficulties, measurement of the emf of galvanic elements in melts in which the Al_2O_3 concentration is below the saturation level has been impossible up to the present time. Accordingly, we have confined ourselves to a study of saturated melts.

EXPERIMENTAL

Apparatus and technique of measurement. The cell used for measurements, and shown in the diagram, consisted of two sintered corundum beakers placed one inside the other. The inner beaker served as a diaphragm and protected the gas electrode from the possible action of "metallic vapor". A diaphragm of this type prevents

diffusion and agitation of the electrolyte, but is sufficiently porous for the passage of a current. The current was fed into the aluminum electrode through a molybdenum* wire protected by a sintered corundum tube. The cell was placed in a graphite beaker, which, in turn, was placed in a steel beaker.

In order to establish the possible influence of the "metallic vapor" on the potential of the gas electrode, measurements were carried out with and without the diaphragm. In the latter case, the gas electrode was immersed directly in the beaker containing the electrolyte and located on the bottom of the aluminum electrode.

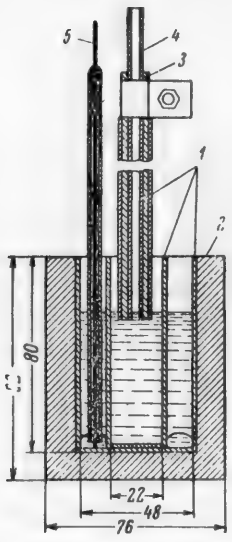

Cell used for emf measurements. 1) Sintered-corundum; 2) graphite crucible; 3) graphite electrode; 4) sintered corundum tube for leading in the gas; 5) tungsten wire (dimensions given in mm).

The gas carrier of the gas electrode was graphite or platinum. In the first instance, the electrode was graphite rod in which a canal had been drilled along the axis; for protection of the outer surface the electrode was tightly packed in a sintered-corundum tube. A sintered-corundum tube was also tightly fitted into the canal drilled through the electrode, gas was passed along this tube for saturating the electrode.

The platinum electrode used was a platinum wire 3 mm in diameter which was fitted into a sintered-corundum tube 12 mm in diameter the latter served for leading in the saturated gases. For investigating the emf of the circuits, synthetic cryolite was used (with a cryolite ratio of $NaF : AlF_3 = 3$), the latter having been obtained by adjusting synthetic industrial cryolite with chemically pure sodium fluoride. The alumina concentration corresponded to a saturated solution of alumina at the experimental temperature.

The gases used were taken from cylinders and were subjected to careful purification before use.

The emf of all the test circuits was measured by the usual compensated setup using a PV-2 type potentiometer, and a needle galvanometer with scale divisions of $0.24 \cdot 10^{-6}$ amperes.

EXPERIMENTAL RESULTS

The emf of the circuit $Al \mid Na_3AlF_6 + Al_2O_3 \mid Pt, (O_2)$ and $(O_2 + N_2)\ Al \mid Na_3AlF_6 + Al_2O_3 \mid Pt$,

The decomposition potential of Al_2O_3 as calculated from the free energy of the reaction $Al_2O_3 = 2Al + 1.5\,O_2$ is equal to 2.12 volts [2].

The same value was obtained from the emf of the element $Al \| Na_3AlF_6 + Al_2O_3 \mid Pt, (O_2)$ at 1000° by Baimakov et al. [3, 4]. A similar value was obtained by Treadwell and Terebesi [5]. It should be pointed out that the decomposition potential of Al_2O_3 determined during the electrolysis of alumina with platinum electrodes, is also in good agreement with the calculated value [6].

All this indicates that the oxygen electrode operates reversibly in the circuit under consideration.

It is known that it is not possible to achieve a reversible oxygen electrode in aqueous solutions. We repeated the measurements of the emf of the circuit $Al \mid Na_3AlF_6 + Al_2O_3 \mid Pt, (O_2)$ both with pure oxygen, and with a mixture of oxygen and an indifferent gas. The electrode was swept with oxygen before immersion in the melt. Measurements were made immediately after immersion of the electrode in the melt, and subsequently every five minutes over a period of an hour. The temperature was kept at 1015°. When pure oxygen was used for sweeping the electrode, the emf of the element established itself at 2.12 volts right at the beginning, and maintained this value, which corresponds to the theoretical value, right throughout without any change. While the electrode Pt, O_2 is reversible, on dilution of the oxygen with an indifferent gas, the potential should change in accordance with the laws governing gas electrodes. Measurements of the emf of the circuit, in which oxygen was diluted with nitrogen, showed that the decrease in partial pressure of the oxygen leads to a drop in the emf.

*In the text the wire used is stated to be molybdenum, while in the diagram, reference is made to a tungsten wire — Publisher's note.

Thus, when the composition of the gas was 12.9% O_2 and 87.1% N_2, the emf was very stable at 2.00-2.01 volts, while for a gas whose composition was 3.5% O_2 and 96.5% N_2, the emf was 1.83 volts.

All the same, the decrease actually found proved to be 2-3 times greater than the theoretical amount: calculation was made on the basis of the equation

$$\Delta E = \frac{RT}{nF} \ln P$$

where $n = 4$ this equation gives, for the first case a drop in emf of 0.056 volts, and for the second a drop of 0.092 volts, as against the results actually obtained of 0.11-0.12 and 0.29 volts respectively.

Thus, a platinum-oxygen electrode is not completely reversible. The deviation from the laws governing gas electrodes, can, presumably, be explained by the incomplete inertness of the platinum toward oxygen. All the same, at a partial pressure of oxygen of 1 atmosphere, the operation of such an electrode approximates to that of a reversible oxygen electrode.

The processes which occur in the element under consideration can be depicted as follows: on the anode, $Al \rightarrow Al^{3+} + 3e$; on the cathode, depending on the nature of the oxygen containing anions, either $O_2 + 4e \rightarrow$ $\rightarrow 2O^{2-}$, or $O_2 + 2Al_2O_3 + 4e \rightarrow 4AlO_2^-$; in the melt, $2Al^{3+} + 3O^{2-} \rightleftharpoons Al_2O_3$ or $Al^{3+} + 3AlO_2^- = 2Al_2O_3$. Finally, the over-all process can be represented as $4Al + 3O_2 \rightarrow 2Al_2O_3$.

The emf of the Circuit $Al \mid Na_3AlF_6 + Al_2O_3 \mid Pt, (CO_2)$

The decomposition potential of alumina, calculated from the free energy of the reaction $4Al + 3CO_2 \rightarrow$ $\rightarrow 2Al_2O_3 + 3C$ is equal to 1.10 volts. The value of the decomposition potential of alumina during electrolysis with carbon electrodes, should also be equal to this, when the primary anode product is CO_2. Measurement of the emf of the circuit $Al \mid Na_3AlF_6 + Al_2O_3 \mid Pt, (CO_2)$ also gives the possibility of determining the decomposition voltage of alumina according to the reaction indicated.

Measurements were carried out at 1000° with and without using the diaphragm around the $\mid Pt, (CO)_2$ electrode. It was established that in all cases, an emf which is constant with time and equal to 1.1-1.12 volts is established, this corresponds to the theoretical value.

The cathodic process in the element under consideration can be represented by the equation $CO_2 + 4e \rightarrow$ $\rightarrow C + 2O^{2-}$ or $CO_2 + 2Al_2O_3 + 4e \rightarrow C + 4AlO_2^-$, while the over-all process is $4Al + 3CO_2 \rightarrow 2Al_2O_3 + 3C$.

The carbon dioxide in this process must be regarded as the electrochemically active, and potential determining material.

The emf of the Circuit $Al \mid Na_3AlF_6 + Al_2O_3 \mid C, (CO_2)$

Since graphite, like platinum in the previous case, can be regarded as a carrier for carbon dioxide gas, then the emf's of the circuits containing graphite and platinum electrodes, saturated with carbon dioxide, should not differ from each other.

The graphite electrode was not subjected to any special treatment before immersion; it was simply held for 15-20 minutes in the oven over the melt while carbon dioxide was used for sweeping it. Measurements were made at 1000°. The results obtained are given below.

Time (in min)	Value of the emf (in volts) in expt. Nos			Time (in min)	Value of the emf (in volts) in expt. Nos.		
	1	2	3		1	2	3
5	1.346	1.46	1.27	60	1.15	1.08	1.00
10	1.27	1.31	1.16	70	1.16	1.12	0.99
15	1.23	1.30	1.13	80	1.14	1.12	0.91
20	1.22	1.28	1.14	90	1.11	1.11	0.78
30	1.116	1.22	1.11	100	1.11	1.11	0.71
40	1.15	1.13	1.11	110	1.11	—	—
50	1.15	1.115	1.041	120	1.11	—	—

At the beginning of the experiment the emf of the circuit was 1.35-1.45 volts, while it subsequently gradually, dropped to 1.11 volts. This value was maintained constant during the whole course of the experiment (Experiments Nos. 1 and 2).

In order to establish whether or not the stable value of the emf is determined by the presence of carbon dioxide on the graphite electrode, i. e., whether the current forming process is the reaction

$$4Al + 2CO_2 \rightarrow 2Al_2O_3 + 3C,$$

in experiment No. 3, after the emf value had reached 1.11 volts, the supply of gas was shut off. The emf of the circuit thereupon started to drop, and fell to 0.72-0.71 volts. This shows that the electrochemically active agent which determines the stability of the potential of the graphite electrode saturated with CO_2, is carbon dioxide, while the current forming reaction is expressed by the equation given above. It follows from this, that during electrolysis with a carbon anode, as long as the primary anode product is CO_2, then the decomposition voltage should be 1.11 volts.

After the carbon dioxide supply has been switched off, and the emf has dropped to 0.72-0.71 volts, the current forming process appears to be carbide formation $4Al + 3C \rightarrow Al_4C_3$, as follows from the work of Baimak, Mashovets, and Kil [3].

The emf, of the element at the start of the experiment, as is evident from the experiments referred to above, is considerably higher than 1.11 volts. It was found that on removing the graphite electrode from the electrolyte after the stable value of the emf had been reached, and keeping it for a few minutes in the air, and then reimmersing the electrode in the melt, the emf of the circuit increased to 1.35-1.45 volts.

Since the initial value of the emf of the circuit with a $|C, CO_2$, cathode is higher than with a platinum-carbon dioxide electrode, but less than with a platinum-oxygen electrode, then the electrochemically active cally active material of the graphite electrode $|C, CO_2$, at the start of the experiment is oxygen, whose chemical potential is less than the chemical potential of molecular oxygen, but greater than the chemical potential of oxygen combined as CO_2. Thus, the material could be oxygen absorbed by graphite during its contact with air.

The stability of the compound of chemisorbed oxygen and carbon can be assessed on the basis of the initial value of the emf which is of the order of 1.45-1.35. volts.

The chemical potential of oxygen entering into the composition of the intermediate carbon-oxygen complexes, differs essentially from the chemical potential of oxygen combined as CO_2. The gradual drop in the emf from 1.45 to 1.11 volts indicates the nonhomogeneity of the chemically sorbed complexes. Since the potential of the carbon electrode before achievement of the stable value of the emf takes on different values, then consequently, various intermediate oxides in which the stability of the oxygen bonds differs must exist on the surface of the carbon. This, in turn, is explained by the nonhomogeneity of the surface of the carbon, in accordance with physicochemical studies of the process of carbon combustion [7-9].

The intermediate oxides originally formed, as shown in the work of Frumkin and co-workers in the case of aqueous solutions [10], change with time, while the bonds between oxygen and carbon become increasingly stable. The change in the stability of the bond between sorbed oxygen and carbon with time is also the reason for the gradual drop in the emf.

As a result of the nonhomogeneity of the intermediate oxides on the surface of a graphite electrode, there exist short circuited microelements. The processes occurring in them lead to the transfer of sorbed oxygen from certain less active parts to other, more active, parts of the graphite electrode. The potential of the electrode at each given moment is determined by the least stable intermediate oxides, in which the chemical potential of oxygen is highest. In these intermediate states, the cathode process is expressed by:

$$C_xO + 2e \rightarrow {}^{x}C + O^{2-}$$

$$C_xO + Al_2O_3 + 2e \rightarrow {}^{x}C + 2AlO_2^{-}.$$

or

After decomposition of the intermediate oxides (discharge of surface microelements) and an emf of 1.11 volts has been achieved, the potential of the graphite electrode is determined by the chemical potential of oxygen entering into the composition of the CO_2.

The emf of the Circuit $Al \mid Na_3AlF_6 + Al_2O_3 \mid C, (O_2)$

The mechanism described for the operation of a graphite-carbon dioxide electrode is also confirmed by measurements of the emf of a circuit, in which the graphite electrode is saturated with oxygen. Measurements were carried out at 1010°.

The results of these experiments, which are given below (Experiments Nos. 1, 2 and 3), show that the initial value of the emf for these circuits also, is either of the same order, or somewhat higher than in the case of graphite saturated with carbon dioxide — about 1.50 volts.

The emf decreases more slowly, but reaches the same stable value of 1.11 v. Experiments Nos. 1 and 2 were carried out with an electrode protected by a diaphragm, while No. 3 was carried out without a diaphragm; the fact that the results obtained are identical confirms the absence of a "depolarizing" action on the part of the "metallic vapor". In Experiment No. 4 the supply of oxygen was shut off before the emf with a value of 1.11 had been reached, this led to a further drop in the emf to 0.8 volts, as in the case of circuits containing a graphite-carbon dioxide electrode.

In Experiment No. 5 the oxygen was diluted with nitrogen to a ratio of 3.5% O_2, 96.5% N_2. The stable, terminal emf dropped by 0.12 volts, while the theoretical decrease should be 0.092 volt. Thus, a graphite-oxygen or, essentially a graphite-carbon dioxide electrode) electrode is closer in its behavior to a reversible gas electrode than is a platinum-oxygen electrode.

Time (in min)	Value of the emf (in volts) in experiments Nos. 1	2	3	4	5
5	1.56	1.46	1.30	1.23	1.40
10	1.47	1.45	1.29	1.21	1.35
15	1.47	1.43	1.27	1.17	1.34
20	1.46	1.42	1.26	1.15	1.33
30	1.45	1.41	1.37	1.08	1.31
40	1.43	1.39	1.21	0.82	1.27
50	1.43	1.38	1.21	0.78	1.16
60	1.36	1.36	1.18	0.81	1.21
70	1.34	1.30	1.17	0.80	1.21
80	1.33	1.12	1.16	0.81	1.20
90	1.30	1.11	1.15	0.80	1.04
100	1.27	1.12	1.13	—	0.98
110	1.22	1.11	1.13	—	1.04
120	1.20	1.11	1.14	—	1.00
130	1.13	1.11	1.14	—	0.99
140	1.10	—	1.12	—	0.99
150	1.11	—	1.11	—	0.95
160	1.11	—	1.11	—	0.99
170	1.12	—	1.11	—	0.99
180	1.11	—	1.11	—	0.99

The agreement between the stable potential of a graphite-oxygen electrode and that of a graphite-carbon dioxide electrode, together with the drop in the initially high value of the potential with time, despite the continuous passage of oxygen, indicate that in this case also, the potential determining agent is carbon dioxide. The initial, high value is determined by oxygen, chemically sorbed by the graphite before the start of the experiment. During saturation with oxygen of an electrode immersed in a melt, the oxygen is only sorbed on the most active parts of the graphite to form carbon dioxide alone. Apparently, this is determined by the fact that during formation of a double layer, the transfer into the melt of chemically sorbed oxygen from the less active parts of the graphite (from the less stable oxides), is accompanied by simultaneous adsorption of electrolyte components, which prevent chemical sorption of oxygen on these parts. Such an explanation is in agreement with a fact noted previously, viz, when an electrode in which the stable potential of 1.11 volts has already been reached, is temporarily

removed from the melt, left in the air, and then reimmersed in the melt, the potential again rises to 1.35 to 1.45 volts.

SUMMARY

During measurements of the emf of galvanic circuits in fused cryolite saturated with alumina at 1000-1015°, using liquid aluminum as the anode, and platinum or graphite saturated with oxygen or carbon dioxide, as cathode, it has been shown that:

1. The emf of the platinum oxygen electrode is 2.12 volts, this agrees with the theoretical value, nevertheless, on diluting the oxygen with nitrogen, the drop in emf does not conform to the laws governing gas electrodes.

2. Cathodes from platinum saturated with carbon dioxide, and of graphite saturated with carbon dioxide or oxygen, a stable emf of 1.11 volts is established, this agrees with the theoretical value when it is assumed that the potential determining material of the cathode is carbon dioxide; the high emf values observed at the start of a test when graphite is used as the carrier for the gas, are determined by the presence of intermediate chemically sorbed carbon oxides C_xO.

LITERATURE CITED

[1] A. I. Belyaev, M. B. Rapoport and L. A. Firsanova, Electrometallurgy of Aluminum, 124 (1953).

[2] V. P. Mashovets, Electrometallurgy of Aluminum, 163 (1938).

[3] Yu. V. Baimakov, V. P. Mashovets and I. G. Kil, Light Metals, 1, 22 (1937).

[4] Yu. V. Baimakov and N. R. Ishmaev, Trans. Leningrad Industrial Inst. 1, 81 (1938).

[5] W. D. Treadwell and L. Terebesi Helv. Chim. Acta, 16, 922 (1933).

[6] A. I. Belyaev, Light Metals, 1, 7 (1938).

[7] S. Z. Roginsky, Adsorption and Catalysis on Heterogeneous Surfaces, 12 (1948).

[8] O. A. Esin and P. V. Geld, Physical Chemistry of Pyro-Metallurgical Processes, 1, 167 (1950).

[9] A. S. Predvoditelev, L. N. Khitrin, O. A. Tsukhanova, Kh. I. Kolodtsev and M. A. Grodzovsky, Combustion of Carbon (1949).

[10] A. N. Frumkin, Prog. Chem. 18, 9 (1949).

Received February 15, 1956

PLATE EFFICIENCY DURING DISTILLATION OF BINARY MIXTURES

E. Rukenshtein

(Bucharest)

In order to compare the fractionating capacity of an actual plate with a theoretical plate, the concept of efficiency has been introduced in the literature. When a liquid is agitated by vapor bubbling through it, intensively enough that the molar fraction $\underline{x}$ of the readily volatile component of the liquid on the plate is constant, fractionation can be compared by means of efficiency alone. When, however, the liquid on the plate is not agitated sufficiently for this state of affairs to occur, it is necessary to introduce two concepts, viz. local and total efficiency. In the literature [1] relations have been derived for determination of total efficiency, only in the limiting case, where agitation of the liquid in the direction of its flow along the plate surface can be disregarded.*

The aim of the present article is to establish a relation for total plate efficiency, taking into account agitation of the liquid along its direction of flow.

In order to simplify the problem we shall confine ourselves to a consideration of cases in which the following conditions are observed:

a) the molar heats of conversion of both components have values which are sufficiently near, so that the molar discharge of the liquid L and the molar discharge of the vapor V are practically constant; b) the vapor is distributed uniformly across the cross section S of the plate. This condition is ensured by the use of plates in the form of sieves which have a sufficiently small enough mesh; c) the carry over of liquid from the plates by the rising vapors is insignificant.

Derivationof the Transport Equation

Bubbling of the vapor through the liquid on the plate leads to agitation of the latter. The number of moles of the readily volatile component which is transferred during the agitation, per unit surface, and in unit time, in directions $\underline{z}$ or l can be expressed by

$$M_z = -\varepsilon \frac{\partial cx}{dz}; \quad M_l = -\varepsilon_l \frac{\partial cx}{\partial l}, \tag{1}$$

where $\underline{z}$ is the distance in the direction of the flow of the liquid along the surface of the plate, l is the distance in the direction measured from the base of the plate to the free surface of the liquid, M_z and M_l are corresponding vectors for the transfer of the material along directions $\underline{z}$ and l, ϵ and ϵ_l are the agitation constants, and $\underline{c}$ is the total molar concentration in the liquid.

For the number N moles which are transferred from the liquid phase into the vapor, per unit surface of contact between the phases, in unit time, we take the equation

$$N = H(y^x - y), \tag{2}$$

*In the other limiting case, i. e., for complete agitation of the liquid on the plate, total efficiency is equal to local efficiency.

where H is the total transfer coefficient, $\underline{y}$ is the molar fraction of the vapor of the readily volatile component, and y^x is the molar fraction of the readily volatile component in the vapor in the case of a thermodynamic equilibrium with a liquid of concentration $\underline{x}$.

Then, from the material balance for the liquid phase, we get the equation: *

$$-\frac{\partial x}{\partial z}\,dz\,dL+\frac{\partial}{\partial z}\left[\zeta f(z)(D+\varepsilon)\frac{\partial cx}{\partial z}\right]dzdl+$$
$$+f(z)\frac{\partial}{\partial l}\left[\zeta_1(D+\varepsilon_1)\frac{dcx}{\partial l}\right]dldz=sf(z)H(y^x-y)\,dzdl, \tag{3}$$

here f(z) is the width of the surface of the plate, through which the liquid flows, ζ is the part perpendicular to the direction $\underline{z}$ of the surface occupied by the liquid, ζ_1 is the part perpendicular to the direction l of the surface occupied by the liquid, D is the diffusion coefficient, $\underline{s}$ is the contact surface between the phases, related to unit volume.

For the vapor phase, from the material balance we derive the equation

$$V'\frac{\partial y}{\partial l}f(z)\,dzdl=sH(y^x-y)f(z)\,dzdl, \tag{4}$$

where V' is the molar discharge of the vapor per unit surface.

Since agitation along the vertical is fairly intense, it can be assumed that $\underline{x}$ is practically independent of l. Accordingly the system of Equations (3) and (4) can be approximately replaced by the following system of equations:

$$-L\frac{dx}{dz}+\frac{d}{dz}\left[\zeta f(z)l_0(D+\varepsilon)\frac{dcx}{dz}\right]=f(z)\int_0^{l_0}sH(y^*-y)\,dl. \tag{5}$$

$$V'\frac{\partial y}{\partial l}=sH(y^x-y), \tag{6}$$

where l_0 is the height of the surface through which the liquid flows.

In order to be able to solve the system of Equations (5) and (6), we make the following simplifying assumptions: d) the total concentration $\underline{c}$ in the liquid phase does not change over wide limits; e) the equilibrium curve, over the range we are interested in, can be approximately replaced by the straight line

$$y^x=mx+p.$$

The latter assumption can be made when the concentration gradient on the plate is not too great. This assumption has already been made (without any special mention at the time) in Equation (2).

The values $\underline{s}$, l_0 and H are constant.

Then by integrating Equation (6) we get

$$y^x-y=(y^x-y_{l=0})\exp-\left(\frac{sHl}{V'}\right). \tag{7}$$

*We assume that dl and dz are small enough to be considered as infinitely small elements, but are large enough at the same time so that the volume $f(z)\,dzdl$ contains the necessary amount of liquid and vapor phases.

Substituting the expression obtained for $y^x - y$ in Equation (5), we get*

$$-L\frac{dx_n}{dz}+\frac{d}{dz}\left[c\zeta f(z)\,l_0(D+\varepsilon)\frac{dx_n}{dz}\right]=$$

$$=\left[1-\exp-\left(\frac{sHl_0}{V'}\right)\right]f(z)\,V'(y_n^x-y_{(n+1)l=l_0}). \qquad (8)$$

Since $$y_n^x-y_{(n+1)l=l_0}=m\,(x_n-x^x_{(n+1)l=l_0},$$

where $\underline{x}$ is the molar fraction of the readily volatile component in the liquid during thermodynamic equilibrium with vapor of concentration $\underline{y}$, then Equation (8) can be transformed into

$$-L\frac{dx_n}{dz}+\frac{d}{dz}\left[c\zeta f(z)\,l_0(D+\varepsilon)\frac{dx_n}{dz}\right]=$$

$$=\left[1-\exp-\left(\frac{sHl_0}{V'}\right)\right]mV'f(z)\,(x_n-x^x_{(n+1)l=l_0}). \qquad (9)$$

Below is given a solution of Equation (9) for the special case, in which:

1) $f(z)\equiv b=\text{const.}$

2) $x^x_{(n+1)l=l_0}\equiv\bar{x}^x_{(n+1)}=\text{const.}$

Condition (2) is fullfilled for a vapor issuing from a distillation vat.

The boundary conditions for $\underline{x}$ are as follows:

$$Lx_{(n-1)z=z_0}=Lx_{(n)z=0}-\zeta f(0)\,l_0(D+\varepsilon)_{z=0}c\left(\frac{dx_n}{dz}\right)_{z=0} \qquad (10)$$

and

$$\left(\frac{dx_n}{dz}\right)_{z=z_0}=0, \qquad (11)$$

where z_0 is the length of a plate.

Since we cannot get an exact relationship between the transfer coefficient ϵ and $\underline{z}$, we replaced it to a first approximation by the mean value ($\bar{\epsilon}$).

We shall introduce the designations**

$$E\equiv 1-\exp-\left(\frac{sHl_0}{V'}\right);\quad a_1\equiv\frac{c\zeta bl_0(D+\varepsilon)}{z_0mVE};$$

$$z^x\equiv\frac{z}{z_0};\quad a_2\equiv\frac{L}{mVE};\quad X\equiv x-\bar{x}^x_{n+1}.$$

*By x_n, $x_{(n+1)}\ldots y_n$, $y_{(n+1)}\ldots$ we imply the molar fractions on plates n, n + 1, . . . The plates are counted from top to bottom.

**Using Equation (7) it is easy to show that

$$E=\frac{y_{(n)l=l_0}-y_{(n+1)l=l_0}}{y_n^x-y_{(n+1)l=l_0}}$$

and, consequently, E is the local efficiency.

Then, Equation (9) and boundary conditions (10) and (11) can be written as follows:

$$a_1 \frac{d^2 X_n}{dz^{x2}} - a_2 \frac{dX_n}{dz^x} - X_n = 0\,, \tag{9'}$$

$$X_{(n-1)z^x=1} = X_{(n)z^x=0} - \frac{a_1}{a_2}\left(\frac{dX_n}{dz^x}\right)_{z^x=0}, \tag{10'}$$

$$\left(\frac{dX_n}{dz^x}\right)_{z^x=1} = 0. \tag{11'}$$

Solving Equation (9') and taking into account the boundary conditions (10') and (11'), we get

$$\frac{X_{(n-1)z^x=1}}{X_{(n)z^x=1}} = \frac{1}{2}\left(1 + \frac{1+\frac{2a_1}{a_2^2}}{\sqrt{1+\frac{4a_1}{a_2^2}}}\right)\exp\left(-\frac{a_2}{2a_1} + \sqrt{\left(\frac{a_2}{2a_1}\right)^2 + \frac{1}{a_1}}\right) +$$

$$+ \frac{1}{2}\left(1 - \frac{1+\frac{2a_1}{a_2^2}}{\sqrt{1+\frac{4a_1}{a_2^2}}}\right)\exp\left(-\frac{a_2}{2a_1} - \sqrt{\left(\frac{a_2}{2a_1}\right)^2 + \frac{1}{a_1}}\right). \tag{12}$$

On the other hand, by definition, total efficiency E_g is characterized by the expression:

(13)

where

$$E_g = \frac{\bar{y}_n - \bar{y}_{(n+1)}}{y_{(n)z=z_0} - \bar{y}_{(n+1)}}\,,$$

$$\bar{y} = \frac{\int_0^{z_0} y_{l=l_0} f_{(z)}\, dz}{\int_0^{z_0} f(z)\, dz}\,.$$

Since

$$V\left(\bar{y}_n - \bar{y}_{(n+1)}\right) = L\left(X_{(n-1)z=z_0} - X_{(n)z=z_0}\right)$$

$$y_{(n)z=z_0} - \bar{y}_{(n+1)} = E\left(y^x_{(n)z=z_0} - \bar{y}_{(n+1)}\right) \equiv mEX_{(n)z=z_0}$$

and

we find that

$$E_g = E\frac{a_2}{2}\left[\left(1 + \frac{1+\frac{2a_1}{a_2^2}}{\sqrt{1+\frac{4a_1}{a_2^2}}}\right)\exp\left(-\frac{a_2}{2a_1} + \sqrt{\left(\frac{a_2}{2a_1}\right)^2 + \frac{1}{a_1}}\right) +\right.$$

$$+\left(1-\frac{1+\frac{2\alpha_1}{\alpha_2^2}}{1+\frac{4\alpha_1}{\alpha_2^2}}\right)\exp\left(-\frac{\alpha_2}{2\alpha_1}-\sqrt{\left(\frac{\alpha_2}{2\alpha_1}\right)^2+\frac{1}{\alpha_1}}\right)-2\Bigg]\equiv E\varphi. \qquad (14)$$

Thus, the total efficiency in the given special case is equal to the product of two factors E and φ: one of these factors, the local efficiency E allows one to compare the actual local fractionation * with the fractionation which would be obtained at a given point, when the vapor leaving the plate at this point is in thermodynamic equilibrium with the liquid. The second factor φ permits evaluation of the fractionation achieved on a plate as compared with the fractionation achieved at the place where the liquid leaves the plate.

Values of φ in Relation to α_1 and α_2

α_2	α_1						
	0	0.01	0.1	0.5	1	2	5
0.5	3.17	2.92	1.93	1.28	1.15	1.08	1.03
1	1.70	1.69	1.50	1.23	1.13	1.06	1.03
2	1.30	1.29	1.25	1.16	1.09	1.06	1.02

It is obvious that $E \leq 1$, E being equal to 1 when thermodynamic equilibrium is attained. One would expect that φ should be greater then unity, or, in the extreme case, equal to unity.

Values of function φ are given in the Table.

From the table it is clear that φ decreases as α_1 and α_2 increase, and becomes practically equal to unity at $\alpha_1 \approx 2$, if $\alpha_2 > 0.5$. Values of φ approaching the maximum are obtained for $\alpha_2 > 0.5$ when $\alpha_1 < 0.1$.

LITERATURE CITED

[1] W. K. Lewis, Ind. Eng. Ch., 29, 399 (1936).

Received November 26, 1956

*By fractionation, we mean the difference between the molar fraction in the vapor leaving the plate, and the molar fraction in the vapor entering the plate.

A STUDY OF THE RELATION BETWEEN THE EXPENDITURE OF MATERIAL IN THE REACTOR AND THE VOLUME OF THE SOLUTION DURING DEVELOPMENT AND CLEARING OF CINE-FILM

I. Blyumberg, G. Bulochnikova and N. Solodovnikova

The necessity of keeping the properties of solutions, which are used in reactors for treatment of certain materials, at a constant level, has compelled technologists to resort to the use of large volumes of these solutions [1]. Increases in the volume of the working solution in a reactor essentially increases the constancy of its properties, but often leads to an increase in the amount of the materials which are used for making up the solution.

In the work described here, this question was investigated taking as examples, bleaching baths in machines used for colored positive cine-film, and for the development of black-white and colored films.

Let us assume that both useful and useless reactions occur in the reaction vessel. Further, let us assume that the useful reactions are those involving oxidation of the metallic silver in the emulsion layer by ferricyanide, and dissolving of this salt by thiosulfate, while the useless reaction is oxidation of thiosulfate by ferricyanide. Solutions of the ferricyanide salt and thiosulfate with concentration c' (in g/liter) are continuously fed into the reaction vessel at the rate of* b_1 and b_2 liters/hour. The total rate of supply of these liquids to the vessel will be $b_1 + b_2 = b$ liters/hour. Solution is also removed from the reaction vessel at a rate of $\underline{b}$ liters/hour, and, consequently, the volume of solution in the vessel will remain constant. Let us assume that the expenditure of any one material (e. g. the ferricyanide salt) on useful reactions (oxidation of Ag) is equal to $\bar{\alpha}_1$(g/hour). The total amount of this material for all reactions which occur in the vessel will then be $\bar{\alpha}_1 + \bar{\alpha}_2 = \alpha$ g/hour.

Under such conditions, after a certain time, there will develop established concentrations of thiosulfate and ferricyanide; we shall denote these by k_1 and k_2. Let us assume that mixing of the solution in the vessel is ideal, and that diffusion of the salts into the emulsion layer proceeds infinitely rapidly. Then, the salt concentrations throughout all points of the vessel and layer will be the same.

We shall derive an expression for the established concentration of any material. If its concentration, and the volume of solution do not change with time, then the total amount of material in the vessel will also remain constant. This state of affairs only holds when the supply of material to the vessel is the same as the amount of it removed.

The amount of expended material is made up of the amount used up in chemical reactions which is equal to $\bar{\alpha}$ (g/hour), and the amount issuing from the vessel with the rejected solution, this being equal to $\underline{bk}$ (g/hour). Material is supplied to the vessel at a rate of $b_1 \cdot c^1$ (g/hour). We substitute b_1 for $\underline{b}$, and, multiplying b_1 by $1 + \frac{b_2}{b_1}$, we assume that the material is introduced into the vessel with $\underline{b}$ liters of liquid. Then the concentration of material in this liquid should be given by $c = \frac{c^1}{1 + \frac{b_2}{b_1}}$ and $cb = c^1 b_1$.

We have:

$$bc = bk + \bar{\alpha}, \text{ откуда } k = c - \frac{\bar{\alpha}}{b} \text{ or } k = c - \frac{\bar{\alpha}_1 + \bar{\alpha}_2}{b}. \quad (1)$$

*Henceforth the rate of supply of replenisher is meant to refer to the volume in liters added to the reactor per hour.

The amount of material used up in useful reactions does not depend on the volume of liquid in the machine, since these reactions only occur in the emulsion layer. The useless reaction occurs throughout the whole volume of the solution, and the greater this volume, the larger the amount of material which is used up in useless reactions. With increases in this useless expenditure, the total expenditure of materials in the vessel increases. Accordingly, $\bar{\alpha}_2$ should depend on the volume of the solution $\underline{v}$. In addition, the amount of material used up in useless reactions in the solution should be determined by the concentrations of the reactants k_1 and k_2 and the velocity constant of the reaction K, which occurs between them. Thus, the value of $\bar{\alpha}_2$ will be equal to

$$\bar{a}_2 = K \cdot k_1 \cdot k_2 \cdot v. \tag{2}$$

Substituting its value in Expression (1), we get

$$k_1 = c - \frac{\bar{a}_1 + K \cdot k_1 \cdot k_2 \cdot v}{b}. \tag{3}$$

From Equation (3) the established concentration of the material which is being used up can be determined

$$k_1 = \frac{bc - \bar{a}_1}{b + K \cdot k_2 \cdot v} \tag{4}$$

and the velocity constant of the useless reaction

$$K = \frac{bc - \bar{a}_1 - bk_1}{k_1 \cdot k_2 \cdot v}. \tag{5}$$

It follows from Equation (3) that under the conditions envisaged above, the established concentration of the material in solution will decrease with increasing volume of the solution. This assumption has been confirmed experimentally.

EXPERIMENTAL

In vessel 1 (diagram) reaction was allowed to occur between two materials A and B, solutions of which were fed into vessel 1 from vessels 2 and 3 at a constant rate. The supply rate of these solutions was regulated by screw clips 4. When the level of the liquid in vessel 1 was kept constant, the supply rate of solutions A and B were independent of the level of the liquids in vessels 2 and 3, assembled on the principle of a Mariott vessel. The level of liquid in vessel 1 was kept constant by means of vessel 5 connected to 1 by a П shaped syphon tube 6. Vessel 5 can be shifted up and down, and the level of its overflow opening determines the level of liquid in 1. The solution in 1 was stirred by a propeller stirrer 7 rotated by motor 8. The rotational rate of the stirrer was kept constant by means of a rheostat.

Experimental procedure. Into vessels 2 and 3 were introduced solutions of materials between which a useless reaction occurs, e. g., $Na_2S_2O_3$ and $K_3Fe(CN)_6$. In experiments with oxidation of developers by oxygen, a solution of developer was placed in one vessel, and a solution of alkali in the other. The oxidizing agent was atmospheric oxygen dissolved in the liquid. Alkali was added to the solution in order to accelerate oxidation of the developer. The solutions were fed at a constant rate into 1 from 2 and 3. After a certain time interval, the concentrations of the materials issuing from 2 and 3 were determined analytically. Samples for determination were taken from 5. The experiment was stopped when the established concentrations of the materials in 1 had been reached.

The supply rate to 1 was established before the start of an experiment from the number of milliliters of solution flowing into a measuring cylinder in one minute. After the start of an experiment, the outflow rate of solutions from 2 and 3 was controlled on the basis of the number of air bubbles passing into the vessel per minute.

Diethylparaphenylenediamine was analyzed colorimetrically. The oxidizing agent was copper ammoniate. The oxidized form of the developer was complexed with 1,3,8-naphtholdisulfonic acid and determined by means

of a photoelectric colorimeter. The alkali was determined titrimetrically. The thiosulfate and ferricyanide which were present together in the same solution were determined as follows. Thiosulfate was determined first by direct iodometric titration, using starch as an indicator. $ZnSO_4$ and KI were then added to the same solution. The ferricyanide oxidized the KI to I_2 which was then determined by titration with thiosulfate.

EXPERIMENTAL RESULTS

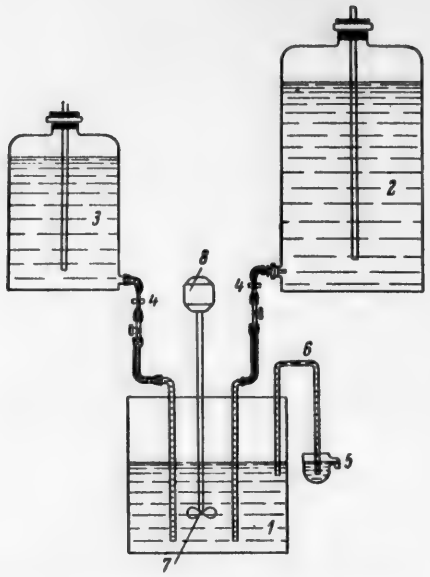

Setup for determination of the relationship between the expenditure of a material in a reactor and the volume of the reaction solution. (Explanation in the text).

Oxidation of Thiosulfate by Ferricyanide. Thiosulfate and ferricyanide are simultaneously present in solution during treatment of color film by the NIKFI* [1] method.

The volume of solution in vessel 1 was 0.5 liter, while the concentration of $Na_2S_2O_3 \cdot 5H_2O$ in vessel 3 was 62.52 g/liter, and the concentration of $K_3Fe(CN)_6$ in vessel 2 was 80.64 g/liter; the supply rate of solution from 3 was 0.75 liter/hour, and the supply rate of solution from 2 was 0.25 liter/hour, $\underline{b} = 0.75 \cdot 1.33 \ldots = 1.0$ liters/hour,

$$C_{Na_2S_2O_3 \cdot 5H_2O} = \frac{62.52}{1.33} = 46.9 \text{ g/liter}, \quad C_{K_3Fe(CN)_6} = \frac{80.64}{4.0} = 20.16 \text{ g/liter}.$$

Time elapsed from start of a test (in hr)	Thiosulfate concentration (in g/liter)	Potassium ferricyanide conc. (g/liter)
0.00	62.52	20.16
0.45	52.70	18.16
1.00	49.60	16.88
1.50	45.85**	15.74**
2.00	45.81**	15.70**
2.25	45.85**	15.74**

Four such experiments were carried out in which different volumes of solution were used. The experimental conditions, and the results obtained are given in Table 1.

TABLE 1

Results of Experiments on the Oxidation of Thiosulfate by Ferricyanide

Vol. of solution in vessel 1 (l)	b (n (l/hr)	$c_{Na_2S_2O_3 \cdot 5H_2O}$ (g/liter)	$c_{K_3Fe(CN)_6}$ (g/liter)	$k_{Na_2S_2O_3 \cdot 5H_2O}$ (g/liter)	$k_{K_3Fe(CN)_6}$ (g/liter)
0.5	1.0	46.90	20.16	45.83	15.73
1.0	1.0	47.02	20.21	44.12	15.16
1.5	1.0	47.02	20.21	40.84	14.01
2.0	1.0	46.96	20.55	37.00	12.82

*Scientific Research Kine-Photo-Institute.

**Equilibrium state achieved.

Oxidation of Hydroquinone by Oxygen. The volume of solution in vessel 1 was 0.5 liter, the hydroquinone concentration in vessel 3 was 13.36 g/liter, while the supply rate of the solution from vessel 3 was 0.75 liter/hour, and the rate of supply rate of solution from vessel 2 was 0.25 liter/hour, $\underline{b} = 0.75 \cdot 1.33 \ldots = 1.0$ liters/hour, $\underline{c}_{\text{hydroquinone}} = \frac{13.36}{1.33} = 10.02$ g/liter.

Time elasped from the start of the test (in hours)	Hydroquinone concentration (g/liter)
0.00	13.36
0.25	12.25
0.50	10.53
1.00	9.72 **
1.50	9.66 **
2.00	9.69 **

Three such experiments were made in which the volume of the solution in vessel 1 was varied. The experimental conditions used as well as the results obtained are given in Table 2.

TABLE 2

Results of Experiments on the Oxidation of Hydroquinone by Oxygen

Volume of solution in vessel 1 (in liters)	$\underline{b}$ (liters/hr)	$\underline{c}_{\text{hydroquinone}}$ (in g/liter)	$\underline{k}_{\text{hydroquinone}}$ (in g/liter)	Time elapsed before equilibrium is reached (hrs)
0.5	1.0	10.02	9.69	1.0
1.0	1.0	10.02	9.72	2.0
2.0	1.0	9.75	9.32	4.85

Oxidation of diethylparaphenylenediamine* by oxygen. The volume of solution in vessel 1 was 0.5 liter, the concentration of material in vessel 3 was 4.85 g/liter, while concentration of NaOH in vessel 2 was 9.60 g/liter; the supply rate of solution from vessel 3 was 0.75 liter/hour, the rate from vessel 2 was the same, $\underline{b} = 0.75 \cdot 1.33 \ldots = 1.0$ liters/hour, $\underline{c}_{\text{dpd}} = \frac{4.85}{1.33} = 3.65$ g/liter, $\underline{c}_{\text{NaOH}} = \frac{9.60}{4.0} = 2.40$ g/liter

Time elapsed from the start of a test (in hours)	Concentration of diethylparaphenylenediamine (in g/liter)
0.00	4.85
0.50	4.00
1.00	3.40
1.50	3.03 **
2.00	3.03 **
2.50	3.03 **

Four such experiments were carried out in which the volume of the solution in vessel 1 was varied. The experimental conditions used, as well as the results obtained are given in Table 3.

DISCUSSION OF RESULTS

In our experiments we determined the values of the established concentration (k). On the basis of these, and using equation (1), and bearing in mind that $\alpha_1 = 0$ (since no useful reactions occur in vessel 1) we determined the values of α_2. These results are given in Table 4.

*Color developing material.

**Equilibrium state reached.

TABLE 3

Results of Experiments on the Oxidation of Diethylparaphenylenediamine by Oxygen

Volume of solution in vessel 1 (liters)	b (liters/hour)	c_{dpd} (in g/liter)	k_{dpd} (in g/liter)
0.5	1.0	3.65	3.03
1.0	1.0	3.75	3.18
2.0	1.0	3.65	3.10
3.0	1.0	3.65	3.13

As the results given in Table 4 show, the values of α_2 for thiosulfate and ferricyanide increase uniformly with increasing volume of the solution, and, for these materials the original assumptions are confirmed. In the case of developers, the reverse is true. Experiments show that the amount of developer oxidized by oxygen is independent of the volume of the solution. This may be explained by the fact that the amount of oxygen passing from the air into solution does not depend on the volume of the solution, but is determined by the area of contact between the solution and air, and this does not change with change in volume of the solution. Consequently, in those cases, where the amount in solution of a second participant in the useless reaction leading to expenditure of one of the components of the working solution, increases, proportionately to the increase in the volume of the

TABLE 4

Results of Determinations of the Values of $\bar{\alpha}_2$

Material		Values of k (in g/liter) and of α_2 (in g/hour) for various volumes of solution in vessel 1 for v values (liter)				
		0.5	1.0	1.5	2.0	3.0
Thiosulfate	k	45.83	44.12	40.84	37.00	—
	α_2	1.05	2.90	6.14	9.94	—
Potassium ferricyanide	k	15.78	15.16	14.01	12.82	—
	α_2	4.42	5.05	6.20	7.72	—
Hydroquinone	k	9.69	9.72	—	9.32	—
	α_2	0.33	0.30	—	0.41	—
Diethylpara-phenylenediamine	k	3.03	3.18	—	3.10	3.13
	α_2	0.62	0.57	—	0.55	0.52

solution, the yield of the useless reaction also increases. In the opposite case, the yield of the useless reaction does not depend on the volume of the solution. Thus an increase in the volume of the working solution leads to an increase in the expenditure of its components, in the case of bleaching baths and persulfate clearing, but does not lead to an increase in the expenditure of the components of developing solutions for black-white, and color films, and of fixing solutions.

Using the experimental results obtained, and on the basis of Equation (5), the velocity constants of the reaction between sodium thiosulfate and potassium ferricyanide were calculated, these values are given below.

Volume (in liter)	0.5	1.0	1.5	2.0
K (in liters/mole · sec)	0.00030	0.00032	0.00030	0.00045

K for the reaction between the developers and oxygen could not be calculated, since the oxygen concentration of the solution was not known.

SUMMARY

In accordance with theory, the useless expenditure of the components of a working solution increases with increasing volume of the solution. An exception is the case where the increase in volume of the solution is not accompanied by an increase in it, of the amount of materials participating in the useless reaction.

LITERATURE CITED

[1] I. Blyumberg, "Chemico-Photographic Processes of Treating Cine-Films", Moscow, (1949).*

[2] N. Kirillov and S. Antonov, "Processes of Color Photography", Moscow, (1951).*

Received October 29, 1955

* In Russian.

THE EFFECT OF TEMPERATURE DURING DETERMINATION OF THE MOISTURE CONTENT OF SULFONATE CATION EXCHANGERS ON THE ACCURACY OF DETERMINATION OF THEIR EXCHANGE CAPACITY

A. A. Vasilyev

Institute of High Molecular Weight Compounds Academy of Sciences, USSR

The fundamental index of ion exchange materials (ionites) is their exchange capacity, which enables one to assess the amount of ions extracted by ion exchangers from an electrolyte solution. For determination of exchange capacity, a number of methods have been suggested, which differ from each other in value and importance; hitherto, there has been lack of agreement of this question. Of considerable importance are those methods which allow the exchange capacity of ion exchangers to be determined on the basis of their content of functional groups. Thus, for sulfonate resins, the sulfonate group content is an important characteristic. This relates, in particular, to the so-called sulfonated phenolic resins, which in addition to the sulfonate groups, also contain phenolic hydroxyl groups, which only participate in ion exchange reactions at high pH values. A simple, and convenient method of determining exchange capacity as a function of the sulfonate group content of cation exchangers, is to titrate an aliquot of the cation exchanger in the H-form with alkali solution, in the presence of an excess of a neutral salt, and using methyl orange as indicator [1]. All the values quoted for exchange capacity in the present article were obtained by this method.

The following circumstance complicates determination of the exchange capacity of ion exchangers.

The exchange capacity is determined on air-dry samples of the ion exchangers, but it is thereby necessary to take into account the moisture content, i. e., to convert the value obtained to that for the dry ("absolutely dry") material. The values for the exchange capacity, when related to the weight of the air-dry material [2, 3], are arbitrary technical characteristics. In this connection, therefore, fairly accurate determination of the moisture content of ion exchangers is very important. A detailed review of existing methods of determining the moisture content of various materials is given in the article by Ryabchikov and Belyaeva [4].

One of the fairly widely used methods for determining the moisture contents of ion exchange resins is the very simple and rapid distillation method of Dean and Stark, which was recommended at one time as a standard [5]. Determination of the moisture content of ion exchangers by means of the Dean and Stark method, is suitable for giving an approximate idea of the characteristics of commercial products. Since it is assumed that sufficient amount of such products will be available for testing, 20-25 g of the test material can be used. The Dean and Stark method is, however, not capable of the accuracy which is sometimes required, particularly for the determination of the exchange capacity of the ion exchanger, when calculations are to be based on the weight of the dry material. While it is difficult to measure the amount of water distilled over in this method, another, added disadvantage, is the difficulty of accurately assessing the amount of moisture adhering to the condenser and receiver walls. The Dean and Stark method requires the use of a comparatively large amount of the test ion exchanger, and such an amount is not always available.

The most widely used methods for moisture content determination are those based on drying the test materials under differing conditions, when, however it comes to a choice of the best conditions for this purpose, there is disagreement. Thus, recommendations have been made that drying be carried out at: 95=100° [6], 100 ± 5° [7], 105 ± 2° [8], 105-110° [2], 115° [9], 110-120° [10], 120° [11]. Some authors recommend that the resins be dried

at normal temperature over phosphorus pentoxide, rather than use elevated temperatures [12, 13]; this, of course, takes longer.

Recommendations to the effect that all types of resin can be dried at one temperature, cannot be regarded as correct [6, 2], since such recommendations do not take into account differences in the thermal stability of resins belonging to various classes of organic compounds. Thus, in the case of some ion exchange resins, precautionary measures which are normally adopted for determination of moisture content, are uneccessary. On the other hand, some of the temperatures recommended may prove to be too high for other types of resins. Such temperatures may lead to appreciable decomposition of the materials, and to mechanical damage from cracking, and breaking up into dust. Revommendations to the effect that the ion exchangers be dried, not to constant weight, but for some arbitrarily determined time, e. g., eight hours [2] cannot be considered as correct either.

As a rule, the moisture content of ion exchange resins can be determined with appreciable accuracy, by drying them to constant weight at a temperature which is lower than the decomposition point of the resin being tested, and which has been established experimentally beforehand. Hitherto, little attention has been given to the thermal stability of ion exchange resins.

In theUSSR, Saldadze [14] started to study the thermal stability of ion exchange resins, nevertheless, further publications relating to the continuation of his work have not yet appeared.

The present article contains results of a study on questions relating to the drying conditions and thermal stability of ion exchange resins, in connection with determination of their exchange capacity. Sulfonate cation exchange resins were studied. T. V. Gerasimyuk and V. S. Matrosova participated in the experimental part of the work.

One of the fundamental criteria which has guided work during assessment of the chemical stability of ion exchangers, has been the absence of any decrease in the exchange capacity of the ion exchangers after various reagents had been allowed to react with them [3, 14].

We used the same criterion when trying to establish the thermal stability of cation exchangers when they are being dried for determination of their moisture content.

EXPERIMENTAL

At the same time as aliquots of the air-dry cation exchanger were taken for titration, samples (about 2 g) of the resin were taken for determination of their moisture content by drying in an oven to constant weight. In view of the high hygroscopicity of the materials, the beakers used for weighing were covered with lids before transferring them to the desiccators, they were cooled in the same state. When the samples had been dried to constant weight, the aliquots of dried material were transferred without loss to flasks and titrated with 0.1 N sodium hydroxide in the presence of 50-100 ml of 0.5 N sodium chloride, and methyl orange used as indicator (the conditions used were the same as those used for titration of the aliquots of air-dry material). The exchange capacities of these and other samples were then calculated and compared, in the case of the air-dry materials the figures obtained were converted to the standard of the dry material by taking into account the moisture content determined. Agreement between the exchange capacities of the air-dry material (calculated back on to the "dry" material),* and that dried in the oven, showed that drying of the resins only led to removal of water, and was not accompanied by decomposition of the resin. When, on the other hand, the exchange capacity of the dried samples was less than the capacity of the air-dry resins, this indicated that decomposition of the resin had occurred. The decomposition processes led to partial loss of sulfonate groups, consequently, the conditions employed for moisture content determination when such losses occur, are not suitable, because of the insufficient thermal stability of the resins under such conditions.

Most of the moisture content determinations carried out on sulfonate resins of different types were made at 105-110°; in the vast majority of cases no drop in the exchange capacity was observed when the cation exchangers were dried at these temperatures. Nevertheless, complete agreement between the exchange capacities of the air-dry and dried samples was comparatively rare. In most cases, a small, but quite definite increase in the exchange capacity of the dried samples as compared with the exchange capacity of the air-dry material, was observed (Table 1).

*In the subsequent text, in all cases where the air-dry cation exchanger is mentioned, the figures have been converted to the standard of the dry material.

TABLE 1

Changes in the Exchange Capacity of Sulfonate Cation Exchange Resins on Drying at 110°

Test cation exchanger	Exchange capacity (in mg-equiv/g)		
	air-dry cation exchanger (d)	dried cation exchanger (e)	$\frac{e}{d}$
Cation exchangers containing both SO_3H and phenolic-OH groups			
KU-1	2.26	2.50	1.10
MSF-3	1.63	2.00	1.23
PFSK	2.44	2.67	1.09
Duolite S-3	3.34	3.40	1.03
Cation exchangers containing SO_3H groups			
SBS	2.78	2.83	1.01
SBS-2	3.54	3.73	1.05
SBS-3	3.49	3.60	1.03
SBS-R	1.91	2.04	1.07
SDV-3	3.75	3.83	1.02
Dowex-50	4.98	5.10	1.02

TABLE 2

Effect of Duration of Heating at 110° on the Exchange Capacity of Type SN Cation Exchangers (Active Groups SO_3H and Phenolic OH)

Time of drying (in hours	Exchange capacity (in mg-equiv/g)		$\frac{e}{d}$
	air-dry cation exchanger (d)	dried cation exchanger (e)	
0	–	3.14	–
11.5	2.97	3.15	1.06
19	2.99	3.19	1.07
44	2.97	3.28	1.10
87	3.03	3.36	1.11
135	3.03	3.44	1.14

Continued heating at 110° led to a further increase in the exchange capacity of the dried sulfonate cation exchangers. The capacity changed very little in the case of air-dry samples, the capacity being calculated by taking into account the moisture content determined experimentally on samples which, after drying, were titrated, and for which there was established a gradually increasing value of the exchange capacity. What has been said is illustrated in Table 2, taking the sulfonated phenolic cation exchange resin SN as an example.

The reason for such an increase in the exchange capacity of the sulfonate cation exchangers subjected to heating, appeared, at first glance to be rather nebulous. It is difficult to conclude that the method used for determining the exchange capacity is not suitable for establishing the sulfonate group content of the cation exchangers [1]. It may be noted, however, that the nature of the "inactive" sulfur which is present in many sulfonate exchangers, and which is not determined by titration, is still far from clear. If it is assumed that heating of the

cation exchangers is accompanied by the formation of numerous cracks in the resin, then, it is possible that as a result of the drying active groups which were not previously available become manifest. The fact that the exchange capacity of air dry sulfonate cation exchangers does not change on grinding them, however, seems to contradict such an explanation. Further, sulfonate exchange resins are known (e. g., MSF, Wofatite R) in which the total sulfur content is very close to the sulfur content as determined by titration; nevertheless, the exchange capacity of such resins increase after drying.

The reasons for the increase in the exchange capacity of sulfonate cation exchange resins on drying, only became clear after experiments were carried out on regeneration of such samples, and after repeated determinations of their exchange capacity. It was found that the enhanced exchange capacity of samples heated in a drying oven, on regeneration, not only became equal to, but proved to be somewhat less than that of the original air-dry samples. What has just been said is illustrated by the figures given in Table 3.

TABLE 3

Effect of a Second Drying at 110° on the Exchange Capacity of Type SN Cation Exchange Resins

Duration of 1st drying (in hrs)*	Moisture content of cation exchange resin samples (%)	Exchange capacity of the samples (in mg-equiv/g)		Duration of 2nd drying (in hrs)	Moisture content of cation exchange resin samples (%)	Exchange capacity of the samples (in mg-equiv/g)	
		air dry	after drying			air dry	after drying
29	23.88	3.13	3.30	30	21.54	3.04	[3.21] **
54	24.47	3.09	3.35	54	21.67	2.98	[3.22]
72	23.78	3.11	3.42	72	21.48	2.95	[3.26]
96	23.76	3.11	3.43	96	21.36	2.91	[3.27]
112	23.74	3.11	3.47	112	20.93	2.95	[3.20]

*The samples used for the first drying treatment, for various time intervals, were taken from a common consignment of air dry material.

**The values for the exchange capacity given in square brackets, were calculated on the basis of the exchange capacity of cation exchange resin subjected to regeneration, and on the basis of the sulfuric acid content of the wash liquors (see Table 4).

As the results given in Table 3 show, only small variations in moisture content were observed for samples subjected to drying in the course of various time intervals, and, consequently, there are only small differences between the exchange capacity of air-dry samples (Column 2). Samples which had been dried in a drying oven and titrated, were subjected to regeneration, washing, and air drying, after which the exchange capacity of both the air dry samples (Column 7) and of samples dried under the conditions described (Column 8), was determined.

It is clear from the table that the exchange capacity of the air-dry samples (Column 7) was much lower than the capacity of the same samples, which was determined after they had been dried in a drying oven (Column 4), and was somewhat lower than the capacity determined for the original air-dry samples (Column 2). At the same time, during titration of samples dried for a new determination of their moisture content, there was again observed an increased value in the exchange capacity (Column 8).

The increase in the exchange capacities of sulfonate cation exchangers which occurs on drying them, can, presumably be explained as follows. Sulfonic acids are known to hydrolyze on heating in acid solution, and even in pure water [15]. When the sulfonate cation exchange resins are heated, as a result of the presence of water in the resin, or of the presence of water as vapor in the drying oven, partial splitting of the sulfonate groups should occur

$$RSO_3H + H_2O \rightarrow RH + H_2SO_4. \quad (a)$$

It is also possible that on heating sulfonate cation exchangers, sulfur dioxide may be formed, which is oxidized by atmospheric oxygen to form sulfur trioxide. The latter then gives sulfuric acid with water:

$$SO_2 + O + H_2O \rightarrow H_2SO_4. \quad (b)$$

Both of these processes, which lead to sulfuric acid formation, may accompany each other, and, under certain heating conditions, one or another may predominate.

One would also expect that some of the gaseous products formed during the splitting of the sulfonate groups, will be lost as a result of volatilization. Thus, if during calculation of the exchange capacity of a sulfonate cation exchanger, one takes into account the amount of water "held" (a) by the resin, or the oxygen and water held (b), then these values of the exchange capacity cannot be regarded as completely reliable.

When sulfonate cation exchangers which have been heated are titrated, both the sulfonate groups and the sulfuric acid contained in the resins will react with the alkali. For titration of a dibasic acid, naturally, double the amount of alkali will be used than for titrating a monobasic acid, which is the source of the dibasic acid. Thus the exchange capacity of the dried material will appear to be high. A cation exchange resin, which, after drying in an oven, is washed with water, does not exhibit this high exchange capacity.

Table 4 contains results for the exchange capacity for two consignments of type SN cation exchange resin. Samples from one consignment were heated at 110° for various time intervals, while the samples from the other consignment were dried at different temperatures over a period of 54 hours.

The results given in Table 4 show what good agreement exists between the values of the apparent exchange capacity as found by direct titration of the cation exchanger (e_1) and those calculated on the basis of the results of the determination of the exchange capacity of the cation exchanger which has been washed free of its decomposition products, and the results for the sulfuric acid content of the wash liquors (e_2).

A consideration of the tables leads one to the following conclusions. Continued heating at 110° leads to a gradual increase in the apparent exchange capacity of dried cation exchangers (e_1, e_2), in actual fact, the exchange capacity of these samples drops appreciably (by 8.5% after heating for 54 hours), since the amount of sulfuric acid split off increases (b, c). Nevertheless, with a slight exception (No. 3), the values for the exchange capacity of the air-dry samples determined directly (d_1), and calculated (d_2, d_3, d_4) are close enough together, and the changes in the apparent capacity of the dried samples are hardly reflected at all in them. The values which are in all probability the closest to the actual figures are those for the exchange capacity (d_2), calculated on the basis of the capacity of the resin samples washed free from its decomposition products, and of the sulfuric acid content of the wash liquors.

When the drying time is kept constant, but the temperature is increased, the apparent exchange capacity of sulfonate cation exchangers again increases. Under these conditions, as previously, there is observed satisfactory agreement between the values of the exchange capacity d_1, d_2, d_3, d_4 although even at a drying temperature of 100°, when the values obtained for the exchange capacity are particularly close to each other, partial decomposition of the cation exchange resin samples is still observed, and, consequently, there is an apparent increase in the exchange capacity of the dried samples. Drying at 150° led to no further increase in the apparent exchange capacity, and the drop in the exchange capacity was considerable.

Decomposition proceeds to an even greater extent at 170°, here, apparently, a considerable fraction of the decomposition products are removed together with the water. The value of the exchange capacity of air dry resin (No. 8, d_1) calculated on the basis of such a "moisture content", proved to be abnormally high, while, on the other hand, the apparent exchange capacity of the dried resin (No. 8, d_2) was lower than the exchange capacity determined for the air dry samples at lower drying temperatures (Nos. 4-7, d_1).

The extent of the change in the apparent exchange capacity of the dried sulfonate exchange resins depends, not only on the temperature at which drying is effected, but also on duration of drying. In a drying oven with improved circulation conditions, conditions for removal of the thermal decomposition products of sulfonate cation

TABLE 4

Calculation of the Exchange Capacity of Type SN Cation Exchange Resins Taking into Account the Sulfuric Acid Content of the Wash Liquors

Sample No.*	Drying conditions for the samples		Moisture content of cation exchange resin samples			Exchange capacity (in mg · equiv/g)									
	Temperature (in °C)	Time (in hours)	Determined by drying, a_1	corrections applied taking into account "held"*		the cation exchanger dried in oven and washed from decomp products, calc on basis of		according to results of H_2SO_4 determinations in wash liquors, calc. on basis of aliquot of dried resin, b_2	Cation exchanger, air dry				of the dried resin (apparent		Coefficient of apparent increase in the exchange capacity of the resin after heating e/d_1
				H_2O a_2	$O + H_2O$ a_3	aliquot of dried resin, with correction applied to H_2SO_4 liberated, b_1	aliquot of dried resin		from results of titration (taking the moisture content into account, a_1)	from exchange capacity of washed resin and H_2SO_4 content of wash liquors d_2**	corrected, taking into account "held"		from results of titration, e_1	from exchange capacity of the washed resin and the H_2SO_4 content of wash liquors, e_2**	
											H_2O d_3**	$O + H_2O$ d_4**			
1	110	30	21.54	21.90	22.22	2.85	2.80	0.41	3.04	3.00 (5)	3.06	3.07	—	3.21	1.05
2	110	54	21.67	22.12	22.52	2.76	2.71	0.51	2.98	2.96 (5)	3.00	3.02	—	3.22	1.08
3	110	96	21.36	22.21	22.39	2.73	2.65	0.62	2.91	2.96	2.95	2.95	—	3.27	1.12
4	100	54	24.11	24.51	24.88	2.74	2.69	0.45	2.90	2.89 (5)	2.92	2.94	3.14	3.12	1.08
5	110	54	24.96	—	—	—	—	—	2.93	—	—	—	3.25	—	1.11
6	130	54	24.68	25.52	26.27	—	—	0.94	2.92	—	2.95	2.98	3.41	—	1.17
7	150	54	25.01	25.93	26.75	2.52	2.40	1.02	2.94	2.91	2.98	3.01	3.42	3.42	1.16
8	170	54	27.37	28.13	28.80	2.45	2.36	0.84	3.03	2.78	3.06	3.09	3.23	3.20	1.05

*Samples Nos. 1, 2, and 3 belong to one consignment, while Nos. 4, 5, 6, 7 and 8 belong to another consignment of SN resin.

**Formulas used for calculating

TABLE 5

Effect of Drying at 110° on the Exchange Capacity of Sulfonate Cation Exchange Resins

Resin type	Sample No.	Drying time	Exchange capacity (in mg · equiv/g) of:		$\frac{e}{d}$
			air-dry resin (d)	dried resin (e)	
Sulfonate-phenolic cation exchange resin (active groups: SO_3H, phenolic OH)					
SN	1	39—44	4.06	4.53	1.11
	2		4.02	4.47	1.11
	3		3.99	4.37	1.10
	4		3.94	4.36	1.11
	5		3.89	4.24	1.09
	6		3.71	4.09	1.10
	7		3.63	3.94	1.09
SN-2	1	6—9	4.81	5.21	1.08
	2		4.67	5.02	1.08
	3		4.38	4.62	1.06
	4		4.29	4.68	1.09
SNF	1	26—33	4.12	4.59	1.11
	2		3.38	3.73	1.10
	3		3.06	3.44	1.12
	4		2.89	3.22	1.11
	5		2.79	3.15	1.13
	6		1.75	1.94	1.11
Mono-functional sulfonate resins (active groups SO_3H)					
SKhV	1	8—12 *	2.21	2.37	1.07
	2		2.02	2.23	1.10
	3		1.99	2.15	1.08
SSE	1	20	4.35	4.39	1.01
	2	19	4.20	4.26	1.015
	3	7	4.02	4.03	1.00
	4	10	4.00	3.99	1.00
	5	12	3.92	3.96	1.01
	6	12	3.56	3.60	1.01

* SKhV resins were dried at 105°.

exchange resins are facilitated. A decrease in the apparent exchange capacity of the resins can be observed at lower temperatures than those given in Table 4 for example. In the work described here drying of samples was carried out in a No. 3 drying oven from the "Electrodelo" factory.

The values given in Tables 2, 3 and 4 are those obtained for sulfonate phenol cation exchangers type SN. Tables 1, 5 and 6 contain results for some other sulfonate cation exchangers.

From the examples given in the Tables, it is clear that, as a rule, mono-functional sulfonate cation exchangers possess greater thermal stability than the sulfonate-phenolic cation exchangers (the coefficient of apparent increase in exchange capacity after heating, is less in the first than in the second). There are exceptions among the individual groups; thus, of three types of mono functional cation exchangers SKhV, SSF, and KU-2, the resins SSF and KU-2 are considerably more thermally stable than resin SKhV (Tables 5, 6).

Results of a study of the sulfonate-phenolic cation exchanger MSF are very illuminating. In this resin, a large part of the sulfur is contained in the sulfonate groups, and the value of the exchange capacity calculated on the basis of sulfur determination by elemental analysis, should not be less than the exchange capacity as determined by titration. From the results given in Table 6, it is clear how distorted are the values for the exchange capacity which are obtained on titrating samples subjected to drying.

TABLE 6

Effect of Drying Temperature on the Exchange Capacity of Sulfonate Cation Exchangers*

Mark of cation exchanger	Drying temperature	Loss in wt. on drying (in%)	Exchange capacity (in mg · equiv./g) of: air dry cation exchenge	Exchange capacity (in mg · equiv./g) of: dried cation exchanger (e)	e/d
MSF	100	21.56	2.48 **	2.67	1.08
	110	24.25		2.72	1.10
	150	24.53		2.14	0.86
	170	31.22		1.40	0.56
KU-2	100	—	4.84	4.86	1.00
	110	—	4.86	4.93	1.01
	120	—	4.89	5.01	1.02

*The drying time for the cation exchange resin MSF was 54 hours; for KU-2 46 hours. The samples of each cation exchanger were taken from one consignment.
**The exchange capacity of the cation exchanger MSF calculated on the basis of the total sulfur content was 2.62 mg-equiv/g.

SUMMARY

1. Heating of sulfonate cation exchange resins is accompanied by partial cleavage of sulfonate groups and, consequently, by a decrease in the exchange capacity of the cation exchange resins.

2. When sulfonate cation exchangers are heated at temperatures below 150°, the greater part of the sulfuric acid formed during the decomposition remains in the cation exchanger, and this leads to an apparent increase in the exchange capacity.

3. When sulfonate cation exchangers are dried for the purpose of determining the moisture content, e. g., for determining exchange capacity, then drying at 100-110° to constant weight is quite permissible. The partial decomposition of the cation exchanger which is observed during drying is not reflected in the accuracy of the determination of exchange capacity.

4. Various types of sulfonate cation exchangers differ appreciably in their thermal stability. As a rule, mono-functional sulfonate cation exchangers possess greater thermal stability than sulfonate-phenolic cation exchangers (the latter split off sulfonate groups as low as 100°).

5. The thermal stability of sulfonate cation exchangers under various heating conditions can be assessed, by comparing the exchange capacity of air dry cation exchangers, calculated on the basis of the dry material and the apparent capacity, determined for dried samples of the cation exchanger taken for determining the moisture content; both high and low values of the apparent exchange capacity indicate partial decomposition of the sulfonate cation exchangers.

LITERATURE CITED

[1] A. A. Vansheidt, A. A. Vasilyev and O. I. Okhrimenko, "Theory, and Practice of the Application of Ion Exchange Materials" Collection of Articles Izd AN SSSR, Moscow, 110 (1955).

[2] I. E. Apeltsin, V. A. Klyachko, Yu. Yu. Lurye and A. S. Smirnov, "Ion Exchange Resins and Their Application", State Publishing House of Literature on Standardization, Moscow, (1949).*

[3] E. B. Trostyanskaya, I. P. Losev and A. S. Tevlina, Progr. Chem. 24, 1, 84 (1955).

[4] D. I. Ryabchikov and V. K. Belyaeva, Progr. Chem. 24, 2, 240 (1955).

*In Russian.

[5] GOST 5695-52 (Introduced by AN SSSR). "Ion Exchange Organic Materials; Test Methods."*

[6] GOST 5695-51 (Introduced by the Ministry of Electric Stations) Cation Exchange Resins; Methods for Determining Qualitative Indices.*

[7] GOST 5695-53 (Introduced by the Ministry of Electric Stations) Ion Exchange Materials; Test Methods.*

[8] H. A. Shah, S. Y. Bafna, J. Indian Chem. Soc. 29, 3, 187 (1952).

[9] R. Kunin and R. Myers, "Ion Exchange Resins," IL, Moscow, 151 (1952).*

[10] E; R. Tompkins, J. Chem. Educ., 26, 1, 32 (1949).

[11] T. R. E. Kressman, and J. A. Kitchener, J. Chem. Soc., 1190 (1949).

[12] N. E. Topp and K. W. Pepper, Z. Chem. Soc., 3299 (1949).

[13] H. P. Gregor and J. I. Bregman, J. Am. Chem. Soc. 70, 2370 (1948).

[14] K. M. Saldadze, "Research in Chromatography," Collection of Articles, Izd. AN SSSR, Moscow, 114 (1952).

[15] Ch. Syuter, "Chemistry of Organic Sulfur Compounds," II, Izd. IL Moscow, 203 (1951).*

Received June 7, 1956

*In Russian

THE TECHNOLOGY OF THE POLYCAPRYLONITRILE FIBER NITRON (NITRILON)*

E. S. Roskin

The S. M. Kirov Leningrad Textile Institute

In a previous article [1], results were given of some studies carried out in the S. M. Kirov Leningrad Textile Institute, with the aim of establishing the conditions for the wet spinning of polycaprylonitrile fibers, and choosing precipitation baths which would ensure formation of a fiber possessing good technical and consumer properties.

The present article is devoted to the method of static polymerization of acrylonitrile already realized under industrial conditions, as a result of which a textile polymer is synthesized and then treated to give the fiber nitron.

By a textile polyacrylonitrile we have in mind a polymer which is readily soluble in dimethylformamide to form solutions which are stable with passage of time and are viscous, colorless, or slightly colored spinning solutions, and which can give high quality textile fibers.

Original products. Acrylonitrile $CH_2=CH-CN$. The technical, stabilized product was freed from inhibitor by shaking it up with 0.5% NaOH solution, it was then washed with water and distilled twice at atmospheric pressure. Since most of the work was carried out in aqueous solutions, the distilled acrylonitrile was not dried.

The dried acrylonitrile had the following characteristics: Boiling point 77°, d_4^{20} 0.8057, n_D^{20} 1.3912.

Potassium persulfate $K_2S_2O_8$. The material used contained 98-99% of the active persulfate.

Sodium hydrosulfite $Na_2S_2O_4$. The material used contained from 65-80% of active hydrosulfite, depending on the consignment.

Sulfuric acid. Chemically pure grade with a specific gravity of 1.84 was used.

Twice distilled water was used. Under production conditions, condensate was used.

EXPERIMENTAL

In order to compare the various methods of polymerizing acrylonitrile and to establish the best one, in the first stage of the investigation, polymerization induced by peroxide compounds was studied [2, 3].

During the second stage of the study, polymerization of acrylonitrile in emulsions and in aqueous solutions was studied, the polymerization being induced by oxidation - reduction systems in which potassium persulfate and sodium hydrosulfite were used.

It was found experimentally that agitation of the medium, as a rule, lengthened the induction period, or even stopped polymerization altogether. When the process was carried out with stirring, the polymer obtained was often only sparingly soluble in dimethylformamide.

The yields of polymer were always greater without stirring than with stirring.

Hunyar and Reichert [4], and also Aybar, Senvar and Akin (Turkey) [5], independantly came to the same conclusion regarding the polymerization of acrylonitrile without stirring.

*Part II of a series of papers on the polymerization of acrylonitrile and the formation of fibers based on it.

Rutkovsky and Goncharov [6] established the inhibiting effect of intensive agitation on the rate of heterophase, emulsifier-less polymerization in the case of methylmethacrylate.

A similar inhibiting effect is shown by ultrasonics (500-200 kilocycles) according to Aybar et al.[5], during polymerization of acrylonitrile and its aqueous solutions, in which hydrogen peroxide and ferric ions participate.

It is natural to speculate what sort of polymerization would occur in the case of a quiescent state of the reaction mixture, i. e., without agitation.

The combination of techniques related to carrying out polymerization in solution without agitation, such as heating, cooling, is termed the static method of polymerization by us. In fact, such polymerization occurs under semi-adiabatic conditions, since complete adiabatic conditions are destroyed by natural heat losses.

Testsshowed that during static polymerization, as established independantly by Hunyar and Reichert [4] as well, the concentrations of the oxidizing and reducing agents dropped, and this should lead to a slowing down of the polymerization process, and simultaneously to an increase in the molecular weight of the polymers. On the other handas the process is continued, heat of polymerization is liberated continuously, and under semi-adiabatic conditions, should lead to an increase in temperature of the reaction mixture, and consequently to a speeding up of the process, which in turn leads to a polymer with a low molecular weight.

Thus, during static polymerization, two conflicting influences are at work. It is essential therefore to find the optimum conditions for carrying out the polymerization, whereby the opposing influences counterbalance each other, and products which are homogeneous with respect to molecular weight are obtained.

A static method of polymerization has been realized by direct mixing of all the components of the mixture, and then allowing the mixture to stand in a quiescent state.

The kinetics of the static polymerization of acrylonitrile have been studied under semi-adiabatic conditions, i. e., under conditions similar to those used in production. Flasks with capacity ranging from 250-2500 ml were used for the work, the flasks being covered on the outside by a layer of asbestos. The experiments were carried out under conditions ensuring a constant external temperature, this being achieved by placing the flasks in a calorimeter in which the temperature was kept constant.

The rate of polymerization $\underline{w}$ is determined by the formula

$$w = \frac{d\eta}{d\tau},$$

where η is the fraction of the acrylonitrile which has reacted up to time τ, τ is the reaction time in minutes.

The value of η is found from the expression

$$\eta = \frac{\Delta t}{\Delta t_{\infty}},$$

where Δt is the increase in temperature of the reaction mixture measured with an accuracy of $\pm$ 0.05°, and Δt_{∞} is the maximum possible theoretical increase in the temperature of the mixture under the given conditions, for complete conversion of the monomer to the polymer.

Corrections for heat losses were applied to the values of the temperature found. Such a method of studying the kinetics of polymerization of acrylonitrile is sufficiently accurate and convenient, since acrylonitrile is comparatively readily soluble in water (about 7% by volume at 20°), and its heat of polymerization is 17.3 $\pm$ 0.5 cal/mole [7]. The induction period was taken as that interval of time between the addition of the last component to the reaction mixture (hydrosulfite) and the first appearance of turbidity in the solution. The duration of polymerization was measured from the end of the induction period.

When polymerization was complete, the contents of the flasks were filtered rapidly on a Buchner funnel. The polymer was washed with distilled water for complete removal of all impurities, after which it was dried to constant weight at 60-70°.

The first experiments showed poor reproductibility. It was established that in order to get reproducible results, it is essential to use freshly distilled acrylonitrile and water, and also to use hydrosulfite taken from the same consignment, which had been carefully stored in a stoppered container in the dark. Before carrying out a test it was essential to check on the content of $Na_2S_2O_4$ in the hydrolysulfite every time. Furthermore, it was found essential for each polymerization to adhere to the same order of addition of the components to the reaction mixture. Reproducible results are only obtained for processes which start off from the same initial temperature of the mixture, and for the same temperature of the external medium.

To illustrate the reproducibility of the processes of static polymerization, we have given results in Table 1 for increases in the temperature of the reaction mixture, related to equal time intervals of polymerization carried out in parallel experiments.

TABLE 1

Reproducibility of Results on Temperature Increases of the Reaction Mixture. (Water 100 g, acrylonitrile 8 g, H_2SO_4 (s. g. 1.84) 0.02 ml, sodium hydrosulfite 0.048 g, potassium persulfate 0.188 g)

Duration of polymerization τ (in min.)	No. of test						Mean temperature (°C)	Maximum deviation in parallel experiments
	I		II		III			
	temp. t (°C)	deviation from mean temperature	temp. t (°C)	deviation from mean temperature	temp. t (°C)	deviation from mean temperature		
0.0	25.0	0.0	25.0	0.0	25.0	0.0	25.0	0.0
1.8	25.0	—0.1	25.0	—0.1	25.2	+0.1	25.1	0.2
5.8	26.1	—0.1	26.2	0.0	26.3	+0.1	26.2	0.2
10.8	27.2	+0.2	27.2	+0.2	26.6	—0.4	27.0	0.6
15.8	28.3	+0.4	28.2	+0.3	27.4	—0.5	27.9	0.9
20.8	29.6	+0.3	29.7	+0.4	28.8	—0.5	29.3	0.8
25.5	30.9	+0.4	30.1	—0.4	30.5	0.0	30.5	0.4
30.8	32.5	+0.2	32.5	+0.2	31.8	—0.5	32.3	0.7
35.8	33.8	+0.3	33.5	0.0	33.2	—0.3	33.5	0.6
40.8	34.0	—0.1	34.0	—0.1	34.5	+0.4	34.1	0.5
45.8	36.0	+0.5	35.1	—0.4	35.3	—0.2	35.5	0.9
50.8	36.7	+0.3	36.7	+0.3	35.9	—0.5	36.4	0.8
55.8	37.0	+0.3	36.9	+0.2	36.2	—0.5	36.7	0.8
60.8	37.1	+0.3	37.1	+0.3	36.2	—0.6	36.8	0.9
65.8	37.0	+0.3	37.1	+0.4	36.2	—0.5	36.7	0.9

From the results given in Table 1, it is evident that parallel determinations of temperature did not differ by more than 0.2-0.9° from each other.

Sulfuric acid was added to the reaction mixture in order to control the pH of the medium. The effect of mixing, and of the initial temperature, and concentration of the components, on the rate of polymerization, the yield of polymer, and its molecular weight (specific or reduced viscosity) was studied. An attempt was also made to explain the nature of the elementary reactions which occur, and to establish the laws governing the kinetics of the process of static polymerization when the latter is carried out under semi-adiabatic conditions.

In all cases, apart from special ones, the tests were carried out with aqueous solutions of the following concentrations (in moles/liter): acrylonitrile 1.2, potassium persulfate $1.6 \cdot 10^{-3}$, sodium hydrosulfite $8.3 \cdot 10^{-4}$, and sulfuric acid $18.8 \cdot 10^{-4}$.

Figure 1 illustrates the effect of mixing on the yield of polymer when a stirrer was used for two hours.

It is clear from this Figure that for a stirrer rate higher than 120-140 revolutions/minute, polymerization did not occur. Maximum yield of polymer was obtained only when no stirring was used. All experiments started at 20°.

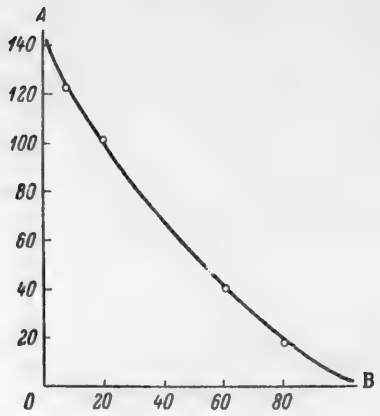

Fig. 1. Effect of mixing on polymer yield. A) Rate of rotation of stirrer (in revolutions per minute); B) yield (in %).

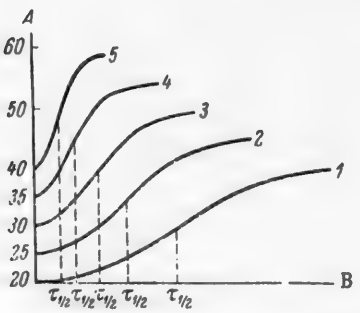

Fig. 2. Curves relating polymer yield to time. A) Temperature of the reaction mixture (in °C); B) duration of the process (in minutes). φ and $\tau_{1/2}$, respectively: 1) 0.035, 91; 2) 0.053, 59; 3) 0.070, 40; 4) 0.098, 25; 5) 0.150, 15.

As one would expect, increasing the working surface of the stirrer led to the same effect as increasing the number of revolutions.

In order to establish the effect of the working surface of the glass stirrers and of the glass of the reaction vessel, pieces of glass were introduced into the reaction mixture. It was found, in many cases, that increasing the surface of contact between the reaction mixture and glass had practically no effect on the polymerization rate.

In Figure 2 are given kinetic curves of polymerization carried out at initial temperatures of 25, 30, 35 and 40°. As the curves show, the yield of polymer and the reaction rate increased with increasing initial reaction temperature. A characteristic feature of the curves is the break which corresponds to the maximum polymerization rate, this is especially noticeable in the case of the lower initial temperatures, as is clearly shown in Figure 3.

Figure 4 illustrates the relation between the logarithm of the initial polymerization rate and 1/T. The initial rate of the reaction (w) was determined graphically, by starting from the part of the curve corresponding to the first 10-15 minutes of the process, and was also determined analytically. The activation energy which was determined graphically, and, analytically by the Arrhenius equation, proved to be 11.1 kilo calories/mole.

In Figure 5 are shown the kinetic curves of polymerization related to various initial temperatures. During the polymerization process, samples of the reaction mixture were taken, together with polymer, they were diluted with five-seven times their amount of cold water and rapidly filtered on a Buchner funnel. The value of the viscosity (η_{specific}/c) was determined for each sample of polymer.

The points on Figure 5 relate to the samples taken, and the appropriate value of the viscosity η_{specific}/c given relative to concentrations of 0.1 g/100 ml. Samples of polymers with reduced viscosities which differ between each other by 0.1-1.5% correspond only to one curve (initial temperature 35°). In all the remaining cases we have samples of polymers which differ considerably in the values of their reduced viscosities.

In Figure 6 are given curves relating changes in the rate of polymerization with time for processes with different initial temperatures of polymerization. Calculations of the rates was made graphically and analytically.

From Figures 2, 3 and 6 it is clear that to each curve there corresponds a maximum reaction rate, which only occurs when about half of the monomer taken initially has reacted. For each case we have

$$A\tau_{\frac{1}{2}} \cong \frac{A}{2},$$

where $\tau_{1/2}$ is the time corresponding to the maximum rate of the process, or the period of half-conversion; and A is the amount of the monomer taken initially.

In Figure 7 is shown the relation between the induction period and the initial polymerization temperature. The duration of the induction period depends, other conditions being equal, on the initial temperature of the process, being shorter the higher this temperature.

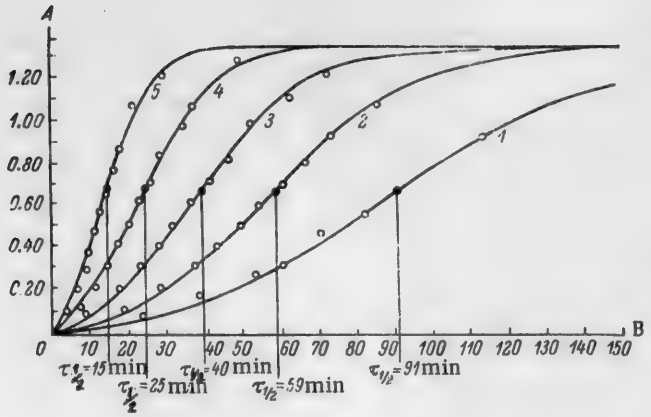

Fig. 3. Comparison of curves for the yield of polymer as a function of time. A) Quantity of reacted monomer (in g mole/liter), B) Duration of process (in min). Initial temperature $t_{init.}$ (in °C): 1) 20, 2) 25, 3) 30, 4) 35, 5) 40.

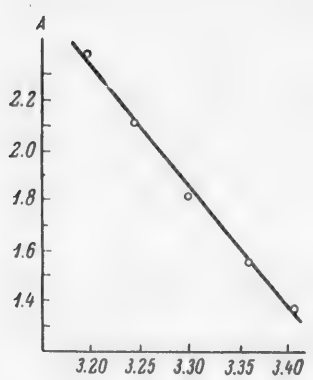

Fig. 4. Relation between the logarithm of the initial polymerization rate and the value of the inverse of the temperature. A) The value of logarithm $W_{init.} + 4$; b) the value of $\frac{1}{T} \times 10^3$.

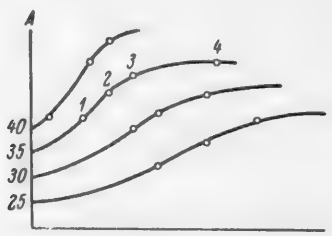

Fig. 5. Curves relating polymerization kinetics and reduced viscosities of the polymer. A) Temperature of the reaction mixture (in °C); B) duration of process (in minutes). Viscosity $\eta_{spec/c}$: 1) 5.482, 2) 5.501, 3) 5.504, 4) 5.509.

In Figure 8 is shown the relation between the value of the molecular weight of the polymers and the concentration of persulfate, for constant amounts of hydrosulfite and monomer. At the lower amounts of persulfate there is observed a sharp increase in the molecular weight of the polymers.

In Figure 9 is shown the relation between the logarithm of the initial rate of polymerization and the logarithm of the monomer concentration. On the basis of this relation, the order of the polymerization reaction with respect to the monomer was found. It proved to be equal to 1.1 . Table 2 contains some results characterizing the kinetics of static polymerization of acrylonitrile under semi-adiabatic conditions.

In order to develop an industrial method for static polymerization of acrylonitrile, tests were transferred from the laboratory to a production scale. The change over from small laboratory volumes to industrial reactors, with volumes of up to 1.5 m^3, and to other factory apparatus, showed that, for correct organization of a

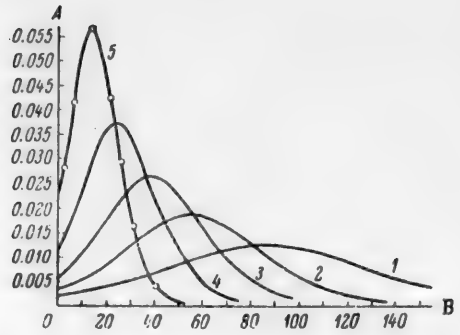

Fig. 6. Curves for change in polymerization rate with time. A) Polymerization rate $\underline{w}$ (in g·mole/liter·minute); B) duration of process (in minutes). Initial temperature $t_{init.}$ (in °C): 1) 20, 2) 25, 3) 30, 4) 35, 5) 40.

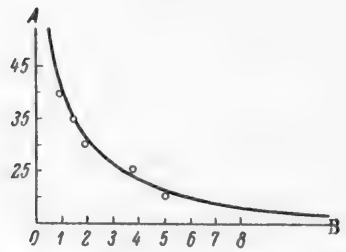

Fig. 7. Change in induction period in relation to the initial temperature of polymerization. A) Initial temperature (in °C); B) duration of the induction period (in minutes).

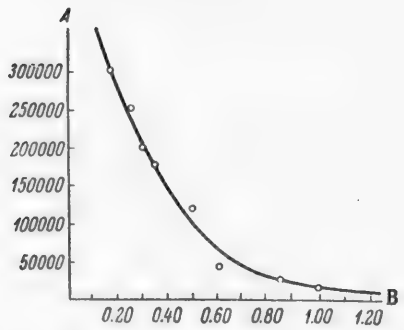

Fig. 8. Effect of potassium persulfate concentration on molecular weight. A) Molecular weight; B) potassium persulfate concentration (in g/liter).

process ensuring production of a textile polymer, it was necessary, not only to increase the amounts of the reaction mixture proportionally, but, to develop additional conditions, and to introduce corrections to the available laboratory results, this is a consequence mainly of changes in heat transfer conditions. This, in turn, was reflected in the kinetics of the process, in the yield of polymer, and the duration of the process [8].

In Figure 10 is shown the effect of hydrosulfite and sulfuric acid on the specific viscosity of a 0,5% solution of polymer in dimethylformamide. As this figure shows, sulfuric acid and sodium hydrosulfite act in opposite directions on the value of the specific viscosity of the polymer. By changing the content of the components of the reaction mixture it is possible to obtain polymers whose molecular weight or specific viscosity fall within the limits given earlier for these indices. Taking into account specifically, work under production conditions, we can recommend the following procedure and conditions for static polymerization of acrylonitrile (based on 100 liters of water): water (condensate) 100 liters, acrylonitrile 7.0-7.4 kilograms, sulfuric acid (s. g. 1.84) 20-25 ml, sodium hydrosulfite 25-30 g, and potassium persulfate 75-80 g.

The initial temperature of polymerization is 20 ± ± 1°. Using the conditions recommended a 98% yield of polymer is obtained when polymerization takes 70-80 minutes, while the induction period is 0-1 minute. The molecular weight of the polymer thereby produced is about 35,000.

The molecular weight was determined from the formula $[\eta] = 1.75 \cdot 10^{-3} M^{0.66}$, while the value of $[\eta]$ was calculated from the formula $[\eta] = \frac{\alpha [\eta]_2 - [\eta]_1}{\alpha - 1}$, [9], [10], where $[\eta]$ is the reduced viscosity for the first concentration η_{1spec}/c_1, $[\eta]_2$ is the reduced viscosity for the second concentration η_{2spec}/c_2, and α is the ratio of the first concentration to the second (c_1/c_2).

DISCUSSION OF RESULTS

It is known that polymerization in the presence of oxidation-reduction systems differs mainly from polymerization induced by peroxides, only in the mechanism of the formation of free radicals [11, 12].

The total activation energy (E_{total}) of the processes of polymerization of acrylonitrile depends on the nature of the induction, and its value is spread over fairly wide limits.

Thus, according to the results of Gritsenko and Medvedev [11], E_{total} in the case of induction by cumene

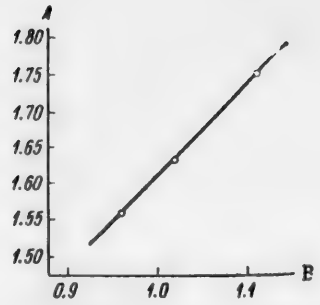

Fig. 9. Relation between the logarithm of the initial polymerization rate and the logarithm of the monomer concentration A) Values of logarithm $W_{init} + 4$; B) values of logarithm $\underline{c} + 1$.

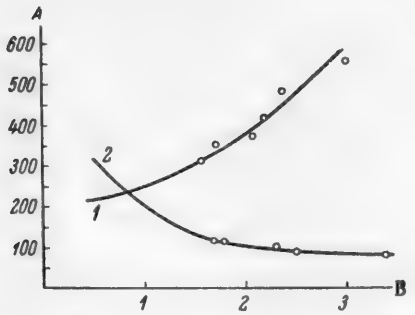

Fig. 10. Effect of H_2SO_4 and sodium hydrosulfite concentrations on specific viscosity. A) Concentration (in g·mole/liter·10^5); B) specific viscosity. 1) H_2SO_4; 2) sodium hydrosulfite.

hydroperoxide alone, is equal to 10.1 kcal/mole, while when hydroquinone is also added [12] the value is 7.2 kcal per mole. On induction by means of potassium persulfate E_{total} is equal to 14.2 kcal/mole [13]. Use of $Fe^{+++} + H_2O_2$ for induction increases the value of E_{total} to 20 kcal/mole [5]. According to our results, E_{total} has the value 11.1 kcal per mole when persulfate and hydrosulfite are used in the static polymerization of acrylonitrile.

The differences in the value of E_{total} testify to the differences in activation energy (E) in reactions involving formation of free radicals, and, consequently, to differences in the mechanisms corresponding to these reactions.

The comparatively low value for E_{total} in the process which we have studied, leads one to conclude, in accordance with the work of Gritsenko and Medvedev, that formation of radicals inducing polymerization of acrylonitrile, occurs as the result of a bimolecular interaction of potassium persulfate with sodium hydrosulfite.

It is possible that, initially, the persulfate ion $\overline{\overline{S_2O_8}}$ dissociates into the sulfate ion and sulfur tetroxide $\overline{SO_4}^+$ which is a strong oxidizing agent

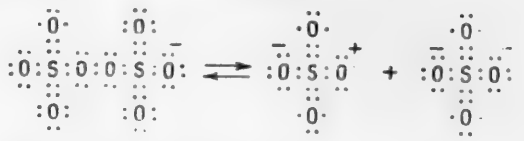

The sulfur tetroxide formed SO_4^+ as a strong electron acceptor seizes one of the electrons on the $\overline{S_2O_8}$ ions and in this way the radical ions $\overline{S_2O_8}$ and $\overline{SO_4}$ are formed.

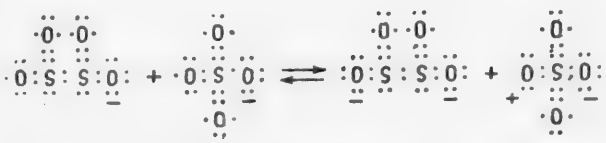

The radical ion $\overline{S_2O_8}^{\cdot}$ changes over into the more stable $\overline{SO_4}^{\cdot}$ radical ion with liberation of an atom of sulfur

The $\overline{SO_4}^{\cdot}$ radical ion seizes one electron from the oxygen of water and changes over into the valency saturated ion $\overline{\overline{SO_4}}$ with formation of a hydrogen ion and a free radical $OH^{\cdot}$

TABLE 2

Some Results on the Kinetics of Static Polymerization of Acrylonitrile

Initial temperature of polymerization	Induction period of polymerization	Half conversion period	Constants				
t_{init} (°C)	τ_{ind}	$\tau_{\frac{1}{2}}$	φ	$a = \frac{1}{1+e^{\tau_{1/2}\varphi}}$	$K = \frac{4w_{1/2}}{(A-B)^2}$	$B = A \cdot a$	$K_0 = BK$
	(in min.)						
20	5.0	91	0.035	0.040	0.0248	0.055	0.0014
25	4.0	59	0.053	0.042	0.0370	0.058	0.0021
30	2.0	40	0.070	0.057	0.0507	0.078	0.0040
35	1.5	25	0.0975	0.080	0.0681	0.110	0.0075
40	1.0	15	0.150	0.105	0.0990	0.144	0.0143

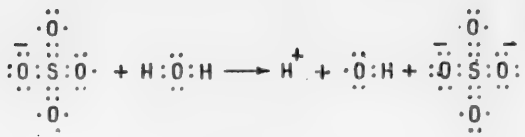

As a result we have the following over-all reaction.

$$\overline{\overline{S_2O_8}} + \overline{\overline{S_2O_4}} + 2HOH \rightarrow 3\overline{\overline{SO_4}} + S + 2H^+ + 2OH^\cdot.$$

Formation of hydrogen ions has been shown experimentally by the decrease in the pH of the medium during polymerization. It is also readily demonstrable that free sulfur is present in the reaction medium.

A reaction following this mechanism would appear to be energetically favorable for compensating the energy expended on formation of the free $OH^\cdot$ and $\overline{\overline{SO_4}}^\cdot$ radicals, as the result of the hydration of hydrogen and sulfate ions.

According to Mishchenko's results, the heat of hydration of H^+ and $\overline{\overline{SO_4}}$ ions is 110 and 243 kcal/g·ion [14].

It can also be assumed, taking into account the low value of E_{total} for our case, that the reason for the primary act of development of free radicals, is the formation of an activated complex during the interaction of the oxidizing agent with the reducing agent according to the scheme

$$\overline{\overline{S_2O_8}} + \overline{\overline{S_2O_4}} \rightleftarrows \begin{matrix} SO_4—SO_4 \\ | \quad\quad | \\ SO_2—SO_2 \\ : \quad\quad : \end{matrix}$$

complex

and further, complex + 2HOH → $3\overline{\overline{SO_4}}$ + S + $2H^+$ + $2OH^\cdot$.

Thus, one can imagine the following elementary reactions occurring during the polymerization process

$$O + B \xrightarrow{K_{OB}} R^\cdot \quad (I) \qquad R^\cdot + M \xrightarrow{K_M} M_1^\cdot \quad (II) \qquad M_1^\cdot + M \xrightarrow{K_p} M_2^\cdot; \qquad M_2^\cdot + M \xrightarrow{K_p} M_3^\cdot,$$

$$M_{n-1}^\cdot + M \xrightarrow{K_p} M_n \quad (III) \qquad R^\cdot + R^\cdot \xrightarrow{K_0'} 2R \quad (IV) \qquad M_p^\cdot + Mq^\cdot \xrightarrow{K_0''} P, \quad (V)$$

where O is the oxidizing agent, R is the reducing agent, $M^{\cdot}_{r}$ is the polymeric free radical. The S-shaped curves for the kinetics of polymerization under semi-adiabatic conditions show that the development of the reaction with time follows the law $e^{\varphi t}$ (where φ is the constant, and t is the time)..

Analysis of the curves shows that they correspond to an equation which formally coincides with the equation of Shilov and Semenov for the case of branched chains of autocatalytic, self accelerating, reactions with degenerated branches [15].

Such an empirical equation is of the form

$$\frac{d\eta}{dt} = AK(1-\eta)\left(\frac{K_0}{KA}+\eta\right), \tag{1}$$

where η is the fraction of reacted monomer, A is the initial amount of monomer, and K_0 and K are constants.

The differences between Equation (1) and the usual Shilov-Semenov equations, are that the former relate, not to isothermal reaction conditions, but to semi-adiabatic conditions, and, in that sense, the constants in the equation are different.

By integration of Equation (1), according to Semenov, under conditions where t = 0 and η = 0, we get [16]

$$\eta = \frac{\frac{K_0}{KA}\left(e^{(K_0+KA)t}-1\right)}{1+\frac{K_0}{KA}e^{(K_0+KA)t}}. \tag{2}$$

Introducing the designations $K_0 + KA = \varphi$, $\frac{K_0}{KA} = a$, ("dimensionless time") we get

$$\eta = \frac{a(e^{\tau}-1)}{1+ae^{\tau}}. \tag{3}$$

When $e^{\tau} >> 1$, we get the approximate equation

$$\eta' = \frac{ae^{\tau}}{1+ae^{\tau}} = \frac{1}{1+1/ae^{-\tau}}$$

and, finally, for $ae^{\tau} = 1$ and $\eta' = 0.5$, we get

$$\eta' = \frac{1}{1+e^{-(\tau-\tau_{max})}} = \frac{1}{1+e^{-\theta}}, \tag{4}$$

where $\theta = \tau - \tau_{max}$.

As is evident from the diagrams given in the text, the curves obtained experimentally coincide well with the curves corresponding to Equations (3) and (4). In exactly the same way, we have good agreement between the curves obtained experimentally for changes in polymerization rate with the analogous curves corresponding to the equations adduced.

As tests showed, inhibition of the polymerization reaction, which occurs on agitation, does not only occur during work in open vessels, when it is possible that atmospheric oxygen may be trapped by the stirrer blades, the oxygen being a strong inhibitor of polymerization. A similar inhibiting effect is also observed in the course of work with closed vessels, the contents of which were stirred by means of an electromagnetic stirring, and by shaking, etc.

This means that the process of agitation itself inhibits the polymerization reaction. It is possible that the inhibiting action of agitation can be explained by an increase in the fracture rate, which is connected with an increase in the rate of coalescence processes of polymer particles containing in themselves the growing polymeric chain.

On the basis of the suggested equation for polymerization kinetics, the values of the initial and maximum rates were calculated.

Below is given a comparison of calculated and experimental results:

Initial temperature (in °C)	Initial rate (in moles per liter · minutes)		Maximum rate (in moles per liter · minutes)	
	experimental	calculated	experimental	calculated
20	0.0025	0.0022	0.0093	0.0127
25	0.0034	0.0035	0.0186	0.0192
30	0.0120	0.0058	0.0244	0.0252
35	0.0124	0.0115	0.0361	0.0374
40	0.0241	0.0237	0.0535	0.0569

V. V. Darvin, V. V. Averyanova, S. N. Dmitrieva who are scientific co-workers at the Institute, and engineers E. A. Kulev and A. I. Konkhin took part in the work.

SUMMARY

1. It has been shown that the kinetics of static polymerization of acrylonitrile under semi-adiabatic conditions, are similar to the kinetics of polymerization under isothermal conditions.

2. It has been shown that agitation has a negative effect on polymerization of acrylonitrile, and on the properties of the polymer obtained.

3. An industrial method has been developed for synthesizing textile polyacrylonitrile by static polymerization methods.

LITERATURE CITED

[1] E. S. Roskin, J. Appl. Chem. XXX, 1, 124 (1957).

[2] E. S. Roskin, Reports of the S. M. Kirov Leningrad Textile Inst. 39 (1954).

[3] E. S. Roskin, Trans. Leningrad Textile Inst. 5, 77 (1955).

[4] A. Hunyar, and H. Reichert, Faserforsch. u. Textiltechn., 5, 1 (1954).

[5] S. Aybar, C. B. Senvar and C. Akin (univ. Ankara, Turkey) Communs. fac. Sci. univ. Ankara, 413, (1952); Ch. A., 48, 7928 (1954).

[6] B. N. Rutkovsky and G. S. Goncharov, J. Appl. Chem. XXVI, 434 (1953).

[7] A. P. Terentyev and A. N. Kost, Collection "Reactions and Methods of Studying Organic Compounds, Cyanoethylation Reactions," Goskhimizdat (1952).*

[8] E. S. Roskin, Textile Industry 11 (1956).

[9] E. S. Roskin, ZhKKh,** 15, 455, (1953).

[10] E. S. Roskin, ZhKKh,** 18, 369 (1956).

[11] T. M. Gritsenko and S. S. Medvedev, J. Phys. Chem. 30, 1238 (1956).

[12] T. M. Gritsenko and S. S. Medvedev, ibid., 30, 1513 (1956).

[13] P. M. Khomikovsky and S. S. Medvedev, J. Phys. Chem. 22, 1027 (1948).

*In Russian.

** Transliteration of Russian journal is unverified — Publisher's note.

[14] K. P. Mishchenko, J. Phys. Chem. 26, 1736 (1952).

[15] N. N. Semenov, "Chain Reactions," Goskhimtechizdat (1934).*

[16] N. N. Semenov, J. Phys. Chem. 27, 899 (1953).

Received October 12, 1955

*In Russian.

WATER PERMEABILITY OF PLASTICIZED COMPOSITIONS*

Sh. L. Lelchuk and V. I. Sedlis

Scientific Research Institute of Polymerized Plastics

The problem of protecting instruments, apparatus, and various metal articles from the action of the weather is of great economical importance.

As practice and special studies have shown, the methods which have been in wide use hitherto, for protecting metallic articles from corrosion, and which include covering the articles with a copious coat of grease, fat, mineral oils, etc, are not completely reliable, and often fail because of the inadequate water stability of such coatings [1].

Recently, the use of film materials made from organic high polymers for protecting metallic articles from corrosion as a result of atmospheric agents, in the first instance from atmospheric moisture, has become widespread. With this aim in view a number of moisture-resistant film materials have been developed for packing and protecting metallic articles and aggregates. It is understood that these materials should exhibit a fairly low moisture permeability, which is characterized by the amount of water vapor penetrating through the protective film in a definite, but fairly long time (from a storage point of view) into an inner space confined by a protective film.

There is a fairly rich literature on the question of the moisture permeability of various high polymers.

Table 1 contains some results for the coefficient of water permeability P for various organic film-forming polymers used in practice.

It is clear from the results given in Table 1 that organic polymers do not possess absolute water impermeability. All of them, to varying degrees, are permeable to water vapor, but differ considerably in their water permeability. Polyisobutylene and polyethylene are the ones which are least permeable to water; the latter, as a result of this fact, and also on account of its outstanding physicomechanical properties is, at the moment, the most effective and valuable moisture proof packing material.

Polyvinylchloride (PVC) is also deserving of attention on account of its low water permeability. It is one of the most important and widely used polymers for the preparation of moisture resistant films and packaging materials. This is a result of its valuable physicomechanical and chemical properties (high mechanical stability, chemical stability, stability to the action of mineral oils, benzine, and also ozone), in addition to its low water permeability, and favorable economic factors (availability, comparative cheapness, plentiful supplies of raw materials).

It would, however, be wrong to be guided solely in the choice of a satisfactory moisture resistant material by the numerical values of the coefficient of water permeability, such as those given in Table 1 for example. Actually, many of the materials listed, including cellulose esters and polyvinylchloride are rarely used for moisture resisting purposes in their pure forms, but are normally used as compositions which contain appreciable amounts of plasticizers. The latter are added to the polymers in order to give the compositions the necessary physicomechanical properties (mainly, pliability, elasticity, frost resistance), and also for lowering the temperature at which the material is processes, for facilitating rolling, calendering, extrusion etc. This refers in particular to polyvinylchloride, which, in the unplasticized form, is hard and brittle at room temperature, and requires a very high temperature, approaching its decomposition, for its processing. The plasticiers added, however, strongly

*Part II of a series of papers on studies relating to the effects of plasticizers on the properties of polyvinylchloride.

TABLE 1

Coefficient of Water Permeability P for Various Film-Forming Materials

Material	$P \cdot 10^9$ ($g \cdot cm^{-1} \cdot hour^{-1} \cdot mm\ Hg$) at 20°
Polyisobutylene (oppanol)	0.2*
Polyethylene	0.2
Vinifol (chlorinated polyvinylchloride)-perchlorvinyl	0.2-0.6
Polystyrene (styroflex)	3.5-4
Polyvinylchloride	0.5
Polyvinylchloride-acetate 95:5	0.7
Benzylcellulose	10.6 [3]
Nitrocellulose	22.5 [2]
Ethylcellulose	77 [2]
Acetylcellulose (triacetate)	71 [2]
Acetylcellulose (diacetate)	114
Cellulose acetobutyrate	52 [2]
Cellophane	260
Polyvinylacetate	30 [2]
Polyamide resin	11 [2]
Bituminous compounds	1-2 [3]

* The coefficients which do not have a reference against them were determined by the authors of the present article.

modify all the physicomechanical properties of the polymer, including its water permeability, in the majority of cases, the water permeability increases. Sometimes, however, this fact seems to be forgotten, and the choice of materials with low water permeability is governed by the values published for the pure polymer, and now and again this leads to trouble.

There is a fairly large amount of published data on the water permeability of various materials, studies have been published which deal with the connection between the chemical structure of polymers and their water permeability [2-7], the results have been given for the values of the coefficients of water permeability of various materials. There is, however, either very little, or no information, on the effect of plasticizers on water permeability.

The present article is devoted to the study of the effect of plasticizers on the water permeability of polyvinylchloride films.

Fundamental Water Permeability Equations

Diffusion phenomena are described by the following fundamental equations of Fick:

$$P = -D\frac{\partial c}{\partial x}, \qquad (I)$$

$$\frac{\partial c}{\partial t} = D\frac{\partial^2 c}{\partial x^2}. \qquad (II)$$

The solution of these equations for the case of a stationary regime leads to a formula which can be used in a number of practical cases for determination of the water permeability of a material

$$Q = \frac{P \cdot S \cdot \Delta p \cdot t}{d}, \qquad (III)$$

from which, the coefficient of water permeability P is determined by means of the formula

$$P = \frac{Q \cdot d}{S \cdot \Delta p \cdot t} \quad g/cm \cdot hour \cdot mm\,Hg \qquad (IIIa)$$

where P is the coefficient of water permeability, Q is the amount of moisture which has diffused through the membrane (in g), d is the thickness of the membrane (film) (in cm), S is the area of the membrane (in cm^2), t is the time (in hours), Δp is the difference in pressure of the water vapor on both sides of the membrane (in mm Hg).

The coefficient of water permeability is also expressed by the equation

$$P = Dh \qquad (IV)$$

where D is the diffusion coefficient, and h is the solubility coefficient.

The solubility coefficient h on the basis of Henry's law, can be determined by means of the formula:

$$h = \frac{\Delta g \cdot \gamma}{g \cdot p} \quad g/cc \cdot mm\,Hg \qquad (V)$$

where g is the initial weight of the sample (in g), Δg is the change in weight of the sample at the saturation point (in g), γ is the specific gravity of the sample (in g/cc), and p is the pressure of water vapor (in mm Hg).

The expression P = Dh has a definite physical meaning. Passage of moisture is nonexistent when one of the factors is zero.

The mechanism of water permeability, under such conditions, is based on ideas regarding sorption-desorption phenomena [6]. The phenomenon of activated diffusion consists of three successive processes: 1) sorption of vapor on one side of a film (dissolution in the film); 2) passage (diffusion) of the dissolved material inside the film in the direction of decreasing concentration of the dissolved material; 3) desorption of the dissolved material on the other side of the film, not subjected to the action of a high concentration of vapor.

The mechanisms of diffusion itself can be represented as follows [8] – adsorbed molecules of vapor move forward in the direction of decreasing vapor concentration. As a result of the thermal movement of the mobile molecules of the polymer in the material, there are formed temporary canals through which the water molecules move forward. It is understandable that with increasing mobility of the macromolecule, e. g., at elevated temperature, or during the efficient plasticization of the polymer molecules, formation of such temporary canals will be facilitated, and the probability of their subsequent formation will be higher, consequently, the rate at which water passes through, i. e., diffusion and water permeability, will increase.

EXPERIMENTAL

Methods for determining constant permeability (P). There are several methods for determining the permeability of water vapor through films, they can be divided into two main groups, which are based on different principles of measurement: 1) gravimetric methods, and 2) methods of measuring pressure.

The most widely used and simplest method is the gravimetric method of determining P, i. e., the direct determination of the moisture which passes through the sample in a given time. Methods of determining P which involve measurement of the vapor pressure are more sensitive, but are more complicated to carry out.

In the work described here, the gravimetric method, in two variants, was used for studying the water permeability of polyvinylchloride films: a) bags, which allow mass tests to be carried out were used; this technique is particularly suitable under factory conditions; b) specially constructed aluminum beakers were used, this allows simultaneous determination of sorption and diffusion of vapor; this second variant was designed for more accurate studies. Results of tests by both methods, in most cases, were in agreement within the limits of experimental error.

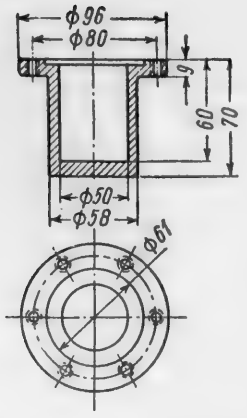

Apparatus for determining the water permeability of films.

Determination of water permeability. The apparatus consisted of an aluminum beaker (diagram) 70 mm long and 50 mm internal diameter, it was provided with a flange having a turned edge 5 mm wide and a clamping ring with an internal diameter of 50 mm. A glass weighing bottle without its lid, and containing water absorbent material was placed in the aluminum beaker. The water absorbent material used was dehydrated (calcined) cupric sulfate ($CuSO_4$), or, more accurately, the monohydrate of the latter ($CuSO_4 \cdot H_2O$). The sample of test film, 60 mm in diameter, was placed on the flange of the beaker and slowly compressed with the clamping ring by means of bolts. The gap between the flange and the clamping ring was filled with paraffin or some other pourable water-impermeable material (for example, a mixture of polyisobutylene and halowax). The assembled apparatus was placed in a hydrostat (in a desiccator) over water, at a constant vapor pressure, at constant temperature. After certain time intervals, from 1 to 7 days, the weighing bottle plus the water absorbent material was withdrawn from the apparatus and weighed on an analytical balance to an accuracy of $1 \cdot 10^{-4}$ g; the increase in weight gave the amount of the water vapor that had penetrated through the films, i. e., the water permeability. At the same time, the film itself was weighed, the increase in weight in this case gave the amount of water sorbed by the film (water absorption).

When a stationary state had been achieved for the process of water penetration, the coefficient of water permeability P was calculated by means of Equation (IIIa).

The relation between the water permeability of polyvinylchloride and the content and chemical nature of the plasticizer. The water permeability of films of high molecular weight compounds (polymers) depends on the molecular structure, which is determined primarily by the flexibility of the molecular chains and by the value of the intermolecular forces. Since addition of plasticizers to polymers is characterized by a decrease in the intermolecular forces, and by an increase in the flexibility of the molecular chains [9], one would expect the water permeability of the polymers to increase. The water permeability, as well as other physicomechanical properties of the compositions, depend on the nature of the plasticizer used, particularly on its efficiency. In order to clarify this relation it is necessary to choose a rational criterion for efficiency, which would actually reflect the nature of the plasticizer and the effect of its interaction with the polymer, and would be a characteristic constant of the plasticizer. We found that such a characteristic constant is the drop in vitrification temperature (ΔT_{vit}) of the composition which is caused by the addition of 1 mole % of a plasticizer, i. e., the value $T_{vit} = T_{vit_0} - T_{vit_1}$, where T_{vit_0} is the vitrification temperature of the pure polymer, and T_{vit_1} is the vitrification temperature of the plasticized polymer containing 1 mole % of the given plasticizer. We have called this value the efficiency number (Э) of the plasticizer [10].

Table 2 contains the efficiency numbers for the most important plasticizers. These numbers were determined for the system polyvinylchloride – plasticizer. It is understood that these numbers will be different for a system containing another polymer.

The water permeability of polyvinylchloride films depends primarily on the amount of plasticizer in the composition, and on the chemical nature of the plasticizer. For any one plasticizer, the water permeability increases with increasing content of the plasticizer in the composition (Table 3).

In all the tables, formulas, and calculations given below, the content of plasticizer in the PVC compositions is expressed in mole percent, by which we mean the amount in centimoles of plasticizer per one basic mole of polyvinylchloride (CH_2CHCl) which is taken as 62.5. In accordance with this, if a composition contains p parts by weight of plasticizer, with molecular weight M per 100 parts by weight of PVC, then for converting the weight ratio to a molar ratio the formula $n = p \cdot 62.5/M$ is used, where n is the amount of plasticizer (in mole %).

It is evident from Table 3 that films containing aliphatic plasticizers (DBA, DOA, DBS, DOS) exhibit a greater water permeability than films which have been plasticized by plasticizers containing aromatic groups (TCP, DBP, DOP etc.).

TABLE 2

Plasticizer Efficiency

Polyvinylchloride-plasticizer	Chemical formula	$T_{vit.}$ (in °C)	(°C) for 1 mole %
Pure polyvinylchloride	$(CH_2—CHCl)n$	65.0	—
Tricresylphosphate (TCP)	$(CH_3C_6H_4O)_3PO$	55.6	9.4
Dibutylphthalate (DBP)	$C_6H_4(COOC_2H_5)_2$	55.2	9.8
Diethylphthalate (DEP)	$C_6H_4(COOC_4H_9)_2$	54.4	10.6
Dioctylphthalate (DOP)	$C_6H_4(COOC_8H_{17})_2$	53.1	11.9
Dibutyladiphate (DBA)	$C_4H_9OCO(CH_2)_4COOC_4H_9$	52.6	12.4
Dioctyladipate (DOA)	$C_8H_{17}OCO(CH_2)_4COOC_8H_{17}$	51.9	13.1
Dibutylsebacate (DBS)	$C_4H_9OCO(CH_2)_8COOC_4H_9$	52.2	13.8
Dioctylsebacate (DOS)	$C_8H_{17}OCO(CH_2)_8COOC_8H_{17}$	49.9	15.1

TABLE 3

Water Permeability of Polyvinylchloride Films Plasticized with Various Plasticizers

Plasticizer	$P \times 10^8$ (g/cm · hr · mm Hg) for a content in mole % of plasticizer of:					
	0	4	6	8	10	12
Tricresylphosphate	0.50	0.55	0.65	0.92	1.74	2.96
Diethylphthalate		0.58	0.86	1.18	2.00	3.38
Dibutylphthalate		0.60	0.94	1.33	2.46	4.02
Dioctylphthalate		0.64	1.16	1.98	3.05	4.97
Dibutyladipate		0.96	1.72	2.67	4.08	5.89
Dioctyladipate		1.45	3.00	4.62	6.81	10.95
Dibutylsebacate		1.09	2.13	3.30	5.00	8.64
Dioctylsebacate		1.64	3.20	5.32	8.03	12.05

TABLE 4

The Relation Between the Efficiency (Efficiency Numbers) of a Plasticizer and the Water Permeability of a Composition (the plasticizer content of the compositions being 8 mole %)

Plasticizer	Efficiency No. (°C)	$P \cdot 10^8$ (g/cm hr · mm Hg)	$D \cdot 10^4$ (cm/sec)	$h \cdot 10^4$ (g/cm³ · mm Hg)
Tricresylphosphate	9.4	0.92	0.58	1.60
Diethylphthalate	9.8	1.18	0.70	1.70
Dibutylphthalate	10.6	1.33	0.74	1.82
Dioctylphthalate	11.9	1.98	0.99	2.00
Dibutyladipate	12.4	2.67	1.15	2.32
Dioctyladipate	13.1	3.30	1.32	2.50
Dibutylsebacate	13.8	4.62	1.84	2.43
Dioctylsebacate	15.1	5.32	1.98	2.69

There is a definite relation between the value of the water permeability of a film and the efficiency of the plasticizer, which is determined by the nature of the plasticizer used, and the amount of it in the composition. The greater the plasticizing effect of a given plasticizer, the greater the water permeability of a film containing this plasticizer (Table 4). Such a relation is completely understandable.

Using the theory of activated diffusion of water vapor through a film, it can be assumed that the addition of a plasticizer to a polymer – as a result of which intermolecular and intramolecular forces decrease – leads to an increase in the mobility of the macromolecules, due to which formation of temporary interstices or "canals" through which water molecules diffuse, is facilitated.

The connection between the efficiency of a plasticizer and the water permeability of films containing the given plasticizer, is so close and uniform, that it should be possible to derive a mathematical expression linking efficiency and the water permeability coefficient.

When a composition contains n moles % of a plasticizer whose efficiency number is ϑ, then the water permeability coefficient P can be calculated by means of the formula:

$$P = P_0 (0.9n - 1.7)(0.265\vartheta - 2.126), \qquad \text{(VI)}$$

where P_0 is the water permeability coefficient for unplasticized PVC, and is equal to $0.5 \cdot 10^{-8}$ according to our measurements.

TABLE 5

Comparative Values of P, Calculated by Means of Formula (VI) and Determined Experimentally for PVC Compositions Containing 8 moles % of Various Plasticizers

Plasticizer	$P \cdot 10^8$ (g/cm · hr, mm Hg)	
	calculated	found
Tricresylphosphate	1.00	0.92
Diethylphthalate	1.30	1.18
Dibutylphthalate	1.37	1.33
Dioctylphthalate	2.82	1.93
Dibutyladipate	3.19	2.67
Dioctyladipate	3.70	3.30
Dibutylsebacate	4.21	4.62
Dioctylsebacate	5.15	5.32

TABLE 6

The Effect of Temperature on Constant Water Permeability $P \cdot 10^8$ (in g/cm · hour · · mm Hg)

Plasticizer content as a % of wt. of PVC)	The coefficient $P \cdot 10^8$ for the system PVC-DOP at temperatures (in °C) of:		
	20	30	40
0	0.50	0.55	0.57
25	1.00	1.13	1.28
50	1.97	2.80	4.07
75	3.55	4.90	7.42
100	5.30	7.30	11.50

Table 5 contains values for the constant P which were calculated on the basis of Formula (VI), and values which were determined experimentally for a content of various plasticizers equal to 8 moles % at 20°.

As these results show, the deviations between the calculated and experimental values of P are fairly considerable, but it should be borne in mind that during the direct determination of P, large deviations are obtained there also, and that the values of P for plasticized PVC obtained by different workers, differ considerably from each other, and vary over the range $3\text{-}4 \cdot 10^{-8}$ to $2\text{-}3 \cdot 10^{-7}$.

Effect of Temperature on Water Permeability. As the temperature increases, not only does the pressure increase [water vapor pressure, and consequently, the factor Δp in Formula (III)], but the mobility of the molecular chains of the polymer also increases, as a result of which, one would expect a significant increase in the water permeability, i. e., in the coefficient P (Table 6).

Barrer [11] has shown that the temperature relationship of the permeability constant, the diffusion constant, and solubility constant are determined by the equations:

$$P = P_0 e^{-E_p/RT}, \qquad \text{(VII)}$$

$$D = D_0 e^{-E_D/RT}, \qquad \text{(VIII)}$$

$$h = h_0 e^{-\Delta H/RT},$$

where P, D and h are the permeability, diffusion, and solubility constants respectively, P_0, D_0 and h_0 are the pre-exponential coefficients; E_p and E_D are the activation energies of permeability and diffusion; ΔH is the heat of solution of the gas in the polymer.

The activation energy of water permeability (E_p), according to our work, amounts to about 1440-2200 kcal/mole, in the case of unplasticized PVC or PVC containing only small amounts of plasticizer, and is equal to 6400-7000 kcal/mole for strongly plasticized compositions.

Table 7 contains results for the values of the water permeability P at a temperature of 40° for the system PVC – DOP, plasticized to different extents; they include results obtained experimentally, and obtained by calculation, using Equation (VII), from the values at 20°.

TABLE 7

Comparison of the Values of P for the System PVC – DOP Containing Different Amounts of Plasticizer, at 20 and 40°

Plasticizer content (as a percentage of the weight of PVC)	$P \cdot 10^8$ at t = = 20°	$P \cdot 10^8$ at t = 40°		Activation energy E_p (in kcal/mole)
		found experimentally	calculated	
0	0.50	0.57	0.56	1440
25	1.00	1.28	1.27	2200
50	1.97	4.07	4.04	6400
75	3.55	7.42	7.35	7600
100	5.30	11.50	11.70	7000

The temperature relationship of the water permeability holds to the degree of accuracy indicated, over the comparatively narrow temperature range, for which the activation energy can be regarded as constant.

Activation energy, however, changes considerably with temperature, particularly at temperatures approximating to the vitrification point. In accordance with the ideas advanced regarding the mechanism of diffusion, one might expect the activation energy to decrease with increasiing plasticizer content of a composition, and to have its highest value for the unplasticized polymer.

Actual results, however, show that the opposite is true. The low value of the permeability activation energy for the pure polymer can be explained by the presence of "cavities" in the solid polymer, which is polyvinylchloride in a vitreous state (20 and 40°, the test temperatures are below the vitrification temperature of polyvinylchloride). Similar relations have also been observed in the case of other solid polymers [11].

The high activation energy observed in the case of plasticized polyvinylchoride may be explained by the increase in the heat of solution ΔH, which is a fraction of the water permeability activation energy, particularly in the highly elastic state, in which strongly plasticized compositions in the temperature range 20-40° are found. Similar phenomena have been observed by other workers [10, 7].

The following approximate formula can be used for calculating the values of P at any temperature T:

$$P_T = 1.5^{\frac{T-20}{10}} \cdot P_{20}, \qquad (X)$$

where P_{20} is the water permeability coefficient at 20°.

Since, for DOS the constant $P_{20} = 5.30$, then for 30° it will be equal to $1.5^{\frac{30-20}{10}} \cdot 5.30 = 1.5 \cdot 5.30 = 7.95$; in fact it was found that $P_{30} = 7.30$. For DOS at 40°, $P_{40} = 1.5^{\frac{40-20}{10}} \cdot 5.30 = 11.92$; the value determined experimentally was 11.50.

SUMMARY

1. Plasticizers have a considerable effect on the water permeability of polymers, as a consequence of which, when making a choice of a water resistant composition, or a composition which has low water permeability, one should not be guided by the water permeability index of the pure polymers alone, it is essential to bear in mind the effect shown by the plasticizer to be used.

2. The water permeability of plasticized polyvinylchloride depends on the chemical nature of the plasticizer used.

3. There is a close connection between the water permeability of a composition and the plasticizing effect of the plasticizer; the greater the plasticizing effect, the higher the water permeability of the composition. The most efficient plasticizers, in particular, the aliphatic plasticizers, make the composition most water permeable.

4. An empirical formula is suggested which relates the value of the water permeability constant to the efficiency of the plasticizer; by means of this formula it is possible to calculate, and forecast, the water permeability of a plasticized material as long as its composition is known.

5. The tendency in recent years to use aliphatic plasticizers of the sebacate, adipate and laurate, etc. type in electrical insulating materials and for water resistant compositions, cannot be regarded as fully justified, since such plasticizers strongly enhance the water permeability of a material, and depress its dielectric and moisture resistant properties, particularly in the case of articles with a highly developed surface and with a small thickness, such as water resistant films and cable insulation.

LITERATURE CITED

[1] V. Skorcheletti and I. S. Vasilyev, J. Appl. Chem. XXVI, 10, 1033 (1953).

[2] G. Deeg and C. Frosch, Modern Plastics, 8, 155 (1944).

[3] Teylor, Hermann and Kemp, Ind. Eng. Ch., 28, 1255 (1936).

[4] S. A. Reitlinger and L. A. Panyunina, J. Appl. Chem. XII, 886 (1939).

[5] S. A. Reitlinger, J. Gen. Chem. 14, 420 (1944).

[6] P. W. Morgan, Ind. Eng. Ch., 10, 2296 (1953).

[7] S. A. Reitlinger, Prog. Chem. 2, 214 (1951).

[8] M. M. Mikhailov, Electricity, 8, 24 (1947).

[9] S. N. Zhurkov, Trans. First and Second Conference on High Molecular Weight Compounds, Izd. AN SSSR (1945).*

[10] Sh. L. Lelchuki and V. I. Sedlis, J. Appl. Chem. XXX, 3, 412 (1957).

[11] R. Barrer, "Diffusion in Solids," Izd. IL (1948).*

Received January 23, 1956

* In Russian.

A STUDY OF THE PHENOLS OBTAINED BY THE THERMAL DECOMPOSITION OF HYDROLYZED LIGNIN*

V. G. Panasyuk

The F. E. Dzerzhinsky Dnepropetrovsk Chemico-Technological Institute

Phenols and neutral materials predominate in the fraction of resin up to 230°, obtained by dry distillation, and also by vacuum thermal decomposition of hydrolyzed lignin from wood and cotton husks. The low boiling phenols may be used as a good source of raw material for the production of plastics, dyes, and other materials. The most valuable phenols from this point of view are: phenol, meta-cresol, meta-ethylphenol, and 1,3,5-xylenol. The composition of the phenols obtained during the dry distillation of hydrolyzed wood and cotton husk lignin, and especially of those obtained during their vacuum thermal decomposition have hardly been studied at all.

We isolated the phenols from the resin fraction boiling between 175-230° by the normal methods using the phenolates. The phenolates were purified from adsorbed oils by extraction with benzene and subsequent steam distillation. This purification was repeated.

The isolated phenols were cut into narrow fractions on a laboratory column.

A study of the phenols from dry-distilled resin. The phenols obtained from cotton husk lignin were distilled after purification. Results of the fractionation and the characteristics of the fractions are given in Table 1.

TABLE 1

Fractionation of Phenols from Cotton Husk Lignin and the Characteristics of the Fractions

Distillation range (°C)	Yield in percent		Characteristics of the fractions	
	with respect to the phenols	with respect to the resins boiling up to 230°	n_D^{20}	d_4^{20}
180-195	26.8	10.7	1.518	1.0376
195-203	27.9	11.2	1.5170	1.0383
203-206	7.9	3.2	1.5150	1.0464
206-212	14.3	5.7	1.5110	1.0380
212-218	5.8	2.3	1.5050	1.0294
Residue	17.3	—	—	—

The narrow fractions of the phenols, as is evident from the refractive index, are not at this stage a mixture of pure phenols. Judging from the yield of the separate fractions, cresols should predominate in the phenols obtained from cotton husk lignin, since almost 55% of them distil up to 203°. On fractionation, the phenols have a bright yellow color, which does not darken on storage.

*Part III of a series of articles on the thermal processing of hydrolyzed lignin. A. Kobeleva and L. Gorodepkaya took part in the experimental work.

TABLE 2

Fractionation of Phenols from Wood Lignin and the Characteristics of the Fractions

Distillation range (°C)	Yield in percent		Characteristics of the fractions	
	with respect to the phenols	with respect to the resins boiling up to 230°	n_D^{20}	d_4^{20}
180-195	3.9	1.7	1.5329	1.0744
195-203	21.2	9.1	1.5465	1.0764
203-206	12.8	5.5	1.5440	1.0858
206-212	20.9	9.0	1.5420	1.0853
212-218	15.6	6.7	1.5400	1.0796
218-225	10.0	4.3	1.5390	1.0828
Residue	15.6	—	—	—

The characteristics of phenols isolated from dry distilled resin of wood lignin (after purification and fractionation) are given in Table 2.

On the basis of the refractive index, the phenol fractions obtained from wood lignin resin would appear to be purer than the corresponding fractions obtained from cotton husk lignin. Their specific gravities are somewhat higher. On storage only the first three fractions darken, the remaining three fractions remain yellow for a long time.

The yield of fractions up to 203°, as a percentage of the total amount of the phenol fractions, amounts to about 25%, this is almost half that from cotton husk lignin.

Determination of the composition of the phenols in each fraction is a very difficult problem. The use of chemical methods gives a far from complete picture. There are published references [1] to the use of paper chromatography for the analysis of phenols, for which purpose it is recommended that the phenols be taken in the form of the products formed by coupling them with diazotized sulfanilic acid. By using derivatives of the phenols, it is possible to carry out a fairly clear cut separation on a paper chromatogram, of the mixture of phenols from each fraction, and, from the value of the mobility, to determine their character. Knowing what the phenols are in each fraction, their isolation presents no difficulty.

We carried out chromatographic separation of the phenols on paper by the method suggested by S. I. Burmistrov. A small amount of the test phenol, dissolved in carbon tetrachloride, was heated with pyridine-sulfotrioxide. The pyridine aryl sulfate formed was then converted into the ammonium salt:

$$ArOH + C_5H_5NSO_3 \rightarrow ArOSO_3H \cdot NC_5H_5,$$
$$ArOSO_3H \cdot NC_5H_5 + NH_3 \rightarrow ArOSO_3NH_4 + C_5H_5N.$$

The ammonium salt obtained in excess ammonia solution was then placed on a sheet of paper for chromatographic separation.

The solvent used was a mixture consisting of an aqueous solution of ammonia and n-butanol in the proportion of 1:1.

Chromatographic separation was carried out on No. 2-Whatman paper made by a Leningrad Factory. The chromatograms were developed by treating the paper sheet with a solution of 4,4'-diazoaminotoluene, with subsequent treatment with hydrochloric acid fumes, after which colored spots appeared.

This reaction can be represented as follows.

1) The ammonium salt of the sulfate ester, on interacting with HCl is hydrolyzed to the free phenol:

$$ArOSO_3NH_4 + HCl \xrightarrow{H_2O} ArOH + NH_4Cl + H_2SO_4.$$

2) 4,4'-Diazoaminotoluene reacts with HCl to form the diazonium compound:

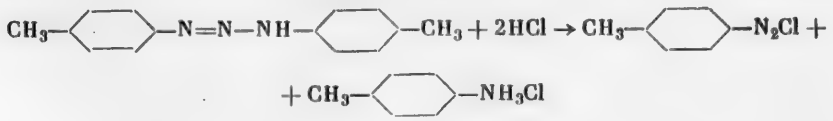

3) The diazonium compound formed then reacts with phenol to give a dye:

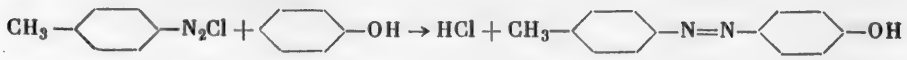

Knowing the mobility (R_f) for the individual phenols, it is possible to establish what phenols are present in each fraction, and, indirectly as well (from the size of the dye spot) to assess the amount of these phenols. We had to determine the R_f values for the pure phenols ourselves. Some phenols were synthesized for this purpose. The R_f values depend on the temperature of the surrounding medium in which the chromatograms are taken.

The R_f values of some of these phenols and their acid ethers are given in Table 3.

The R_f values of some phenols were too close to each other, some of them being identical, for example the R_f values of ortho-cresol, ortho-ethylphenol and cresol. We differentiated them by the colors of the respective dyes formed by them.

Using the R_f values which we established, we were able to establish the nature of the phenols obtained from the resin derived from cotton husk and wood lignins. Results of studies on the phenolic fractions from cotton husk lignin are given in Table 4.

The chromatographic results confirmed that, by far the most abundant phenols present were the cresols, including meta-cresol; guaiacol was detected in the third and fourth fractions. Creosol was not detected. Of the xylenols, only 1,3,4-xylenol (meta) could be found in the phenols from cotton husk lignin.

Table 3

Determination of the Mobility of Some Pure Phenols at 12°

Phenol	B. p. (in °C)	R_f value	Color of the spot
Phenol	181	0.43	Yellow-orange
Ortho-cresol	191	0.54	Dark-orange
Meta-cresol	203	0.48	Orange
Para-cresol	202	0.58	Dark-orange
Guaiacol	205	0.40	Violet-red
Ortho-ethylphenol	207	0.54	Yellow-orange
1,3,4-Xylenol	211	0.62	Orange-red
Meta-ethylphenol	214	0.58	Ditto
Para-ethylphenol	219	0.66	Orange-rose
Creosol	221	0.54	Reddish-gray
1,2,4-Xylenol (ortho)	225	0.60	Yellow-orange

TABLE 4

Chromatographic Analysis of Phenolic Fractions from the Dry Distillation of Cotton Husk Lignin

Boiling range of the fractions (in °C)	R_f value	Detected	Observations
180—195	0.43	Phenol	Little
	0.53	Ortho-cresol	Predominates
	0.58	Para-cresol	Little
	0.48	Meta-cresol	Little
195—203	0.40	Guaiacol	Meta-cresol predominates
	0.57	Para-cresol	
	0.48	Meta-cresol	
203—206	0.40	Guaiacol	All components in equal amounts
	0.49	Meta-cresol	
	0.57	Para-cresol	
206—212	0.39	Guaiacol	Traces in equal amounts
	0.58	Meta-ethylphenol	
	0.64	1,3,4-Xylenol (meta)	
212—218	0.66	Para-ethylphenol	Little
	0.63	1,3,4-Xylenol (meta)	Predominates

TABLE 5

Chromatographic Analysis of Phenolic Fractions from Wood Lignin (Dry Distillation Process)

Boiling range of the fraction (in °C)	R_f value	Detected	Observations
180—195	0.39	Guaiacol	Traces
	0.43	Phenol	Predominates
	0.54	Ortho-cresol	Little
195—203	0.39	Guaiacol	Little
	0.48	Meta-cresol	Predominates
	0.59	Para-cresol	Little
203—206	0.39	Guaiacol	In equal amounts
	0.58	Para-cresol	
	0.47	Meta cresol	Little
206—212	0.39	Guaiacol	Large amounts
	0.57	Meta-ethylphenol	Predominates
212—218	0.39	Guaiacol	Little
	0.53	Creosol	Little
	0.62	Meta-1,3,4-Xylenol	Predominates
218—225	0.40	Guaiacol	Traces
	0.54	Creosol	Large amounts
	0.65	Para-ethylphenol	Little

Results of studies carried out on the phenolic fractions from wood lignin are given in Table 5.

We detected a mixture of various phenols and their ethers in all the phenolic fractions; guaiacol was detected in all the fractions.

Nine of all the simple phenols and their ethers were detected in the resins obtained from both types of lignin. The difference in the composition of the phenolic fractions is insignificant. Thus, very little phenol

was found in the cotton husk lignin, creosol was not detected, while of the xylenols, only one of the meta-isomers was found; guaiacol was found in large amounts in wood lignin resin.

Cresols, among them the meta-isomer predominate in all the fractions from cotton husk lignin; cresols and guaiacol were present in approximately equal amounts in the resin from wood lignin. The total amount of phenols obtained as a result of dry distillation is insignificant – only 2% of phenols could be isolated from the light fractions obtained from cotton husk lignin, while from the resin obtained from wood lignin only about 1% of phenols could be obtained from the same fractions.

A study of the phenols from the resin obtained by the vacuum-thermal decomposition of lignin in the liquid phase. Phenols from the resin obtained by vacuum-thermal decomposition of both types of lignin in anthracene oil were studied. During the vacuum process, the yield of the low boiling part of the resin (up to 230°) was equal to 25-30%. From this resin we obtained 10-12% by weight on the dry lignin of the low boiling phenols, the amounts being practically the same from both types of lignin. The phenols were separated from each other by the same technique as the phenols from the dry distillation process. Their yields, and the characteristics of each low temperature fraction are given in Table 6.

The total yield of low boiling phenols as a percentage of the lignin was greater than 9%, this indicates that it would be expedient to use hydrolyzed wood lignin for the preparation of phenols by vacuum-thermal decomposition in the liquid phase.

Results of the chromatographic analysis of the individual fractions are given in Table 7.

TABLE 6

Fractionation of Phenols from Wood Lignin Resin and Characteristics of the Fractions Obtained (Vacuum-Thermal Process)

Boiling range (in °C)	Yield (in percent) with respect to:			Characteristics of the fraction	
	phenols	resin	lignin	d_4^{20}	n_D^{20}
180—195	7.07	2.79	0.84	1.0782	1.5450
195—203	19.90	7.86	2.36	1.0928	1.5453
203—206	14.71	5.87	1.76	1.0975	1.5435
206—212	18.35	7.34	2.20	1.0987	1.5395
212—218	11.02	4.41	1.32	1.0884	1.5379
218—225	4.72	1.89	0.57	1.0834	1.5368
Total	24.73	—	—	—	—
Residue	100	30.16	9.05	—	—

With respect to composition, the phenols in each fraction are exactly the same as in the corresponding fractions from the dry distillation process, but their amounts calculated on the basis of the weight of lignin taken are considerably greater. Guaiacol was determined in all fractions. In order to determine the amount of guaiacol and to identify it, guaiacol was isolated from fractions 2,3, and 4 by the barytes method [2]. The guaiacol obtained was distilled at 204-206°. In all, 35.6% was isolated from these fractions, this amounts to 2.25% on the weight of the dry lignin.

The characteristics of the phenols isolated from the resin obtained by means of the vacuum-thermal process from cotton husk lignin are given in Table 8.

More than 10% of the low boiling phenolic fractions, expressed as a percentage of the weight of lignin, can be obtained. Cresols were found to predominate in these fractions as noted previously in the case of the phenolic fractions obtained from dry distilled resin.

TABLE 7

Chromatographic Analysis of Phenolic Fractions from Wood Lignin Resin (Vacuum-Thermal Process)

Number of the fraction	Boiling range of the fraction (in °C)	R_f value	Detected	Observations
1	180—195	0.40	Guaiacol	Traces
		0.44	Phenol	In equal amounts
		0.55	o-cresol	
2	195—203	0.40	Guaiacol	Both cresols predominate
		0.49	m-cresol	
		0.58	p-cresol	
3	203—206	0.40	Guaiacol	Large amount
		0.48	m-cresol	Cresols in equal amounts
		0.58	p-cresol	
4	206—212	0.40	Guaiacol	Large amount
		0.48	m-cresol	Traces
		0.58	m-ethylphenol	Predominates
5	212—218	0.40	Guaiacol	Little
		0.53	Creosol	Traces
		0.62	m-xylenol 1,3,4	Predominates
6	218—225	0.40	Guaiacol	Traces
		0.53	Creosol	Little
		0.65	p-ethylphenol	Predominates

TABLE 8

Fractionation of the Phenols from Resin Obtained by the Vacuum-Thermal Process from Cotton Husk Lignin, and the Characteristics of the Fractions

Boiling range (in °C)	Yield (in %) with respect to:			Characteristics of of the fractions	
	Phenols	Resin boiling up to 230°	Lignin	d_4^{20}	n_D^{20}
180—195	24.1	10.36	2.90	1.0577	1.5405
195—203	40.5	17.42	4.87	1.0444	1.5391
203—206	8.9	3.82	1.07	1.0426	1.5369
206—212	6.1	2.62	0.73	1.0446	1.5351
212—218	6.0	2.60	0.72	1.0410	1.5320
218—225	1.4	0.60	0.17	—	1.5300
Residue . . .	13.0	—	—	—	—
Total	100	37.42	10.46	—	—

Results of the chromatographic analysis of these fractions are given in Table 9.

It is evident that the composition of the phenolic fractions obtained during the vacuum-thermal process is practically the same as that for the fractions obtained by the dry distillation method.

Guaiacol was isolated in an amount which was equal to 3% of the total weight of the phenolic fractions, calculated in terms of the weight of dry lignin this was a very insignificant amount. The total amount of meta-cresol in the phenolic fractions was determined by means of trinitrocresol. The nitrated product had a melting

TABLE 9

Chromatographic Analysis of the Phenolic Fractions from the Resin Obtained from Cotton Husk Lignin (Vacuum-Thermal Process)

Boiling range of the fraction (in °C)	R_f value	Detected	Observations
180—195	0.44	Phenol	Little
	0.53	o-cresol	Predominates
	0.46	m-cresol	Little
	0.57	p-cresol	Little
195—203	0.40	Guaiacol	Traces
	0.46	m-cresol	Predominates
	0.57	p-cresol	—
203—206	0.40	Guaiacol	Little
	0.47	m-cresol	Predominates
	0.57	p-cresol	Traces
206—212	0.40	Guaiacol	Traces
	0.58	m-ethylphenol	—
	0.64	(Meta)- 1,3,4-Xylenol	Predominates
212—218	0.63	(Meta)- 1,3,4-Xylenol	In equal amounts
	0.67	p-ethylphenol	In equal amounts
	0.59	m-ethylphenol	Little
218—225	Not determined		

point of 105-106°. The total amount of meta-cresol in the first and second fractions was about 30.0% or, on the basis of the dry lignin 2.3%. The total amount of meta-cresol which can be obtained from cotton husk lignin will be slightly higher. The phenol content of the first fraction was 6.2%, or about 0.17% on the dry lignin.

SUMMARY

1. Phenols isolated from resin obtained by the dry distillation of lignins, amounted to 1% for wood lignin, and 2% for cotton husk lignin; these phenols were studied by means of paper chromatography; nine different phenols and their ethers were found by this technique in the fractions boiling up to 225°.

2. The same phenols were isolated from the resins obtained by both dry distillation and vacuum-thermal degradation.

3. The phenol obtained in the greatest amount from wood lignin was guaiacol, calculated on the basis of the dry lignin it was present to the extent of more than 2%. Of the phenols from cotton seed lignin, the ones present in the greatest amount were the cresols, the meta-isomer predominating.

LITERATURE CITED

[1] R. Blok, R. Lestran and G. Tsveig, "Paper Chromatography," IL (1954).*

[2] K. Bauer, "Analysis of Organic Compounds," IL (1953).*

Received July 29, 1955

DEVELOPMENT OF A PROCESS OF HYDROGENATION REFINING, UNDER LOW HYDROGEN PRESSURES, OF GASOLINES OBTAINED BY THERMAL LIQUEFACTION AND SEMICOKING OF ESTHONIAN SHALES

M. K. Dyakova, A. B. Vol-Epshtein, E. A. Aleksi and E. I. Vasilchikova

In the modern shale-processing industry, semicoking gasolines are purified by means of sulfuric acid. The losses in the purification comprise about 19% of the weight of the gasoline; an unstable product with a high sulfur content (0.6%) and a sharp unpleasant odor is obtained [1].

In the All-Union Scientific Research Institute for Shale Processing a method has been worked out, in laboratory conditions, for stabilization and desulfurization of shale gasolines by two-stage treatment with aluminosilicate clays [2, 3].

At the first stage (at 150-300° and a space rate of 2 liters/liter of catalyst·hour) most of the neutral oxygen compounds and some of the sulfur compounds are removed from the gasoline in polymer form. At the second stage (at 430° and a space rate of 0.5 liter/liter of catalyst·hour) additional and more extensive removal of sulfur takes place. The yield of stable and desulfurized gasoline with octane number 73 is about 79 wt. %, and coke formation is 3.5% on the second-stage crude. The polymers can be used for the production of lubricants and partly as components of Diesel fuel [3]. The catalysts are regenerated by burning out the coke in air. Not enough is known about the stability and life of the catalysts.

Hydrogenation purification at low pressures is an effective method for desulfurization of motor fuels, including shale gasolines.

Moldavsky and Pokorsky [4], in the 1930's used a large-scale laboratory flow unit for hydrogenation purification of gasolines from tars obtained from Gdov and Veimarn shales (sulfur content 1.0-0.74%, phenols 3.2-3.7%, bromine number 60.8-74.6, density d_4^{15} 0.78-0.79). Under a pressure of 20 atm , at 440°, with space rates up to 0.4 liter/liter of catalyst·hour, and molar ratio of feed to hydrogen 1:3.5, with Cr_2O_3 catalyst, sulfur could be removed down to 0.05% and stable gasoline was obtained (induction period over 4 hours) of a lighter fractional composition. The hydrogen consumption was up to 1.0% on the feed, the hydrogenation product yield was 98.0-99.5%. Unfortunately, the life of the chromium oxide catalyst was not studied and the octane number of the purified gasoline was not determined.

Shale distillates heavier than gasoline can also be effectively purified by hydrogenation under pressures of up to 100 atm [5, 6].

Hydrogenation refining is successfully used in industry for refining of crude benzene for the production of pure benzene, toluene, xylene, or motor fuel components. The process is carried out under conditions which exclude hydrogenation of aromatic hydrocarbons and ensure thorough removal of heteroatomic and unsaturated compounds.

At the hydrogenation works in Scholven [7], crude benzene of b. p. 210° is purified under a pressure of 70-80 atm , at 350° over a static $MoO_3 + Al_2O_3$ catalyst, which can be regenerated when necessary by combustion of the deposited coke in oxygen-containing gases. The hydrogen comsumption, including mechanical losses, is about 0.4%.

Crude benzene contains small amounts of highly unstable compounds (cyclopentadiene, indene, coumarone, etc.) which can undergo polymerization in the course of heating up to the reaction temperature, forming plugs in the heat exchanger and preheater tubes. This difficulty was avoided in the pilot plants by means of a preliminary hydrogenation stage at 220-240°. In the Scholven plant these unsaturated compounds were removed by polymerization at about 200°, the depolymerized crude being subjected to the subsequent heating.

At the Nurenberg gas works [8] a unit has recently been started for the purification of crude benzene (b. p. up to 200°, by means of coke-oven gas at 35 atm and 320-350° over a sulfur-resistant catalyst) with an output of 500 tons/month. The yield of the pure hydrogenation product is 98% at both works. Operating experience has shown that hydrogenation purification of technical benzene is economically feasible, and compares favorably with the sulfuric acid method, giving a product of better quality.

The possibility of deep purification of brown coal tar distillates and its thermal cracking products with b. p. up to 350° by hydrogenation by a staggered-cycle process over $MoO_3 + Al_2O_3$ aromatization catalyst under a pressure 50 atm , by means of gases containing 54-68% of hydrogen by volume has been deconstrated in a laboratory unit and the "DHD" production unit [9].

There is an extensive literature on the hydrogenation refining of petroleum distillates. The process developed by the Shell Company for the hydrodesulfurization of aromatized aviation gasolines obtained by thermal and catalytic cracking, over a static $WS_2 + NiS$ (40%W, 25% Ni, 35% S) catalyst, similar to that used in the present investigation, is of interest. The process was put into operation at two refineries and proved to be simple and economic. The experimental unit was operated at 50 atm., 343°, a volume feed rate of about 10 volumes of feed/volume of catalyst·hour, and 1:7 molar ratio of feed to hydrogen.

Purification of gasoline containing 0.25% of sulfur, mainly in the form of thiophene, and with bromine number 25, yielded a product which was almost entirely free from sulfur (the sulfur content was a few thousandths of one per cent) with a yield of 100% by volume. It was also shown that gasolines of higher sulfur contents and bromine numbers can be purified.

It was found that low pressures cause a rapid fall of catalyst activity, and that total pressure should not decrease below 43 atm ; the best results are obtained if the purification is carried out at 50-70 atm. Catalyst life is longer at lower temperatures. As the activity of the catalyst decreases, the temperature must be raised to 427° and the volume feed rate lowered from 15 to 5 volumes of raw materal/volume of catalyst·hour. Although an increase of the molar ratio of the raw material to hydrogen above 1:2 has little effect on the degree of desulfurization, it should be maintained at 1:7 in order to preserve the activity of the catalyst.

Deposition of tarry products lowers the catalyst activity. This effect can be partly avoided by circulation of hydrogen without the feed for several hours between 490 and 540°. The catalyst can be activated in this was only 2-3 times between complete regenerations. Regeneration is carried out after 2000 hours of continuous operation (after the passage of 15,000-20,000 volumes of feed per 1 volume of catalyst), and is effected by removal of the carbonaceous deposits by treatment of the catalyst with superheated steam (at 460-510°), followed by steam with a small admixture of air, and steam with hydrogen sulfide to sulfidize the catalyst (at a temperature below 680°). This treatment fully restores the initial activity of the catalyst. After 2-3 complete regenerations (4000-6000 operating hours) mechanical crumbling of the catalyst resulted in considerable pressure differences, and it was necessary to screen off the fines. The remaining catalyst was used again. To decrease deposition of tarry substances, the authors recommend the use of small transportable sections with spent catalyst, and state that freshly distilled feed should be hydrogenated.

According to Sherwood [11], good results similar to those described above are obtained by hydrogenation desulfurization of gasolines at 50 atm and 360-380° over a cobalt—molybdenum—aluminum catalyst. The author notes the high strength, cheapness, and long service life of the catalyst, which is not inferior to $WS_2 + NiS$ catalyst in its desulfurizing action.

In recent years modifications of reforming processes have been developed whereby it is possible to obtain high-grade motor and aviation gasolines and aromatic hydrocarbon concentrates from sulfur-containing gasoline and ligroine fractions, containing unsaturated hydrocarbons [12]. The possibility of using processes of this type for the purification of shale gasolines is not excluded.

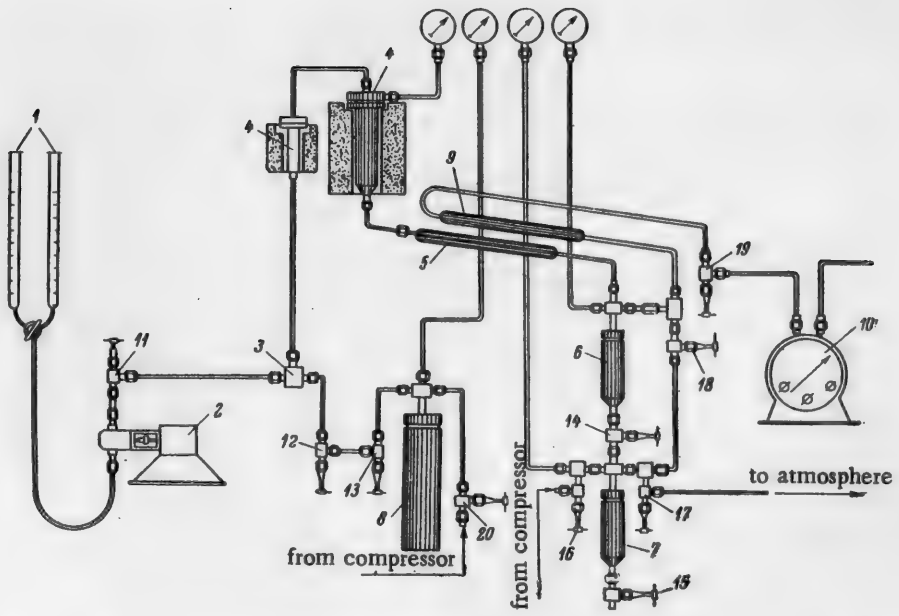

Fig. 1. Diagram of a continuous unit for hydrogenation of shale gasolines. 1) Buret for crude, 2) liquid pump, 3) T-piece, 4) reactors, 5) condenser, 6,7) receiver for product, 8) buffer vessel with hydrogen, 9) condenser, 10) gas flow meter, 11) feed valve, 12, 16) hydrogen feed valves, 13) hydrogen feed control valve, 14, 18) valves for cutting off the upper receiver, 15) product discharge valve, 17) pressure reduction valve, 19) pressure control valve, 20) valve for hydrogen inlet into buffer vessel.

Thus, numerous investigations and refinery practice have demonstrated the effectiveness of low-pressure hydrogenation for purification of a wide range of raw materials — petroleum gasolines, ligroines, gas oils (direct distillation and obtained by catalytic cracking), coal tar benzene, shale distillates, and others.

The purpose of the present investigation was the development of a hydrogenation process with industrial tungsten sulfide catalysts for the purification of gasolines obtained by thermal liquefaction and semicoking of Esthonian shales, at moderate pressures.

EXPERIMENTAL

The hydrogenation of shale gasolines was carried out in a continuous unit with two reactors (Fig. 1). The 1st reactor, 25 cc in capacity, was completely filled with $WS_2 + NiS + Al_2O_3$ catalyst; 100 cc of the corresponding catalyst was placed in the middle region of the second reactor. Some of the experiments were carried out without the 1st reactor, which was installed to prevent high-temperature coking of the unstable components of semicoking process gasoline (this effect was not observed in gasolines obtained by thermal liquefaction).

The characteristics of ths starting materials are given in Table 1. Freshly distilled materials were used in prolonged tests of catalyst activity.

The catalysts used for the investigation were fresh industrial catalysts; for the preliminary hydrogenation stage — $WS_2 + NiS + Al_2O_3$, WS_2 — and for the gasoline reforming stage — WS_2 + aluminosilicates. The properties of these catalysts, their use in industry, and their preparation are described in the literature [13]. The catalysts were charged into the reactor in the form of cylinders or in pieces obtained by breaking the latter into 5 parts.

TABLE 1

Characteristics of Shale Gasolines

Physicochemical properties	Semicoking gasoline, Sample I, neutral	Thermal liquefaction gasolines	
		Sample II, crude	Sample III, neutral
Density d_4^{20}	0.7580	0.7886	0.7745
Sulfonables (vol. %)	68.0	–	32.3
Phenols (vol. %)	–	3.8	–
Iodine number	113.6	89.5	36.6
Sulfur content (wt. %)	0.87	1.56	0.92
Boiling commences at (°C)	54	44	75
10% boils out at (°C)	84	80	91
50% boils out at (°C)	126	135	139
90% boils out at (°C)	186	198	187
97.5% boils out at (°C)	225	210	208
Octane number (engine method)	60	–	53.4
Octane number with 1.5 ml of R-9 per 1 kg gasoline after H_2SO_4 purification (engine method)	–	–	62.0

To determine the optimum conditions for hydrogenation refining of shale benzenes, the influence of the process conditions on the degree of desulfurization and on the octane number of the purified products was determined, and the activity of the catalysts in prolonged operation was then studied under constant conditions in which A-66 and A-70 motor gasolines were formed.

The nature of the catalyst, as is clear from the data in Table 2, has a significant influence on the hydrogenation refining of shale gasolines. Under comparable conditions, the catalysts for the first stage of vapor-phase hydrogenation, WS_2 + NiS + Al_2O_3 and WS_2, have considerable greater desulfurizing activity than WS_2 + + aluminosilicate catalysts. The gasoline with b. p. up to 200°, obtained over the WS_2 + NiS + Al_2O_3 catalyst, has a very low octane number (60.8 with 1.5 ml of R-9 per 1 kg of gasoline); this is because of its high content of alkanes (over 50%), mainly of normal structure. The WS_2 catalyst, which activates the cracking and to some extent the isomerization of normal paraffins at 400-420°, raises the properties of the hydrogenation product to the standard specifications for motor fuel. This catalyst, as compared with WS_2 + NiS + Al_2O_3 , gives a lighter fractional composition with a lower yield of hydrogenation product, with a higher hydrogen consumption.

The hydrogenation temperature influences the degree of removal of sulfur and unsaturated compounds (Fig. 2) and the octane number of the gasoline (Table 3). The rate of hydrogenation of unsaturated compounds, and the reduction of sulfur and oxygen compounds, rises rapidly with an increase of temperature from 250 to 350°. The additional effect produced by further rise of temperature is slight.

A-66 motor gasoline (with 1.5 ml of R-9 per kg of gasoline) is obtained by the hydrogenation of shale semicoking gasoline at 400° and a volume feed rate of 1.2 liters/liter of catalyst · hour calculated on all the catalyst (or 1.5 liters/liter · hour calculated on WS_2). Increase of the temperature to 420° under the same conditions makes it possible to obtain A-70 motor gasoline (with 1.5 ml of R-9 per kg of gasoline). Hydrogenation refining of thermal-liquefaction gasoline at 400° and a feed rate of 1.2 liters/liter · hour yields A-70 gasoline.

However, if the gasolines are merely to be stabilized and desulfurized, without simultaneous improvement of octane rating, it is possible, as shown by the experimental results (Tables 3 and 4) to increase the feed rates and lower the process temperatures considerably.

Increase of the feed rate from 1.2 to 3.2 liters/liter · hour (Table 4) gives a higher yield, with a heavier fractional composition, and with a decrease of the octane number from 66.0 to 61.0 (with 1.5 ml of R-9 kg of gasoline). The contents of unsaturated hydrocarbons and sulfur change little and irregularly.

TABLE 2

Effect of the Nature of the Catalyst in the Hydrogenation Refining of Gasoline from the Thermal Liquefaction of Shale (Sample II) Pressure 50 atm ; Volume Feed Rate 1.5 liters/liter Catalyst · Hour, $M_{feed} : M_{H_2} = 1 : 5$

Catalyst	Temperature (°C)	Characteristics of neutral product						Hydrogen consumption (% of raw feed)	Yields (% on raw feed)			
		sulfur content (%)	octane No.		distils at (°C); hydrogenation product (in vol. %)				motor gasoline	phenols	water	gas + losses
			with 1.5 ml R-9 per kg of gasoline	without R-9	10	50	90					
$WS_2+NiS+Al_2O_3$ . .	400	0.14	—	—	—	—	—	—	—	—	—	—
WS_2	400	0.14	67.0	56.0	82	119	169	1.6	93.2	0.4	1.3	6.7
WS_2+aluminosilicate	410	0.23	67.0	—	80	121	173	—	—	—	—	—
$WS_2+NiS+Al_2O_3$ . .	350	0.14	60.8	46.0	81	125	180	0.9	96.6	0.5	0.9	2.9
WS_2	420	0.14	70.0	—	79	117	169	—	90.6	0.1	1.4	7.9

TABLE 3

Effect of Temperature in the Hydrogenation Refining of Shale Gasolines. Pressure 100 atm ; 1st Reactor Contained $WS_2 + NiS + Al_2O_3$ (25 ml); 2nd Reactor Contained WS_2 (100 ml); Volume Feed Rate 1.2 liters/liter · hour, Hydrogen Feed 1400 liters/liter raw feed · hour

Process conditions and properties of product	Semicoking gasoline, sample I			Thermal liquefaction gasoline, sample III	
Operating time of catalysts (hours)	280—285	266—274	274—280	299—306	306—310
Temperature of second reactor (°C)	382	400	420	400	420
Boiling commences at (°C)	42	41	37	41	41
10% boils out at (°C)	60	58	54	59	58
50% boils out at (°C)	101	99	92	105	101
90% boils out at (°C)	166	163	170	175	189
97.5% boils out at (°C)	201	197	198	195	198
Iodine number	6.1	3.3	3.2	1.2	0.8
Sulfonables (vol. %)	—	6.5	6.6	9.9	11.1
Octane number with 1.5 ml or R-9 kg of gasoline	65.0	66.0	73.0	71.0	74.0
Sulfur content (in wt%)	0.035	0.037	0.023	0.029	0.021
Yield of hydrogenation product (wt.%)	—	94.2	90.3	92.7	90.5

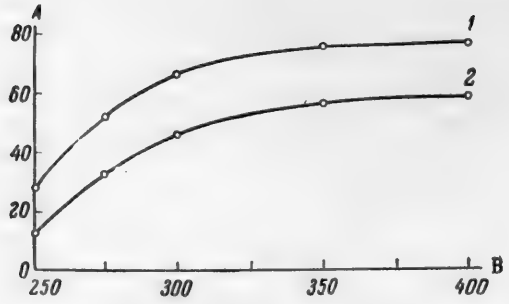

Fig. 2. Effect of temperature on the degree of removal of sulfur and unsaturated compounds in hydrogenation (Sample II). Pressure 20 atm , volume feed rate 3 liters per liter of catalyst · hour, catalyst $WS_2 + NiS + Al_2O_3$. A) Amount of sulfur and unsaturated compounds removed (in %), B) temperature (°C). Curves: 1) sulfur compounds, 2) unsaturated compounds.

The influence of pressure (between 10 and 100 atm) and molar ratio of feed to hydrogen on the degree of desulfurization of shale gasolines was studied. Increase of pressure raises the degree of purification, and increase of the molar ratio of feed to hydrogen from 1:4.5 to 1:8 has almost no effect on the degree of reduction of sulfur compounds and hydrogenation of unsaturated hydrocarbons.

Hydrogenation of shale gasolines results in the simultaneous removal of sulfur and unsaturated compounds. The hydrogenation refining could not be carried out selectively either by variations of the process conditions — variations of pressure from 10 to 100 atm , of temperature from 250 to 420°, of feed rate from 1.1 to 3.2 liters/liter · hour or of the molar ratio of feed to hydrogen — or by the use of different catalysts.

The next stage in the investigation was a study of the prolonged use of tungsten sulfide catalysts for the hydrogenationof shale gasolines under constant conditions in which A-66 and A-70 gasolines were obtained; pressure 100 atm , $WS_2 + NiS + Al_2O_3$ catalyst (25 ml) in the 1st reactor, temperature 350-360°, WS_2 catalyst (100 ml) in the second reactor, temperature 400°, raw feed rate 150 ml per hour, with 1400 liters of hydrogen per 1 liter of gasoline.

TABLE 4

Effect of Volume Feed Rate in the Hydrogenation Refining of Shale Semicoking Gasoline (Sample I) Pressure 100 atm , $WS_2 + NiS + Al_2O_3$ (25 ml) in the 1st Reactor, 350-360°; WS_2 (100 ml) in the 2nd Reactor, Temperature 400°, Hydrogen Feed 1300-1500 liters/liter feed · hour

Operating time of catalysts (hours)	266—274	259—264	264—266
Volume feed rate (in liters/liter catalyst · hour)	1.2	1.9	3.2
Boiling commences at(°C)	41	40	38
10% boils out at (°C)	58	64	64
50% boils out at (°C)	99	107	114
90% boils out at (°C)	163	166	176
97.5% boils out at (°C)	197	201	210
Iodine number	3.3	2.1	4.3
Sulfonables (vol. %)	6.5	7.4	7.4
Octane number	46.3	—	—
Octane number with 1.5 ml of R-9 per 1 kg of gasoline	66.0	63.0	61.0
Sulfur content (wt. %)	0.037	0.028	0.016
Yield of hydrogenation product (wt. %)	94.2	98.7	97.4

In order to study the effect of the hydrogenation conditions on the quality of the gasoline, these conditions were varied somewhat during the operation.

The tests of catalyst life were continued for 473 hours. During this time the operation of the unit was interrupted 9 times, the catalysts remaining under hydrogen pressure the whole time.

The results, given in Figure 3, show the high hydrogenation activity of the catalysts: the iodine number decreased from 113.6 to 2-4 and the sulfur content fell from 0.77 to 0.02-0.04%. The changes of the iodine number indicate that interruptions in the operation of the unit, accompanied by rapid cooling and subsequent heating of the catalysts, lead during the first 150 hours to a decrease of the hydrogenation activity of the catalysts, but this is rapidly restored. During the subsequent 320 hours the degree of hydrogenation remains at a constant high level, with extensive hydrogenation of unsaturated compounds and removal of sulfur compounds (about 97%).

The cracking activity of the catalysts is greatest during the first stages of operation — the yield of the product is less than 90% by weight, and the gasoline formed has the lightest fractional composition. The yield increases with progressive age of the catalysts, reaching about 96% after 6-10 runs.

The octane numbers of the purified gasolines vary slightly and irregularly with catalyst age, with an average value, from five determinations, of 67 (with 1.5 ml of R-9 per 1 kg of gasoline). The pure gasoline has the low octane number of 46.3, despite its light fractional composition and high susceptibility to ethyl fluid (an increase of about 20 in the octane number is produced by addition of 1.5 ml of R-9 to 1 kg of the gasoline); this indicates that the hydrogenation product has a high content of normal paraffins of poor engine qualities. Hydrogenation products of gasolines obtained by thermal liquefaction have higher octane numbers.

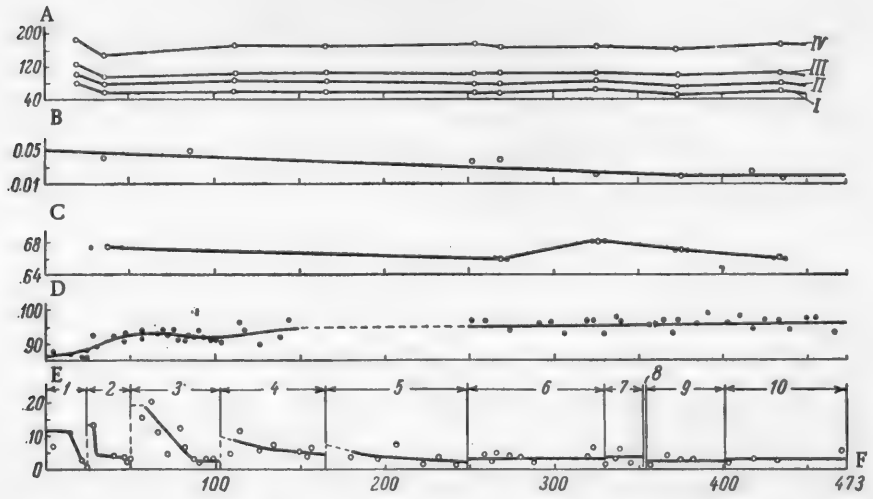

Fig. 3. Hydrogenation of shale semicoking gasoline (sample I: S = 0.87%, iodine number 113.6, octane number 60). Pressure 100 atms WS_2 + NiS + Al_2O_3 catalyst (25 ml) in the 1st reactor, temperature 350-360°; WS_2 catalyst (100 ml) in the 2nd reactor, temperature 400°, volume feed rate 1.2 liters/liter · hour, 1300-1500 liters of hydrogen per 1 liter raw feed. A) Temperature (°C), B) sulfur content (wt. %) C) octane number (1.5 ml of R-9 per 1 kg), D) yield of hydrogenation product (in wt. %), E) iodine number, F) service life of catalyst (hours). Fractional composition of gasoline: vol. % distilled over: I) 10, II) 30, III) 50, IV) 90. The arabic numbers on the diagram are the numbers of the runs.

TABLE 5

Material Balances for the Hydrogenation Refining of Shale Gasolines. Pressure 100 atm, WS_2 + NiS + Al_2O_3 (25 ml) in the 1st Reactor, 350-360°; WS_2 (100 ml) in the 2nd Reactor, Feed Rate 150 ml/hour, Hydrogen Rate 1400 liters/liter feed

Operating time of catalysts (hours)	Temp. in 2nd reactor (°C)	Origin of raw gasoline	Yields (% on raw feed)			Hydrogen consumption (% on raw feed)	Characteristics of product		
			gasoline	water	gas + losses		iodine No.	sulfur content (%)	octane No. with 1.5 ml of R-9
373—377	400	Semicoking (sample I)	95.8	0.7	5.4	1.9	2.4	0.018	67.0
377—386	420	Semicoking (sample I)	95.2	0.8	6.5	2.5	3.0	0.017	72.0
386—397	400	Semicoking (sample III)	98.2	0.6	2.4	1.2	1.4	0.042	70.0

The material balances for the hydrogenation refining of gasolines obtained from Esthonian shale by the semicoking and thermal liquefaction processes are given in Table 5.

The gasolines obtained by hydrogenation at 400° had the following group composition (% by weight):

	Alkenes	Alkanes	Cyclanes	Aromatic hydrocarbons
Semicoking gasoline	1.6	66.5	27.2	4.7
Thermal-liquefaction gasoline	0.6	57.9	32.2	9.3

Gasoline made by thermal liquefaction is a better raw material than gasoline made by semicoking of shale, because of the lower hydrogen consumption (owing to its lower contents of unsaturated hydrocarbons and neutral oxygen compounds), the higher octane characteristics of the hydrogenation product (owing to its higher content of cyclic hydrocarbons), and a much lower tendency to coke formation on heating.

The foregoing experimental data show that there is no deactivation of the industrial catalysts WS_2 + NiS + + Al_2O_3 and WS_2 during prolonged operation (20 days) under constant conditions in which high yields of good-quality motor gasoline are obtained, and prove convincingly that the process can be continued for long periods.

SUMMARY

1. It was shown in the development of a process for the hydrogenation refining of gasolines obtained by thermal liquefaction and by semicoking of Esthonian shales over industrial tungsten catalysts at moderate pressures (100 atm) that gasolines obtained by thermal liquefaction of shales are better raw materials than semicoking shale gasolines for the production of motor gasoline by hydrogenation, because of the lower hydrogen consumption, higher octane characteristics of the product, and the considerably lower tendency to coke formation on heating.

2. The investigation demonstrated the stable performance of industrial tungsten catalysts in the hydrogenation refining of unstable sulfur-containing shale gasolines.

LITERATURE CITED

[1] N. I. Zelenin, Liquid Fuel From Shale, 44 (State Fuel Tech. Press, 1948).*

[2] N. I. Zelenin, O. S. Kuratova, N. E. Shirokova and M. S. Varakisich, Trans. All-Union Sci. Res. Inst. for Shale Processing 1, 57 (1948); E. E. Feofilov, O. S. Kuratova and G. V. Tatarkina, ibid, 1, 67 (1948).*

[3] E. E. Feofilov and G. N. Garnovskaya, Chemistry and Technology of Shale Products II, 106 (1954).*

[4] B. L. Moldavsky and V. N. Pokorsky, Chemistry of Solid Fuel 6, 943 (1935).*

[5] B. L. Moldavsky and S. E. Livshits, Chemistry of Solid Fuel 5, 1, 91 (1934).*

[6] E. L. Clark, R. W. Hiteshul, H. I. Kandiner and B. Morris, Ind. Eng. Ch., 43, 2173 (1951).

[7] A. M. Stammer, World Petrol. VII, 24, 8 (1953).

[8] H. Novak and H. G. Liebich, Brenstoff Chemie, 35, 19/20 (1954).

[9] R. Birthler and C. H. R. Czkibik, Chem. Techn., 7, 373 (1954).

[10] R. M. Cole, and D. D. Davidson, Ind. Eng. Ch., 41, 12, 2711 (1949).

[11] P. W. Sherwood, Erdöl u. Kohle, 10, 617 (1953).

[12] R. A. Steel, I. A. Bock, W. R. Hertwig and L. W. Russum, Petroleum Refiner, 33, 5, 167 (1954); Petrol. Eng., 26, 4, C, 14, 24 (1954) etc.

[13] I. B. Rappoport, Synthetic Liquid Fuel (State Fuel Tech. Press, 1949)*; W. Kronig, Katalytische Druckhydrierung von Kohlen, Teeren, und Mineralolen (Berlin, 1950); F. Stitz, Osterreiche Chem. Z. 48, 3-4, 86 and 5-6, 113 (1947); S. V. Tatarsky, K. K. Papok and E. G. Semenido, Petroleum Economy 2 (1946)*; A. I. Vavul and E. S. Silchenko, Chemistry and Technology of Synthetic Liquid Fuel and Gas (State Fuel Tech. Press, 1951)* 3, 159; A. V. Lozovoi, S. A. Senyavin and A. B. Vol-Epshtein, J. App. Chem. 28, 2, 175 (1955).

Received September 12, 1955

* In Russian.

PRODUCTION OF SYMMETRICAL 4,4'-DINITROCARBANILIDES*

A. A. Spryskov, S. N. Solodushenkov and V. N. Klyuev

The Ivanova Institute of Chemical Technology

Among the extensive group of azo dyes, the so-called phosgenated dyes include a number of representatives with high fastness. Therefore an extension of the range of intermediates for the synthesis of phosgenated dyes is of definite interest. The problem of the synthesis of symmetrical 4,4'-dinitrocarbanilides has also arisen in relation to the possible use of the corresponding diaminocarbanilides as amines for ice dyeing.

Therefore the object of the present investigation was a search for possible means of preparing these compounds. Eight symmetrical derivatives of 4,4'-dinitrocarbanilide were prepared, five of which had not been described previously. Some properties of these compounds have been studied and their structure established.

Losanitch [1] treated carbanilide with nitric acid and obtained a product which he thought to be tetranitrocarbanilide. Similar results were obtained by Fleischer and Nemes [2]. Reudler [3], who also studied the nitration of carbanilide, considered that the products obtained by Fleischer and Nemes were most probably the dinitro derivatives. Curtius [4] nitrated carbanilide to obtain a product which was hydrolyzed to give m-nitroaniline. This led him to conclude that 3,3'-dinitrocarbanilide is formed by nitration. However, Reudler [3] did not detect 3,3'-dinitrocarbanilide on repeating Curtius's experiments. Ryan and O'Toole [5] obtained 4,4'-dinitrocarbanilide by the nitration of carbanilide in organic solvents. Coffey and Scholfield [6] nitrated carbanilide derivatives with methoxyl groups in the 2 and 2' positions, in acetic acid as a medium, and obtained 3,4'-dinitro-2,2'-dimethoxycarbanilide, 4,4'-dinitro-2,2', 5,5'-tetramethoxycarbanilide, and 4,4'-dinitro-2,2'-methoxy-5,5'-dichlorocarbanilide.

Harrison [7], who studied the nitration of symmetrical substituted carbanilides in acetic acid, found that in the nitration of 2,2'-dimethyl-3,3'-dimethyl-, 2,2'-dichloro-, and 3,3'-dichlorocarbanilides the nitro groups enter the ortho and para positions relative to the carbamide group, forming mixtures containing from 33 to 50% of the ortho isomers. In the nitration of 4,4'-dichlor- and 2,2', 4,4'-tetramethylcarbanilides the nitro groups only enter the ortho position relative to the carbamide group. Tsuda and Sakamoto [8] prepared 4,4'-dinitrocarbanilide by nitration of carbanilide in acetic acid.

Kogan and Kutepov [9] consider that the carbamide group — NHCOR is the directing group in nitration. Since in nitration the nitro group predominantly enters the para position to the acylamino group, and enters the ortho position to only a slight extent, the nitration of carbanilide should predominantly yield 4,4'-dinitrocarbanilide. They found that only small amounts of the ortho isomer were formed under various nitration conditions. They did not observe the formation of any 3,3'-dinitrocarbanilide.

Previous research on the nitration of carbanilide and its chloro, alkyl, and alkoxy derivatives shows that the directing effect is always exerted by the carbamide group. The 4,4'-dinitro isomer and a small amount of the 2,2'-dinitro isomer are always formed; the amounts of 3,3'-dinitro isomer are so small that it cannot be detected.

In addition to the nitration of carbanilide and its derivatives, other methods may be used for the preparation of 4,4'-dinitrocarbanilides. For example, Vittenet [10] heated p-nitroaniline with diphenylcarbonate and obtained 4,4'-dinitrocarbanilide. On heating of 2-amino-5-nitrotoluene with phosgene in toluene solution, Vittenet obtained 4,4'-dinitro-2,2'-dimethylcarbanilide. He used this method to prepare other isomeric dinitrodimethylcarbanilides and dinitrotetramethylcarbanilides. Reudler [3] prepared 4,4'-dinitrocarbanilide by Vittnet's

* Communication I in the series on the synthesis and applications of carbanilide derivatives.

method. This method, with certain modifications, was patented in Germany [11]. Coffey and Schofield's method [12] for the preparation of 4,4'-dinitrocarbanilide from p-nitroaniline in presence of dimethylaniline in an inert solvent is also recommended for the production of symmetrical halo, nitro, alkyl and alkoxy derivatives. They prepared 4,4'-dinitro-2,2'-methoxy-5,5'-dichlorocarbanilide and 4,4'-dinitro-2,2', 5,5'-tetramethoxycarbanilide. The preparation of the latter by the same method is claimed in a Swiss patent [13]. Lastovsky [14] prepared 2,2'-, 3,3'-, and 4,4'-dinitrocarbanilides by phosgenation of the corresponding nitroanilines in nitrobenzene.

Other methods for the preparation of nitrocarbanilides are not described here, as they are of no practical significance, with the possible exception of the method of preparation through the isocyanates.

Carbanilide and its derivatives may be hydrolyzed by the action of ammonia [15]. Gershzon and Lastovsky [16] showed that under increased pressures the hydrolysis of carbanilide with acids is almost complete. Coffey and Schofield [6] proposed the hydrolysis of derivatives of 4,4-dinitrocarbanilide by aqueous ammonia solutions under pressure. Harrison [7] hydrolyzed dinitrodimethyl- and dinitrodichlorocarbanilides by boiling aqueous pyridine solution or by glacial acetic acid. Kogan and Kutepov [9] consider that aqueous ammonia is the best hydrolyzing agent for 4,4'-dinitrocarbanilide. At low concentrations of the latter the hydrolysis is almost complete.

EXPERIMENTAL

Synthesis of 4,4'-dinitro-2,2', 5,5'-tetrachlorocarbanilide. 81 g (0.5 mole) of 2,5-dichloroaniline was dissolved in 180 ml of toluene, 50 g of soda in 1000 ml of water was added to the solution from a dropping funnel, and a current of phosgene was simultaneously passed through the mixture. The phosgenation was continued for 4 hours at 40-50°. The precipitate of 2,2', 5,5'-tetrachlorocarbanilide was filtered off; toluene was removed from it by steam distillation; it was again filtered, washed, and dried. Yield 85 g (97% of theoretical) of a white crystalline product, m. p. 296°.

For the nitration, 35 g (0.1 mole) of 2,2', 5,5'-tetrachlorocarbanilide was dissolved in 95 ml of sulfuric acid (s. g. 1.84); 17 ml of nitric acid (s. g. 1.36) was added dropwise to the solution at 20°, and the nitration was continued for 3 more hours at the same temperature. The nitration product was isolated by pouring the reaction mixture into cold water. The yellow precipitate was filtered off and washed with water. The crude 4,4'-dinitro-2,2', 5,5'-tetrachlorocarbanilide melted at 215°, the yield being 33 g (75% of the theoretical). It dissolves in 80% acetic acid on heating, and dissolves readily in acetone; crystallizes from a mixture of 2 volumes of acetone with 1 volume of water, in the form of pale yellow needles with m. p. 251°; it has not been described in the literature.

Hydrolysis of the nitration product by boiling in a mixture of pyridine and water for 4 hours gave 2,5-dichloro-4-nitroaniline which separated out on cooling in the form of yellow needles with m. p. 153-153.5° after recrystallization from pyridine diluted with water. The agreement with the m. p. of 153° given in the literature for 2,5-dichloro-4-nitroaniline shows that the nitro groups enter the 4,4' positions in nitration.

Synthesis of 4,4'-dinitro-2,2'-dimethyl-5,5'-dichlorocarbanilide. A solution of 44.5 g (0.25 mole) of 2-methyl-5-chloroanilinehydrochloride in 350 ml of water was added dropwise to a solution of 80 g of soda in 600 ml of water. A slow stream of phosgene was passed through the mixture at 30-35° with stirring. The precipitated 2,2'-dimethyl-5,5'-dichlorocarbanilide was filtered off and washed with water. This gave a product with m. p. 270-271°, in a yield of 17 g (44% of the theoretical).

For nitration, 15 g of 2,2'-dimethyl-5,5'-dichlorocarbanilide was added to a mixture of 30 ml of glacial acetic acid and 44 ml of nitric acid(s . g. 1.4) and nitrated at 55-60° for 1 hour. The thickened mixture was diluted with 100 ml of glacial acetic acid, and the heating was continued for a further 12 hours. When the mixture was poured into water, 4,4'-dinitro-2,2'-dimethyl-5,5'-dichlorocarbanilide (not described previously) was obtained in a yield of 6 g (31% of the theoretical). It is soluble in pyridine, acetone, methanol, and ethanol, and sparingly soluble in benzene; the compound recrystallized from ethanol is yellow, and melts at 226° with decomposition (the capillary was introduced into the apparatus at 200°).

0.1310 g wt.: 16.79 ml N_2 (24°, 737 mm Hg).
Found %: N 14.28 $C_{15}H_{12}O_5N_4Cl_2$. Calculated %: N 14.04.

Two g of the nitration product was hydrolyzed by boiling in a mixture of 25 ml of pyridine and 15 ml of water for 2.5 hours. The precipitate formed on dilution with water was filtered off, recrystallized from benzene, and obtained in the form of yellow crystals with m. p. 159°. Acetylation gave the acetyl derivative with m. p. 178°. 2-methyl-5-chloro-4-nitroaniline melts at 163°, and its acetyl derivative at 181° [17]. This proves that the nitro groups enter the 4 and 4' positions. (2-methyl-5-chloro-6-nitroaniline melts at 60°, and its acetyl derivative at 194°.)

Synthesis of 4,4'-dinitro-2,2'-dimethoxy-5,5'-dimethylcarbanilide. A solution of 40 g of 4-methoxy-3-aminotoluene in 75 ml of toluene was added dropwise with stirring at 35-40° to a solution of 70 g of soda in 1 liter of water, with a stream of phosgene passed through for 3 hours. The precipitate of 2,2'-dimethoxy-5,5'-dimethylcarbanilide was filtered off and treated with steam to remove toluene. The yield was 32.8 g (75% of the theoretical) of a white product with m. p. 199°.

For nitration, 2,2'-dimethoxy-5,5'-dimethylcarbanilide was treated with 10 moles of 15% nitric acid for 15 hours at 50-70°. When the mixture was poured into water a greenish yellow nitration product was obtained in 86.5% of the theoretical yield, with m. p. 255-260°. After recrystallization from pyridine, 4,4'-dinitro-2,2'-dimethoxy-5,5'-dimethylcarbanilide consisted of yellow crystals with m. p. 277°.

0.1278 g wt.: 15.80 mm N_2 (20°, 752 mm Hg).
Found %: N 14.25. $C_{17}H_{18}O_7N_4$. Calculated %: N 14.36.

Hydrolysis of 4,4'-dinitro-2,2'-dimethoxy-5,5'-dimethylcarbanilide with 25% ammonia in a sealed tube for 4 hours at 180° gave 2-methoxy-5-methyl-4-nitroaniline in the form of yellow needles with m. p. 132° before purification. Acetylation with acetic anhydride gave the acetyl derivative with m. p. 156°. A mixture with 2-methoxy-5-methyl-4-nitroacetanilide gave no depression. The same melting points for 2-methoxy-5-methyl-4-nitroaniline and its acetyl derivative are given in the literature [18]. This demonstrates the structure of the nitrocarbanilide, not described previously.

Synthesis of 4,4'-dinitro-2,2'-diethoxy-5,5'-dimethylcarbanilide. 4-ethoxy-3-aminotoluene was dissolved in toluene, and an emulsion in aqueous alkali was phosgenated with vigorous stirring at 35-40° for 4.5 hours. Near the end of the phosgenation the temperature was raised to 60-70° and the product was isolated as in the preceding synthesis. The yield of 2,2'-diethoxy-5,5'-dimethylcarbanilide was about 60% of the theoretical, with m. p. 198°.

For nitration, the product was dissolved in glacial acetic acid and added during 0.5 hour to a solution of 5 moles of 30% nitric acid in glacial acetic acid. The nitration was continued for 8 hours at 60°. The 4,4'-dinitro-2,2'-diethoxy-5,5'-dimethylcarbanilide formed was yellow in color, and melted at 205° without purification; it has not been described in the literature.

Synthesis of 4,4'-dinitro-2,2', 5,5'-tetraethoxycarbanilide. Hydroquinone was converted into 1,4-diethoxybenzene by the method for the preparation of phenetole. The subsequent nitration and reduction were performed by the method used in the preparation of 2,5-dimethoxyaniline [19]. The 2,5-diethoxyaniline was obtained in the form of white crystals with m. p. 78-82°, darkening in air.

A solution of 18 g of 2,5-diethoxyaniline in 100 ml of 3% hydrochloric acid was added with stirring to a solution of 75 g of soda in 300 ml of water at room temperature, and a stream of phosgene was passed through at the same time for 1.5-2 hours. The 2,2', 5,5'-tetraethoxycarbanilide was obtained in the form of a gray precipitate, the yield being 18 g (93.5% of the theoretical), with m. p. 194.5-196°; it was crystallized from toluene as colorless crystals with m. p. 199°.

0.1812 g wt.: 12.1 ml N_2 (24°, 740 mm Hg).
Found %: N 7.47. $C_{21}H_{28}O_5N_2$. Calculated %: N 7.22.

For nitration, 18 g of 2,2', 5,5'-tetraethoxycarbanilide was suspended in 140 ml of water; 16.5 ml of nitric acid, s. g. 1.5, was added dropwise to the suspension at about 30°, and the nitration was then continued for 5 hours at 70°. The mixture was poured into water to give a greenish yellow product with m. p. 204-205° in a yield of 19 g (86% of theoretical).

4,4'-dinitro-2,2', 5,5'-tetraethoxycarbanilide is soluble in glacial acetic acid and in pyridine; it crystallizes from a mixture of equal volumes of water and pyridine in the form of long thin needles, melting with decomposition at 215°.

0.1204 g wt.: 12.7 ml N_2 (24.5°, 738 mm Hg).
Found %: N 11.75. $C_{21}H_{26}O_9N_4$. Calculated %: N 11.75

Synthesis of 4,4'-dinitro-2,2', 5,5'-tetramethylcarbanilide. p-Xylidine was phosgenated in an aqueous alkaline emulsion at 45-50° for 1.5-2 hours. The white precipitate of 2,2', 5,5'-tetramethylcarbanilide was filtered off and washed with hot water and methyl alcohol. The yield was 72% of the theoretical, with m. p. 264°.

Harrison [7] nitrated 2,2', 5,5'-tetramethylcarbanilide with 12 moles of nitric acid (s. g. 1.5) in acetic acid. We used 10 moles of 30% nitric acid at 65-70°; after 1 hour the mixture was poured into cold water to give a yellow product with m. p. 244°. The yield was 69% of the theoretical, the same as obtained by Harrison.

Nitration in acetic acid with 5 moles of nitric acid at room temperature for 8 hours gave an 84% yield, the melting point being 244° as before.

After recrystallization from acetone 4,4'-dinitro-2,2', 5,5'-tetramethylcarbanilide melts at 276° (at 280° according to Harrison), and is easily hydrolyzed by boiling pyridine with water. This gives a product with m. p. 142°, with an acetyl derivative melting at 168°. The literature gives m. p. 142° for 2,5-dimethyl-4-nitroaniline, and 168-169° for its acetyl derivative.

Synthesis of 4,4'-dinitro-2,2'-dichlorocarbanilide. Phosgenation of 172.5 g of 2-chloro-4-nitroaniline with m. p. 106° in 450 ml of toluene and 113 ml of dimethylaniline at 50° for 3 hours gave a product of m. p. 237° which separated out on cooling in a yield of 170 g (92.5% of theoretical). It is fairly easily soluble in hot glacial acetic acid, and better in hot pyridine. After threefold recrystallization from pyridine yellow needles with m. p. 242.5° were obtained. The m. p. of 255° given by Harrison [7] for 4,4'-dinitro-2,2'-dichlorocarbanilide obtained by nitration of 2,2'-dichlorocarbanilide is probably too high. For confirmation of its structure, the product was hydrolyzed in aqueous pyridine to give 2-chloro-4-nitroaniline with m. p. 106° before purification; the acetyl derivative had m. p. 139°.

Synthesis of 4,4'-dinitro-2,2', 5,5'-tetramethoxycarbanilide. Patents [12, 13] describe the preparation of the carbanilide by phosgenation of 4-nitro-2,5-dimethoxyaniline, or by nitration of 2,2', 5,5'-tetramethoxycarbanilide in acetic acid [6].

We prepared the carbanilide as follows. Phosgene was passed through a solution of 18 g of soda in 250 ml of water at 35-40° with stirring, and a solution of 25 g of 2,5-dimethoxyaniline hydrochloride in 150 ml of warm water was added dropwise. After 30-40 minutes, with a constant alkaline reaction of the medium, 14 g (64% of theoretical) of almost colorless 2,2', 5,5'-tetramethoxycarbanilide with m. p. 209° was precipitated.

For nitration, 13 g of 2,2', 5,5'-tetramethoxycarbanilide was stirred into 133 g of 15% nitric acid; the mixture was heated to 60° during 1 hour, and kept at that temperature for 3-4 hours. The mixture was then poured into water, when 14.5 g (87.5% of theoretical) of yellow crystals of 4,4'-dinitro-2,2', 5,5'-tetramethoxycarbanilide separated out; the compound melted at 275° with decomposition.

Found %: N 13.51. $C_{17}H_{18}O_9N_4$. Calculated %: N 13.27.

We were not concerned with the optimum synthesis conditions, and therefore the yields of the products may be increased.

All the melting points were determined in sealed capillaries with the aid of short thermometers in a sulfuric acid bath or (above 270°) in an aluminum block. Many of the dinitrocarbanilides decompose without melting on prolonged heating at high temperatures and therefore the usual melting-point determinations do not give sharp results. The capillary was therefore introduced into the apparatus at a temperature 5-30° below the approximately determined melting point, and the heating was carried out more rapidly than usual. In such cases the melting points below 270° were determined in the Friedrichs apparatus [20], where the capillary can be inserted quickly at the required temperature.

SUMMARY

The dinitrocarbanilides prepared can be used after reduction for the synthesis of azo dyes.

LITERATURE CITED

[1] S. Losanitch, Ber., 10, 690 (1877).

[2] A. Fleischer, and G. Nemes, Ber., 10, 1295 (1877).

[3] M. Reudler, Rec. trav. chim., 33, 35 (1914).

[4] Th. Curtius, J. pr. Ch. [2], 52, 213 (1895).

[5] Ryan and O'Toole, Sci. Proc. Royal Soc. Dublin 17, 146 (1922/24).

[6] S. Coffey and E. Schofield, British Patent 375414 (1931); Zbl. II, 3920 (1933).

[7] E. Harrison, J. Soc. Chem. Ind., 54, Trans. 282 (1935).

[8] K. Tsuda and S. Sakamoto, J. Pharm. Soc. Japan, 64, 221 (1944).

[9] I. M. Kogan and D. F. Kutepov, J. Gen. Chem. 21, 1297 (1951);* ibid., 21, 2028.*

[10] H. Vittenet, Bull. Soc. Chim., [3] 21, 150 (1899); ibid 21, 660 and 948 (1951).

[11] MLB, German Patent 319970 (1912); Frdl., 13, 237.

[12] S. Coffey and E. Schofield, U. S. Patent 2093265 (1932); Zbl., II, 3954 (1937).

[13] J. R. Geigy A.-G., Swiss Patent 240993 (1946); Ch. A., 43, 6426 (1949).

[14] R. P. Lastovsky, J. Gen. Chem. 18, 923 (1948).

[15] A. Claus, Ber., 9, 694 (1876).

[16] G. I. Gershzon and R. P. Lastovsky, J. Appl. Chem. 9, 2058 (1936).

[17] J. Kenner, C. Tod and E. Witham, J. Chem. Soc., 127, 2346 (1925).

[18] L. Limpach, Ber., 22, 790 (1889).

[19] S. V. Bogdanov and V. A. Ivanova, Aniline Dye Ind. 4, 7 (1934).

[20] J. Houben, Die Methoden der Organischen Chemie, I, 799 (1925).

Received January 16, 1956

*Original Russian pagination. See C. B. Translation.

BRIEF COMMUNICATIONS

EXTRACTION OF SMALL AMOUNTS OF GOLD FROM CYANIDE, HYDROCHLORIDE, AND IODIDE SOLUTIONS BY MEANS OF ION-EXCHANGE RESINS

N. A. Ezerskaya and N. V. Markova

Scientific Research Institute for Geological Prospecting of Gold

The determination of gold in cyanide, hydrochloride, and iodide solutions is usually preceded by separation of the gold from the solutions in order to remove impurities and to concentrate it.

Most of the methods for the precipitation of gold described in the literature, based on the easy reduction of gold compounds to the metal, or on the formation of sparingly soluble compounds, do not give complete extraction of gold at very low concentrations (10^{-4}-10^{-6} mole/liter). Coprecipetation of gold with the use of collectors improves the extraction of gold, but the process is laborious, as it involves the subsequent separation of gold from the collector.

One of the commonest methods for the separation of gold from iodide solutions — extraction in the form of an amalgam [1] — is simple and fairly accurate, but it is inconvenient for extraction of gold from large volumes of solution. Moreover, the necessity of using mercury is a disadvantage.

Therefore it seemed very desirable to attempt to use ion-exchange resins, capable of extracting down to 10^{-5} - 10^{-6} moles of gold per liter from dilute hydrochloride, iodide, and cyanide solutions.

The possibility of using ion-exchange resins for the extraction of gold from hydrochloride solutions was first demonstrated in 1945 by Sussman, Nachod, and Wood [2]. Later Hussey [3] used weakly basic anion-exchange resins for the extraction of gold from cyanide solutions. Burstall, Forrest, and Wells [4] made a detailed study of the adsorption of gold on a strongly basic anion-exchange resin, Amberlite IRA = 400.They studied the influence of a number of metals and anions present in industrial cyanide liquors on the extraction of gold, and attempted to remove gold from the resin by means of various organic solvents. The best results were obtained when the resin was treated with acetone containing 5% of hydrochloric acid and 5% of water. However, 100% recovery of the gold could not be achieved. In 1955 Popova and Fridman [5] used a number of Soviet weakly basic anion-exchange resins for the extraction of gold from industrial cyanide liquors. Gold adsorbed by the resin was determined by the assay method. A test for the completeness of the extraction of gold, carried out with the aid of radioactive tracers, showed that gold was extracted completely from solutions containing tenths or hundredths of a milligram of gold per liter.

The object of the present investigation was the extraction of gold from various dilute solutions followed by chemical determination (without the use of assay methods). Hydrochloride, cyanide, and iodide solutions were analyzed.

Hydrochloric acid solutions of gold ($HAuCl_4$) are obtained in the analysis of minerals, alloys, and other gold-containing products. Extraction of gold from such products is necessary either for its determination or to separate it from other elements which have to be determined (such as copper, iron, etc.).

Cyanide solutions of gold in the form of $NaAu(CN)_2$ are obtained in the cyanide treatment of gold ores. Analysis of these solutions is important in control of the cyanidation process and of the subsequent precipitation of gold. Gold cyanide solutions are used in electroplating practice for gold plating. The necessity for precise analysis of gold electrolytes is obvious.

Iodide solutions of gold ($NaAuI_4$) are met in the determination of gold, in the so-called "iodine test" [1], i. e., in the treatment of the ore with a solution of iodine in potassium iodide. To determine the gold which is dissolved in this test, it must be extracted from the solution.

EXPERIMENTAL

The weakly basic anion-exchange resins An-2F, EDE-10, and Aspatit TM were used in the investigation. The resins were first converted into the chloride form by treatment with hydrochloric acid. The resins were brought into contact with the solutions under test in static conditions, the solution being mechanically stirred with the resin. After the stirring, the resin was filtered off and burned. The residue after the combustion was dissolved in aqua regia, and the solution was evaporated almost to dryness on the water bath. It was then evaporated twice with hydrochloric acid. The $HAuCl_4$ solution was then analyzed polarographically [6], volumetrically, or colorimetrically [7].

TABLE 1

Extraction of Gold from Hydrochloric Acid Solutions (2 g of AN-2F resin, stirring time 1.5 hours, solution volume 200 ml)

Au taken (mg)	Au found (mg)	Difference (mg)	Au taken (mg)	Au found (mg)	Difference (mg)
0.970	0.970	0	0.029	0.031	+ 0.002
0.290	0.260	− 0.030	0.029	0.031	+ 0.002
0.097	0.089	− 0.008	0.022	0.022	0
0.058	0.060	+ 0.002	0.015	0.015	0

TABLE 2

Extraction of Gold by Anion-Exchange Resin From Hydrochloric Acid Solutions in Presence of Copper and Iron (2 g of AN-2F resin, stirring time 1.5 hours, solution volume 200 ml; Au determined polarographically)

Taken (mg)			Found (mg)		
Au	Cu	Fe	Au	Cu in filtrate	Fe in filtrate
0.5	–	–	0.5	–	–
0.5	0.5	–	0.5	0.5	–
0.5	2.0	–	0.5	2.0	–
0.5	–	1.0	0.5	–	1.0
0.5	–	4.0	0.5	–	4.0

Extraction of gold from hydrochloric acid solutions. The experiments showed that gold can be extracted from hydrochloric acid solutions (pH ≈ 3) equally fully by means of the weakly basic resins AN-2F, TM, and EDE-10. A disadvantage of EDE-10 is its "creeping" during combustion. The stirring time needed is 1-1.5 hours. The minimum amount of resin is 1.5-2 g. The results in Table 1 show that the extraction of various amounts of gold is fairly complete.

Copper and iron, present as cations in hydrochloric acid solutions, are not adsorbed by the resin and do not interfere in the subsequent determination of gold (Table 2).

Extraction of gold from cyanide solutions. AN-2F, EDE-10 and TM resins were used for the extraction of gold. The time required for the stirring of the solution with the resin was 1-1.5 hours. The resin after filtration was burned in a porcelain crucible. The residue was dissolved in aqua regia in the same crucible, and the gold was then converted into $HAuCl_4$. The gold was determined polarographically or colorimetrically.

All three resins extract gold completely from the solutions. The advantage of TM and EDE-10 resins is their rapid combustion.

TABLE 3

Polarographic Determination of Gold in Industrial Cyanide Liquors After Extraction with an Anion Exchange Resin (Resin — AN-2F, stirring time 1 hour)

Concentration of Au (mg/g)	Amount of solution (mg)	Au present (mg)	Amount of resin (g)	Au found (mg)	Difference (mg)
14.02	100	1.40	2	1.28	— 0.12
7.01	100	0.70	2	0.63	— 0.07
2.80	100	0.28	2	0.28	0
1.40	200	0.28	3	0.26	— 0.02
0.28	500	0.14	3	0.15	+ 0.01
0.14	500	0.07	3	0.08	+ 0.01
0.070	1000	0.07	3	0.066	— 0.004
0.035	2000	0.07	4	0.063	— 0.007
0.028	2000	0.056	4	0.060	+ 0.004

The conditions for the adsorption of gold from synthetic cyanide solutions had been thoroughly studied in the investigation cited above [5]; therefore we did not repeat these experiments, and extracted gold directly from industrial cyanide liquors which contained considerable amounts of copper and zinc, and a little iron, in addition to gold. Copper, zinc, and iron, present as complex cyanides, are adsorbed by anion exchangers together with gold. As only copper interferes with polarographic determination of gold in an alkaline medium, it must be removed. For this, the residue after combustion of the resin was treated several times with HNO_3 (1 : 1) on heating, and the solution was decanted from the residue. Aqua regia was added to the residue; this was followed by evaporation with aqua regia to convert the gold into $HAuCl_4$, and by polarographic determination of gold.

TABLE 4

Extraction of Gold from Iodide Solution (2 g of TM resin, stirring time 1-1.5 hours, solution volume 200 ml, pH = 2-3, iodine combined with Na_2SO_3)

Au taken (mg)	Au found (mg)	Difference (mg Au)	Au taken (mg)	AU found (mg)	Difference (mg Au)
0.740	0.722	—0.018	0.014	0.014	0
0.390	0.370	—0.020	0.007	0.007	0
0.056	0.055	—0.001	0.003	0.003	0
0.028	0.028	0	0.0014	0.0016	+0.0002
			0.0007	0.0007	0
			0.0003	Not found	—0.0003

The results of the determination of gold in several cyanide solutions are given in Table 3.

Extraction of gold from iodide solutions. Solutions prepared from a standard gold solution were used for the studies of the extraction of gold by anion-exchange resins. To prepare the standard solution, an accurately weighed sample of metallic gold was dissolved in 100 ml of a 2% iodine solution in 4% potassium iodide solution. The gold solution was standardized as follows: 3 ml of the solution was evaporated to dryness in a lead basin, and the residue was then analyzed for gold by the usual assay procedure.

Direct extraction of gold by anion-exchange resins from iodide solution does not give the desired results. The resin vigorously adsorbs iodine from the solution, with a considerable decrease of its exchange capacity. The greater proportion of the gold ions remains in solution. The extraction of gold is improved if the iodine is combined with alkali solution. The best results were obtained with EDE-10 resin. However, the extraction of small amounts of gold is incomplete. The reason is the increase of the solution pH, which, as is known, lowers the exchange capacity of weakly basic anion exchangers. Therefore in the subsequent experiments the iodine was combined with sodium sulfite. To the iodide solution containing gold a few milliliters of 10% soda solutions was added, followed by crystalline sodium sulfite until the solution became decolorized. The resin was then added and the solution was agitated by means of a mechanical stirrer. The resin with the adsorbed gold was burned and treated as in the preceding experiments. Gold was determined polarographically, volumetrically, or colorimetrically. The most complete extraction of gold was obtained with TM resin.

A change of pH from 2 to 3.5 did not affect the extraction of gold. Further increase of pH decreased the extraction.

For 500 ml of solution, 2-3 g of resin is needed. The time of stirring is 1-1.5 hours. Under these conditions gold is effectively extracted from iodide solutions with different gold contents (Table 4).

When ore or sand is treated with iodine solution for determination of gold, iron may be dissolved together with gold. Experiments with artificial iodide mixtures containing gold and iron showed that iron is not adsorbed by the anion-exchange resins in these conditions, and does not interfere with the determination of gold. Copper in presence of iodine forms CuI_2, which rapidly passes into Cu_2I_2, which is insoluble in water and does not interfere with the determination of gold.

SUMMARY

1. Gold is extracted almost completely from hydrochloric acid solutions (pH $\approx$ 3) by AN-2F, EDE-10, and Aspatit TM anion-exchange resins, and can be determined polarographically, volumetrically, or colorimetrically.

2. Gold in industrial cyanide liquors can be determined polarographically, volumetrically, or colorimetrically after extraction from the liquors by means of the above-named resins.

3. Gold is extracted almost completely from iodide solutions by Aspatit TM after iodine has been combined with sodium sulfite.

LITERATURE CITED

[1] Austen, Trans. Inst. Mining and Metallurgy, XX, 516 (1911); V. Ya. Mostovich, The Art of Assaying (State Sci.-Tech. Press, Moscow-Leningrad-Sverdlovsk, 1934)* p. 110; O. E. Zvyagintsev, V. A. Vorobyeva and S. K. Shabarin, Factory Labs. 9, 909 (1939); G. K. Kropachev, Jubilee Coll. Trans. Irkutsk Mining Metallurg. Inst. 139 (1941).

[2] Sussman, Nachod and Wood, Ind. Eng. Ch., 37, 618 (1945).

[3] Hussey, Rept. Invest. U. S. Bur. Mines 4374 (1949).

[4] Burstall, Forrest, Kember and Wells, Ind. Eng. Ch., 45, 8, 1648 (1955).

* In Russian.

[5] N. N. Popova, I. D. Fridman, Trans. Sci. Res. Inst. Geol. Prospecting Gold (1956).

[6] N. A. Ezerskaya, Ann. Sector Platinum 32 (1956).

[7] Pollard, Analyst, 62, 597 (1937); Pevzner and Paulsen, J. Appl. Chem. 11, 6 (1938).

Received June 2, 1956

USE OF RADIOACTIVE SULFUR (S^{35}) FOR DETERMINATION OF SULFONIC GROUPS IN SULFONATED COAL

N. P. Drozdov and A. N. Popov

The treatment of certain coals with oleum [1] produces sulfonated coal (a cation exchanger) containing sulfonic and carboxyl groups formed in the course of sulfonation. It is known that coal contains sulfur even before sulfonation. In the Donets coal used in our experiments some sulfur is present in the form of pyrite [2] mixed with the coal, and some is in organic form. We shall refer to the content of this sulfur in coal as the "initial" content.

Our purpose in the present investigation was to determine the sulfonic group content of sulfonated coal. This can be done by chemical analysis only if the "initial" sulfur content does not decrease during sulfonation and the sulfur is not oxidized to sulfonic groups. To solve this problem, we prepared under different conditions 4 samples of sulfonated coal containing labeled sulfur in the form of sulfonic groups.

The sulfonated coals were made by the action of oleum containing 27% of excess SO_3 on powdered Donets coal, in 6 : 1 weight ratio of oleum to coal.

Coal fractions with 0.25-0.5 mm particles were used. S^{35} was introduced into the oleum in the form of $H_2S^{35}O_4$.

The preparation of the 1st, 2nd, and 4th sulfonated coal samples was carried out for 3 hours at 20, 100 and 200° respectively, while the 3rd sample was prepared in 20 minutes at 150°. The sulfonated coal samples were washed with water, 10% HCl solution, and again with distilled water until neutral to methyl orange, and then dried at 100°. To find whether the "initial" sulfur is oxidized to sulfonic groups during the oleum treatment of the coal, several experiments were carried out on the thermal decomposition of the sulfonated coal samples. A weighed sample of moistened sulfonated coal was heated in a heat-resisting retort in a nitrogen atmosphere for 3 hours at 500°. In these conditions sulfur oxides were formed only from the sulfonic groups present in the sulfonated coal. The liberated gases were passed through $CuCl_2$ solution, where the sulfur oxides formed sulfuric acid, and the hydrogen sulfide which was also formed during the decomposition produced a precipitate of copper sulfide.

At the end of the experiment the solution was filtered. Barium sulfate containing S^{35} was precipitated from the filtrate, and its specific activity was compared with the specific activity of a precipitate obtained from the oleum used for sulfonation of the coal.

In all the experiments on the thermal decomposition of the 3 samples of sulfonated coal prepared at 20, 150 and 200° the specific activities of the barium sulfate coincided within the limits of experimental error. This shows that the sulfur present in coal is not oxidized to sulfonic groups.

Sulfonic groups are formed only when they are introduced into the coal by treatment with oleum.

The determinations of the "initial" sulfur in the coal (q_0) and of the total sulfur in the sulfonated coal (q_1) were carried out chemically, the sulfur being weighed as $BaSO_4$ [3].

The sulfonic group content (q_2) of the sulfonated coal was determined by two methods.

In the isotopic dilution method [4], it was found from the expression

$$q_2 = \frac{q_1 \cdot A_1}{A_0} \text{ m-eq/g}$$

where q_1 is the total sulfur in the sulfonated coal (in meq/g), * found by chemical analysis; A_1 is the activity (in pulses /minute) of the $BaSO_4 + BaS^{35}O_4$ precipitate obtained in the chemical analysis of sulfonated coal tagged with S^{35}; A_0 is the activity (in pulses/minute) of the $BaSO_4 + BaS^{35}O_4$ precipitate obtained by the action of $BaCl_2$ on the oleum used for sulfonation of the coal. The accuracy of the determinations was ± 3 %.

The specific activities of $BaSO_4 + BaS^{35}O_4$ and sulfonated coal were measured with the aid of an end-type radiation counter to an accuracy of ± 1%.

The thickness of the layer of precipitate used for the measurement was greater than the saturation thickness for the β^--particles emitted by S^{35}.

The decrease of the "initial" sulfur content on treatment of the coal with oleum was found from the expression

$$\Delta q = q_{0\text{av}} - (q_1 - q_2)$$

or (in %)

$$\frac{\Delta q}{q_{0}\text{av}} \cdot 100,$$

where q_0 is the average value from 3 determinations of the "initial" sulfur content of the coal (in meq/g).

The other method for sulfonic group determination was the method of standard additions; a definite amount (a meq) of sodium sulfate ($Na_2SO_4 + Na_2S^{35}O_4$) prepared from NaOH and the oleum used for sulfonation of the coal was added to 1 g of the sulfonated coal free from radioactive sulfur.

The sodium sulfate solution was added in small portions; the sulfonated coal was dried and mixed after each addition. Analogously, a meq of inactive Na_2SO_4 was added to 1 g of sulfonated coal containing S^{35} in its sulfonic groups. In this case the gram-equivalent of Na_2SO_4 is numerically equal to the molecular weight, as the tagged sulfur is present in the sulfonated coal in the form of $R-SO_3H$ groups. Both samples of the sulfonated coal were conditioned in air to constant moisture content, and the S^{35} activity was determined in each.

The tagged sulfur content (q_2) of the sulfonated coal was found from the expression

$$q_2 = \frac{a \cdot A_3}{A_2},$$

where A_3 is the activity of the sulfonated coal containing S^{35} in its sulfonic groups; A_2 is the activity of the sulfonated coal into which a meq of sodium sulfate containing radioactive sulfur had been introduced per 1 g of the sulfonated coal.

The sulfonic group content of the sulfonated coal determined by the two methods was correlated with the exchange capacity of its sulfonic groups (at pH = 7), which was determined by the usual method [5], with slight modifications.

The procedure was as follows. Through a column containing 2 g of the sulfonated coal in the H form, 0.5 liter of 10% $CaCl_2$ solution was passed at a rate of 2 ml/cm^2 · minute. The solution leaving the column was

* The sulfur content of coal and total sulfur in sulfonated coal are given in meq/g, 1 meq of sulfur being taken as 32 mg.

collected in a measuring flask. The hydrogen ion content of this solution was determined by titration with 0.05 N NaOH solution. The titration results were used to calculate the exchange capacity in meq/g of dry sulfonated coal. To convert the sulfonated coal back into the H form, 300 ml of 10% HCl solution was passed through the column. The coal was then washed with distilled water until neutral to methyl orange.

The results of the determinations of exchange capacity and sulfonic group contents of different samples of sulfonated coal are given in the Table.

Exchange Capacities and Sulfonic Group Contents of Different Samples of Sulfonated Coal

Sulfonated coal sample No.	Exchange capacity (meq/g)	Tagged sulfur (sulfonic groups) (in meq/g) q_2 in the sulfonated coal, determined by		"Initial" sulfur content q_1 of sulfonated coal (in meq/g)	Decrease of "initial" sulfur content on sulfonation of coal in %, $\frac{\Delta q}{q_{av}} \cdot 100$	Total sulfur content q_3 of sulfonated coal (in meq/g)
		isotopic dilution	standard additions			
1	1.95	2.39	2.31	1.42		
	1.98	2.27	2.39	1.43		
	1.97	2.39	2.34	1.42		
Average	1.97	2.35	2.35	1.42	28.6	3.35
2	2.36	2.40	2.38			
	2.36	2.43	2.37			
	2.37	2.39	2.38			
Average	2.36	2.41	2.38	1.42	41.6	3.22
3	1.96	1.93	2.01			
	1.97	1.94	1.94			
	1.97	1.95	1.98			
Average	1.97	1.94	1.97	1.42	47.2	2.72
4	1.86	1.26	1.24			
	1.87	1.23	1.25			
	1.85	1.28	1.27			
Average	1.86	1.26	1.25	1.42	74.6	1.62

It is seen that the "initial" sulfur content decreases during sulfonation of the coal. The total sulfur content is lower in sulfonated coals made at higher temperatures.

In sulfonated coals Nos. 2 and 3, prepared at 100 and 150°, the sulfonic group (tagged sulfur) contents are practically equal to their exchange capacities at pH = 7. In sulfonated coal No. 1, prepared with the reaction mixture cooled to 20°, the sulfonic group (tagged sulfur) content is greater than the exchange capacity. In sulfonated coal No. 4, prepared at 200°, other groups are apparently more active and take part in ion exchange even in neutral solution. As a result, the sulfonic group content of this sample is lower than its exchange capacity at pH = 7.

SUMMARY

1. It is shown that in the sulfonation of coal the "initial" sulfir is not oxidized to sulfonic groups.

2. The contents of sulfonic groups (tagged sulfur) in sulfonated coals were determined by the isotopic dilution and standard addition methods.

3. It is shown that the sulfur group content of sulfonated coal cannot be found from the results of chemical analysis (without the use of tagged sulfur), as 29-75% of the sulfur present in Donets coal is removed during sulfonation.

4. It was found that the sulfonic group contents of sulfonated coal samples prepared at 100 or 150° are practically equal to their exchange capacities at pH = 7.

LITERATURE CITED

[1] M. S. Shkrob, Modern Methods of Water Preparation and Boiler Water Treatment (1947) p. 136.*

[2] B. A. Pavlov and A. S. Solovyeva, Technology of Inorganic Substances (1954), p. 61.

[3] Treadwell and Hall, Analytical Chemistry. Gravimetric Analysis (Russian Translation) (1935) pp. 348-350.

[4] S. E. Bresler, Radioactive Elements (1952), pp. 411-414.

[5] R. Kunin and R. Myers, Ion Exchange Resins (Russian Translation) (IL, 1952), p. 159.

Received January 13, 1956

*In Russian.

ACTION OF ENAMEL MELTS ON STEEL

G. I. Belyaev

The Dnepropetrovsk Chemicotechnological Institute

Enamel ground coats in direct contact with the metal are formed during firing of the ware at high temperatures (875-975°). During this firing, steel is oxidized under the enamel layer with the formation of a thin surface film of scale which then reacts and dissolves in the silicate melt. Excess of iron oxides in the enamel leads to the supersaturation and crystallization; this increases the number of surface faults and lowers the quality of the ground coat [1].

The literature contains very few publications on the mechanism of the solution of metals in fused silicates, and there is no common opinion concerning the effect of enamel composition on the dissolution of steel. In 1953, we put forward the view that "with increasing basicity of enamel glasses the oxidizing action of silicate melts on steel increases" [1].

Azarov [2, 3], who studied many problems relating to the formation of enamel coatings, also carried out experiments on the corrosion of steel in silicate melts. To determine the action of borate and boron-free enamels on the metal, he exposed steel plates to the action of borate frit Nos.1-18, 41 and 2015, and boron-free Nos.1-35, 60 and 10 melts for 10 minutes; after treatment in 20% caustic soda solution, he determined the corrosion losses of the specimens. He concluded from these experiments that ". . . the composition of the enamel does not have any significant influence on the oxidation of steel during exposure to the melts" [2]. In another paper [3], containing a description of the same experiments, he repeats this conclusion and states that ". . . the composition of the enamel did not have any significant influence, in the experimental conditions described, on the oxidation of steel during exposure to the melts."

Mazurek [4] considered that the oxidizability of steel under an enamel coating is determined by the sintering temperature of the enamel rather than by the nature of the silicate melt. He wrote "The oxidizability of steel under the enamel layer varies within narrow limits for borate and boron-free enamels; i. e., it does not depend on the presence of boric anhydride." We do not deny the influence of the frit-sintering temperature on the oxidation of steel, but we consider that, for ground coat enamels of the same fusibility, the oxidizability of the steel depends considerably on the basicity of the melt, and in particular on the presence of boric anhydride in the enamel.

In many papers on the action of fused salts on steel [5-7] there are direct indications that the corrosion losses depend not only on the melting point but also on the composition of the fused electrolyte. It is also known that basic slags have a considerably stronger oxidizing action than acidic on metals [8].

It was therefore decided to study the corrosion of steel in fused electrolytes in relation to enameling technology. In particular, the action of melts of simple silicate and borate glasses of different basicity, and of industrial borate and boron-free enamel frits on low-carbon sheet steel was studied.*

EXPERIMENTAL

Silicate and borate glasses of the following compositions were prepared for the corrosion tests: 1) $Na_2O \cdot SiO_2$; 2) $Na_2O \cdot 1.5\ SiO_2$; 3) $Na_2O \cdot 2SiO_2$; 4) $Na_2O \cdot B_2O_3$; 5) $Na_2O \cdot 1.5\ B_2O_3$; 6) $Na_2O \cdot 2B_2O_3$; 7) $Na_2O \cdot$

*N. F. Smakota assisted in the experiments.

· · $3B_2O_3$ and 8) B_2O_3. The batches were made from quartz and sand washed in hydrochloric acid, and chemically pure sodium carbonate and boric acid. The glasses were melted in fireclay crucibles in a laboratory electric furnace at 1100-1200°. The melts were poured onto refractory plates, cooled, crushed, and powdered in a porcelain ball mill. The glass powders were again heated to 1100°, when the melts were poured out into crucibles containing the steel specimens.

Specimens of thin cold-rolled sheet steel from the "Zaporozhstal" mill were used in the experiments. The size of the plates was 20 × 80 × 0.5 mm. The chemical composition of the steel (in %) was: C 0.08, Mn 0.33, Si traces, S 0.029 and P 0.013. The specimens were cleaned with emery paper, treated with ethyl alcohol, and kept in a desiccator for 30 minutes before being weighed on an analytical balance. The prepared specimens were put into ceramic crucibles, covered with the molten glass, and kept for 1 hour in the furnace at 1100°. Each experiment was carried out with "fresh" melt and repeated at least 3 times. Only 1 steel specimen was put into each crucible. The crucibles were then taken out of the furnace, the steel specimens were quickly removed from the melts and immersed in cold water; after the melt had been removed from the metal surface the specimens were washed in alcohol, dried, and weighed.

Observations during the heating showed that the melt liberates a gas which takes fire at the surface. This gas is probably hydrogen and oxides of carbon. After the experiments the color of the glass near the plate changed, the melt became brown, and a thin layer of glass saturated with iron oxide formed on the surface of the steel. This layer was easily detached on sharp cooling of the specimen in water.

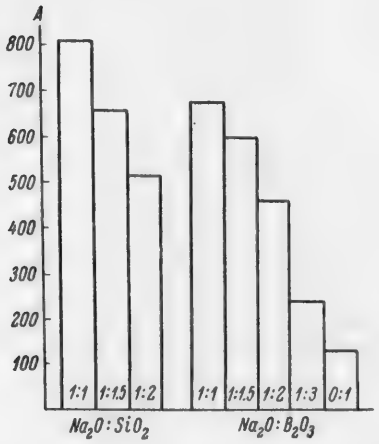

Fig. 1. Corrosion losses of steel in silicate and borate melts. A) Loss in weight (in mg/dm²).

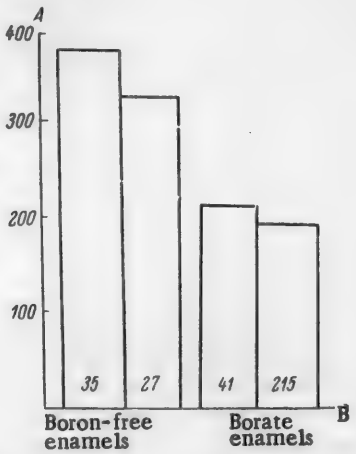

Fig. 2. Dissolution of steel in borate and boron-free enamels. A) Loss in weight (in mg/dm²), B) numbers of enamels.

Gurovich [5] showed that, with complete immersion of the specimens in chloride melts, the results with and without use of vacuum agreed within the limits of experimental error. Therefore all our tests in silicate melts were carried out without the use of vacuum.

The corrosion loss was used as a measure of the solution rate of iron in the fused electrolytes. The effect of glass composition on the corrosion of steel is given in Table 1 and Figure 1.

The method described above was also used for testing the action of borate and boron-free enamels on steel. Table 2 gives the compositions of these enamels, and Table 3 and Figure 2 give data on the dissolution of iron in fused industrial enamels.

TABLE 1

Corrosion of Steel in Molten Silicate and Borate Glasses

Glass composition	Wt. of steel plate (in g)		Loss of wt. of the specimen (in mg)	Area of specimen (in dm^2)	Corrosion of specimen (in mg/dm^2)	Average corrosion rate (in $mg/dm^2 \cdot hr$)
	before immersion in melt	after immersion				
$Na_2O \cdot SiO_2$	2.2244	2.1214	103.0	0.121	851.2	810.0
	2.1277	2.0312	96.5	0.122	791.0	
	2.2057	2.1072	98.5	0.125	788.0	
$Na_2O \cdot 1.5SiO_2$	2.2236	2.1450	78.6	0.121	644.2	653.1
	2.2864	2.2052	81.2	0.123	665.5	
	2.2530	2.1730	80.0	0.122	655.7	
$Na_2O \cdot 2SiO_2$	2.1713	2.1067	64.6	0.125	516.8	509.6
	2.1340	2.0716	62.4	0.123	507.3	
	2.1727	2.1091	63.6	0.126	504.7	
$Na_2O \cdot B_2O_3$	2.1585	2.0780	80.5	0.119	668.0	672.4
	2.2725	2.1883	84.2	0.124	679.0	
	2.2060	2.1249	81.1	0.121	670.0	
$Na_2O \cdot 1.5B_2O_3$	2.2565	2.1803	76.2	0.128	595.3	596.6
	2.2448	2.1723	72.5	0.121	599.1	
	2.3154	2.2415	73.3	0.124	596.0	
$Na_2O \cdot 2B_2O_3$	2.1107	2.0575	53.2	0.122	436.0	455.5
	2.0908	2.0450	55.7	0.122	456.6	
	2.2217	2.1671	54.6	0.123	443.9	
$Na_2O \cdot 3B_2O_3$	2.1583	2.1273	31.0	0.124	250.0	244.4
	2.1537	2.1231	30.6	0.124	248.9	
	2.2106	2.1808	29.8	0.126	236.5	
B_2O_3	2.2955	2.2774	18.1	0.132	137.1	134.7
	2.2485	2.2307	17.8	0.130	136.9	
	2.1011	2.0855	15.6	0.120	130.0	

The results show that the corrosion rate depends on the composition of the silicate melt. Iron dissolves less rapidly in simple borate glasses than in silicate glasses of analogous composition (Fig. 1). This is probably because boric anhydride is a more acidic oxide than silica, and melts of sodium silicates are more basic than melts of sodium borates. As was to be expected, the corrosion losses were lowest in fused boric anhydride. Experiments with enamels of more complex composition (Table 2) also show convincingly (Table 3 and Fig. 2) that the corrosive action of enamel melts on steel decreases with increasing boric anhydride content.

The explanation is that ordinary boron-free ground enamels are weakly basic, while borate enamels are acidic [9]. Of the boron-free melts studied No. 35 is considerably more corrosive to steel than No. 27, of analogous composition. The cause of the higher chemical activity of No. 35 melt is probably its higher basicity as compared with No. 27 (the $Na_2O : SiO_2$ ratio is 0.41 in the former case, and 0.38 in the latter).

Many workers [5-7] have reported that the presence even of traces of moisture in the melt increases the corrosion loss of steel considerably. It is known [8, 10-12] that molten glasses and slags have high contents of gases, consisting mainly of H_2O dissociated into H^+ and OH^-, and that the solubility of H_2O increases with increasing basicity. The large cations Na^+ and K^+ [8] are especially effective in raising the solubility of gases in slags. On the basis of these considerations, the mechanism of the dissolution of iron in a silicate melt can be represented as an electrochemical process, in which hydrogen ions are discharged at the cathodic regions of the microcouples in the metal according to the equation [6]

$$2H^+ + 2e = H_2,$$

TABLE 2

Enamel No.	Contents (%)					
	SiO_2	B_2O_3	Al_2O_3	Na_2O	CaF_2	Fe_2O_3
42	51.75	13.65	7.70	17.60	9.00	0.30
215	46.90	18.84	8.07	20.02	5.81	0.36
27	59.29	—	1.56	22.35	14.59	2.21
35	58.68	—	3.36	24.25	12.56	1.15

while at the anodic regions iron ions enter the glass:

$$Fe - 2e = Fe^{2+}.$$

SUMMARY

1. Iron dissolves vigorously in molten silicate and borate glasses and enamels, with evolution of gases.

2. The corrosion rate of iron depends on the chemical composition and the basicity of the silicate melt. Sodium silicates are more corrosive to steel than sodium borates. The solvent action of glass melts on steel increases considerably with increasing Na_2O and decreasing B_2O_3 and SiO_2 contents.

TABLE 3

Corrosion of Steel in Molten Enamels

Enamel No.	Wt. of steel plate (in g)		Loss of wt. of the specimen (in mg)	Area of specimen (in dm^2)	Corrosion of specimen (in $mg/dm^2 \cdot$ hour)	Average corrosion rate (in $mg/dm^2 \cdot$ hour)
	before immersion	after immersion				
41	2.1635	2.1356	27.9	0.118	236.4	212.4
	2.1811	2.1566	24.5	0.120	204.1	
	2.3163	2.2913	25.0	0.127	196.9	
215	2.2140	2.1900	24.0	0.122	196.7	198.7
	2.2250	2.2004	24.6	0.121	203.3	
	2.3574	2.3321	25.3	0.129	196.1	
27	2.2493	2.2089	40.4	0.124	325.5	331.3
	2.2027	2.1633	39.4	0.119	331.0	
	2.2480	2.2062	41.8	0.124	337.0	
35	2.2908	2.2446	46.2	0.124	372.6	384.0
	2.1960	2.1482	47.8	0.120	398.3	
	2.2310	2.1845	46.5	0.122	381.1	

3. Steel is oxidized more vigorously by melts of boron-free ground coat enamels than by melts of borate enamels.

4. The solution of iron in silicate melts is probably an electrochemical process which involves liberation of gaseous hydrogen and oxides of carbon, and release of iron ions into the melt.

LITERATURE CITED

[1] G. I. Belyaev, Coll. Trans. Novocherkassk Polytech. Inst. 24 (38) (Industrial Construction Press, 1953).*

[2] K. P. Azarov, Coll. Trans. Novocherkassk Polytech. Inst. 24 (38) (Industrial Construction Press, 1953).*

[3] K. P. Azarov, J. Appl. Chem. 27, No. 1 (1954).

[4] Yu. V. Mazurek, Author's Summary of Dissertation, Lensoviet Technol. Inst. Leningrad (1955).

[5] E. I. Gurovich, J. Appl. Chem. 27, No. 4 (1954).

*In Russian.

[6] V. P. Kochergin, A. V. Kabirov and O. N. Skornyakova, J. Appl. Chem. 27 (1954).

[7] V. P. Kochergin, M. S. Garpienko, O. N. Skornyakova and M. Sh. Minushena, J. Appl. Chem. 29, No. 4 (1956).*

[8] O. A. Esin and P. V. Geld, Physical Chemistry of Pyrometallurgical Processes II (Metallurgy Press, 1954).**

[9] K. P. Azarov, Coll. Trans. Novocherkassk Polytech. Inst. (Industrial Construction Press, 1954).**

[10] W. Eitel, The Physical Chemistry of the Silicates (Russian translation) (ONTI, 1936).

[11] V. T. Slavyansky, J. Phys. Chem. 25, No. 9 (1951).

[12] S. E. Krasikov, Glass Ind. 7 (1938).

Received June 17, 1956

*Original Russian pagination. See C. B. Translation.
**In Russian.

DETERMINATION OF THE SOLUBILITY OF CARBON DIOXIDE IN AQUEOUS SOLUTIONS OF SODIUM SULFATE AND ITS MIXTURES WITH SULFURIC ACID BY THE ISOTOPIC DILUTION METHOD

M. K. Shchennikova, G. G. Devyatykh and I. A. Korshunov

The N. I. Lobachevsky State University, Gorky

Determinations of the solubility of carbon dioxide in aqueous solutions of sodium sulfate and its mixtures with sulfuric acid are of practical importance, as solutions of these substances are formed in the recocery of carbon dioxide from alkaline liquors by means of sulfuric acid.

Little information is available in the literature on the solubility of carbon dioxide in aqueous sodium sulfate solutions [1-3], and there are almost no data on its solubility in mixtures of sodium sulfate with sulfuric acid.

The determinations were carried out by the isotopic dilution method, with C^{14} radioactive carbon isotope as the tracer. The experimental procedure was similar to that described in the preceding communication [4].

RESULTS AND DISCUSSION

The results of our determinations of the solubility of carbon dioxide in aqueous solutions of sodium sulfate and its mixtures with sulfuric acid are given in Table 1. The solubility is expressed in terms of the coefficient of absorption α (the volume of gas in ml, reduced to standard conditions, absorbed by 1 ml of solvent at the temperature of the experiment when the partial pressure of the gas is 760 mm) and the mole fraction N_s.

Effect of temperature on the solubility of carbon dioxide in aqueous solutions of sodium sulfate and its mixtures with sulfuric acid. The curves for the solubility of carbon dioxide as a function of the temperature are given in Figure 1. The values of $\log N_s$ and $1/T$ were used for graphical determination of the differential heats of solution. The results are given in Table. 2.

Table 2 shows that the differential heats of solution of carbon dioxide in these solutions are of the same order as the value for pure water which, according to Zelvensky's data [5], is 5870 cal /mole at 25° and atmospheric pressure. This shows that the ratio of physically dissolved to chemically combined carbon dioxide is the same in sodium sulfate solutions as in water.

Effect of sodium sulfate concentration on the solubility of carbon dioxide. The effect of sodium sulfate concentration on the solubility of carbon dioxide is shown in Figure 2. The solubility of carbon dioxide in aqueous sodium sulfate solutions at 17° was studied by Secenow [1]* who showed that this equation

$$N_s = N_0 e^{-KC} \qquad (1)$$

is applicable to this case. Here N_S is the solubility of carbon dioxide in sodium sulfate solution of concentration C, N_0 is the solubility of CO_2 in water at the same temperature; K is the constant which depends on the nature of the electrolyte and the temperature.

*Here and further on the Russian name transliterates as Sechenov – Publisher's note.

TABLE 1

Solubility of Carbon Dioxide in Aqueous Solutions of Sodium Sulfate and Its Mixtures with Sulfuric Acid

Composition of solvent	Temperature (°C)	α (in ml/ml)	$N_s \cdot 10^4$
0.4 N Na_2SO_4 (2.84%)	26	0.658	5.34
	26	0.678	5.41
	35	0.473	3.85
	45	0.340	2.78
	45	0.336	2.75
	65	0.183	1.51
0.83N. Na_2SO_4 (5.6%)	25	0.608	4.93
	50	0.332	2.72
	75	0.154	1.28
1.24 N. Na_2SO_4 (8.2%)	25	0.521	4.23
	25	0.531	4.32
	50	0.280	2.30
	75	0.115	0.95
2.05 N. Na_2SO_4 (13%)	26	0.403	3.29
	26	0.419	3.42
	35	0.320	2.62
	43	0.270	2.22
	55	0.176	1.46
	65	0.128	1.07
2.6 N Na_2SO_4 (16.1%)	25	0.295	2.42
3.36 N Na_2SO_4 (20%)	25	0.253	2.14
	25	0.247	2.09
	30	0.232	1.97
	35	0.164	1.40
	50	0.123	0.84
0.4 N Na_2SO_4 + 9.25% H_2SO_4	25	0.660	5.52
	25	0.642	5.36
0.83N Na_2SO_4 + 9.25% H_2SO_4	25	0.574	4.82
	25	0.550	4.62
	50	0.341	2.86
1.24N Na_2SO_4 + 9.25% H_2SO_4	25	0.491	4.16
	25	0.496	4.20
1.67 N Na_2SO_4 + 9.25% H_2SO_4	25	0.435	3.71
	25	0.432	3.69
2.6 N Na_2SO_4 + 9.25% H_2SO_4	25	0.304	2.63
0.4 N Na_2SO_4 + 30% H_2SO_4	25	0.590	5.43
	25	0.592	5.45
0.4 N Na_2SO_4 + 42% H_2SO_4	25	0.585	5.60
	25	0.593	5.67
	35	0.438	4.21
	45	0.342	3.30
	55	0.257	2.50
	65	0.212	2.08
0.83 N Na_2SO_4 + 42% H_2SO_4	25	0.524	5.15
	25	0.524	5.15
1.24 N Na_2SO_4 + 42% H_2SO_4	25	0.518	5.09
	50	0.240	2.40
	75	0.099	1.0
0.4 N Na_2SO_4 + 4.6% H_2SO_4	25	0.717	5.91
	25	0.694	5.72
	50	0.346	2.90
0.4 N Na_2SO_4 + 2.3% H_2SO_4	25	0.706	5.79
	25	0.667	5.46

TABLE 2

Differential Heats of Solution of Carbon Dioxide

Solvent	Temperature range (°C)	− L (in cal /mole) (± 10%)
0.4 N Na_2SO_4	25-65	5800
2.05 N Na_2SO_4	25-50	5900
3.36 N Na_2SO_4	25-50	5800
0.4 N Na_2SO_4 + 42% H_2SO_4	25-65	5400

The variation of log N_0/N_S with the molar concentration of sodium sulfate, from our data, is plotted in Figure 3. It is seen that the solubility − concentration relationship for carbon dioxide conforms to Secenow's equation for all the temperatures studied. The values of the constant K in Equation (1) are given below.

Temperature (in °C) . . .	25	30	40	50	75
K	0.65	0.67	0.72	0.86	1.53

It is seen that K increases with temperature. The solubility curves become correspondingly more flat (Fig. 2). The variation of K with temperature is plotted in Figure 4.

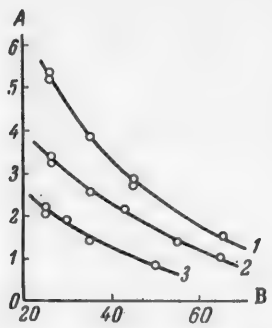

Fig. 1. Effect of temperature on the solubility of carbon dioxide. A) Solubility of $CO_2 - N_S \cdot 10^4$, B) temperature (°C). Na_2SO_4 concentration (N): 1) 0.4, 2) 2.05, 3) 3.36.

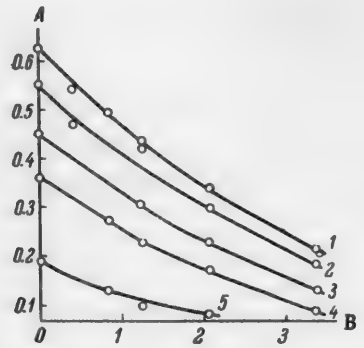

Fig. 2. Solubility of carbon dioxide in aqueous sodium sulfate solutions at various temperatures. A) Solubility of $CO_2 - N_S \cdot 10^3$, B) concentration of Na_2SO_4 (in g-equiv/liter). Temperature (°C): 1) 25, 2) 30, 3) 40, 4) 50, 5) 75.

The graph in Figure 4 can be used for determining the solubilities of carbon dioxide in sodium sulfate at concentrations and temperatures for which no experimental data are available. In illustration, solubilities of carbon dioxide in aqueous sodium sulfate solutions at 30°, determined from experimental data (N_S exptl.) and calculated from Equation (1) for K = 0.67 are given below.

$C\ Na_2SO_4$ (moles/liter)	0	0.2	0.4	0.5	0.6	1.0	1.5
$N_s \cdot 10^3$ (exptl.) . . .	0.55	0.48	0.43	0.41	0.385	0.300	0.213
$N_s \cdot 10^3$ (calc.) . . .	—	0.48	0.42	0.39	0.368	0.282	0.202

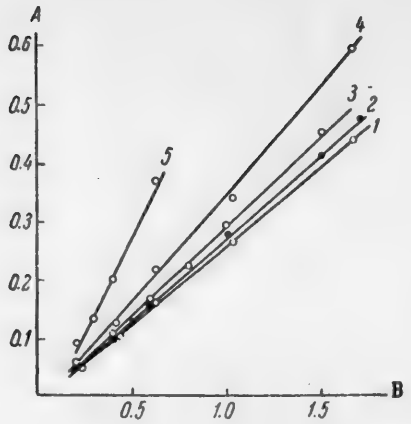

Fig. 3. Variation of log N_0/N_S with molar concentration of sodium sulfate at various temperatures. A) Log N_0/N_S, B) Na_2SO_4 concentration (moles/liter). Temperature (°C): 1) 25, 2) 30, 3) 40, 4) 50, 5) 75.

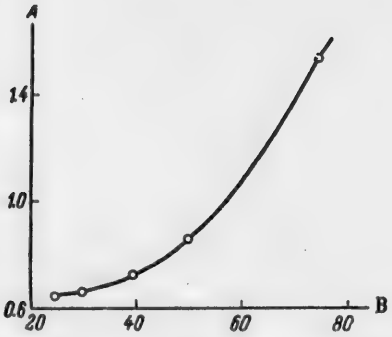

Fig. 4. Variation of the constant in the Secenow equation with the temperature. A) Secenow constant K, B) temperature (°C).

SUMMARY

1. The isotopic dilution method with the aid of radioactive C^{14} isotope was used to determine the solubilities of carbon dioxide in aqueous sodium sulfate solutions of 0.4 to 2.6 N concentrations in the 25-65° temperature range, and in a series of solutions of sodium sulfate with sulfuric acid. The differential heats of solution of carbon dioxide were determined.

2. It is shown that the solubility of carbon dioxide in aqueous sodium sulfate solutions conforms to the Secenow equation for all the temperatures studied.

LITERATURE CITED

[1] J. Secenow, Ann. Chim. Phys. 6, 226 (1892).

[2] A. E. Markham and K. A. Cobe, J. Am. Chem. Soc. 63, 449 (1941).

[3] K. A. Cobe and J. S. Williams, Ind. Eng. Ch., anal. 7, 37 (1935).

[4] M. S. Shchennikova, G. Devyatykh and I. Korshunov, J. Appl. Chem. 30, 6, 833 (1957).*

[5] Ya. Zelvensky, J. Chem. Ind. 14, 1250 (1937).

Received December 10, 1956

*Original Russian pagination. See C. B. Translation.

RELATIONSHIP BETWEEN THE FROST RESISTANCE OF CEMENTS AND THE THERMODYNAMIC POTENTIAL* OF THEIR CHEMICAL AND MINERALOGICAL COMPONENTS

E. M. Kolobov

Regarding the frost resistance of hardened cement as its specific maximum work of resistance to the disruptive forces of the ice crystallizing in the pores, and also to the stresses arising from the thermal deformation of its mineralogical components, we attempted to find a method of physicochemical characterization of the individual constituents of cement which would determine qualitatively the comparative frost resistance of dicalcium hydrosilicate, calcium hydroxide, tricalcium hydroaluminate, tricalcium hydroferrite, and calcium trisulfohydroaluminate.

The relative frost resistance of specimens consisting of prisms 1 × 1 × 3 cm in size from cements of approximately one-component composition was determined experimentally in conjunction with the above investigation.

The postulates of the theory of frost resistance of cement could then be verified by comparison of the theoretical and experimental data.

The resistance of a solid to destruction depends on forces of molecular attraction. For any given individual substance, these forces can be expressed most completely in terms of its thermodynamic potential.

The thermodynamic potential is the part of the internal energy of a substance which can be converted into work. It is expressed by the function

$$F = H - TS,$$

where F is the thermodynamic potential (in joules/g · degree), H is the enthalpy (in joules/g · degree), T is the temperature (in °K), and S is the entropy (in joules/g · degree^2).

For calculations of the thermodynamic potential of the compounds in hardened cement within the temperature range of the USSR climate, the following relationships should be used:

$$S_0^T = \int_0^T c_P^0 d\,(\ln T),$$

$$\Delta F = \int_{T_1}^{T_2} - S dT,$$

where c_p is the heat capacity (in joules/g · degree), and ΔF is the change of free energy (in joules/g · degree).

The problem therefore reduces to determination of entropy from heat capacity data, followed by calculation of the function from the entropy data.

*"Free energy" is the more common term in Western literature – Publisher's note.

By the additivity rule, according to which the heat capacity of a solid is almost exactly the sum of the heat capacities of its constituent atoms and molecules, the heat capacities of the mineralogical components of cement stone at different temperatures can be calculated. The calculation results are given in Table 1. The variation of heat capacity with temperature is shown in Figure 1.

From known heat capacities of the cement compounds at different temperatures, their entropies and entropy changes with temperature can be calculated.

TABLE 1

Heat Capacities of Cement Compounds (in joules per mole · degree)

Temperature (°C)	CH*	C_2SH	C_3AH_6	C_3FH_6	$C_3A \cdot 3CZ \cdot H_{30}$
—73	61.15	142.53	341.1	342.3	1206.92
—23	76.0	164.36	421.7	381.8	1571.42
0	80.2	170.16	446.5	447.4	1685.97
+25	119.5	212.95	667.1	663.9	2817.56

* The following notation is used in this paper: CH for $Ca(OH)_2$, C_2SH for $2CaO \cdot H_2O$, C_3AH_6 for $3CaO \cdot Al_2O_3 \cdot 6H_2O$, C_3FH_6 for $3CaO \times Fe_2O_3 \cdot 6H_2O$ and $C_3A \cdot 3CZ \cdot H_{30}$ for $3CaO \cdot Al_2O_3 \cdot 3CaSO_4 \cdot 30H_2O$.

The graph in Figure 2 was used for these calculations. The area ghMN gives the entropy changes of C_2SH in the temperature ranges from + 25 to 0°; from 0° to −23°; and from −23° to −73°. The corresponding changes are found for C_3FH_6 from the area MNQr, for CH from MNba; for $C_3A \cdot 3CZH_{30}$ from MNed, and for C_3AH_6 from MNki.

The results of the graphical calculation of entropy are given in Table 2 and Figure 3.

A number of useful conclusions can be drawn even from the existing data. The compounds in cement form the following series in order of increasing heat capacities and entropy changes: C_2SH, C_3FH_6, CH, $C_3A \cdot 3CZH_{30}$, C_3A. The first three compounds constitute a group of related compounds, with the highest stability in temperature changes between + 25° and −73°. C_3AH_6 is an extremely unstable component. Calcium trisulfohydroaluminate is intermediate between these compounds.

Figure 3 is used for calculation of the quantitative changes of the thermodynamic potentials of the cement compounds with temperature from the areas of the corresponding entropy − temperature figures.

It is seen that each compound in cement has the characteristic thermodynamic potential, i. e., part of the internal energy of the substance convertible into work. In the temperature range in question, the thermodynamic potentials of all cement compounds undergo considerable changes. The greatest change is found for C_3AH_6. The other compounds for the following series in order of decreasing ΔF: $C_3A \cdot 3CZ \cdot H_{30}$, CH, C_3FH_6, and C_2SH has the lowest ΔF. The higher the value of ΔF, the more thermodynamically unstable the given substance is. Consequently, the greater the change of thermodynamic potential of a given substance, the greater is its change of strength.

TABLE 2

Changes of Entropy with Temperature (in joules/g · degree · 10^{-3}) for Compounds in Cement

Compounds	Entropy in temperature range (°C)			
	from + 25 to 0°	from 0 to − 23°	from −23 to − 73°	from + 25 to −73°
C_2SH	1.93	1.60	3.78	7.21
C_3FH_6	2.24	1.80	4.08	8.12
CH	2.30	2.00	5.20	9.50
$C_3A \cdot 3CZH_{30}$	3.60	2.90	6.10	12.60
C_3AH_6	4.65	3.90	9.0	17.55

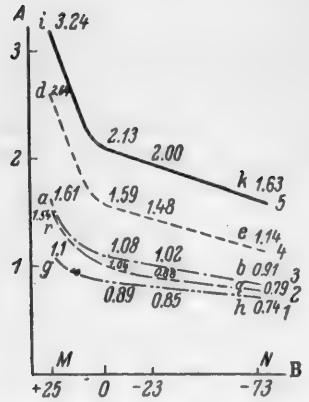

Fig. 1. Effect of temperature on the heat capacities of cement compounds. A) Heat capacity c_p (in joules/g·degree), B) temperature (°C). Cement compounds:
1) C_2SH, 2) C_3FH_6, 3) CH,
4) $C_3A \cdot 3CZ \cdot H_{30}$, 5) C_3AH_6.

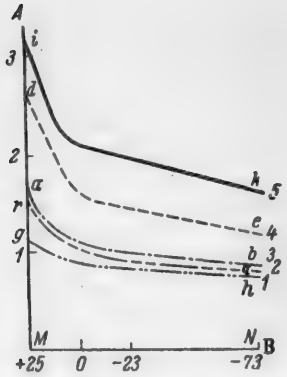

Fig. 2. Graph for calculation of the entropies of compounds in hydrated cement. A) Heat capacity c_p (in joules/g·degree), B) ln T. Numbering of the curves as in Figure 1.

In relation to comparative changes of the thermodynamic potentials of different substances, it may be asserted that the decrease or increase of the strength of an ideal solid is proportional to the change of the thermodynamic potentials of the substances constituting this solid.

The strength of real solids is considerably less than the theoretical calculated value owing to the presence of pores, capillaries, and microcrevices. However, the relative values of the strengths of real solids remain the same.

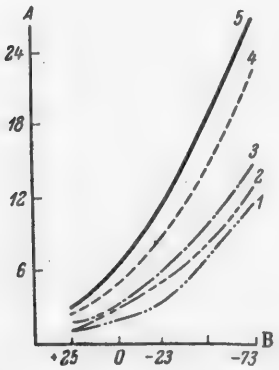

Fig. 3. Graph for calculation of the thermodynamic potentials of cement compounds. A) Entropy increase (in joules/g·degree·10^{-3}), B) temperature (in°C). Numbering of the curves as in Figure 1.

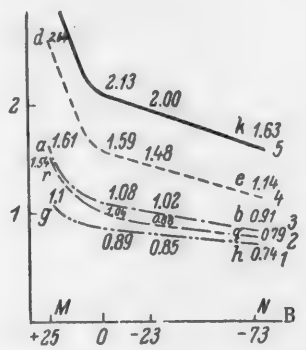

Fig. 4. Frost resistance of single-mineral cements. A) Coefficient of frost resistance, B) number of cycles. The curve numbers are explained in the text.

Therefore we consider that it is permissible to evaluate the strength changes in these materials on the basis of changes of the thermodynamic potential of their constituents.

The practical basis of the evaluation of the influence of the mineralogical composition of cement on its frost resistance can be formulated as follows. The highest stability from the energy aspect, with respect both to strength and water adsorption, when the temperature is decreased from + 25 to −73°, is found in C_2SH; C_2FH_6 is very close to this compound; C_3AH_6 is extremely unstable; finally, trisulfohydroaluminate occupies an intermediate position between the group of stable compounds and the unstable C_3AH_6. Calcium hydroxide is more stable than trisulfohydroaluminate, but it cannot be classified as a stable compound.

The above theoretical deductions provided the basis of a method for preliminary evaluation of the frost resistance of cements differing in mineralogical composition. It follows from these deductions that 1) belite cements should have the highest frost resistance; 2) the frost resistance should diminish with increasing contents of C_3S in the cement, or in passing from belite to alite cements; 3) tricalcium aluminate, which gives the least stable hydration products, is an undesirable component in frost-resistant cements; 4) increase of C_4AF in the fluxing agents raises the frost resistance, as C_3FH_6 is a very stable compound.

These preliminary data, based on theoretical considerations, were used in experimental determinations of the frost resistance of single-mineral cements in the form of specimens consisting of 1 × 1 × 3 cm prisms made without sand (1 : 0 cement paste).

After hardening for a year, the specimens were subjected to 100 freezing cycles. The relative strength decrease was found to be least in cement II, containing 88% of belite. Specimens of aluminate cement III failed after 8 cycles. Aluminoferrite cement IV proved to be very frost-resistant (Fig. 4). Finally, an increase of the alite content of cement I to 75% produced a considerable decrease of frost resistance in comparison with cement II (Table 3).

TABLE 3

Results of Experimental Determinations of the Frost Resistance of Cements

Cement	Calculated mineral composition (%)	Water-cement ratio	Amount of additive (%)	Bending strength (kg/cm²) after hardening (months)				Bending strength (kg/cm²) after freezing (cycles)			Coefficient of frost resistance after freezing (cycles)		
				12	13	14	15	30	60	90	30	60	90
I	(75, 20, 3, 2)	0.31	2	117	119	124	123	96	37	0	0.80	0.32	0
II	(8, 88, 2, 2)	0.22	2	138	134	135	132	120	118	80	0.91	0.78	0.59
III	(0, 3, 96, 1)	0.36	8	41	37	35	36	failed after 8 cycles					
IV	(3, 0, 0, 97)	0.26	4	105	97	91	89	84	64	43	0.88	0.71	0.48

SUMMARY

1. The thermodynamic potential of cement constituents is an important physicochemical characteristic which relates the thermodynamic properties of the cement constituents with the structural properties of the cement.

2. The agreement between the changes of thermodynamic potential and strength changes in the course of freezing-thawing cycles confirms the view that the stability of the compounds in hydrated cement in variable temperature conditions can be determined by means of thermodynamic analysis.

Received August 16, 1955

LAWS GOVERNING THE SIMULTANEOUS CATHODIC DISCHARGE OF THE PRINCIPAL METAL IONS AND IMPURITIES IN THE ELECTROLYTIC PRODUCTION OF COBALT

A. L. Rotinyan, V. L. Kheifets and A. M. Yakovleva

It was shown in our earlier papers [1-3] that in the electrolytic refining of metals some impurities are discharged at the limiting current, and others, with chemical polarization. The quantitative equations derived in these papers express the laws of simultaneous discharge and correlate the degree of contamination of the cathodic deposit with the composition of the solution and the electrolysis conditions.

The laws derived for the simultaneous discharge of ions in the refining of metals were verified and confirmed in experiments on the incorporation of a number of impurities in cathodic nickel deposits [1]. Baimakov and his associates [4, 5] later studied the simultaneous discharge of copper and arsenic in the electrolytic deposition of copper and showed that the incorporation of arsenic is determined to a considerable extent by chemical polarization, while Salin and Ponomarev [6] showed that in the electrodeposition of zinc, lead is incorporated in the deposit at the limiting current.

Some of these relationships have now been verified for the electrolytic refining of cobalt.

If an impurity is discharged at the limiting current in electrolysis, its content in the cathodic deposit is given by the equation [1, 3]:

$$A_i = \frac{100\, K_{gi} C_{ib}}{\eta J}, \qquad (1)$$

where K_{gi} is the convective diffusion rate constant; C_{ib} is the concentration of the contaminating ions (it is assumed that C_{ib} is the same throughout the electrolyte owing to adequate stirring); J is the cathode current density; η is the cathode current efficiency.

It should be noted, however, that the concentration of the contaminating ions in the cell is not the same as in the incoming electrolyte. In practice, electrolysis is carried out with the electrolyte flowing through the cell, where the impurities are deposited, and this naturally lowers their concentration in comparison to their concentration in the incoming solution. The relationship between the concentration of the impurity in the cell and in the incoming electrolyte is given by the material balance equation

$$QC_{in} = QC_{ib} - K_{gi} C_{ib}, \qquad (2)$$

where Q is the flow rate of the electrolyte through the cell; C_{in} is the concentration of the i-th impurity in the incoming electrolyte.

We find C_{ib} from Equation (2):

$$C_{ib} = \frac{QC_{in}}{Q + K_{gi}} . \quad (3)$$

Substituting (3) into (1), we have

$$A_i = \frac{100\, K_{gi} Q C_{in}}{\eta I\,(Q + K_{gi})} . \quad (4)$$

If $Q \to \infty$, then $Q \gg K_{gi}$, and we again have Equation (1); if, on the contrary, $Q \ll K_{gi}$ then A_i is directly proportional to Q.

It follows from this equation that A_i should be a linear function of C_{in}, as in Equation (1), but with a different slope factor.

The experimental results confirming Equation (1) are given in Figure 1; it is seen that the experimental points are ranged around a straight line. In this case, as in the electrodeposition of nickel, not only such an electropositive impurity as copper, but also such an electronegative impurity as zinc is deposited at the limiting current. The fact that, as in the electrodeposition of nickel, the experimental points for all the impurities are ranged around a common straight line once again confirms the view, advanced earlier, that the convective diffusion constants of all bivalent metals have the same value. Further, it follows from Equation (4) that the degree of contamination of the metal should not depend either on the nature of the principal metal, or on its concentration. This may be demonstrated by calculations of K_{gi} for the electrodeposition of nickel [1], cobalt, and tin [7]. The results of such calculations are given in the Table; the last column shows that the values of K_{gi} are fairly constant.

Values of K_{gi} for the Discharge of Impurities at the Limiting Current in the Electrodeposition of Nickel, Cobalt, and Tin

Principal metal	Temperature (°C)	Q (ml/sec · cm²)	C_{in} g-atoms per cc	A_i (atomic %)	I (g-atoms/sec · cm²)	η	K_{gi}
Nickel	55	$0.25 \cdot 10^{-3}$	10^{-6}	0.25	$0.78 \cdot 10^{-7}$	1.0	$0.86 \cdot 10^{-3}$
Cobalt	60	$0.28 \cdot 10^{-3}$	10^{-6}	0.164	$1.04 \cdot 10^{-7}$	1.0	$0.44 \cdot 10^{-3}$
Tin	20	$0.74 \cdot 10^{-3}$	10^{-6}	0.25	$1.04 \cdot 10^{-7}$	0.95	$0.37 \cdot 10^{-3}$

If the discharge rate of the impurity is determined by diffusion, and the deposition rate of the principal metal is determined by delay of the discharge stage,* it follows from the equality of the convective diffusion constants for all bivalent metals that the relative content of an impurity in the solution (C_i/C_{in}) will always be less than the relative content of the impurity in the cathodic deposit. In such a case the bisector of the angle between the coordinate axes will lie below the experimental straight line. If the deposition rate of the principal metal is determined by diffusion, or occurs with a small degree of chemical polarization, which may be neglected, then the $A_i - C_{in}$ lines and the bisector will coincide. Finally, if both the principal metal and the impurity are discharged with chemical polarization, the discharge rate constant of the principal metal should be greater than that of the impurity,** and therefore the experimental $A_i - C_{in}$ lines should lie below the bisector. For the

*This can only be the case when the rate constant for the discharge of the principal metal is considerably less than the rate constant of convective diffusion.

**If the rate constant for the principal metal is less than that of the impurity, then the impurity must be discharged at the limiting current, because of its low concentration.

electrodeposition of cobalt, the experimental $A_i - C_{in}$ line does in fact lie above the bisector. This shows that in the electrodeposition of cobalt the discharge of ions in the slow step. The same is found in the electrodeposition of nickel.

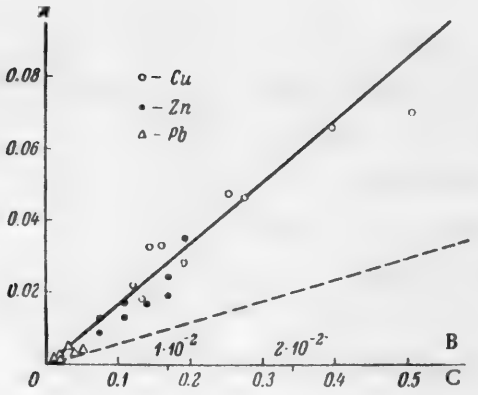

Fig. 1. Effect of the concentrations of impurities in the electrolyte in the electrodeposition of cobalt on their contents in the cathodic deposit. Composition of solution (in moles/liter): $CoSO_4$ 1.7; H_3BO_3 0.4; pH = 4.83. Electrolysis conditions: J_c 2 amp/dm², Q 50 ml/amp-hr; t 60°. A) A_i (atomic %); B) $\frac{C_i}{C_{in}}$ (atomic %); C) $C_i \cdot 10^3$ (moles/liter).

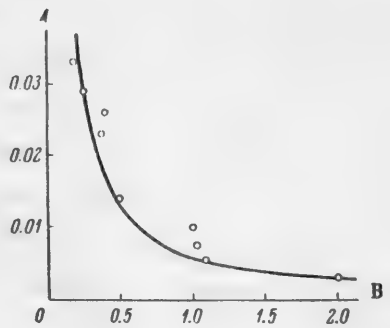

Fig. 2. Effect of current density on the lead content of a cathodic cobalt deposit. Concentration of impurity $0.019 \cdot 10^{-3}$ moles/liter, Q = 50 ml/hour, t = 60°. Composition of electrolyte is given in Figure 1. A) A_i (atomic %); B) D_c (amp/dm²).

If follows from Equation (1) or (4) that the amount of the impurity in the cathodic cobalt deposit should decrease with increase of cathode current density. The results of our experiments on the influence of current density on the inclusion of lead in the deposit, given in Figure 2, show satisfactory agreement between the theoretical curve (continuous line) and the experimental data.

All the impurities studied were discharged at the limiting current. The explanation is that cobalt is a fairly electronegative metal and its electrodeposition is accompanied by strong polarization. However, according to published data, an impurity such as nickel is included in cobalt deposits in consequence of delayed discharge.

Fedotyev and Mikhailov's experiments [8], and the older work of Pletenev and Kuznetsova [9] and of Jong and Engerman [10], show that the nickel content of the deposit increases with increasing current efficiency with respect to cobalt and with increasing current density.

This fact may be explained on the assumption that both nickel and cobalt are deposited with chemical polarization, and that $\alpha_{Ni} z_{Ni} > \alpha_{Co} z_{Co}$. In this case we have in accordance with the equation [3]

$$A_i = \frac{100\, BC_{ib}\, (\eta J)^{\frac{\alpha_i z_i}{\alpha_M z_M}}}{C_M^{\frac{\alpha_i z_i}{\alpha_M z_M}}} - 1 \qquad (5)$$

In this equation C_M is the concentration of the principal metal, B is a constant, α_i and α_M, z_i and z_M are the respective fractional coefficients and ionic valences of the impurity and the principal metal.

As regards the influence of cobalt concentration in the solution on the incorporation of the nickel impurity in the cathodic deposit, most of the published results indicate that, in agreement with theory, the nickel content of the deposit decreases with increasing cobalt concentration in the electrolyte.

Thus, our new experimental results and literature data confirm the relationships established earlier.

LITERATURE CITED

[1] V. L. Kheifets and A. L. Rotinyan, Proc. Acad. Sci. USSR 82, 423 (1952).

[2] A. L. Rotinyan, V. L. Kheifets, E. S. Kozich and O. P. Kalganova, Proc. Acad. Sci. USSR 88, 301 (1953).

[3] A. L. Rotinyan and V. L. Kheifets, Nonferrous Metals 2, 24 (1954).

[4] Yu. V. Baimakov and A. G. Syrovegin, Trans. Leningrad Polytech. Inst. 6, 5 (1953).

[5] Yu. V. Baimakov and V. Ya. Terekhin, Trans. Leningrad Polytech. Inst. 6, 165 (1953).

[6] A. A. Salin and V. D. Ponomarev, Nonferrous Metals 2 (1953).

[7] V. L. Kheifets, E. S. Kozich and O. M. Danilovich, Proc. Acad. Sci. USSR 113, 138 (1957).*

[8] N. P. Fedotyev and S. V. Mikhailov, Trans. Leningrad Inst. Chem. Technol. 3 (1940).

[9] S. A. Pletenev and V. V. Kuznetsova, Nonferrous Metals 5 (1933).

[10] C. B. Jong and C. Egerman, Trans. Electrochem. Soc. 72, 447 (1938).

Received October 15, 1956

*Original Russian pagination. See C. B. Translation.

THE POTENTIALS OF COPPER, ANTIMONY, BISMUTH, AND LEAD IN NITRIC ACID SOLUTIONS

V. V. Tenkovtsev

Scientific Research Storage Battery Institute

The electrode potential is one of the principal factors determining the direction and rate of many electrode processes. In a study of the reduction of copper, antimony, and bismuth ions on metallic lead, it was first decided to investigate the influence of various factors on the potentials of these metals in nitric acid solutions. The electrode potentials were determined by a compensation method against a saturated colomel electrode with the aid of the AP-310 potentiometer with 1 mV scale divisions; the null instrument was a galvanometer with a current sensitivity of $1.2 \cdot 10^{-6}$ amp. The electrodes in all cases were rods cast from the analytical-grade metals. The electrode tips were turned on a lathe down to 3.5 mm diameter, covered with an insulating layer, and the exposed ends were ground on a fine carborundum block to leave a clean surface of about 0.1 cm^2 visible area. The electrode ends were cleaned each time immediately before immersion in the electrolyte.

It was found in preliminary experiments that the electrode potentials of these metals in nitric acid solution reach constant values within 1-2 minutes after immersion, changing very little after that. Therefore the determinations of potential were carried out 2 minutes after immersion of the electrode in every case.

Average values of three determinations are given in the graphs. The results were reproducible to within ± 1-2 mv.in every case.

The potential of a metallic electrode immersed in a solution varies in proportion to log $a_{M^{+n}}$, and at high dilutions, to log $C_{M^{+n}}$. When plotted in $\epsilon_M - \log C_{M^{+n}}$ coordinates, this relationship is represented by a straight line which does not pass through the origin but cuts off an intercept along the ϵ_M axis, numerically equal to the standard potential of the metal. However, a study of the effect of the concentrations of their respective ions in 1 N HNO_3 solution on the potentials of lead, bismuth, and antimony showed that a linear relationship holds only at relatively high concentrations of the metal ions, namely, above about 0.01 N for lead and copper, and 0.001 N for antimony and bismuth. The slope factor of the experimental straight lines plotted in $\epsilon_M - \log C_{M^{+n}}$ coordinates does not agree with the theoretical factor (0.058/n), although the lines are somewhat steeper for the bivalent metals than for bismuth and antimony.

Further decrease of the metal ion concentration has no appreciable influence on the electrode potential, which remains constant for the given background solution (Fig. 1). It has been reported in the literature [1, 2] that in some instances, at very low M^{+n} concentrations, the electrode potential of the metal ceases to depend on the concentration of its ions in solution. Some authors attribute this to adsorption of the metal ions on the electrode surface or to the establishment of irreversible potentials owing to formation of basic salts. However, in our experimental conditions (in 1 N HNO_3 solution) the formation of basic salts is unlikely. The effect may be ascribed to the fact that a metallic electrode may begin to dissolve when immersed in a particular medium. A definite concentration of the metal ions is then set up in the layer of liquid adjacent to the electrode, constant for the given medium, and the electrode potential corresponds to this concentration of its ions. Increase of the metal ion concentration in the solution has no effect on the electrode potential until the M^{+n} concentration in the bulk of the solution begins to exceed the concentration of these ions in the layer around the electrode. After this the electrode potential is displaced in the positive direction with increasing log $C_{M^{+n}}$, and varies linearly with log $C_{M^{+n}}$. Tomashev [2] gives a similar explanation of this effect.

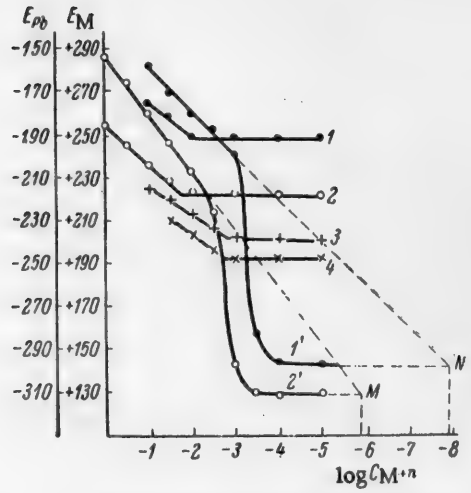

Fig. 1. Variations of the electrode potentials E_M and E_{pb} with the metal ion concentration log $C_{M^{+n}}$. 1) Copper, 2) lead, 3) bismuth, 4) antimony, in 1 N HNO_3 solution; 1') copper, and 2') lead in 0.1 N KNO_3 solution.

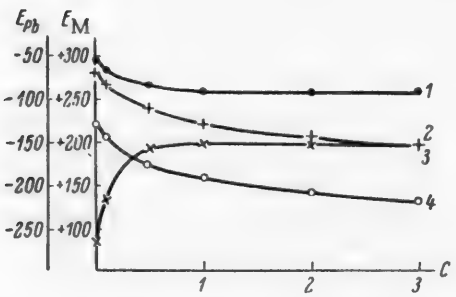

Fig. 2. Variations of the electrode potentials E_M and E_{pb} with the HNO_3 concentration (C in terms of normality). Metal concentrations (N): 1) 2.10^{-2} Cu, 2) 4.10^{-2} Bi, 3) 1.10^{-2} Sb, 4) 1.0 Pb.

It follows from the above that the break in the ϵ_M − log $C_{M^{+n}}$ plot corresponds to the concentration of the metal ions in the layer at the electrode which is established when the metal dissolves in the medium, and can serve as a measure of the corrosive activity of the medium with respect to the metal. A decrease in the corrosive activity of the medium should shift the break in the ϵ_M − log $C_{M^{+n}}$ line in the direction of lower concentrations, as a decrease of the rate of solution must decrease the concentration of the metal ions in the layer around the electrode.

To verify these views, we determined the potentials of lead and copper in neutral media. Analogous experiments with bismuth and antimony could not be performed because of the precipitation of basic salts. The method used for the determinations was the same as before, but the potentials were determined in presence of 0.1 N potassium nitrate solution at pH 5-6. The results are given in Figure 1 (Curves 1' and 2'). It is seen in Figure 1 that at high concentrations of M^{+n} ions in the solution, ϵ_M varies linearly with log $C_{M^{+n}}$, and the slope of the linear region (the prelogarithmic coefficient in the Nernst equation) is equal to the theoretical value for lead, and somewhat lower than the theoretical for copper, but is nevertheless greater than in 1 N nitric acic solution. Thus, the background solution not only alters the absolute value of the potential, but has a significant influence on the slope factor.

If the metal ion concentrations are decreased to below $5 \cdot 10^{-3}$ N for lead and $1 \cdot 10^{-3}$ N for copper, the electrode potentials are shifted sharply in the negative direction, but beyond a definite limit are no longer influenced by further decreases of M^{+n} concentration. A sharp shift of the potential in the negative direction is generally associated either with complex formation or with the establishment of irreversible potentials owing to formation of sparingly soluble compounds. In the present instance the latter is the more probable. It is known that lead salts are readily hydrolyzed in neutral solutions. At high dilutions ($C_{pb} < 1 \cdot 10^{-3}$ N) and relatively high pH (about 6) the possibility of the deposition of basic salts or lead hydroxide on the electrode surface is not excluded. This gives rise to an electrode of the second kind, of the type $Pb \mid Pb(OH)_2 \mid OH'$, the potential of which is determined by the solubility of lead hydroxide. Therefore the limit reached by the potential of a lead electrode in these conditions with decreasing lead ion concentration must be determined by the solubility of $Pb(OH)_2$. In fact, if the ϵ_M − log $C_{M^{+n}}$ curve is continued into the region of lower concentrations, it intersects the continuation of the linear sloping region of the curve at the point M (Fig. 1), corresponding to a lead concentration of $0.9 \cdot 10^{-6}$ mole/liter, which is close to the concentration of lead in saturated $Pb(OH)_2$ solution, $4.2 \cdot 10^{-6}$ mole/liter [3]. This confirms once again that the abrupt change of potential on the ϵ_M − log $C_{M^{+n}}$ curve is caused by the formation of an electrode of a second kind, the potential of which is determined by the solubility of $Pb(OH)_2$.

The analogous abrupt change of potential on the $\epsilon_M - \log C_{M^{+n}}$ curve for copper is probably also the consequence of the establishment of irreversible potentials. It is true that the salts of bivalent copper have a lower tendency to hydrolysis than lead salt, but several authors report [1, 4] that at copper concentrations below $\simeq 10^{-4}$ mole/liter univalent and not bivalent copper ions are stable in aqueous solutions. Therefore when the Cu^{++} concentration is decreased below 10^{-3} - 10^{-4} N in a neutral medium, the formation of an electrode of the type $Cu|\ Cu_2O\ |OH'$ is possible, leading to an abrupt shift of the potential of the copper electrode in the negative direction.

The continuations of the horizontal and sloping regions of the curve intersect at a point (N) (Fig. 1) corresponding to a copper concentration of $0.6 \cdot 10^{-8}$ mole/liter. The solubility product of $Cu_{20}(Cu^{+}\overline{OH}^{-})$ is $1.2 \cdot 10^{-15}$ [3], which corresponds to a copper concentration of $3.5 \cdot 10^{-8}$ mole/liter. Here we again have adequate confirmation of the fact that the abrupt change of potential with decreasing copper concentration in neutral media is caused by the establishment of irreversible potentials owing to the formation of sparingly soluble Cu_2O on the electrode surface.

In presence of 1 N nitric acid there is no abrupt shift of potential in the negative direction with decreasing concentration of the metal in solution, as nitric acid prevents hydrolysis and gives rise to a fairly high concentration o M^{+n} in the layer near the electrode owing to dissolution of the metal.

It follows from the above data that solution acidity has a significant influence both on the electrode potential of the metal and on the variation of ϵ_M with the concentration of the corresponding metal ions (the prelogarithmic coefficient in the Nernst equation). It is clear from the graph (Fig. 1) that with increasing concentration of nitric acid in the solution (Curves 1 and 1', 2 and 2'), the potentials of lead and copper are shifted in the negative direction to an increasing extent with increasing concentrations of the corresponding metals in the solutions.

To determine the effect of acidity of the medium on metal potentials, we studied the changes in the potentials of copper, bismuth, lead, and antimony with increase of nitric acid concentration from $1 \cdot 10^{-3}$ N to 3.0 N. The experimental procedure was the same as before. The results are given in Figure 2. It follows from the curves (Fig. 2) that an increase of the nitric acid concentration produces considerable shifts of the potentials of lead, bismuth, and copper in the negative direction. Increase of the corrosive activity of the medium evidently intensifies the transfer of metal ions into solution and increases the negative charge of the electrode. The changes in the potential of the antimony electrode are of the directly opposite character. The explanation is that antimony is almost insoluble in nitric acid, and increase of nitric acid concentration does not result in intensified dissolution, but to intensified passivation of the electrode surface and a shift of the potential in the positive direction.

SUMMARY

1. It was found in a study of the variations of the potentials of lead, copper, antimony, and bismuth in nitric acid solutions with the concentrations of the corresponding ions and with acidity of the medium that a linear relationship between ϵ_M and $\log C_{M^{+n}}$ holds, in acid solutions, only at relatively high concentrations of these ions — of the order of 10^{-2} N for lead and copper, and 10^{-3} N for bismuth and antimony.

2. It is shown that the cause of the abrupt shift of the potentials of lead and copper in the negative direction with decreasing concentrations of the metal ions in a neutral medium is the establishment of irreversible potentials owing to the formation of basic salts or hydroxides.

LITERATURE CITED

[1] G. V. Akimov and V. P. Batrakov, J. Phys. Chem. 13, 12, 1807 (1939).

[2] N. D. Tomashev, Theory of Metal Corrosion (Metallurgy Press, 1952) p. 84*.

[3] I. M. Kolthoff and V. A. Stenger, Volumetric Analysis (Russian translation) 1 (State Chem. Press, 1950).

[4] E. M. Zaretsky and G. V. Akimov, J. Appl. Chem. 11, 7-8, 1161 (1939).

* In Russian.

Received October 22, 1955

THE CAUSES OF LOCAL SPONGY FORMATIONS ON THE CATHODE IN ZINCATE ELECTROLYTES

N. T. Kudryavtsev, R. Yu. Bek and I. F. Kushevich

It has already been reported [1] that one of the causes of local spongy growths on the cathode in zincate solutions at low current densities is the presence of dispersed (colloidal) particles of zinc or of incompletely oxidized zinc. These particles are transferred to the cathode cataphoretically or mechanically, and form centers of random growth of crystals of the depositing metal. It was shown that these particles may originate by irregular dissolution of zinc at the anode, contamination of the solution with zinc dust, and spontaneous dissolution of zinc at the cathode by the action of microcells arising on its surface; for example, differential aeration cells at the solution – air boundary. The latter is possible because cathodic polarization in zincate electrolytes up to the limiting current is low [2], of the order of 7-10 mv.

Additions of very small amounts (fractions of a gram per liter) of lead, tin, or mercury salts to zincate electrolytes prevent sponge formation on the cathode. The mechanism of the action of these additions is interpreted [1] as the complete oxidation of ultrafine particles of zinc by ions of more positive metals and the dissolution of the zinc in the form of ions.

In the present investigation additional experiments were carried out to verify and amplify the previously proposed explanations of the causes of local spongy formations on the cathode in zincate solutions at low current densities.

The electrolytes used for the experiments had the following composition: Zn from 0.2 to 0.4 N, $NaOH_{total}$ 2.5 N. The temperature was about 20°. The current densities in all the experiments were below the limiting values, about 0.2 amp/dm^2.

The cathodes were copper tubes or rods, previously coated with zinc in acid solution. The anodes were chemically pure zinc, platinum, and nickel. The electrolytes were prepared by chemical dissolution of freshly precipitated zinc hydroxide in hot (~ 60°) concentrated NaOH solution. The solution was then diluted and decanted after settling.

The first experiments showed that local spongy zinc growths are formed in electrolysis both with soluble zinc anodes and with insoluble (Pt and Ni) anodes. However, in the latter case they differed sharply in appearance and amounts from the spongy deposits formed in electrolysis with soluble anodes.

Whereas in electrolysis with soluble anodes the spongy growths are distributed in large numbers over the entire cathode surface, in electrolysis with insoluble anodes they are mainly formed at the regions of the cathode near the solution – air boundary (at the water line). Only occasional spongy formations were found on the rest of the surface (Fig. 1).

This confirms the view put forward earlier [1] that the formation of spongy zinc in the upper region of the cathode, at the solution – air boundary, is due to the formation and action of differential aeration couples or galvanic cells. As a result, zinc is dissolved at the anodic regions, with the formation of colloidal zinc particles together with zinc ions. Observations whowed that individual spongy growths formed after some time (15-20 minutes) at the lower regions of the cathode arise as the result of the separation of particles accumulating in the upper zone and their adherence to other regions of the cathode.

In order to confirm that the colloidal particles are formed in the upper zone of the cathode by the action of differential aeration couples or local galvanic cells, zinc was deposited on a bent cathode with one end below and the other above the electrolyte level (Fig. 2). This experiment showed that hardly any spongy deposit was formed on the end of the cathode submerged in the solution, while it formed and grew as before at the region at the solution level.

Interesting results were also obtained in experiments on the deposition of zinc from zincate solutions on copper cathodes, with insoluble anodes. When a copper cathode was immersed in a zincate electrolyte before the current was switched on, the deposition of zinc (after the current was switched on) was irregular. Some regions of the cathode surface remained without a zinc coating for a long time, evidently as the result of passivation — oxidation by the alkali before electrolysis. Subsequently, as deposition proceeded, spongy growths appeared randomly distributed all over the cathode in these regions.

Fig. 1. Spongy deposits on cathodes in electrolysis of zincate solutions without additives, at low current densities. a) With soluble (zinc) anode, b) with insoluble (Pt) anode.

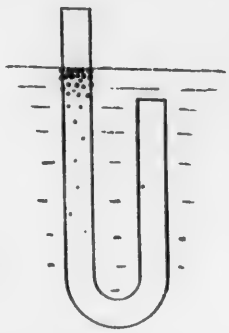

Fig. 2. Spongy deposits on cathodes in zincate solutions without additions, with an insoluble anode (Pt) at low current densities.

When the copper cathode was immersed in the electrolyte with the current switched on, its entire surface was coated with zinc simultaneously, and a spongy deposit was formed only in the upper zone of the cathode at the metal — solution boundary. An explanation of this difference between the deposits on copper cathodes is that in the first case local galvanic cells were formed between zinc and (oxidized) copper, and these gave rise to sponginess all over the cathode surface. The action of galvanic cells in the formation of spongy deposits on the cathode is also clearly illustrated by the following experiment. When a zinc cathode is brought into contact with a copper plate, dark spongy deposits rapidly appear at the point of contact during electrolysis at very low current densities.

In order to find any other possible causes of sponge formation on the cathode, experiments were also carried out with zincate electrolytes prepared in different ways: 1) by the mixing of 5 N solutions of $ZnSO_4$ and NaOH, followed by dilution to the required concentration; 2) by the dissolving of both freshly precipitated (from zinc sulfate solution) zinc hydroxide, and zinc hydroxide which had been kept under water; 3) by the dissolving of ZnO prepared by calcination of freshly precipitated basic zinc carbonate. In methods 2 and 3, the zinc hyxroxide or oxide was first added to hot (70°) concentrated caustic alkali, and the solution was then diluted with water to the required concentration. The solutions were always used for electrolysis both immediately after preparation and after prolonged keeping ("aging") for 30-40 days.

It is known [3] that the solubility of zinc hydroxide depends on the conditions of its preparation, because of the differences in the structure of the hydroxide formed. It seemed likely that the character of the cathodic deposit also depends on the structure of the zinc hydroxide, which may in some cases be present as a colloidal suspension.

In Flerov's paper [4] on a study of the aging of sodium zincate solutions and its influence on electrode processes it is noted that a spongy deposit is formed on the cathode if amorphous zinc hydroxide is used, while no sponginess is found on the cathode if crystalline hydroxide is used. Unsaturated zincate solutions, which initially gave spongy deposits, did not give rise to sponginess on the cathode after "aging" (prolonged keeping). However, our experiments on the electrolysis of zincate electrolytes prepared by different methods, with and without aging, showed that they all gave rise to zinc deposits of the same nature.

As has already been stated, according to the results obtained by Kudryavtsev and Nikiforova [5], additions of tin, lead, and mercury salts to zincate electrolytes prevent the formation of spongy deposits on the cathode at low current densities (below the limiting value).

In addition to these metals, we also studied salts of arsenic, antimony, and selenium, which have more positive potentials than zinc. The experiments showed that additions of all these salts at very low concentrations, of the order of 0.005-0.01 g/liter, also prevent the formation of spongy deposits on the cathode. The most reproducible results were obtained with selenium. At higher contents in the electrolytes, these metals, like zinc, themselves favor the formation of spongy cathodic deposits. Evidently at higher concentrations the ions of these metals are discharged at the cathode at the limiting current. It is known [1, 6] that the discharge of metal ions at the limiting current leads in most cases to the formation of spongy deposits on the cathode. At high concentrations it may be displaced by contact with cathodic zinc (when its polarization is very low) also in spongy form, just as zinc, when immersed in solutions of simple salts of copper, lead, and other more electropositive metals, becomes coated with a spongy mass containing these metals.

It is also possible that electropositive metals displaced by zinc on contact form microcells with it at the cathode, the action of these microcells dissolving the zinc. Here, as in anodic dissolution, colloidal particles of zinc are formed and act as muclei for the spongy deposits on the cathode.

The action of hydrogen peroxide, potassium nitrate, chromic anhydride, and other oxidizing agents was also investigated. In small amounts these additions did not have any appreciable effect on the nature of the cathodic deposits in zincate electrolytes. At higher concentrations of these additions, spongy deposits appeared on the cathode in electrolysis with both soluble and insoluble anodes. An investigation of the causes of this effect showed that in the presence of large amounts of these oxidizing agents the cathodic zinc is redissolved. The current efficiency with respect to the metal falls to 0 and below — the layer of zinc on which the new layer was being deposited was itself dissolved.

SUMMARY

1. Experiments on the electrolysis of zincate solutions at low current densities, with soluble (zinc) and insoluble anodes, with and without added tin, lead, and mercury salts, confirmed the results of earlier investigations on this subject.

2. It is shown that, besides tin, lead, and mercury, additions of other metals more electropositive than zinc to zinc electrolytes, such as small amounts (0.005-0.01 g/liter) of selenium, arsenic, or antimony, prevent the formation of spongy deposits on the cathode at low current densities.

3. It was found that in presence of sufficient amounts of certain chemical oxidizing agents spongy deposits may also be formed on the cathode in consequence of the dissolution of zinc and the resultant appearance of ultrafine particles of zinc in the solution.

4. All the experimental results are in harmony with the previously advanced explanation of the causes of formation of spongy deposits and of the mechanism of the action of additives which prevent these deposits in zincate electrolytes at low current densities.

LITERATURE CITED

[1] N. T. Kudryavtsev, J. Phys. Chem. 26, 2 (1952).

[2] N. T. Kudryavtsev, J. Phys. Chem. 23, 7 (1949).

[3] R. Scholder and N. Weber, Z. anorg. allg. Ch., 215, 355 (1933); R. Scholder and Hendrich, ibid, 241, 76 (1939).

[4] V. N. Flerov, Author's summary of Candidate's Dissertation, Gorkii Polytech. Inst. (1956).

[5] N. T. Kudryavtsev and A. A. Nikiforova, Corrosion and its Prevention, 5-6 (1940).*

[6] M. Loshkarev, A. Ozerov and N. Kudryavtsev, J. Appl. Chem. 22, 3 (1949).

Received June 8, 1956

*In Russian.

COLLOIDAL AND SUSPENDED PARTICLES IN PHYSICOCHEMICAL PROCESSES IN BOILERS

S. A. Durov and N. G. Chen

The Sergo Ordzhonikidze Polytechnic Institute, Novocherkassk

Suspended particles of various degrees of dispersion are formed in steam boilers during the boiling of water. The effect of these particles on physicochemical processes in boilers is of considerable interest. Their influence on foaming has been studied in detail by Durov [1]. It follows from his work that highly disperse suspended particle of insoluble mineral substances, which strengthen considerably the steam bubble films on the free evaporation surface, should have a considerable influence on continuous entrainment, which is caused mainly by destruction of steam bubbles. There are indications of this influence in the literature, but they are highly contradictory. For example, Kostrikin [2] states that, before the critical salt content is reached solid particles should be carried over selectively with the steam. Therefore their presence in boiler water should lead to a high degree of contamination of the steam. The opposite view is held by Levitsky [3] and others, who conclude from their investigations that finely divided suspended substances decrease the amounts of salts carried over.

Clarification of this problem is of great practical importance, as solid particles of various degrees of dispersion are always present in boiler water. It was therefore decided to study this question in greater detail. It was first required to determine the ratio in which the suspended particles are distributed between the liquid and the steam bubble films, the destruction products of which, in the modern view, constitute the chief factor in the entrainment of salts at low and moderate steam pressures.

The transfer of solid particles into the bubble films was studied with the aid of C^{14} and Ca^{45} radioactive isotopes contained in the compounds $Na_2C^{14}O_3$ and $Ca^{45}Cl_2$. The experiments were carried out with solutions of salts capable of forming precipitates of $Mg_2(OH)_2C^{14}O_3$ and $Ca^{45}CO_3$ with the compounds containing the isotopes, according to the equations:

$$2MgSO_4 + 2Na_2CO_3 + H_2O = Mg_2(OH)_2C^{14}O_3 + 2Na_2SO_4 + CO_2,$$
$$Ca^{45}Cl_2 + Na_2CO_3 = Ca^{45}CO_3 + 2NaCl.$$

The inactive salts were always taken in excess, and the solutions foamed during boiling.

Samples were taken from the liquid layer and from the foam which, in Academician Rebinder's definition [4] is "a continuous lamellocellular structure in which the individual bubbles are close together, being separated by thin liquid films." Equipment B [5] was then used to determine the activity of the samples, and the coefficient of transfer of the suspended particles into the bubble films was calculated by means of the formula

$$K = \frac{A_1}{A_2} \cdot 100,$$

where K is the required coefficient, and A_1 and A_2 are the specific activities of samples of the foam and liquid layers of the boiling solution (in pulses/minute · ml). The results of these experiments show that the coefficient of transfer of $Mg_2(OH)_2C^{14}O_3$ into the liquid films was 311.6%, and that of $Ca^{45}CO_3$ 136.6%, that is, the bubble films had a considerably higher content of suspended particles than the liquid layer of the boiling solution. It

follows that in entrainment caused by foaming, selective transfer of solid particles of a certain optimum size is inevitable. However, in absence of foam entrainment, and when the steam height is considerable, the suspended particles are not only not carried over selectively, but greatly reduce the amounts of salts carried over. For example, the entrainment coefficient of $Na_2S^{35}O_4$, found by the usual radioactive tracer method [6] for the boiling of 0.01 N solution, is 0.49%; but if the boiling solution contains suspended particles* of $Mg_2(OH)_2CO_3$ then, under the same conditions, the coefficient decreases to 0.08%. The effect of suspended particles in decreasing the amounts of salts carried over with the steam was also confirmed by a gravimetric method. In these experiments, in order to avoid large errors in weighing, we used solutions with salt concentrations considerably above that of boiler water. The results of these experiments** are given in Table 1.

TABLE 1

Determination of Substances Carried Over in Steam (forced circulation 100 $kg/m^2 \cdot hour$)

Substance	Steam height (mm)	Substances carried over (in mg/liter) from boiling solution	
		1 N	2 N
NaCl	650	56.5	43
NaCl + $Fe(OH)_3$	650	7	4
NaCl + $Al(OH)_3$	650	7	4
NaCl + $Mg_2(OH)_2CO_3$	650	20.5	16
NaCl + $Ca_3(PO_4)_2$	650	42	13
NaCl + $CaCO_3$	650	45	20

It follows from the data in Table 1 that suspended substances decrease the amount of NaCl carried over to different degrees, as represented by the following series: $Fe(OH)_3 \geq Al(OH)_3 > Mg_2(OH)_2CO_3 > Ca_3(PO_4)_2 > > CaCO_3$. This shows that ferric and aluminum hydroxides have the same effect in diminishing the amount of salt carried over. The only explanation for this behavior of colloidal $Fe(OH)_3$ and $Al(OH)_3$ in the boiler process is that their colloidochemical properties are similar.

Moreover, $Fe(OH)_3$ and $Al(OH)_3$ solutions, whichare more stable in boiling solution, decrease the entrainment of NaCl to a greater extent than does calcium carbonate, which crystallizes rapidly under such conditions. Calcium carbonate decreases the amount of salt carried over only slightly, while basic magnesium carbonate, which is an amorphous precipitate and partially a colloid [1] decreases it to a greater extent than calcium phosphate and carbonate precipitates, but less than ferric and aluminum hydroxide solutions. These facts indicate that the influence of suspended substances on the entrainment of salts in steam is associated not only with the physical properties of the solid particles, as Folk [8] asserted, but depends to a greater extent on the colloidochemical properties of the disperse phases.

For an explanation of this fact, we turn to Table 2, which gives the amounts of NaCl carried over with forced circulation of 100 $kg/m^2 \cdot hour$ at different steam heights, both in absence of solid particles and in presence of a precipitate of basic magnesium carbonate in the solution.

We see in Table 2 that with a low steam space (170 mm) addition of the colloidal fraction to the boiling solution increases sharply the amount of NaCl carried over with the steam. At heights of 350 mm and over the $Mg_2(OH)_2CO_3$ precipitate present in the boiling solution decreases, although only slightly, the amount of salt carried over. With a higher steam space, solid particles reduce appreciably the amount of NaCl carried over with steam. Two facts may be noted: first, the amount of NaCl carried over decreases fairly smoothly with increase of the steam height if no solid particles are present in the solution (Fig. 1); second, if the boiling solution

*The experiments were preformed with forced circulation at 150 $kg/m^2 \cdot hour$, with a steam height of 788 mm. The possibility of adsorption of the tagged atoms was taken into consideration [6].

**Samples of condensate for determinations of the salt content were taken in all cases in absence of foam on the evaporation surface [7].

***See footnote at end of Literature Cited.

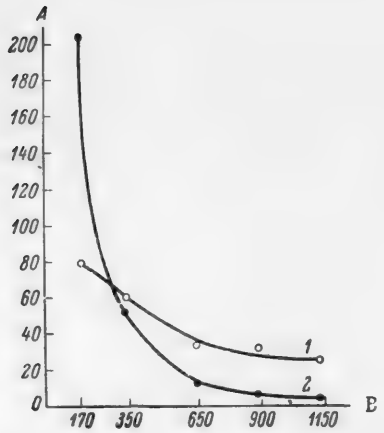

Fig. 1. Effect of steam space height on the entrainment of NaCl. A) NaCl carried over (in mg/liter), B) steam space height (mm). 1) NaCl, 2) NaCl + + $Mg_2(OH)_2CO_3$.

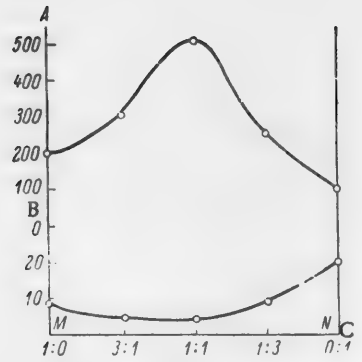

Fig. 3. Effect of composition of the mixture on foaming and entrainment of NaCl solution. A) Foam height (mm), B) salt carried over (in mg per liter), C) composition of $Fe(OH)_3$ + $Mg_2(OH)_2CO_3$ mixture, M) $Fe(OH)_3$, N) $Mg_2(OH)_3CO_3$.

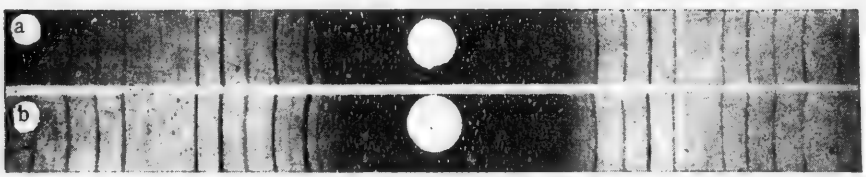

Fig. 2. X-ray pattern of material carried over from NaCl + $Mg_2(OH)_2CO_3$.

TABLE 2

Sodium Chloride Carried Over in Absence and Presence of Basic Magnesium Carbonate

Substances	NaCl carried over (in mg/liter) with steam height (mm)				
	170	350	650	900	1150
NaCl	80	60	35	32.5	25
NaCl + $Mg_2(OH)_2CO_3$	204	55	15	7	4

contains suspended $Mg_2(OH)_2CO_3$ particles, the amount of salt carried over falls steeply with increase of the steam height, indicating very strong natural separation of the droplets. The only cause of this can be that when the steam bubbles break down the solid particles assist the formation of large drops which separate out naturally and, if the steam space is high, these drops are not carried over but return to the solution. This probably accounts

for the decreasing effect of the solid particles on the amount of salt carried over. The results of x-ray phase analysis show that the suspended particles are absent from the salt carried over if the steam space is high enough. Figure 2 is an x-ray pattern of the substance carried over from a solution containing NaCl + $Mg_2(OH)_2CO_3$ (a), which has well-defined lines completely coinciding in intensity and position with the characteristic lines of sodium chloride in the standard (b), but contains no lines or background indicating the presence of another phase — magnesium compounds. This indicates that the larger and heavier drops, containing $Mg_2(OH)_2CO_3$ particles, underwent natural separation under our experimental conditions. However, if the steam space is low, when these drops can bounce into the zone of high steam velocities, they are entrained by the steam, with a considerable lowering of the quality of the steam. Therefore highly disperse particles of insoluble mineral substances present in boiling water in steam boilers can improve the quality of the steam appreciably only if the steam space is high enough. In fact, it has been found in boiler practice that the use of organic colloids produces very favorable results in such cases [9].

In Figure 3, interesting curves are given, representing the results of experiments carried out with 0.5 N NaCl solution in presence of mixtures of $Fe(OH)_3$ + $Mg_2(OH)_2CO_3$ in the following ratios: 1:0, 3:1, 1:1, 1:3, 0:1 (the total content being 2 meq/liter). It is seen that maximum foaming of the NaCl solution occurred when the $Fe(OH)_3$ + $Mg_2(OH)_2CO_3$ mixture was in 1:1 ratio. The minimum amount of salt entrainment corresponded to this same composition. Thus, maximum foaming corresponds to minimum entrainment of sodium chloride in steam. The foaming curve is concave with respect to the abscissa axis, whereas the entrainment curve is convex with respect to it. Therefore a mixture of basic sodium carbonate and ferric hydroxide solution decreases entrainment more and causes more foaming than either of its constituents. The probable reason is the stabilization of particles of basic magnesium carbonate, at the optimum degree of dispersion for foaming, by the ferric hydroxide solution, which can be adsorbed on suspended particles to form a colloidal film [10]. The foaming action of a mixture of suspended particles, and in particular $Fe(OH)_3$ + $Mg_2(OH)_2CO_3$, does not conform to the additivity rule: the experimental curve for the mixture deviates considerably from the additivity line.

SUMMARY

1. The content of solid particles of a certain degree of dispersion in foam exceeds considerably their concentration in the liquid layer of a boiling solution.

2. It is shown that, if the steam space is high enough, suspended particles reduce considerably the entrainment of salts in steam, while if the steam space is low and foam entrainment occurs, they sharply increase the amount of salt carried over.

3. A mixture of basic magnesium carbonate and ferric hydroxide solution causes much more foaming than either of the components separately; their foaming effect does not conform to the additivity rule.

4. The same mixture decreases entrainment to a greater extent than either of the components separately.

LITERATURE CITED

[1] S. A. Durov, Physicochemical Principles of Foam Priming in Boilers,(Izd. AN SSSR, 1948).*

[2] Yu. M. Kostrikin, Electrical Power Stations 1 (1953).

[3] M. V. Levitsky, Trans. North Caucasian Mining and Metallurgical Institute 11 (1949).

[4] P. A. Rebinder, J. Phys. Chem. 11,*6 (1931).

[5] V. Bochkarev et al., Measurement of the Activity of Beta and Gamma Radiation Sources (Izd. AN SSSR, 1953).*

[6] M. A. Styrikovich and Ya. G. Vinokur, Proc. Acad. Sci. USSR 90, 2, 179-182 (1953).

[7] N. G. Chen, Author's Summary of Candidate's Dissertation, Novocherkassk (1955).

* In Russian.

[8] Pauli, EOT, 2 (1938). *

[9] I. I. Magire and I. T. Topolasky, EOT 9, 44-46 (1937).*

[10] G. V. Zakharova, Colloid J. 4, 2-3 (1938).

Received June 8, 1956

*References [8] and [9] as well as the journal EOT are unverified. The names of the authors seem Western. "Magire" could well be McGuire and Folk referred to in the text who is cited in [8] could be Volk — Publisher's note.

RECTIFICATION OF METHANOL – ETHANOL – WATER MIXTURE IN A CONTINUOUS-ACTION COLUMN*

M. E. Aerov, G. L. Motina and M. M. Potarin

Rectification with the collection of two products in the distillate is often met in industry. The present investigation deals with the rectification of the three-component mixture methanol–ethanol–water, with both alcohols collected in the distillate. The purpose of the work was to determine the distribution of the components along the column in this rectification, about which not enough information is available in the literature.

The rectification of the mixture was carried out by the continuous method in a laboratory sieve-plate column, described previously [1]. The feed was supplied at 40-50° at the ninth plate from the top; Regularity of the bubbling on the plates was checked visually, and the pressure drop in the column was also measured. Otherwise the experimental procedure and the methods used for analysis of the mixtures obtained were as described previously [1].

The experimental data were treated by the graphical stepwise separation method in vapor–liquid equilibrium diagrams.

The results of two of the most typical experiments are given below. Characteristics of the rectification process are given in Table 1.

The compositions of samples of the liquid phase taken along the column are given in Table 2.

TABLE 1

Characteristics of the Rectification Process

Experiment No.	Feed rate (kg/hour)	Distillate withdrawal rate (kg/hr	Composition (molar %)									Reflux ratio (for top of column)	Ratio of theoretical to actual plates
			feed			distillate			residue				
			methanol	ethanol	water	methanol	ethanol	water	methanol	ethanol	water		
12	0.426	0.220	12.2	17.5	70.25	64.3	29.9	5.8	0.9	0.5	98.6	5.85	16.5/20
18	0.328	0.125	12.2	17.5	70.25	58.0	34.1	7.9	0.3	0.1	99.6	12.0	12/20

Figures 1-2 and 3-4 give the graphical constructions for the numbers of theoretical plates and separation steps in vapor–liquid equilibrium diagrams. The construction method for the theoretical plates was described previously [1]. The construction method for the separation steps was similar to that described in the literature [2]. On the y-x diagram for the individual components a line is drawn equidistant from the operating line and the equilibrium line. Then from the point in the operating line corresponding to the final concentration (the concentration in the distillate) a horizontal line is drawn, and along it is taken an intercept equal to double the

*Communication II.

intercept of the horizontal distance from the operating line to the middle line. From this point a vertical line is drawn to intersect the operating line. The construction is repeated at this point, and continued to the point corresponding to the concentration in the still. It is seen that the concentration difference between neighboring "steps" is equal to the average driving force over the given section of the column. The number of these "steps" is the number of separation steps. Combined vapor–liquid equilibrium diagrams for the system methanol–ethanol–water, considered in detail earlier [1], were used for the constructions.

TABLE 2

Compositions of Liquid Phase Samples Along the Column

Sampling point		Concentration (molar %)					
		experiment No. 12			experiment No. 13		
		methanol	ethanol	water	methanol	ethanol	water
Plate	1	64.3	29.9	5.8	58.0	34.1	7.9
	2	50.4	34.3	15.3*	45.0	42.3	12.7
	3	45.0	46.5	8.6	43.0	42.5	14.5
	5	38.6	49.0	12.2	37.6	44.6	17.7
	7	34.3	53.3	12.4	31.6	48.5	19.9
Feed		12.2	17.55	70.25	12.2	17.55	70.25
Plate	11	21.0	65.5	13.5	23.6	53.5	22.9
	13	16.5	63.7	19.8	20.0	56.9	23.1
	15	14.0	50.1	35.9	11.6	38.1	50.4
	17	10.0	35.5	54.5	5.8	32.3	62.0
Still		0.86	0.51	98.7	0.3	0.16	99.7

* Total alcohol content apparently too low (experimental error).

The operating line was drawn through points corresponding to the methanol and ethanol concentrations in the distillate and residue on the corresponding diagrams. A correction for the underheating of the original mixture below its boiling point was applied to the stripping line. The compositions of the vapor phase in equilibrium with the liquid on the theoretical plates are indicated in Figures 3 and 4 by points.

In all the constructions the number of separation steps practically coincides with the number of theoretical plates. The concentrations determined by graphical analysis (in the theoretical-plate construction) were compared with the experimental values. Satisfactory agreement was found. For example, in Experiment No. 12 the maximum concentration of ethanol found by analysis of the samples was 65.5 molar %, while the calculated value was 68.0 molar %.

The concentration distributions along the column are plotted in Figure 5. The concentrations of methanol, ethanol, and water are marked off successively along the line corresponding to any given plate. The points corresponding to the concentrations of methanol and of ethanol are joined by curves. The concentration distributions determined experimentally and by the method of graphical analysis (theoretical-plate construction) are given in the diagrams.

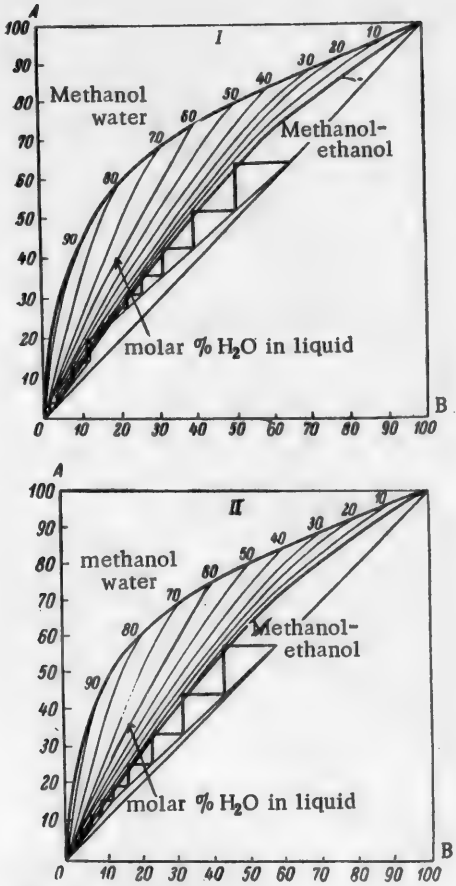

Fig. 1. Construction of theoretical plates on the diagram for methanol. A) Methanol in vapor (molar %), B) methanol in liquid (molar %). I) Experiment No. 12, II) Experiment No. 13.

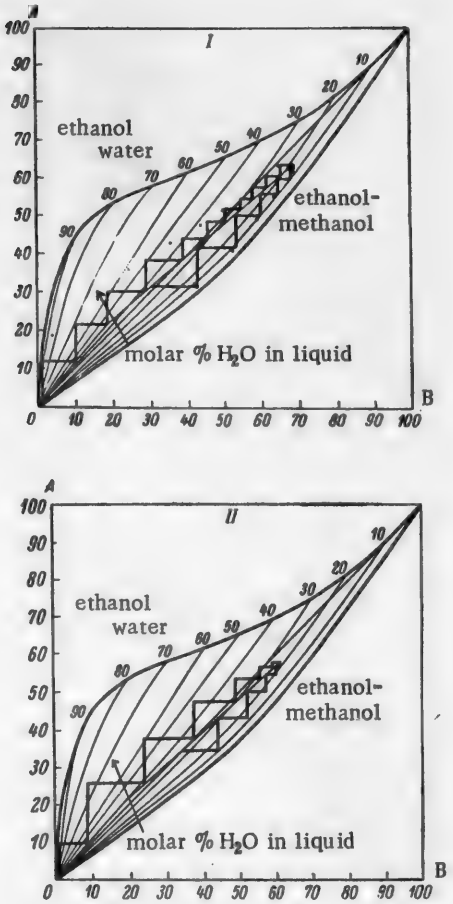

Fig. 2. Construction of theoretical plates on the diagram for ethanol. A) Ethanol in vapor (molar %), B) ethanol in liquid (molar %). I) Experiment No. 12, II) Experiment No. 13.

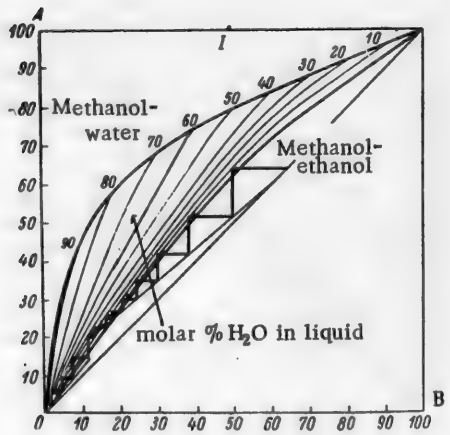

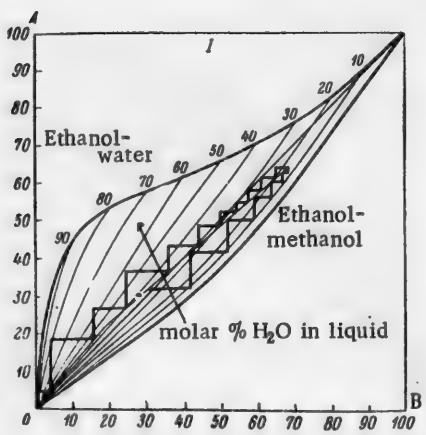

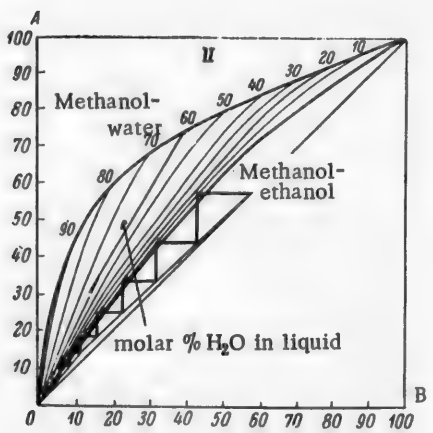

Fig. 3. Construction of separation steps on the diagram for methanol. A) Methanol in vapor (molar %), B) methanol in liquid (molar %). I) Experiment No. 12, II) Experiment No. 13.

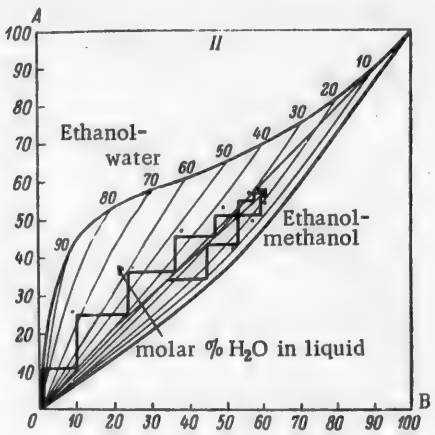

Fig. 4. Construction of separation steps on the diagram for ehtanol. A) Ethanol in vapor (molar %), B) ethanol in liquid (molar %). I) Experiment No. 12, II) Experiment No. 13.

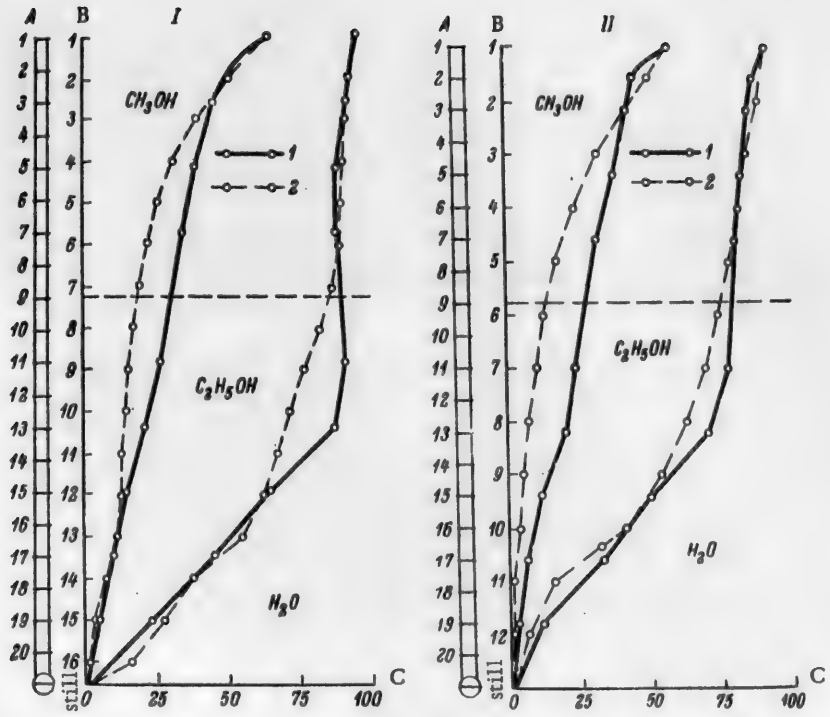

Fig. 5. Comparison of experimental data and the results of graphical analysis for the distribution of the components of the mixture along the column. A) Number of actual plates, B) number of theoretical plates, C) composition of liquid phase (in molar %). 1) Experimental data, 2) results of graphical analysis; I) Experiment No. 12, II) Experiment No. 13.

SUMMARY

1. Experimental data on the distribution of concentrations along the column are in satisfactory agreement with the calculated results obtained by graphical analysis of the theoretical plates.

2. In the separation of a mixture of the two alcohols from water, ethanol is the more volatile component in the lower part of the column, and the less volatile in the upper part.

LITERATURE CITED

[1] M. E. Aerov, G. L. Motina and L. P. Golovanova, J. Appl. Chem. 30, 567 (1957).*

[2] V. M. Ramm, Absorption Processes in Chemical Industry (Goskhimizdat, 1951), pp. 87-90.**

Received September 19, 1955

*Original Russian pagination. See C. B. Translation.

**In Russian.

PREPARATION OF TRIHYDROXYSTEARIN

G. V. Pigulevsky and A. E. Saprokhina

The A. A. Zhdanov State University, Leningrad

In 1951 one of us published a paper [1] on the preparation of hydroxy acid triglycerides. It was shown in this paper that crystalline palmitodihydroxystearin (m. p. 62.5°) can be prepared by the oxidation of peach oil with acetyl hydroperoxide followed by catalytic hydrogenation. The formation of this mixed triglyceride shows that the oil contains palmitodiolein. It was also pointed out that studies of hydroxy acid triglycerides may provide a new route to investigations of the structure of triglycerides in vegetable oils.

The present communication deals with the results obtained by application of this method to oil of the spurge plant (Euphorbia lathiris). As is known, spurge oil contains 87-90% of oleic acid, 3.8-6.0% of linoleic acid, and 6-7.4% of saturated acids. Oxidation of spurge oil with acetyl hydroperoxide yielded the triglyceride of oleic acid epoxide (m. p. 57-58°), which gave trihydroxystearin (m. p. 65-65.5°) on catalytic hydrogenation.

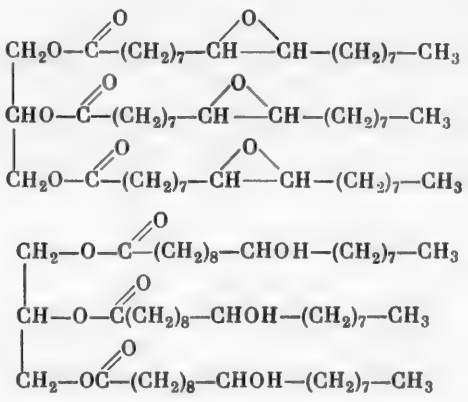

The structure of trihydroxystearin was confirmed by the formation of hydroxystearic acid on saponification of the triglyceride. The formation of trihydroxystearin indicates the presence of triolein in spurge oil.

EXPERIMENTAL

Oxidation of spurge oil with acetyl hydroperoxide. To 300 g of spurge oil (iodine number 84) dissolved in 600 ml of ether, there was added 305 ml of an ether solution of acetyl hydroperoxide containing 20.54 g of active oxygen (30% excess). Acetyl hydroperoxide was prepared as described by B. A. Arbuzov. The oxidation was continued for 4 days. A white precipitate began to form even during the oxidation. The white precipitate was filtered off and washed with water to remove acetic acid. The yield of the white substance was 130 g; after recrystallization from alcohol and ligroine it had m. p. 57-58°.

Found %: C 73.24, 73.23; H 11.15, 11.23. M 939.3, 923.3. $C_{57}H_{104}O_9$. Calculated %: C 73.34; H 11.23. M 933.4.

Saponification of substance with m. p. 57-58°. 3.73 g of the compound was saponified with 0.5 N caustic potash solution at room temperature. After two days the reaction mixture was diluted with twice its volume* ofwater and acidified with 10% sulfuric acid. The substance which separated out was filtered off and washed with water. After recrystallization from alcohol and ligroine a substance [2, 3] was obtained with m. p. 56-57° and neutralization number 187.8. A mixed sample with oleic acid epoxide gave no depression.

Hydrogenation of triolein oxide [4]. The reaction was carried out in a special hydrogenation vessel in glacial acetic acid in presence of palladium black prepared by Willstatter's method.

Eight grams of triolein oxide, 40 ml of acetic acid, and 0.81 g of palladium black were taken. The hydrogenation temperature was 60°. The theoretical amount of hydrogen required is 576 ml (at 0°, 760 mm); 495 ml was absorbed in 3 hours. The hydrogenation was 86% complete.

Isolation of the hydrogenation product. An acetic acid solution of the hydrogenated substance, separated by decantation from the palladium black, was diluted to 2/3 with water. The white precipitate was filtered off and washed with water. Recrystallization from alcohol yielded 4.76 g of a crystalline substance with m. p. 65-65.5°.

Found %: C 72.69, 72.54; H 11.58, 11.65. M 960.2, 959.1.
Calculated %: C 72.85, H 11.81. M 939.45.

Saponification of substance with m. p. 65-65.5°. The presumed trihydroxystearin was saponified with 0.5 N alcoholic caustic potash at room temperature. The compound, isolated as described above, had m. p. 80-81.5° after recrystallization from alcohol.

Found %: C 71.87, 71.91; H 12.18, 12.26. Neutralization number 188.1, 184.7, hydroxyl number 2.08, 2.15. $C_{18}H_{36}O_3$. Calculated %: C 71.94, H 12.08. Neutralization number 186.7, hydroxyl number 2.0.

SUMMARY

Triolein trioxide, m. p. 57.58°, has been prepared for the first time; it was hydrogenated to give trihydroxystearin, m. p. 65-65.5°. The new class of compounds, hydroxy acid triglycerides, may be used in studies of the structure of mixed triglycerides in vegetable oils.

LITERATURE CITED

[1] G. V. Pigulevsky and T. A. Starostina, Proc. Acad. Sci. USSR 79, 261 (1951).

[2] G. V. Pigulevsky and M. A. Petrova, J. Russ. Chem. Soc. 58, 1062 (1926).

[3] J. Böeseken, and A. Belifante, Ber. 45, 914 (1926).

[4] G. V. Pigulevsky and Z. Ya. Rubashko, J. Gen. Chem. 9, 831 (1938); 25, 2227 (1955).**

Received February 21, 1957

* This phrase is ambiguous in the Russian. It literally translates as "diluted twice".
** Original Russian pagination. See C. B. Translation.

INVESTIGATION OF THE COMPOSITION OF DRY-DISTILLED RETORT TURPENTINE FROM THE RESIN OF KOREAN PINE

(Pinus koraiensis sieb. et Zucc)

N. I. Uvarova and I. I. Bardyshev

Chemical Division of the Far Eastern Branch of the Academy of Sciences USSR
and the Belorussian Institute of Wood Technology

The composition of turpentines obtained from the oleoresins of various conifers has been studied fairly fully. Less is known about the composition of dry-distilled turpentines, although the total output of such turpentines is several thousands of tons per year. There are only a few papers [1-4] on this subject in the literature.

The purpose of the present investigation was to study the composition of dry-distilled retort turpentine from the resin of Korean pine. Lyubarsky investigated the turpentine from this source and found that it contained 75% of a fraction distilling at 155-180°. He did not report the qualitative or quantitative characteristics of this turpentine [4].

Our sample of turpentine had the following approximate composition in %: *l* - α-pinene 25, *l* -camphene 7, cyclodihydromyrcene (?) 5, D-Δ^3-carene 13, mixture of *l* -limonene and dipentene 25, p-cymene 3, terpene alcohols 4, and high-boiling constituents 14. The percentage composition of the turpentine was calculated by Bardyshev's method [5].

In addition to substances of the terpene series, the first fraction also contained products of the dry distillation of wood, the nature of which was not studied.

EXPERIMENTAL

The turpentine sample was obtained by the dry distillation of so-called "resinified logs" in a Vyatka retort belonging to one of the works of the Maritime Region Industrial Soviet of the Spassk region. The crude turpentine had d_4^{20} 0.8920, n_D^{20} 1.4862, acid number 18.50.

The crude turpentine was first distilled, and the fraction boiling in the 155-190° range was collected. This fraction was purified by repeated shaking with dilute aqueous caustic alkali followed by distillation in steam. This fraction, referred to as "purified turpentine" was then investigated.

The purified turpentine had the following physicochemical characteristics: d_4^{20} 0.8541, n_D^{20} 1.4726, $[\alpha]_D^{20}$ − 20.8°, acid number 0.3, ester number 5.8. The content of alcohols calculated as $C_{10}H_{17}OH$ was 4.0 %. The turpentine was distilled by the Engler method at 750 mm Hg; start of boiling 158°; 5 ml 163.5°; 10 ml 165°; 15 ml 165.5°; 20 ml 166°; 30 ml 167°; 40 ml 168.8°; 50 ml 171°; 60 ml 172°; 70 ml 174°; 80 ml 177.5°; 90 ml 184°; 95 ml 195°. 400.0 g of the purified turpentine was fractionated under vacuum in a column of 25 theoretical plates at reflux ratio 25.

The results of the fractional distillation (at 20 mm) are represented graphically in Figure 1.

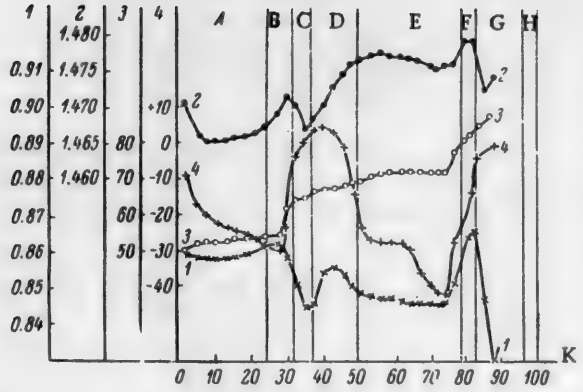

Fig. 1. Rectification data for dry-distilled Korean pine turpentine. 1) d_4^{20}, 2) n_D^{20}, 3) boiling point at 20 mm Hg (°C), 4) $[\alpha]_D^{20}$. Zones: A) l-α-pinene, B) l-camphene, C) cyclodihydromyrcene (?), D) d-Δ^3-carene, E) l-limonene with dipentene, F) terpene alcohols, G) high-boiling components and residues, H) losses, K) Contents of fractions (%).

l-α-Pinene. Fractions 3-4 of zone A were distilled twice over metallic sodium to give l-α-pinene with b. p. 154-155° at 751 mm Hg, d_4^{20} 0.8574, n_D^{20} 1.4653m $[\alpha]_D^{20}$ − 23.30°. The nitrosochloride obtained from this fraction melted at 102° (with decomposition), and pinonic acid at 103-104°.

Fractions 6-11 of zone B, 12-17 of zones C and D, and 23-28 of zone E were distilled twice under vacuum through a column of 50 theoretical plates at reflux ratio 25.

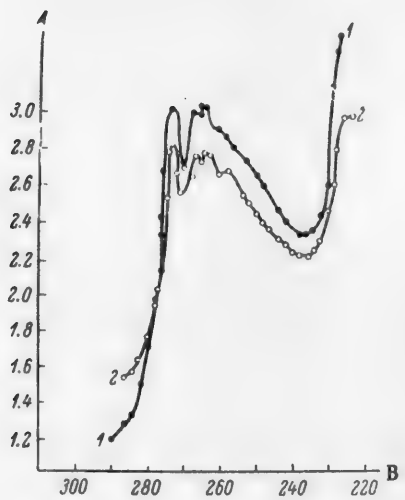

Fig. 2. Absorption curves. A) Logarithm of the molar absorption coefficient (log Σ), B) wavelength (in mμ). 1) Log Σ for pure p-cymene*, 2) log Σ for the fraction studied.

l-Camphene. The product obtained in the second distillation of fractions 6-11 had b. p. 54° at 20 mm Hg, d_4^{20} 0.8620 n_D^{20} 1.4722, $[\alpha]_D^{20}$ − 34.34° When this fraction was cooled to −70°, crystals melting at room temperature were formed. This fraction was converted into isoborneol acetate by the method of Bertram and Walbaum [6], and the camphene content was calculated by Bardyshev's formula [7]. The camphene content of these fractions was 42.3 %, or 7% on the total amount of turpentine.

Cyclodihydromyrcene (?) and d-Δ^3-carene. Two fractions were isolated from fractions 12-17 by a second fractionation: Fraction I, b. p. 65.0° at 20 mm Hg, d_4^{20} 0.8364, n_D^{20} 1.4645, $[\alpha]_D^{20}$ − 0.48°. Fraction II, b. p. 67.5° at 20 mm Hg, d_4^{20} 0.8606, n_D^{20} 1.4717, $[\alpha]_D^{20}$ + 13.59°.

Fraction I did not react with maleic anhydride, and yielded the following fractions by distillation over metallic sodium:

a) b. p. 157.5-162° at 747.2 mm Hg, n_D^{20} 1.4628;

b) b. p. 162-166° at 747.2 mm Hg, d_4^{20} 0.8366, n_D^{20} 1.4625, $[\alpha]_D^{20}$ −0.72°;

* The spectroscopic determinations were carried out by Kh. A. Cherches, to whom we express our gratitude.

** See footnote at end of paper

c) b. p. 166-167° at 747.2 mm Hg, d_4^{20} 0.8341, n_D^{20} 1.4626, $[\alpha]_D^{20}$ −0.48°.

By its physical constants, fraction "c" resembles cyclodihydromyrcene [8].

Elementary analysis.

Found %: C 87.24, 87.21; H 12.23, 12.28. $C_{10}H_{18}$. Calculated %: C 86.87; H 13.13.

The nature of this hydrocarbon will be studied further.

Fraction II was distilled over metallic sodium, and had the following constants: b. p. 169-170° at 748 mm, d_4^{20} 0.8622, n_D^{20} 1.4717, $[\alpha]_D^{20}$ + 13.6°. This fraction was converted by the usual method into d- Δ^3-carene nitrosate in good yield; this melted with decomposition at 139°. Recrystallization of the nitrosate from ethyl acetate did not raise its melting point.

l-Limonene and dipentene. A second distillation of fractions 23-28 yielded a substance which had the following properties after distillation over metallic sodium: b. p. 173-174° at 747.8 mm Hg, d_4^{20} 0.8434, n_D^{20} 1.4752, $[\alpha]_D^{20}$ −44.43°.

The titration of 1.1 g of the substance in a mixture of anhydrous ether and absolute alcohol cooled to −5° took 2.7 g of bromine. The crystalline dipentene tetrabromide melted at 126° after recrystallization from absolute ethanol. A mixed sample with known pure dipentene tetrabromide gave no m. p. depression.

p-Cymene. The first runnings of limonene and dipentene contained a substance of higher density and refractive index than limonene. It has been reported in the literature that p-cymene may distil together with limonene and dipentene, raising the density and refractive index of these fractions [9].

The fraction with d_4^{20} 0.8460 and n_D^{20} 1.4765 was oxidized twice with aqueous 3% $KMnO_4$ solution. This yielded a product (50.3 g) with d_4^{20} 0.8479, n_D^{20} −18.72°. This product was distilled under vacuum through a column of 50 theoretical plates at a reflux ratio of 50. The fractions obtained, with d_4^{20} 0.8477-0.8512, n_D^{20} 1.4775-1.4808, $[\alpha]_D^{20}$ − 3.15-1947°, were again oxidized with 3% $KMnO_4$ solution and then distilled in steam; this gave 2.3 g of a substance with n_D^{20} 1.4882.

The logarithm of the molar absorption coefficient in the ultraviolet region of the spectrum for this fraction is plotted in Fig. 2, Curve 2. For comparison, the logarithm of the molar absorption coefficient of pure p-cymene, with n_D^{20} 1.4911, d_4^{20} 0.8560, MR_D 45.47 and $[\alpha]_D^{20}$ = 0° * is also plotted in the same diagram.

The substance was chromatographically separated in a column filled with silica gel; a fraction with d_4^{20} 0.8581, n_D^{20} 1.4908, $[\alpha]_D^{20}$ = 0°, which was p-cymene, was isolated. Oxidation of the p-cymene gave p-hydroxyisopropylbenzoic acid, which had m. p. 155° after three recrystallizations.

Distillation residue. The distillation residue contained 55.5% of terpene alcohols, calculated as $C_{10}H_{17}OH$; these were not investigated further.

SUMMARY

1. Dry-distilled retort turpentine from the resin of Korean pine consists of approximately 25% of *l* - α-pinene, 5 % of cyclodihydromyrcene (?), 13% of d- Δ^3-carene, 25 % of *l*-limonene and dipentene, 3% of p-cymene, 4% of terpene alcohols, and 14% of high-boiling components which were not investigated.

LITERATURE CITED

[1] B. A. Arbuzov, J. Appl. Chem. 3, 867 (1930).

[2] V. M. Nikitin, J. Appl. Chem. 19, 1401 (1946).

[3] I. I. Bardyshev, A. L. Piryatinsky, K. V. Bardysheva and O. I. Chernyaeva, J. Appl. Chem. 23, 552 (1950).

[4] E. I. Lyubarsky, Industry 6, 39 (1927).

* The spectroscopic determinations were carried out by Kh. A. Cherches, to whom we express our gratitude.

[5] I. I. Bardyshev, Coll. Trans. Central Sci. Res. Inst. Wood Industry 10, 129 (1951).

[6] Bertram and Walbaum, J. pr. Ch., 2, 49 (1894).

[7] I. I. Bardyshev, J. Appl. Chem. 26, 1299 (1953).

[8] V. M. Nikitin, Chemistry of the Terpenes and Resin Acids (State Wood and Paper Press, Moscow-Leningrad, 1952) p. 57. *

[9] I. I. Bardyshev, Proc. Acad. Sci. USSR 101, 2, 263 (1953).

Received March 8, 1956

Footnote:

The following is found in the Russian beneath the text for Fig. 2. It seems to relate to a figure similar to Fig. 1 but not given – Publisher's note. Rectification data for turpentine from Ayan spruce. 1) d_A^{20}. 2) n_D^{20}. 3) b. p. at 20 mm, 4) $[\alpha]_D^{20}$ zones: A) L-α-pinene, B) L-β-pinene. C) D-Δ^3-carene, D) L-limonene with dipentene, E) terpene alcohols, F) high-boiling components and residues, G) losses, H) contents of fractions (%).

*In Russian.

PREPARATION OF BENZIDINE BASES WITH THE USE OF ALIPHATIC ALCOHOLS AS REDUCING AGENTS

D. F. Kutepov and V. E. Reinshtein

Benzidine and its derivatives are very valuable intermediates which are extensively used for the production of a large group of azo dyes.

As is known, benzidine or 4,4'-diaminodiphenyl was first synthesized by N. N. Zinin by the action of sulfuric acid on hydrazobenzene.

Considerably later, methods were developed for the rearrangement of the corresponding hydrazo compounds for the production of other technically valuable diamines, of the diphenyltolidine, dianisidine, benzidine-2,2'-disulfonic acid, tolidine-2,2'-disulfonic acid, benzidine-3,3'dicarboxylic acid, and other series [1, 2].

Alexejev [3] showed that an alkaline medium is required for the reduction of nitro compounds to azoxy, azo, and hydrazo compounds. He was the first to use sodium amalgam and zinc in presence of alkali as reducing agents.

For the preparation of azobenzene-4,4'-dicarboxylic acid, Sokoloff [4] proposed a method of reduction of nitro compounds with zinc dust in ammonia solution.

Apart from these reducing agents, those of magnesium in conjunction with methyl alcohol or with aqueous ammonium chloride solution has been proposed [5] for the preparation of azoxy derivatives from nitro compounds. The work of Zinin and later authors [6] is worthy of special attention; here azoxybenzene was prepared by reduction of nitrobenzene with boiling alcoholic solution of sodium methoxide. Greater yields were obtained when nitrobenzene was heated with excess of dry sodium methoxide suspended in acid. In industrial reduction of nitro compounds in an alkaline medium, especially for partial reduction of polynitro compounds, metal sulfides such as Na_2S, Na_2S_2, NaHS, $(NH_4)_2S$ etc., are also used. Solutions of ammonium sulfide in alcohol or dioxan are used in laboratory practice.

The industrial production of benzidine and its derivatives is usually effected by reduction of the corresponding aromatic nitro compounds with zinc dust in an alkaline medium. The reduction is carried out in two stages, azoxy compounds being obtained in the first stage, and hydrazo compounds in the second. Rearrangement of the latter in an acid medium forms benzidine bases.

In view of the fact that the original nitro compounds and their reduction products are insoluble in aqueous caustic soda solution, and zinc dust and zinc oxide are present in the form of precipitates, vigorous stirring is used. An inactive organic solvent (benzene, toluene, xylene, etc. [7]) is sometimes added to the reaction mixture to make it more mobile and to dissolve the reaction products.

We have shown in the present investigation that, if alcohols (methyl, ethyl and others) are used as reducing agents, nitro compounds are reduced fairly smoothly to azo compounds, which are isolated and reduced further with zinc dust to the hydrazo compounds.

The sodium salt of the corresponding carboxylic acid formed in the first reduction stage, after separation of the reduction products and distillation of excess alcohol, was subjected to further treatment with sulfuric acid. The organic acid was then obtained pure by distillation.

This method for the preparation of benzidine bases by the reduction of nitro compounds with alcohols has not been used in industry.

We found the optimum conditions for the reduction and determined the proportions of alcohols, nitro compounds, and alkali, which give azoxy compounds in high yields, and with a much lower consumption of alcohol and alkali than in the methods described in the literature [6]. The azoxy compounds were subjected to further reduction with zinc dust to the corresponding hydrazo compounds without being separated from the reaction mass; the hydrazo compounds were converted into benzidine bases in an acid medium, in high yields calculated on the starting nitro compounds.

It is also shown that not only monohydric alcohols, but higher alcohols such as ethylene glycol, can be used under suitable conditions for the reduction of aromatic nitro compounds to azoxy compounds.

Our combined method for the reduction of nitro compounds by various alcohols in the 1st reduction stage, and by other reducing agents in the 2nd reduction stage, can be used for the preparation of benzidine, dianisidine, tolidine, benzidinecarboxylic acid, benzidinedisulfonic acid, and other benzidine derivatives.

The method was subjected to trials on the industrial scale at the Dorogomilov Chemical Works,* and proved entirely satisfactory.

It was established in these trials that hydrazo compounds are obtained in high yields without previous isolation of the azoxy or azo compounds. Benzidine bases are obtained in high yields calculated on the original nitro compounds. The consumption of the highly scarce zinc dust can be decreased by 60-100%, depending on the substance used for the reduction of the azoxy and azo compounds.

The production of benzidine bases is made much cheaper, and the output rate is increased by a decrease of the time required for reduction of the nitro compounds.

EXPERIMENTAL

Preparation of Benzidine Bases with the Use of Methyl Alcohol

Preparation of benzidine. 1) To a boiling solution of 50 g of caustic soda (100%) in 75 ml of methyl alcohol, contained in a flask under reflux, 123 g of nitrobenzene was added gradually with stirring over a period of 2 hours. After the nitrobenzene had been added the reaction mixture was stirred for 3-4 hours more at the boil until the odor of nitrobenzene disappeared. After removal of the methyl alcohol by distillation, 96 g of azoxybenzene with m. p. 35° was obtained; this was 97% of the theoretical yield on the nitrobenzene.

Found %: C 71.8, 72.3; H 54,**4.97; N 14.6, 14.9. $C_{12}H_{10}N_2O$.
Calculated %: C 72.9; H 5.05; N 14.07.

Evaporation of the aqueous solutions yielded 60.5 g of sodium formate. The salt was treated with sulfuric acid; 33 g of formic acid was distilled off.

100 ml of water was added to the azoxybenzene, followed by the addition of 90 g of zinc dust (in 5 g portions at 15-20 minute intervals) to the mixture at 80° with vigorous stirring. This reaction yielded 87.2 g of hydrazobenzene with m. p. 126° (96% of the theoretical yield calculated on nitrobenzene).

Found %: C 77.96, 78.4; H 6.1, 6.2; N 15.8, 15.5. $C_{12}H_{12}N_2$.
Calculated %: C 78.3; H 6.5; N 15.2.

In addition to the hydrazobenzene, 3.73 g of aniline was obtained (4% calculated on nitrobenzene).

To isolate the hydrazobenzene, the reaction mixture was acidified with sulfuric acid, and the hydrazobenzene was then separated from the zinc sulfate solution by filtration. In other cases the reaction mass was filtered and the precipitate, consisting of hydrazobenzene and zinc hydroxide, was treated with mineral acid.

*O. V. Korsunsky, G. B. Bernshtein and I. F. Ivonin took part in the trials.

**Probably 5.4 — Publishers note.

The hydrazobenzene was subjected to rearrangement in hydrochloric acid. The yield was 76.3 g of benzidine with m. p. 127.5° (83% calculated on nitrobenzene).

Found %: C 78.6, 78.2; H 6.3, 6.4; N 15.9, 16.7. $C_{12}H_{12}N_2$.
Calculated %: C −78.3, H 6.5; H −6.5; N 15.2.

2) To 123 g of nitrobenzene at 85-90° a solution of 50 g of caustic soda in 145 g of methyl alcohol was added gradually with stirring during 2 hours. After the addition, the mixture was boiled until the odor of nitrobenzene disappeared. The reduction was less vigorous when alcoholic alkali was added to nitrobenzene, and the yields of hydrazobenzene and benzidine were accordingly somewhat higher.

The yields were: 97 g of azoxybenzene (98% calculated on nitrobenzene), 89.2 g of hydrazobenzene (97% calculated on nitrobenzene), and 77.3 g of benzidine (84% on nitrobenzene).

2.8 g of aniline (3% on nitrobenzene) was also formed in the reaction.

3) The reaction mass obtained after reduction of nitrobenzene with methyl alcohol, as in Experiment 1, was diluted with 200 ml of ethyl alcohol and 200 ml of 20% aqueous ammonia after removal of excess methanol. A rapid stream of hydrogen sulfide was passed through the mixture at 60° until the separation of hydrazobenzene ceased. The ethyl alcohol was then distilled off and the hydrazobenzene was used for the preparation of benzidine.

The yields were: 84.6 g of hydrazobenzene (92% on nitrobenzene), and 73.8 g of benzidine (80% on nitrobenzene).

Preparation of dianisidine. To a boiling solution of 50 g of caustic soda in 75 ml of methyl alcohol 153 g of o-nitroanisole was added gradually during 2 hours. The mixture was then stirred at the boil for 3 hours, the excess methanol was driven off, and the reaction mixture was diluted with 100 ml of water

The second stage of reduction with zinc dust was performed as in Experiment 1. The consumption of zinc dust was 85 g. At the end of the reduction the reaction mass was diluted with 40 ml of water and acidified with dilute sulfuric acid at 10°. Hydrazoanisole was separated by filtration. The yield of hydrazoanisole was 116 g (95% on o-nitroanisole).

Found %: C 68.3, 68.7; H 6.45, 6.6; N 11.9, 11.6. $C_{14}H_{16}N_2O_2$.
Calculated %: C 68.85; H 6.56; N 11.48.

Rearrangement of the hydrazoanisole in dilute sulfuric acid yielded 105 g of dianisidine (84.5% on o-nitroanisole).

Found %: C 68.9, 68.2; H 6.4, 6.2; N 11.3, 11.7. $C_{14}H_{16}N_2O_2$.
Calculated %: C 68.85; H 6.56; N 11.48.

If the first stage of the reduction of the nitro compounds is carried out at 120-150° under pressure, azo compounds in about 98% yield are obtained.

Preparation of benzidine bases with the use of ethylene glycol. To a mixture of 123 g of nitrobenzene and 60 g of ethylene glycol, heated to 125°, 80 g of 50% caustic soda solution was added with stirring. The temperature of the mixture gradually rose to 140-145° during the addition, water was continuously distilled off through the condenser, together with a little nitrobenzene, which was returned into the reaction flask through a Florentine vessel. After the addition of the alkali the reaction mass was stirred at 140-145° until the nitrobenzene odor disappeared (1.5 hours). The yield of azoxybenzene was 97 g (98.2% on nitrobenzene).

To azoxybenzene (not purified) 50 ml of water was added, and the second reduction stage was performed at 80° by means of zinc dust which was added in 5 g portions at 15-20 minute intervals. The zinc dust was added in the form of an alkaline suspension (100 g of zinc dust to 50 g of 5% caustic soda solution).

Water was added simulatneously with the zinc dust (50 ml of water per 20 g of zinc). The consumption of zinc dust was 80 g. The yield of hydrazobenzene was 89.1 g (97.5% on nitrobenzene).

Rearrangement of the hydrazobenzene in dilute hydrochloric acid gave 78.2 g of benzidine (85% on nitrobenzene).

If the first reduction stage is performed with an increased amount of ethylene glycol (80-85 g) at 170-175°, the reaction product is azobenzene. The consumption of zinc dust in the second reduction stage is then decreased to 40-50 g. The yields of hydrazobenzene and benzidine remain the same.

A mixture of ethylene glycol and glycerol may be used for the reduction, and lime can be used instead of caustic soda.

Dianisidine, tolidine, and other benzidine bases can be obtained analogously in high yields.

SUMMARY

1. It is shown that in the preparation of benzidine bases by the proposed method the hydrazo compounds formed by reduction are easily converted into benzidine bases in an acid medium.

2. The consumption of zinc dust is considerably decreased in this method. Benzidine bases are obtained in high yields.

LITERATURE CITED

[1] N. N. Vorozhtsov, The Fundamentals of Synthesis (1950) pp. 275-292.*

[2] V. O. Lukashevich, Org. Chem, Ind. 7, 506 (1940).

[3] P. P. Alexejev, Bull. (2), 1, 324-326 (1864).

[4] N. V. Sokoloff, Bull. l'Arc St.-Petersbourg, 7, 476 (1864).

[5] German Patent 446867, 26 XI 1926; Frd. XV, 227.

[6] N. N. Zinin, J. pr. Ch., (1), 36, 98 (1845); H. Schmidt , G. Schultz, Annalen, 207, 328 (1881); A. Lachman, J. Am. Soc., 94, 1180 (1902; J. W. Bruhl, Ber., 37, 2076 (1904).

[7] U. S. Patent 1633123, 1644484, Z,1, 1613 (1929); U. S. Patent 1718393, Z, 1,2010 (1930).

Received June 11, 1956

*In Russian.

HIGH-MELTING ABIETIC ACID

N. F. Komshilov

Laboratory of Wood Chemistry, Karelian Branch, Academy of Sciences USSR

The literature on the resin acids describes in satisfactory detail abietic acid with m. p. 174-175°, $[\alpha]_D^{20}$ −115.6° (in alcohol), but as long ago as 1905 Levy [1] obtained abietic acid with somewhat different properties by distillation of rosin. This had m. p. 181-183°, $[\alpha]_D^{20}$ −66.5°, while in 1908 Shkatelov [2] reported that he found sylvic acid with m. p. 179-180°, $[\alpha]_D$ 0° in the oleoresin of Pinus silvestris. He prepared this acid by distillation of rosin under atmospheric pressure. The properties of sylvic acid were similar to those of Levy's acid. Later an acid of almost the same properties with m. p. 182°, $[\alpha]_D$ −30.7° was prepared by Aschan and Virtanen [3] by the distillation of talloil; they named this pinabietic acid. A similar product with m. p. 182°, $[\alpha]_D$ − 3.0° was obtained by Ruzicka and Meyer [4] by vacuum distillation of rosin. Krestinsky, Persiantseva, and Novak [5] proved the individuality of a resin acid with m. p. 186-188°, $[\alpha]_D^{20}$ −17.36° (in alcohol) and named it high-melting abietic acid, in distinction from low-melting abietic acid with m. p. 174-175°, $[\alpha]_D^{20}$ −115.6° (in alcohol). The same authors [6] studied the structure of abietic acids and ascribed the following Formula (I) to high-melting abietic acid:

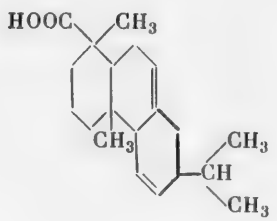

(I)

Earlier investigations of the pyroabietic acids and disproportionated rosin [7-10] obtained by the action of palladium deposited on carbon at 250-270° on rosin and resin acids cast considerable doubts on the existence of high-melting abietic acid, as the pyro products contained a mixture of dehydro-dihydro- and tetrahydroabietic acids. Evidence was put forward that simple heating also leads to a rearrangement of the hydrogen atoms.

In our investigations in the field of resin acids we thought it necessary to return to the question of abietic acids. We desired to obtain additional information which would prove or disprove the existence of the high-melting form of abietic acid. A pure sample of low-melting abietic acid with m. p. 174°, $[\alpha]_D^{20}$ −107.7° was prepared and subjected to isomerization by distillation under atmospheric pressure. After separation of the distillation products and recrystallization of the resin acids obtained, there was found 6.5%, on the weight of the original sample, of high-melting abietic acid with m. p. 182°, $[\alpha]_D^{20}$ + 12.61°. This high-melting abietic acid was undoubtedly free of dextropimaric and other resin acids of the oleoresin.

Another sample of pure low-melting abietic acid was subjected to the action of acid isomerization agents. After an alcoholic solution containing low-melting abietic acid and 0.1% of hydrochloric acid had been boiled for 14 hours, the specific rotation of the resin acid fell to $[\alpha]_D^{20}$ −43.54° and its crystalline form changed, and no longer corresponded to low-melting abietic acid. After a further exposure of the resin acid to an alcoholic acid solution for 40 days a mixture with $[\alpha]_D^{20}$ + 15.37° was obtained. This mixture could contain oxidation

products, but not dehydro-dihydro- or tetrahydroabietic acids, as redistribution of the hydrogen atoms is impossible under these conditions.

Additional purification of the high-melting abietic acid with m. p. 183° and $[\alpha]_D^{20}$ + 20.5° (from alcohol) through the diacetonamine salt [11] showed that a somewhat purer acid can be obtained, with m. p. 186° and $[\alpha]_D^{20}$ + 30.2° (from alcohol), but that it was in the main a homogeneous high-melting abietic acid which could not be separated by this method.

Determination of the content of double bonds by Kaufmann's method showed the presence of two double bonds in the molecule of high-melting abietic acid. If this had been a mixture of dehydro-dihydro- and tetrahydroabietic acids, considerably smaller amounts of the halogen would have reacted.

Combustion of different samples of high-melting abietic acid confirmed that its elementary composition corresponds to the formula $C_{20}H_{30}O_2$.

On the grounds of all the above data it may be claimed that high-melting abietic acid is an individual compound with elementary composition corresponding to the formula $C_{20}H_{30}O_2$. The molecule of the acid contains two double bonds, and it has m. p. 186°, $[\alpha]_D^{20}$ + 30.2° (in alcohol).

EXPERIMENTAL

Preparation of pure low-melting abietic acid by the isomerization method. 100 g of rosin was dissolved in 100 ml of acetone containing 0.5% of hydrochloric acid. The crystalline mass (50% on the original rosin) was separated on a Buchner funnel and then recrystallized. After the first recrystallization from alcohol, the product (25%) had m. p. 170° and its crystalline form was that of abietic acid. After the second recrystallization the abietic acid, which comprised 15% of the original substance, had m. p. 172°. This abietic acid was purified further through the diacetonamine salt [11]. Recrystallization yielded 4 fractions of salts, and from these, acids:

Fraction I $[\alpha]_D^{20}$ — 3.20 at l = 1.9009 dm C = 1.6456, $[\alpha]_D^{20}$ —102.3°;
Fraction II $[\alpha]_D^{20}$ — 3.15 at l = 1.9009 dm C = 1.5388, $[\alpha]_D^{20}$ —107.7°;
Fraction III $[\alpha]_D^{20}$ — 3.06 at l = 1.9009 dm C = 1.6783, $[\alpha]_D^{20}$ — 95.9°;
Fraction IV $[\alpha]_D^{20}$ — 2.48 at l = 1.9009 dm C = 1.4730, $[\alpha]_D^{20}$ — 88.6°.

Fraction II of abietic acid, with m. p. 174° and $[\alpha]_D^{20}$ −107.7°, which represented about 7-8 % of the original rosin, was used in the subsequent experiments.

The lower specific rotation of Fraction I can be attributed to the presence of other resin acids, and in particular, to dextropimaric acid.

Isomerization of pure low-melting abietic acid with m. p. 174° $[\alpha]_D^{20}$ −107.7° by the action of acid reagents. 0.2054 g of low-melting abietic acid was dissolved in alcohol. To the solution hydrochloric acid was added to give about 0.1 % of hydrochloric acid per 20 ml of the resin acid solution.

The changes in the rotation of the resin acid are shown in Table 1.

Neither in this nor in the subsequent experiments could the high-melting abietic acid be obtained free from oxidation products, but the crystal form of the isomerization product corresponded to high-melting abietic acid.

Distillation, under atmospheric pressure, of pure low-melting abietic acid with m. p. 174°, $[\alpha]_D^{20}$ −107.7°. 2.90 g of low-melting abietic acid was distilled at normal pressure from a retort. 91.7% of distillate was obtained. 23.1% of hydrocarbons and 68.6% of acid products were isolated from this distillate. From the acids 37.6% of a crystalline acid was isolated by crystallization. Additional twofold crystallization yielded 6.44% of high-melting abietic acid with m. p. 182°, $[\alpha]_D^{20}$ + 12.61 (from alcohol).

TABLE 1

Changes in the Rotation of the Resin Acid

Isomerization conditions: C = 1.027, 0.1% HCl	Isomerization time	α_D^{20} at $l = 1.9009$ dm	$[\alpha]_D^{20}$
—	0	—2.05	—105.01
In the cold	5 min	—1.95	— 99.89
At the boil	20 min	—1.90	— 97.32
	2 hrs	—1.30	— 66.60
	4 hrs	—1.05	— 53.78
	6 hrs	—0.95	— 48.66
	14 hrs	—0.85	— 43.54
Rest of the time in the cold	40 days	+0.30	+ 15.37

Preparation of high-melting abietic acid from rosin. 251.25 g of rosin was distilled under atmospheric pressure. This gave 75.84% of rosin oil, from which 47.26% of hydrocarbons and 28.58% of crystalline acids were isolated.

After tenfold fractionation, high-melting abietic acid was obtained with m. p. 183°, $[\alpha]_D^{20}$ + 0.45 at l = 1.9009 dm, C = 1.2514, $[\alpha]_D^{20}$ + 20.56.

Elementary analysis

0.0794 g subst. CO_2 0.2308 g; H_2O 0.0711 g
0.0782 g subst. CO_2 0.2277 g; H_2O 0.0705 g

$C_{20}H_{30}O_2$. Found %: C 79.33, 79.46; H 10.02, 10.09.
Calculated %: C 79.42; H 10.00.

Determination of equivalent

0.1240 g subst: 8.22 ml 0.1 N. KOH, equivalent 302.66.
0.1802 g subst : 11.91 ml 0.1 N. KOH, equivalent 302.68.

Determination of iodine number, by Kaufmann's method, and of the number of double bonds

0.0610 g substance: 7.77 ml 0.1 N thiosulfate, iodine number 161.92; number of double bonds 1.93. 0.1974 g substance: 25.95 ml 0.1 N thiosulfate, iodine number 166.80; number of double bonds 1.99.

Additional purification of high-melting abietic acid with m. p. 183°, $[\alpha]_D^{20}$ 20.5. 2.1 g of high-melting abietic acid was purified through the diacetonamine salt [11]. Five fractions were obtained by the purification. After twofold recrystallization of each fraction, high-melting abietic acid with the constants given in Table 2 was obtained.

TABLE 2

Constants of Abietic Acid

Fraction No.	Wt. of fraction (g)	% of fraction	M. P. (°C)	$[\alpha]_D^{18}$
I	0.27	12.86	185	+ 7.33
II	0.21	10.00	185	+24.28
III	0.61	29.04	186	+30.24
IV	0.73	37.76	183	+32.22
V	0.28	13.34	177	+30.95

The lower positive rotation of the first fraction of the high-melting acid is the result of the presence of other resin acids, especially low-melting abietic acid, while the depression of the melting point of the fifth fraction is caused by the presence of hydrocarbon impurities.

The three middle fractions were subjected to elementary analysis.

2nd fraction	0.779 g subst.:	CO_2 0.2260 g;	H_2O 0.0719 g.
	Found %:	C 79.17 ;	H 10.33.
3rd fraction	0.788 g subst.:	CO_2 0.2287 g;	H_2O 0.0712 g.
	Found %:	C 79.20 ;	H 10.12.
4th fraction	0.778 g subst.:	CO_2 0.2261 g;	H_2O 0.0749 g.
	Found %:	C 79.31 ;	H 10.77.
$C_{20}H_{30}O_2$.	Calculated %:	C 79.42 ;	H 10.00.
$C_{20}H_{32}O_2$.	Calculated %:	C 78.89 ;	H 10.60.

SUMMARY

The investigation confirmed the individuality of high-melting abietic acid, $C_{20}H_{30}O_2$. The molecule of the acid contains two double bonds, and it has m. p. 186°, $[\alpha]_D^{18}$ + 30.2° (in alcohol).

LITERATURE CITED

[1] S. Levy, Z. ang. Ch., 18, 1739 (1905).

[2] V. V. Shkatelov, Monit. Scient. 22, 1, 217 (1908); P. A. Bobrov, Trans. Vyatka Sci. Res. Inst. of Regional Study II, 29 (1926); V. V. Shkatelov, Mem. Belorussian State Academy of Agriculture 4, 113 (1927).

[3] O. Aschan, and A. Virtanen, L. Ann., 424, 150 (1920).

[4] L. Ruzicka and I. Meyer, Helv. Chim. Acta, 5, 315 (1922).

[5] V. N. Krestinsky, N. I. Persiantseva and A. A . Novak, J. Appl. Chem. 12, 1407 (1939).

[6] V. N. Krestinsky, A. A. Novak and N. E. Komshilov, J. Appl. Chem. 12, 1514 (1939).

[7] E. Fleck and S. Palkin, J. Am. Chem. Soc., 59, 1593 (1937); 60, 921 (1938).

[8] L. F. Fieser and W. P. Campbell, J. Am. Chem. Soc., 60, 159 (1938).

[9] T. Hasselstrom, E. A. Brennan and I. D. Mc Pherson, J. Am. Chem. Soc. 60, 1267 (1938).

[10] E. R. Littmann, J. Am. Chem. Soc., 60, 1419 (1938).

[11] E. V. Roginskaya, J. Appl. Chem. 20, 564 (1947).

Received October 27, 1956

METHOD FOR THE PREPARATION OF BARIUM ALKALIES IN THE PURE STATE

M. M. Kushnir

The uses of pure barium alkalies are wide and varied. Organic synthesis, the production of special varieties of glass and rubber, of phosphors, of drugs — these are only a few of the applications of pure barium alkalies.

Industrial practice has shown that the principal difficulty in the production of pure barium alkalies lies in the purification of the crude product (technical barium hydroxide) to remove chlorides and iron.

Removal of iron from barium hydroxide. To a solution of technical barium hydroxide containing 180-185 g/liter, 10-12 kg/m^3 of technical quicklime is added, the reaction mixture is agitated for 20 minutes, and filtered through a frame filter press. To facilitate filtration, the mixture is sometimes left to settle for 20 minutes. The temperature of the liquid after addition of quicklime and during filtration must not exceed 75°. The iron content of the liquor is decreased 10 to 15-fold, and generally falls to 0.001-0.0013 g/liter. More complete removal of iron by means of technical quicklime is not possible because of the iron content of the latter (about 0.1-0.08%), and because of the reversibility of the purification process. Further purification of barium hydroxide (which is rarely necessary) can be effected by means of reactive calcium oxide containing about 0.003% of iron. The iron content after the second purification stage, with the use of reactive calcium oxide, is less than 0.0001 g/liter.

With careful filtration, the calcium content of the purified solution does not increase (and sometimes it even decreases) because of the negligibly low solubility of calcium hydroxide in concentrated caustic solutions.

Removal of chlorides from barium hydroxide. Technical barium hydroxide was formerly purified by centrifugal washing. This method has been abandoned because of its ineffectiveness — the chloride content was decreased by only 30% (from 0.04 to 0.003-0.0028%) and more than 20% of the barium hydroxide was lost in the wash liquors. It was therefore proposed to remove chlorides by recrystallization of technical barium hydroxide and washing of the newly formed $Ba(OH)_2 \cdot 7H_2O$. In this way the chloride content can be decreased 30 to 40-fold, down to about 0.001-0.0012%. The mother liquor and wash liquors are purified to remove iron and carbonated to commercial barium carbonate.

Calcium oxide cannot be replaced by the hydroxide, as the removal of iron from the barium hydroxide becomes much less effective.

Barium carbonate of a high degree of purity is obtained by carbonation of 20% barium hydroxide solution previously purified to remove iron and chlorides. It has been found that adsorption of chlorides and other soluble impurities predominates at the start of the precipitation, when the carbonate is in the colloidal state and is positively charged. As the precipitation proceeds, the adsorption of impurities decreases, as a considerable part of the barium carbonate is precipitated on existing centers of crystallization and the specific surface of the precipitate decreases. It was therefore proposed to commence the carbonation of barium hydroxide in presence of recycled barium carbonate paste. The amount of recycled paste is 10% of the total volume of barium carbonate produced in the operation.

Adoption of this method has improved the quality of the product and doubled the output rate.

Received October 13, 1956

BOOK REVIEWS

R. M. Fedorovich. Measurement of temperature (Laboratory Manual of Chemical Technology, No. 1). Moscow University Press (1957).

Temperature measurement and control in technological processes are of great importance in the national economy, especially in the chemical industry.

The laboratory manual of chemical technology, entitled "Measurement of Temperature" (Issue No. 1), compiled by R. M. Fedorovich and published by the Moscow University in the beginning of 1957, deals with practical measurements of temperatures.

This is the first issue of the proposed publication, in the form of separate issues, of a useful manual of laboratory practice in chemical technology for chemical students of the Moscow State University.

A close examination of this booklet shows that it can be used not only within the framework of Moscow University, but on a wider scale — by students, scientific workers, industrial chemists, and others who come into contact with temperature control and regulation of technological processes in their daily work.

The booklet consists of 6 short chapters and an appendix giving auxiliary tables for calculations.

The introductory chapter "Temperature Measurement" provides the theoretical basis for the four laboratory investigations described in the booklet.

This chapter describes the purpose of the work, the international temperature scale, and the fundamental principles of the design of instruments for temperature measurement (dilatometric and manometric instruments, resistance thermometers, and radiation pyrometers). The names and compositions of thermoelectric alloys, characteristics of thermocouples, thermocouple circuits, and the potentiometer circuit are given. The other 4 chapters (under the titles of the corresponding studies) give detailed descriptions of the laboratory work, and are all designed on the same plan.

In Study No. 1 (Chapter 1) "Comparison of the Readings of a Technical Mercury Thermometer and a Manometric Thermometer" there are descriptions of the design of mercury thermometers, the principal methods for their calibration, stem corrections, and the use of standard thermometers. The designs of various types of manometric thermometers and the principal characteristics of the substances used in them are analyzed.

In the section on "Manometric Thermometers" their contemporary Soviet code marks should have been given. The first part of the chapter should have been illustrated with diagrams or photographs.

Study No. 2 deals with a method for comparing the readings of a radiation pyrometer with a millivoltmeter, and a thermocouple with an automatic potentiometer. The circuits of the automatic electromechanical SP potentiometer, the radiation pyrometer, and photographs of the SP-3 automatic potentiometer and the mechanical design of the SP-1 potentiometer are given.

Study No. 3 is a comparison of the readings of the optical pyrometer with those of a thermocouple with an automatic electronic potentiometer.

This chapter is illustrated with photographs of the automatic electronic potentiometer, the scheme of the optical pyrometer, and the electrical circuit of the EPD potentiometer.

Study No. 4 consists of comparisons of the readings of a mercury thermometer and a resistance thermometer with an automatic electronic bridge circuit.

The principal defects of the booklet are errors of method and general inconsistencies.

There is some lack of clarity in the terminology used: the substance used to fill the bulb of a manometric thermometer is sometimes termed the working body (p. 16) or the working substance (p. 17), or the thermometric substance (p. 18). Thermodynamic and thermometric terms are confused.

The nomenclature of some instruments lacks clarity. For example, thermoelectric instruments are described as "thermoelectric thermometers" on page 8, and "thermoelectric pyrometers" on page 7 and page 35. Vapor pressure thermometers are described on the same page (17) both as vapor manometers and vapor thermometers.

The term "rheochord" is used both in the masculine (pp. 24, 28, 37) and in the femine gender (p. 19, Figure 4).

There are some obscure points and contradictions: on page 7 it is stated that mercury thermometers can be used between −30 and + 750°, while on page 14 the upper limit is said to be + 500°.

The lower limit of applicability of radiation thermometers is said to be above 800° (p. 12), and also 800° (p. 34).

The data in the "Appendix" are inadequately correlated with the main text. The reliability of some of the reference data is dubious. For example, the student will be puzzled why it is possible to use a chromel−copel thermocouple (used in the RP radiation pyrometer, p. 25) within the measurement range of this instrument, i. e., from 900 to 1800° (p. 26), as its upper working limit of temperature measurement (radiation measurements − I. F.) is only 600-800° (p. 9).

The question is not clarified by Table 3 (p. 44), which gives almost the same radiation temperature limits (800-1800°), especially as there is no mention anywhere of the use of another type of thermocouple in this instance, or of any other reason. It would be desirable to give here the formula relating the true to the radiation temperature:

$$T = T_y \sqrt[4]{\frac{1}{\varepsilon}}\,*,$$

which is used for the calculations. This is especially necessary in view of the unsuitability of Table 3 (p. 44) for calculations in Study No. 2, as the temperature measurements are to be made at intervals of 50° (p. 27), while the radiation temperatures in the table are given at intervals of 200°.

Table 1 (p. 43) lacks calibration data for iron−constantan and copper−constantan thermocouples, mentioned in the text on page 9, although such data are given for other types of thermocouples.

No concrete examples of the fields of practical application of the thermometric instruments discussed are given. Such data would make the factual material clearer.

Elimination of all the above-mentioned defects, which are particularly undesirable in a teaching aid, would improve the publication.

It should be pointed out that the booklet on the whole is worthy of favorable evaluation. It fulfills its purpose and achieves the intended aim, "to acquaint the student with the design and operation of instruments for measurement and recording of temperature" (p. 5). The booklet can also be used by those who have to measure temperatures (pyrometricians, technologists, thermochemists, etc.).

I. G. Filatov

* Great Soviet Encyclopedia, 2nd ed. 35, 477 (1955).

Proceedings of the Technical Conference on the Roasting of Materials in Fluidized Layers (May 25-29, 1954). Metallurgy Press, 162 pages, gratis (1956).

In recent years conferences have often been held on specific aspects of science or technology. For example, there was a conference on the use of tagged atoms in analytical chemistry (Kiev), a conference on the chemistry and technology of selenium and tellurium (Moscow), etc. There is no doubt that such conferences are very profitable and effective, as they bring together representatives of undertakings, institutes, laboratories, main committees, and other organizations, and make it possible to summarize past work and plan future tasks in a businesslike and uncrowded atmosphere.

The conference called by the State Institute of Nonferrous Metals (Gintsvetmet) on one of the most advanced technical methods of roasting, the "fluidized layer" method, was of this kind.

The proceedings of this conference have been published in a separate book, which is of great interest to metallurgists and chemists. It contains 10 papers on the results of laboratory investigations and the industrial adoption of the process in which finely divided solids in the semisuspended state react with gases in a "fluidized layer", with short reports of the discussions and the resolution of the conference.

The conference was attended by 124 delegates from 17 works and 15 scientific research and planning institutes of various organizations: The Academy of Sciences USSR, the Ministries of Nonferrous Metallurgy, Ferrous Metallurgy, Chemical Industry, the Petroleum, Paper, and Wood Processing Industries, and of teaching institutions.

The papers were concerned with the following subjects: 1) investigation and industrial adoption of the roasting of zinc concentrates in a fluidized layer, 2) investigations of the oxidative roasting of other sulfide materials, and 3) reductive roasting of various materials.

For chemists, the greatest interest lies in the second and third sections, which contain the following papers: A. M. Malets (Scientific Research Institute of Fertilizers and Insectofungicides) on the roasting of pyrite in a fluidized layer, L. N. Sidelkovsky (Moscow Institute of Power Engineering) on the intensive roasting of flotation pyrite with the use of waste gas heat, I. V. Babin (State Institute of Nonferrous Metals) on the dissociative roasting of calcium sulfate and V. A. Teplenko (Institute of Ferrous Metallurgy) on the magnetizing roasting of iron ores.

The discussions and the conference resolution unanimously noted the necessity for the rapid adoption of this new and progressive roasting method in industrial practice; this necessitates intensified work on the design and construction of various types of furnaces of different capacities, on the automatic control of the processes, and scientific research on the theory of roasting processes in fluidized layers, on the determination of the most rational process conditions, and on the utilization of the heat liberated in the roasting process.

The new method of "roasting in a fluidized layer" will undoubtedly be extended to branches of industry where it is not yet used, and to processes beyond the limits of the concept of "roasting."

The methods used in roasting can undoubtedly be extended to a wide range of gas–solid interactions, making these processes considerably more rapid and safer. The interaction of gases with fluidized solid particles can probably be applied in processes of chlorination, sulfating, hydrogenation, etc.

The organizers of the conference and the Metallurgy Press must be reproved for the delay in publishing the proceedings of the conference: more than 2 years elapsed between the conference and the presentation of the proceedings to the press, while the printing took about six months. It is regrettable that the proceedings do not include the paper by G. Ya. Leizerovich, which had been circulated by the Central Institute of Information of the Ministry of Nonferrous Metallurgy. Because of this, the wider circle of readers of the proceedings of the conference have no opportunity of reading this paper.

O. E. Zvyagintsev

LETTERS TO THE EDITOR

We request you to publish the following comments on the paper by R. Z. Temkina "Production of Phenol – Formaldehyde Resin Adhesives Containing Practically no Free Phenol," published in J. Applied Chem. 29, No. 9, 1442-1444 (1956).

Phenol – formaldehyde resins containing practically no free phenol or formaldehyde were prepared by G. S. Petrov and N. S. Shcherba (authors' certificate No. 75871; priority September 13, 1948, class $\frac{12, d, 20/01}{39, c, 22}$).

The preparation of these resins was tested in January 1950 at the experimental unit of the Scientific Research Institute of Plastics, Ministry of Chemical Industry USSR; these trials established that:

1) the actual conditions for the making of these resins, in accordance with Author's Certificate No. 75871, conform to the specified conditions and do not require special equipment; i. e., the same equipment as is used for the usual phenol–formaldehyde resins is suitable;

2) the advantages of these resins over the usual resoles are: a) these resins are soluble in aqueous ammonia solutions, and b) it is possible to obtain rapidly hardening thermosetting resins practically free from free phenol or formaldehyde;

3) the yield of precipitated and washed anhydrous resins is over 140 % on the weight of the phenol, whereas industrial phenol–formaldehyde resins are obtained only in 107-110% yields.

In addition, the production and properties of such resins are described in the Transactions of the D. I. Mendeleev (Order of Lenin) Moscow Institute of Chemical Technology (No. 18, pp. 202-206, 1956).

The introduction of urea and other substances into the reaction mixture at a definite condensation stage is described in the literature (O. Nuvel, Production of Phenol–Aldehyde Resins, 1933, p. 39).

G. S. Petrov and N. S. Shcherba

*Original Russian pagination. See C. B. Translation.

JOURNAL OF APPLIED CHEMISTRY OF THE U. S. S. R. IN ENGLISH TRANSLATION

July 1957

TABLE OF CONTENTS

	Page	Russ. Page
Separation of Calcium Chloride From Solvay Spent Liquor Through Calcium Hydroxy-Chloride. I. I. Volnov and E. I. Latysheva	1039	977
Isotherms for the Reciprocal Aqueous System Ammonium Monophosphate – Sodium Nitrate – Water at + 30, +20 and 0°. S. Ya. Shpunt	1047	985
Removal of Scale From Steels at Elevated Temperatures. B. S. Krasikov and B. I. Lavrentyev	1055	993
The Corrosion Stability of Galvanic Films Deposited on a Passivated Surface. L. I. Kadaner and A. Kh. Masik	1060	998
The EMF of Some Galvanic Circuits in Cryolite-Alumina Melts. V. P. Mashovets and A. A. Revazyan	1069	1006
Plate Efficiency During Distillation of Binary Mixtures. E. Rukenshtein	1075	1012
A Study of the Relation Between the Expenditure of Material in the Reactor and the Volume of the Solution During Development and Clearing of Cine-Film. I. Blyumberg, G. Bulochnikova and N. Solodovnikova	1080	1016
The Effect of Temperature During Determination of the Moisture Content of Sulfonate Cation Exchangers, on the Accuracy of Determination of their Exchange Capacity. A. A. Vasilyev	1086	1022
The Technology of the Polycaprylonitrile Fiber Nitron (Nitrilon). E. S. Roskin	1095	1030
Water Permeability of Plasticized Compositions. Sh. L. Lelchuk and V. I. Sedlis.	1106	1041
A Study of the Phenols Obtained by the Thermal Decomposition of Hydrolyzed Lignin. V. G. Panasyuk	1114	1049
Development of a Process of Hydrogenation Refining, Under Low Hydrogen Pressures, of Gasolines Obtained by Thermal Liquefaction and Semicoking of Esthonian Shales. M. K. Kyakova, A. B. Vol-Epshtein, E. A. Aleksi, and E. I. Vasilchikova	1121	1056
Production of Symmetrical 4,4'-Dinitrocarbanilides. A. A. Spryskov, S. N. Solodushenkov and V. N. Klyuev	1130	1065
Brief Communications		
Extraction of Small Amounts of Gold from Cyanide, Hydrochloride, and Iodide Solutions by Means of Ion-Exchange Resins. N. A. Ezerskaya and N. V. Markova	1135	1071
Use of Radioactive Sulfur (S^{35}) for Determination of Sulfonic Groups in Sulfonated Coal. N. P. Drozdov and A. N. Popov.	1140	1074
Action of Enamel Melts on Steel. G. I. Belyaev.	1144	1077
Determination of the Solubility of Carbon Dioxide in Aqueous Solutions of Sodium Sulfate and its Mixtures with Sulfuric Acid by the Isotopic Dilution Method. M. K. Shchennikova, G. G. Devyatykh and I. A. Korshunov	1149	1080

TABLE OF CONTENTS (continued)

	Page	Russ. Page
Relationship Between the Frost Resistance of Cements and the Thermodynamic Potential of their Chemical and Mineralogical Components. E. M. Kolobov	1153	1084
Laws Governing the Simultaneous Cathodic Discharge of the Principal Metal Ions and Impurities in the Electrolytic Production of Cobalt. A. L. Rotinyan, V. L. Kheifets and A. M. Yakovleva	1157	1087
The Potentials of Copper, Antimony, Bismuth and Lead in Nitric Acid Solutions. V. V. Tenkovtsev	1161	1090
The Causes of Local Spongy Formations on the Cathode in Zincate Electrolytes. N. T. Kudryavtsev, R. Yu. Bek, and I. F. Kushevich	1164	1093
Colloidal and Suspended Particles in Physicochemical Processes in Boilers. S. A. Durov and N. G. Chen	1168	1096
Rectification of Methanol – Ethanol – Water Mixture in a Continuous-Action Column. M. E. Aerov, G. L. Motina and M. M. Potarin	1173	1100
Preparation of Trihydroxystearin. G. V. Pigulevsky and A. E. Saprokhina	1178	1104
Investigation of the Composition of Dry-Distilled Retort Turpentine from the Resin of Korean Pine (Pinus koraiensis sieb. et Zucc). N. I. Uvarova and I. I. Bardyshev	1180	1105
Preparation of Benzidine Bases with the Use of Aliphatic Alcohols as Reducing Agents. D. F. Kutepov and V. E. Reinshtein	1184	1108
High-Melting Abietic Acid. N. F. Komshilov	1188	1111
Method for the Preparation of Barium Alkalies in the Pure State. M. M. Kushnir	1193	1115
Book Reviews	1194	1117
Letters to the Editor	1197	1120

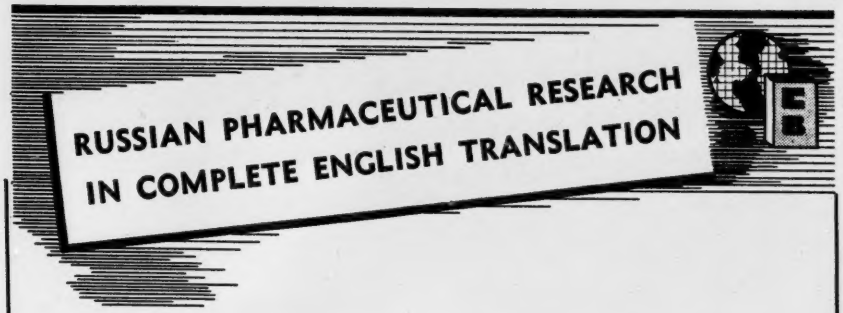

SOVIET PHARMACEUTICAL RESEARCH
Chemistry Collection No. 4 — Just published

Covers all aspects of Soviet pharmaceutical research; papers selected by one of the top pharmaceutical research chemists, of one of the major drug companies, from all Russian chemistry journals translated by Consultants Bureau, **1949–1955.** Sections may be purchased as follows:

I. PHARMACEUTICAL CHEMISTRY. Sections: Solubility; Stability: Ion Exchange; Emulsions, Suspensions, Gels; Miscellaneous. 74 papers, 447 pages, **$95.00**

II. PHARMACOGNOSY. Sections: Alkaloids; Oils; Glycosides; Miscellaneous. 87 papers, 399 pages, **$90.00**

III. MEDICINAL CHEMISTRY. Sections: Structure-Activity Relationships; General. 91 papers, 556 pages, **$100.00**

THE COMPLETE COLLECTION, 252 papers, 1,402 pages, **only $200.00**

*Single articles available — Table of Contents sent on request

All Consultants Bureau's translations by bilingual scientists, equally familiar with Russian and the technical terminology. All diagrammatic and tabular material integral with the text is included; text is clearly reproduced by multilith process from IBM cold type; books are staple bound in durable paper covers. Complete catalogs of Consultants Bureau translations available

CONSULTANTS BUREAU, INC.
227 WEST 17th STREET, NEW YORK 11, N. Y. — U.S.A.
Telephone: ALgonquin 5-0713 • Cable Address: CONBUREAU, NEW YORK

Chemistry Collection No. 2

SOVIET RESEARCH IN

GLASS and CERAMICS

(1949-1955)

One hundred and forty six reports, in complete English translation, with all tabular material and diagrams integral with the text. Selection and Preface by W. G. Lawrence, Chmn., Dept. of Ceramic Research, State University of New York College of Ceramics at Alfred University.

The complete collection . . . $150.00

The one hundred and forty six reports included in this collection originally appeared in the Soviet Journals of General and Applied Chemistry and the Bulletin of the Academy of Sciences of the USSR, beginning with 1949. The collection comprises over 900 pages, more than 400,000 words of recent research on glass and ceramics by Soviet scientists, in complete English translation.

The Collection is divided into sections, which may be purchased separately, as follows:

Basic Science: (70 reports)	$ 90.00
Glass; glazes and enamels (32 reports)	40.00
Refractories (12 reports)	20.00
Cements, limes and plasters (28 reports)	35.00
Miscellaneous (4 reports)	7.50

CONSULTANTS BUREAU, INC.

227 WEST 17th STREET, NEW YORK 11, N. Y. — U.S.A.

Telephone: ALgonquin 5-0713 • Cable Address: CONBUREAU, NEW YORK